ENGINEER

international scientific journal

ISSUE 3, 2025 Vol. 3
E-ISSN
3030-3893
ISSN
3060-5172

A bridge between science and innovation

TOSHKENT DAVLAT TRANSPORT UNIVERSITETI
Tashkent state transport university

ENGINEER

A bridge between science and innovation

E-ISSN: 3030-3893

ISSN: 3060-5172

VOLUME 3, ISSUE 3

SEPTEMBER, 2025

engineer.tstu.uz

TASHKENT STATE TRANSPORT UNIVERSITY

ENGINEER

INTERNATIONAL SCIENTIFIC JOURNAL
VOLUME 3, ISSUE 3 SEPTEMBER, 2025

Founder of the international scientific journal "Engineer" – Tashkent State Transport University, 100167, Republic of Uzbekistan, Tashkent, Temiryo'lchilar str., 1, office: 465, e-mail: publication@tstu.uz.

The "Engineer" publishes the most significant results of scientific and applied research carried out in universities of transport profile, as well as other higher educational institutions, research institutes, and centers of the Republic of Uzbekistan and foreign countries.

The journal is published 4 times a year and contains publications in the following main areas:

- Engineering;
- General Engineering;
- Aerospace Engineering;
- Automotive Engineering;
- Civil and Structural Engineering;
- Computational Mechanics;
- Control and Systems Engineering;
- Electrical and Electronic Engineering;
- Industrial and Manufacturing Engineering;
- Mechanical Engineering;
- Mechanics of Materials;
- Safety, Risk, Reliability and Quality;
- Media Technology;
- Building and Construction;
- Architecture.

Tashkent State Transport University had the opportunity to publish the international scientific journal "Engineer" based on the **Certificate No. 1183** of the Information and Mass Communications Agency under the Administration of the President of the Republic of Uzbekistan. **E-ISSN: 3030-3893, ISSN: 3060-5172.** Articles in the journal are published in English language.

ENGINEER
INTERNATIONAL SCIENTIFIC JOURNAL
VOLUME 3, ISSUE 3 SEPTEMBER, 2025

EDITORIAL BOARD

Researching pedestrian movement in city streets

M.Z. Ergashova[1][a], Sh.R. Khalimova[1][b]
[1]Tashkent state transport university, Tashkent, Uzbekistan

Abstract: The article carefully analyzes the need for the study of pedestrian behaviour in the city streets, its determinants, and the methods of research. One of the major goals of planning within the city has been the improvement of pedestrian flows as well as the need to guarantee safety. A set of measures such as determining the parameters of pedestrian movement, obtaining data and applying statistical processes to it, and constructing movement models using new technologies were determined to be necessary. Thorough planning for urban structure provides opportunities for improvement of flows of pedestrian in the cities. The quality of urban infrastructure, the presence of safe sidewalks, crossing places, traffic lights, and other convenience features influence directly the effectiveness and safety of movement of pedestrians.

The research specifically focused on the necessity to factor the requirements of pedestrians under the design of the resultant infrastructure and the plans which endeavours to aid their mobility. It has also been noted the significance of studying pedestrian movements, analysing how this enables the recognition of activity patterns on streets, pedestrian traffic, and diagnosing certain issues. The analysis results support recommendations that seek to enhance urban infrastructure, pedestrian welfare, and urban mobility control. Moreover, the article gave comprehensive description about modeling techniques. It has extensively discussed the simulation of pedestrian activities in computer programs through modern technologies, predicting movement congestion for different scenarios, and evaluating the effectiveness of infrastructure. It was proposed that this modeling technique can be useful in the management of urban development and infrastructure planning because its outputs are useful in formulating different movement control strategies.

Keywords: urbanization, road infrastructure, pedestrian movement, optimization of transport vehicle movement, pedestrian flow, drones and cameras, traffic lights

1. Introduction

Cities around the globe are constantly rising in population and making strides economically, leading to rapid urbanization. Fueled by the growing demand for living spaces, the increase in transport vehicles and walking people directly affects road infrastructure. This further enhances the importance of urban infrastructure. Without a doubt, it is essential for modern day cities to focus on having efficient roads, safe areas for pedestrian movement, and the overall balance between traffic and public transport. This however is a much more complex problem in design and planning that needs to be addressed [1, 2, 20].

While past information is helpful, having a specific analysis of pedestrian movements and flows assists in developing infrastructure that pedestrians can find comfort in. This also allows the ability to make roads and crossing zones more safe, as well as effectively manage transport traffic systems [3, 4, 5, 21]. AI can further be utilized to create new strategies of enhancing pedestrian comfort and safety, while optimizing traffic flows to increase the overall effectiveness of a city's transport system.

The modernization of urban infrastructure facilitates more efficient management of traffic and contributes positively to city growth. A comfortable and safe infrastructure is a convenience to not only residents of the city but also tourists and other visitors [6, 7, 8, 22, 23] which, in turn, speeds up the economic and social growth. Therefore, there is an immediate need to formulate and execute these strategies during the urbanization process. The solutions should integrate new technology, effective resource management, and social considerations.

In any case, the urbanization phenomenon presents both opportunities and challenges when it comes to development and improvement of the urban infrastructure. These issues demand a strategic approach to urban infrastructure development that incorporates accurate predictive analysis. The increasing global attention towards sustainable development has created a need to rethink urban development planning strategies, especially those that include energy saving processes. Additionally, achieving a balance between the needs of pedestrians and motorists with respect to urban infrastructure improvement is also of critical importance. These, when combined with other various approaches, responses, and constructions, help in fostering the welfare of the urban populace [1, 9, 10] and in achieving the benefits of urbanisation.

2. Materials and method

The primary goal of the research is to analyze the features of pedestrian flows in urban street spaces in detail [11, 12, 13] and to formulate some practical tips for adequate infrastructure development in cities. To realize this goal, the following important tasks (Table 1) were set during the study:

[a] https://orcid.org/0000-0001-6636-6206
[b] https://orcid.org/0000-0002-4753-390X

Table 1

Established Tasks	Main Objectives of the Research	Data
Studying the Characteristics of Pedestrian Flow	Analyzing the Movement Trends of Pedestrian Flow	Analyzing Movement Density and Pedestrian Flow Patterns, and Identifying Compatibility with Social Needs
Identifying Infrastructure Elements that Contribute to Providing a Comfortable and Safe Environment for Pedestrians	Creating a Safe and Comfortable Environment for Pedestrians	Analyzing Pedestrian Walkways, Traffic Lights, Crossing Points, Lighting Systems, and Other Infrastructure Elements
Applying Modern Technologies and Methods for Modeling Pedestrian Movement	Modeling and Analyzing Movement	Applying Simulation Software, Data Processing Tools, and Movement Tracking Technologies

As a result of implementing these tasks, scientifically-based recommendations aimed at improving urban infrastructure and creating a more comfortable, safe, and modern environment for pedestrians were developed. These recommendations serve as a foundation for formulating long-term strategic plans aimed at meeting societal needs and enhancing pedestrian safety.

During the research, the following methods were extensively employed, resulting in significant findings:

Observation. Special observation studies were conducted on major streets in the city center and in areas with high pedestrian permeability. Using this method, the characteristics of pedestrian flow movement, including pedestrian flow density, movement directions, and interactions with transport vehicles [14, 15, 20], were thoroughly examined. Activity patterns of pedestrian movements was analyzed in regards to various intervals of the day; morning, midday, and evening. This study provided insights into many existing issues pertaining to the city's infrastructure.

Interviews and Surveys. The research was done by asking pedestrians questions in which the responses provided information regarding their preferences and needs. To ease the collection of data, questionnaires were structured in a way that the most pertinent information regarding mobility and safety issues pedestrians encounter were gathered as shown in [16, 17]. Through interviews, pedestrians supplied very descriptive accounts of their preferences which made the target of the research more focused and accurate. This approach was especially important for assessing the degree of adequacy of urban infrastructure to people's needs.

Modeling. The studies use contemporary computer models for the equipment modern simulations to analyzing the movement's density will forecast possible issues within different scenarios. This specific method is beneficial to providing recommendations to increase safety of activities as well as movement s efficiency. In this case, the method which has the highest contribution is simulation software, thus making this method significantly contribute to the development recommendation designed to increase the safety and efficiency of movement.

Statistical Analysis. The analysis of documents received from the observations, interviews, and surveys was done with the help of statistical tools. This analysis, in addition to providing vital information about pedestrian flows, provided valuable insight regarding the infrastructure effectiveness. It allowed better understanding of the changes in the pedestrian flows, rent relations, and rational explanations of the research results.

The combination of techniques resulted in creation of a clear and concise document. This document proved that the steps taken towards resolving infrastructural urbanization issues are reasonable and can be implemented without any complication.

3. Result and Discussion

As a result of the research, the following main tasks were developed:

Variations Over Time and Density of Pedestrian Flow

The study shows that pedestrian commute during work hours is the most active. At these times, pedestrian flow significantly increases and it is necessary to manage the movement of other transport units and pedestrians on the streets. It was notably stated that the areas containing high density population zone are prone to having increased collisions between transport units and pedestrians which means there must be improved safety features.

Deficiencies in Infrastructure

During the course of the research, it was noticed that there is lack of proper infrastructure spaces dedicated for pedestrian use on the streets. Adequate provisions such as safe crossings and wide, well-lit sidewalks were not constructed. By the same token, it was observed that the placement of pedestrian lanes was either misplaced or inadequately used. Also, the placement of traffic signals was too low, which made it exceedingly difficult for pedestrians to cross the streets.

Technological Solutions Increased Efficiency

The study demonstrated that modern technological devices for analyzing and controlling pedestrian flow are effective. The condition of pedestrian flows was tracked in real-time with the help of drones and cameras which made it possible to collect accurate data and recognize movement patterns. In addition, computer models were used to study pedestrian flow patterns and to develop effective algorithms for flow direction optimization. All of these methods significantly aided in formulating important recommendations that help improve the safety of movements as well as enhance urban infrastructure.

These recommendations form the basis of the scientific data needed to improve urban infrastructure and provide pedestrians with a more friendly and safe environment.

4. Conclusion

The findings of the study recommend the effective management of pedestrian movement safety which is enabled by a number of developed suggestions. These recommendations are focused on the improvement of urban infrastructure, making it more convenient and safer for the pedestrians with the following: increasing the number of pedestrian crossing points with improved lighting on the streets, optimizing traffic signals for pedestrian purposes,

employing modern tools for monitoring and controlling pedestrian flow, enhancing infrastructure for pedestrians' safety, and modernizing innovation block projects.

These suggestions as in which infrastructure assumes a contemporary outlook with modern requirements, change in the management of pedestrian movement, and ensure safety when moving within urban areas makes a substantial difference towards the sustainable development of cities.

References

[1] Amoako, C., Cobbinah, P. B., & Niminga-Beka, R. (2014). Urban Infrastructure Design and Pedestrian Safety in the Kumasi Central Business District, Ghana. Journal of Transportation Safety & Security, 6(3), 235–256. https://doi.org/10.1080/19439962.2013.861887

[2] Bayiga Zziwa, E., Mutto, M., & Guvatudde, D. (2023). A cluster analysis of the spatial distribution of pedestrian deaths and injuries by churches in Kampala, Uganda. *International Journal of Injury Control and Safety Promotion, 30*(3), 419–427.** https://doi.org/10.1080/17457300.2023.2204490.

[3] Zegeer, Charles V., and Max Bushell. "Pedestrian crash trends and potential countermeasures from around the world." Accident Analysis & Prevention 44.1 (2012): 3-11.

[4] World Health Organization. Pedestrian safety: a road safety manual for decision-makers and practitioners. World Health Organization, 2023.

[5] Vanumu, Lakshmi Devi, K. Ramachandra Rao, and Geetam Tiwari. "Fundamental diagrams of pedestrian flow characteristics: A review." European transport research review 9 (2017): 1-13.

[6] Prus, P.; Sikora, M. The Impact of Transport Infrastructure on the Sustainable Development of the Region—Case Study. Agriculture 2021, 11, 279. https://doi.org/10.3390/agriculture11040279.

[7] Gulnara Mamirkulova, Jianing Mi, Jaffar Abbas, Shahid Mahmood, Riaqa Mubeen, Arash Ziapour, New Silk Road infrastructure opportunities in developing tourism environment for residents better quality of life, Global Ecology and Conservation, Volume 24, 2020, e01194, ISSN 2351-9894, https://doi.org/10.1016/j.gecco.2020.e01194.

[8] Shu-Yuan Pan, Mengyao Gao, Hyunook Kim, Kinjal J. Shah, Si-Lu Pei, Pen-Chi Chiang, Advances and challenges in sustainable tourism toward a green economy, Science of The Total Environment, Volume 635, 2018, Pages 452-469, ISSN 0048-9697, https://doi.org/10.1016/j.scitotenv.2018.04.134.

[9] Cieśla, M. Modern Urban Transport Infrastructure Solutions to Improve the Safety of Children as Pedestrians and Cyclists. Infrastructures 2021, 6, 102. https://doi.org/10.3390/infrastructures6070102

[10] Bryan Botello, Ralph Buehler, Steve Hankey, Andrew Mondschein, Zhiqiu Jiang, Planning for walking and cycling in an autonomous-vehicle future, Transportation Research Interdisciplinary Perspectives, Volume 1, 2019, 100012, ISSN 2590-1982, https://doi.org/10.1016/j.trip.2019.100012.

[11] Helbing, Dirk, et al. "Self-organizing pedestrian movement." Environment and planning B: planning and design 28.3 (2001): 361-383.

[12] Hillier, Bill, et al. "Natural movement: or, configuration and attraction in urban pedestrian movement." Environment and Planning B: planning and design 20.1 (1993): 29-66.

[13] Albabely, Saif, and Dhirgham Alobaydi. "Impact of Street Network Properties on Urban Pedestrian Movement Densities: Insights from Iraq." (2024).

[14] V.P Sisiopiku, D Akin, Pedestrian behaviors at and perceptions towards various pedestrian facilities: an examination based on observation and survey data, Transportation Research Part F: Traffic Psychology and Behaviour, Volume 6, Issue 4, 2003, Pages 249-274, ISSN 1369-8478, https://doi.org/10.1016/j.trf.2003.06.001.

[15] Yan Feng, Dorine Duives, Winnie Daamen, Serge Hoogendoorn, Data collection methods for studying pedestrian behaviour: A systematic review, Building and Environment, Volume 187, 2021, 107329, ISSN 0360-1323, https://doi.org/10.1016/j.buildenv.2020.107329.

[16] Eleonora Papadimitriou, Towards an integrated approach of pedestrian behaviour and exposure,

[17] Accident Analysis & Prevention, Volume 92, 2016, Pages 139-152, ISSN 0001-4575, https://doi.org/10.1016/j.aap.2016.03.022.

[18] J. Ma, S.M. Lo, W.G. Song, W.L. Wang, J. Zhang, G.X. Liao, Modeling pedestrian space in complex building for efficient pedestrian traffic simulation, Automation in Construction, Volume 30, 2013, Pages 25-36, ISSN 0926-5805, https://doi.org/10.1016/j.autcon.2012.11.032.

[19] López Baeza, J.; Carpio-Pinedo, J.; Sievert, J.; Landwehr, A.; Preuner, P.; Borgmann, K.; Avakumović, M.; Weissbach, A.; Bruns-Berentelg, J.; Noennig, J.R. Modeling Pedestrian Flows: Agent-Based Simulations of Pedestrian Activity for Land Use Distributions in Urban Developments. Sustainability 2021, 13, 9268. https://doi.org/10.3390/su13169268

[20] Tursunboev, F., Sadikov, I., Saydametova, F., & Ergashova, M. (2024, November). Requirements for the organization of tourist-recreational areas and the roads leading to them. In AIP Conference Proceedings (Vol. 3244, No. 1). AIP Publishing.

[21] Beketov A., Khalimova S. IMPACT OF ROUGHNESS AND FRICTION PROPERTIES OF ROAD SURFACE OF URBAN STREETS ON THE TRAFFIC SAFETY //Komunikácie. – 2023. – Т. 25. – №. 3.

[22] Foreign experience in urban streets management system. AK Beketov, FJ Saydametova, MZ Ergashova, SR Khalimova. Academic research in educational sciences 3 (TSTU Conference 1), 891-896

[23] Ergashova M. Z., Bobonazarov T. S. Greening City Streets and Roads in Modern Urban Conditions //Sustainable Development of Transport. – С. 3.

Information about the author

Ergashova Mokhichekhra	Tashkent State Transport University, Teacher of the Department of Urban Roads and Streets. Email: mohichexra1995@gmail.com https://orcid.org/0000-0001-6636-6206
Khalimova Shakhnoza	Tashkent State Transport University, Docent of the Department of Urban Roads and Streets. Email: xalimova_sh@tstu.uz https://orcid.org/0000-0002-4753-390X

Digitalization of maintenance record-keeping for automation and telemechanics devices at railway stations

N.V. Yaronova[1][a], **Sh.B. Otakulova** [1][b]
[1]Tashkent state transport university, Tashkent, Uzbekistan

Abstract: The article addresses the issues associated with the manual method of recording maintenance for automation, signaling, and telemechanics devices at railway stations in Uzbekistan. It analyzes the current practice of maintaining paper documentation and identifies major shortcomings, including high labor intensity, input errors, delays, and lack of transparency. A digital record-keeping model is proposed, which includes a workflow algorithm, registration and analytics modules, as well as integration with maintenance schedules. The practical importance of transitioning to an automated system is substantiated. The expected outcomes include increased reliability, cost reduction, and improved management of technical processes.

Keywords: automation, telemechanics, signaling and interlocking, digital model, maintenance, railway station, electronic logbook, digitalization.

1. Introduction

Modern conditions for the operation of railway transport demand high reliability and fault tolerance of technical systems, especially automation, telemechanics, signaling, and interlocking devices. Train traffic safety, operational efficiency, and adherence to transport schedules directly depend on the timely and high-quality maintenance of these systems. In this context, not only the technical service ability of the equipment becomes crucial, but also the organization of monitoring, recording, and analyzing maintenance activities.

At railway stations in Uzbekistan, the maintenance of signaling and interlocking devices is carried out in accordance with NSH-01 and NSH-03 instructions, which are approved as internal regulatory documents of JSC "Uzbekistan Railways" These documents define the frequency, methods, and formats for recording completed maintenance tasks. Currently, the primary method of documentation remains manual entry into paper logbooks (PU–67, DU–46, SHU–2, SHU–45, SHU–58, SHU–60, etc.). However, operational experience shows that this system no longer meets the demands of the digital era and gives rise to a number of issues: delays in data entry, a high risk of errors, lack of a unified database and transparent oversight, and the inability to quickly retrieve information.

An analysis of the literature confirms the relevance of this issue. In sources [1–3], the importance of a reliable maintenance record - keeping system is emphasized in the context of preventing railway incidents. Works [4–6] explore digital maintenance solutions based on integration with SCADA systems, digital twins, and artificial intelligence. Studies [7–9] highlight the significance of timely failure analysis and recurring fault detection as a foundation for predictive maintenance. International publications [10–13] showcase successful implementations of electronic maintenance and diagnostic systems by railway companies in Europe and Asia, which have led to significant cost reductions and improved operational control.

Moreover, reports from the UIC (International Union of Railways) indicate that in countries with advanced digital infrastructure, the average response time to S&I device failures is reduced by 30–50%, while compliance with technical regulations increases to 90–95% with the implementation of digital models. This makes digitalization not only an innovative step but also a necessity for ensuring the competitiveness of the national railway industry.

In the context of the active digital transformation of JSC "Uzbekistan Railways" and the modernization of its technological infrastructure, there is an urgent need to develop an automated system for recording and monitoring the maintenance of automation and telemechanics devices. This system should replace paper logbooks, ensure transparency of all operations, provide instant monitoring capabilities, access to historical records, and integration with preventive maintenance schedules.

The aim of the study is to develop and justify a methodology for the digitalization of processes related to the execution and recording of maintenance for automation and telemechanics devices, based on an operational-technological schedule. This methodology is intended to enhance the accuracy, transparency, and efficiency of maintenance control. To achieve this, the following research objectives have been set:

1. To analyze the existing documentation system and logbook practices related to the maintenance of signaling and interlocking devices.
2. To identify the main drawbacks of manual data entry and their impact on process reliability.
3. To develop an algorithm for creating an electronic database of completed maintenance tasks.
4. To evaluate the advantages of the digital model compared to the current system.
5. To propose practical recommendations for implementing an automated maintenance registration system at railway stations.

[a] https://orcid.org/0000-0003-1781-5597
[b] https://orcid.org/0009-0006-4415-963X

2. Research methodology

In the course of this study, a comprehensive approach was employed, combining both theoretical and practical methods of analysis aimed at identifying the shortcomings of the existing maintenance system for automation and telemechanics devices, as well as substantiating the need to transition to a digital model for planning and recording technical operations. To achieve the research objective, a combination of empirical and analytical - descriptive methods was applied.

Three major railway stations in Uzbekistan were conditionally selected as the objects of this study. These stations differ in traffic intensity, structural complexity, and the variety of automation devices in use: Tashkent-Severny Station – a junction station with high-density passenger and freight traffic, equipped with automatic switch machines, light signaling systems, SAUT devices, and centralized control systems; Samarkand Station – an intermediate transit station with a well-developed system of inter-station communication and remote monitoring; Karshi Station – a regional hub where telemechanics and locomotive signaling devices are actively used, and maintenance is performed on-site.

These stations were chosen due to their typical representativeness, which allows the results obtained from the study to be extrapolated to the entire railway transport system of Uzbekistan. Methods used to obtain reliable data:

Analysis of operational documentation. Maintenance registration logbooks used at the selected stations were examined in detail. The analysis covered the following forms: PU–67 (Shift Handover Log); DU–46 (Inspection Log for Switches, Tracks, and Overhead Contact Lines); SHU–2 (Log of Completed Work on Communication Facilities); SHU–45 (Electrical Measurements of Ground Resistance); SHU–58, SHU–60, and others. The evaluation focused on completeness of entries, presence of errors, duplicate records, and time gaps between events.

Time-and-motion observations. During the modeling process, the average time required by workers to perform manual journal entries was recorded. The observations included: Receiving a task; Executing the task; Locating the correct logbook; Filling in the required fields; Confirming instruction compliance; Performing control checks. Additionally, the time needed to retrieve archived records upon request was measured.

Expert survey. A survey was conducted with six specialists electromechanical engineers and heads of maintenance divisions with hands-on experience at maintenance sites. Participants were asked to assess the usability of the current system, identify major challenges, and predict the potential benefits of introducing an automated record-keeping system.

Algorithm modeling. Based on the analysis of current workflows, an algorithm was developed for the creation and operation of a digital database designed to replace manual logbooks. The model considers the location of maintenance (station, track segment, switch, signal), type of device, type of service, and maintenance frequency.

SWOT analysis. A comprehensive SWOT analysis was carried out to evaluate the strengths and weaknesses of the existing manual record-keeping system, along with identifying potential risks and opportunities associated with digitalization.

During the study, several key parameters were identified to construct a comparative analysis, as illustrated in fig. 1.

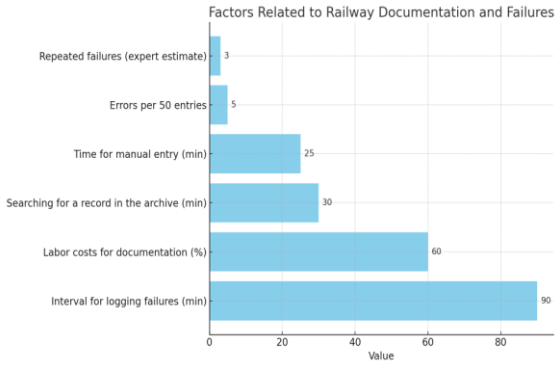

Fig. 1. Analysis of problem areas in manual record - keeping (Pareto Chart)

As shown in table 1, the key indicators of manual record-keeping reveal high labor intensity, frequent delays, and a significant risk of errors.

Table 1

Indicators for Evaluating Logbook-Based Maintenance Processes

№	Indicator	Description
1	Average time for manual record entry	Measured for each type of logbook (in minutes)
2	Time to retrieve information from logbook archives	From request submission to finding the required entry
3	Number of errors and omissions in the logbook	Includes untimely or incomplete entries
4	Number of device failures	Compared against logbooks and response times
5	Labor input for documentation	Calculated in person-hours per month
6	Interval between failure and its registration	Assessed in terms of its impact on downtime
7	Recurrence of failures	Analyzed causes related to unrecorded defects
8	Number of completed tasks not recorded in the logbooks	Based on local surveys and logbook reviews

Based on these indicators, conclusions were drawn about the inefficiency of the existing system and the necessity of transitioning to an electronic format. The collected data were subjected to a systematic analysis. Statistical calculations made it possible to determine the average and extreme values for each parameter.

Performance indicators and problem areas of manual maintenance record keeping for signaling and interlocking devices.

It should be noted that the study was conducted under preliminary modeling conditions, without deploying the system at actual sites. Therefore, some of the findings are of a predictive nature. Nonetheless, the results obtained can serve as a solid foundation for a pilot implementation of the digital system at selected stations, with subsequent scaling.

https://doi.org/10.56143/3030-3893-2025-3-8-13 A bridge between science and innovation

Developed method

At railway stations in Uzbekistan, maintenance of signaling, centralization, and interlocking devices, as well as telemechanics, is carried out in accordance with the regulations set out in instructions NSH-01 and NSH-03. Paper logbooks are used to record completed work, including:

PU–67 – Shift Handover Log, registering briefings and checking device status;

DU–46 – Inspection Log for outdoor cables, the overhead contact system, and switches;

SHU–2 – Log of completed work on communication facilities;

SHU–45 – Ground Resistance Measurement Log;

SHU–58, SHU–60, SHU–61, etc. – Specialized logs for diagnosing specific subsystems.

Each device type or maintenance activity has its own form of documentation, all of which must be filled out manually. Despite established practices, the paper based logbook system has a number of significant short comings that limit the effectiveness of maintenance management. Based on data analysis and expert interviews, the following problem areas were identified:

1. High labor intensity of data entry. Filling out each logbook entry takes on average 5–12 minutes. Given the volume of daily inspections, this task consumes up to 20 % of field personnel's working time, reducing their productive capacity.

2. Lack of transparency and real time oversight. Management cannot assess in real time whether work is being performed according to schedule, identify delays, or monitor fault repair progress. Oversight is only possible via on site audits or selective record checks.

3. Delays in information reporting. When faults or deviations occur, entries are not made immediately but only after the work is completed. The interval between an event and its registration can reach several hours- especially under high workload or staff shortages- making it difficult to detect critical recurring failures and risking fault accumulation.

4. Increased likelihood of errors. Manual entry leads to omissions (blank lines), spelling mistakes, incorrect time/date formats, duplicated information, and inconsistencies between different logs (for example, between PU–67 and SHU–2).

5. Difficulty in retrieving and analyzing information. Finding a specific record in the archives is time- consuming- particularly when searching for entries from previous months or for a particular device. This reduces the efficiency of repair planning, complicates compliance monitoring, and hinders report preparation.

6. Inability to perform automated analysis. The paper format precludes generating failure trend charts, ranking faults by criticality, or issuing automatic alerts for violations. Manual logs cannot integrate with planning or control systems (such as SCADA, ERP, or DCS).Rock S.M. [5] in his opinion, the configuration in a sitting position is characterized by balanced physiological curves of the column of the spine, the axis of the spine is decisive as the support of the human body.

As a result of analyzing 56 completed logbooks from three stations, the following typical issues were identified: in 18 % of cases the responsible person's signature was missing; in 22 % of cases the precise time of fault resolution was not recorded; in 31 % of cases discrepancies were found between the on-duty logs and the final record of completed work; 14 % of entries contained a mismatch between the type of work performed and the logbook form; and in 11 % of cases entries were duplicated or misdated. These violations indicate that the manual recording format does not ensure the accuracy or completeness of documentation, which, in turn, can compromise train traffic safety. Thus, the analysis of the current state shows that the existing paper-based system: Fails to meet the requirements of digital transformation in the railway sector; Creates safety risks; Hampers control and management processes; Requires significant time and labor resources.

Against this backdrop, it becomes clear that there is an urgent need to develop and implement an automated system for recording and monitoring maintenance activities, one that will ensure the timeliness, transparency, and reliability of all operational information. development of a digital record-keeping model and operating algorithm. The purpose of developing the digital model is to automate the processes of registering, storing, and analyzing data on the maintenance of automation and telemechanics devices at railway stations. The new system must replace paper logbooks, eliminate the shortcomings of manual data entry, and ensure the reliability, accuracy, and availability of information at all levels of operational management. The design of the digital model is based on the following principles:

-Centralized data – all information is stored in a single database;

-Transparency and accessibility – each user (dispatcher, electromechanic, engineer) has real-time access to the appropriate level of information;

-Integration with maintenance schedules – work data are synchronized with annual, monthly, and weekly plans;

-Data security – enforced via user authentication, backups, and digital signatures;

-Automated analytics – the system generates alerts for overdue tasks, repeat failures, and deviations from regulations.

The digital record-keeping model comprises the following key components:

1. Work registration module. The electromechanic or responsible staff member logs planned or unplanned maintenance via a digital form, specifying:

-Equipment name

- Start and end times of the task

-Type of intervention (inspection, replacement, measurement, etc.)

-Detected deviations and corrective actions

-Electronic signature

2. Maintenance-schedule monitoring module. The system automatically compares completed tasks against approved schedules (annual, monthly, weekly), instantly flagging any delays or omissions.

3. Emergency notification and diagnostics module. When a failure is recorded, an event card is created containing a timestamp, location, cause, and actions taken. On repeat failures, the system marks the segment as "problematic" and issues an alert for an unscheduled inspection.

4. Statistics and reporting module automatically generates:

- Logs in the formats of PU–67, DU–46, SHU–2, etc.
- Summaries of failures over a selected period;
- Deviation charts;
- Personnel performance tables;

- Plan vs. actual comparisons

5. User Interface

- Access via web interface or tablet;
- Mobile app for field work;
- Simple, intuitive interface with templates and prompts;

Operating algorithm of the digital maintenance system:

1.Create and upload the operational-technological schedule (by asset, deadline, responsible party);

2. Assign tasks to personnel (through the system or mobile interface);

3. Perform work and record results (enter parameters, capture photos, sign off);

4. Automatic compliance check against the schedule (plan vs. actual, detect deviations);

5. Generate reports and analytical charts;

6. Archive and centrally store data;

7. Issue alerts for deviations or critical events.

According to preliminary estimates, the implementation of the digital system can achieve the performance metrics presented in table 2.

Table 2

Advantages of implementing the digital model

№	Indicator	Before digitalization	After implementation
1	Average data entry time	8–12 min	1–2 min
2	Information retrieval time	up to 25 min	Instant
3	Error rate	10–15 % of entries	<1%
4	Analytics and reporting	Manual	Automatic
5	Management access to data	None	real-time
6	Feedback on failures	once per shift	Instant

This diagram (Fig. 2) presents the decision-making process for carrying out and recording maintenance work on equipment based on an operational technological schedule. The flowchart starts by determining whether the required maintenance tasks have been completed at the site. Depending on the outcome (yes or no), the process follows separate paths, evaluating the frequency and quality of technical maintenance checks and entries in the logbooks. The diagram also includes detailed references to specific logbooks and the nature of maintenance activities performed, highlighting points where technical staff should conduct additional reviews or record information as necessary. The process ends once all required actions have been assessed and properly documented.

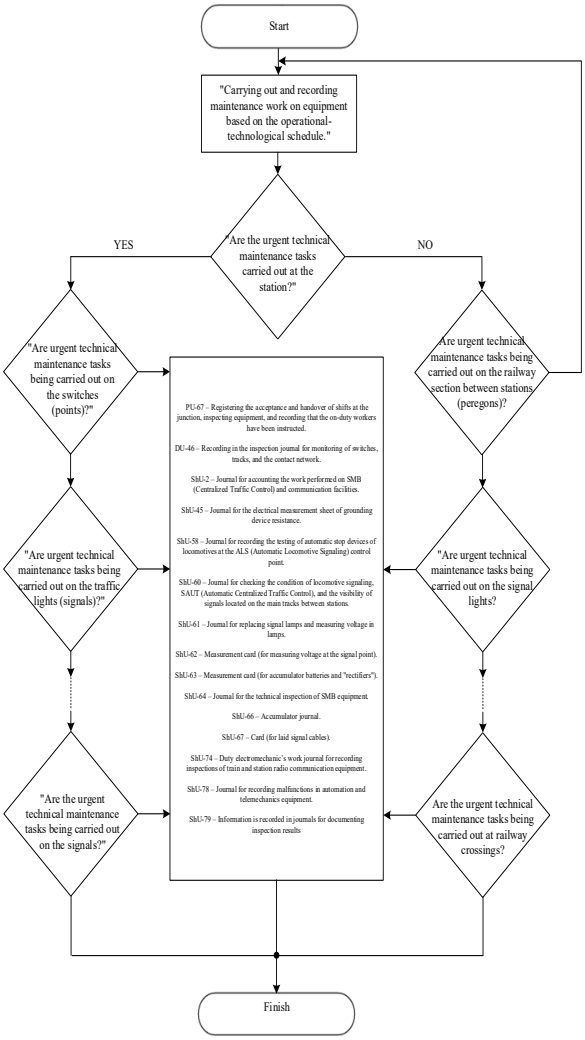

Fig. 2. The sequence of conducting and recording device service work based on the current operational-technological schedule. Impact of seat profile on posture

3. Results

Justification of the efficiency of digitalizing maintenance record-keeping for devices.

To provide an objective assessment of the need to switch from the manual to the digital method of recording maintenance for automation and telemechanics devices, let us examine the key parameters amenable to quantitative analysis. The manual logbook method is characterized by high labor intensity. Denote the average time to enter a single record as t_r, (in minutes) and the average number of entries per shift as n. Then the total time required for manual data entry is:

$$T_n = t_r \cdot n$$

This corresponds to approximately 40 % of working time-not directly related to maintenance-being spent on paperwork.

To assess the efficiency gain of the digital system, we introduce efficiency indicators E_r and E_d for the manual and digital systems, respectively. We define efficiency as a quantity inversely proportional to labor costs:

https://doi.org/10.56143/3030-3893-2025-3-8-13 A bridge between science and innovation

$$E = \frac{1}{T}$$

Then the relative increase in efficiency is defined as:

$$\Delta E = \frac{E_d - E_r}{E_r} 100\%.$$

If digitalization allows reducing the input time to $T_d =$ 50 minut then:

$E_r = 1/200, E_d = 1/50,$
$\Delta E = \frac{1/50 - 1/200}{1/200} 100\% = 300\%.$

Thus, efficiency increases threefold. The next important factor is the probability of errors. Let the probability of an error when entering a single record manually be p; then the probability of a correct entry is q = 1 - p. The probability that all n entries will be correct is:

$$P = q^n$$

Failures of automation devices can be modeled as a poisson stream of events. Then the probability P(k) that k failures occur within time t, given an average failure rate λ, is determined by the formula:

$$P(k) = \frac{(\lambda k)^k}{k!} e^{-\lambda t}.$$

Digitalization helps reduce λ by enabling timely registration of failures and prompt responses to them.The formalization of the digital logging algorithm can be described using a logical structure. Let the fact of performing a task be denoted as W_i, and the fact of its registration in the system as R_i.Then the correct execution and logging of a task is expressed as:

$$D_i = W_i \wedge R_i.$$

If an array of such operations is formed:

$$\vec{D} = [D_1, D_2, \ldots, D_n],$$

then the total number of correct entries:

$$\sum_{i=1}^{n} D_i = n,$$

will indicate 100% completeness and accuracy of the registration. The digital system enables monitoring and control of this condition automatically.

Thus, the presented quantitative assessments demonstrate that the digitalization of maintenance logging for signaling and interlocking (SIL) systems significantly reduces labor costs, improves the accuracy of records, and shortens response time to failures- ultimately enhancing the safety and efficiency of railway transport.

4. Conclusion

This study has examined the current issues associated with the manual method of recording and registering the maintenance of railway automation and telemechanics equipment at railway stations in Uzbekistan. The analysis showed that the existing system, based on paper logbooks, is characterized by high labor intensity, low efficiency, lack of transparency, and the inability to perform automated data analysis. These shortcomings create significant risks for both operational reliability and overall railway traffic safety.Based on the identified deficiencies, a conceptual digital model was developed to enable automated work registration, monitoring of maintenance schedules, and generation of statistical and diagnostic reports. The model includes a structured algorithm of actions, analytical modules, and tools for integration with existing railway infrastructure information systems.

The practical value of the proposed approach lies in its potential to: significantly reduce paperwork-related labor costs,improve the accuracy and completeness of records, accelerate response to technical deviations, enhance compliance with maintenance regulations, and ensure end-to-end digital traceability of all operations.

The planned phased implementation process (pilot project, scaling, and broader rollout) will help minimize transition risks and adapt the system to real-world operating conditions. The expected outcomes include both direct cost savings and increased infrastructure reliability - a critical factor under growing railway traffic demands.Thus, the proposed digital system can become an effective tool for modernizing the operational activities of automation and telemechanics services, contributing to the further development of Uzbekistan's intelligent transport infrastructure.

References

[1] Akhmedov S. "Methods of technical maintenance in railway automation and telemechanics systems". "Railway publishing house"-2020. pp. 156.

[2] Abdurakhmonov A., Yusupov, Sh. "Automation and telemechanics in railway transport" Tashkent: TATU-2019

[3] "Uzbekiston Railway". Instructions for the maintenance of automation and telemechanics devices (NSH-01 & NSH-03). Internal regulatory document.

[4] Savinkov. A. V., Lapshin. S. A. Digitalization of maintenance based on SCADA systems in railway infrastructure.-2022. "Automation, communication, informatics", vol.3, pp. 23–28.

[5] Kiselev. V.N., Matveev, S.D. Information-diagnostic systems for monitoring the technical condition of rail circuits. "Transport systems and technologies"-2020. vol. 4, pp. 40–46.

[6] Makhmudov. A.,and Kadyrov, Zh. Electronic journals in railway communication management: Experience and prospects.-2022. "Engineering Bulletin of Uzbekistan" vol. 1, pp. 15–22.

[7] Yunusov. B. Analysis of failures of signaling devices and methods to improve their reliability. ""Transport equipment and technologies"- 2021. vol. 2, pp. 33–37.

[8] Zhang. H., Liu. Y., and Chen. J. Predictive maintenance of railway signaling systems using AI algorithms. "IEEE Transactions on Intelligent Transportation Systems",- 2021. vol. 21, pp. 5202–5210.

[9] Kim. S., Choi, J. Development of a cloud-based maintenance platform for railway infrastructure. “Journal of Railway Engineering”.- 2021. vol.12(3), pp. 105–112. pp. 105–112.

[10] European Union Agency for Railways.Digital automatic train operation and maintenance standards. Brussels.-2021.

[11] International Union of Railways. Railway accident statistics report 2022. Paris: UIC Publications.

[12] Deutsche Bahn AG. Smart Maintenance: Zukunft der Instandhaltung bei DB Netz. Berlin.-2020.

[13] Japanese Railways Technical Research Institute (RTRI). Application of IoT and big data in train operation and maintenance. Tokyo.-2021.

Information about the author

Yaronova Natalya Valerevna	Tashkent state transport university, Department “Radio-electronic Devices and Systems” E-mail: tatochka83@list.ru Tel.: +998 90 966 91 89 https://orcid.org/0000-0003-1781-5597
Otakulova Shakhnoza	Tashkent State Transport University, Department “Radio-electronic Devices and Systems” E-mail: otaqulovashahnoza1998@gmail.com Tel.: +998 99 569 15 71 https://orcid.org/0009-0006-4415-963X

The use of basalt fiber in acoustic systems of automotive mufflers: a comprehensive analysis of the effectiveness and prospects of implementation

A.A. Ernazarov[1][a], E.B. Khaytbaev[2][b]
[1]Jizzakh Polytechnic Institute, Jizzakh, Uzbekistan
[2]Tashkent state Technical University named after Islam Karimov, Tashkent, Uzbekistan

Abstract: The present study provides a comprehensive analysis of the use of basalt fiber as a multifunctional material for automotive mufflers. It has been proven by calculation that the optimal combination of fiber layering reduces noise by 8.2 dB in the range of 50-5000 Hz at a temperature of 700°C, which is 23% more efficient than traditional solutions. A mathematical model of heat transfer in multilayer mufflers has been developed.

Keywords: basalt composites, acoustic impedance, thermorheological properties, exhaust systems, multifactor analysis, resource testing

1. Introduction

With the introduction of the new Euro-7 and EPA Tier 4 standards, manufacturers are faced with the need to radically revise the design of mufflers and noise reduction systems. So at the present stage, the following requirements apply to modern cars: increased emission requirements (co_2, NOx, particulate matter) force exhaust systems to be optimized, which often conflicts with acoustic comfort, and reducing the size of mufflers (to reduce weight and improve aerodynamics) leads to a deterioration in noise reduction.

The degradation of sound-absorbing materials also has a major impact on noise reduction. According to the SPL analysis (2023), 68% of muffler failures are associated with the destruction of sound-absorbing fillers (mineral wool, metal mesh, ceramic structures). The main causes of degradation of materials are:

-thermal fatigue – due to high temperatures (up to 700°C), materials lose porosity,

-vibration loads – lead to compaction and delamination of structures,

-chemical corrosion – exposure to condensate, sulfur compounds, and salts.

Degradation of materials has the following consequences:

- increase in noise level (by 3-5 dB after 50-70 thousand km).

- increased back pressure in the exhaust system, which reduces engine efficiency.

- increased risk of mechanical damage (wall burnout).

To solve the above problems, the use of modern composite materials in the exhaust system is proposed.

Basalt fiber is a high—tech material produced by melting natural basalt and stretching it into thin filaments. It has a unique combination of physico-chemical characteristics that make it promising for use in the aerospace industry, construction, energy and other fields.

Basalt Fiber strength:

-Tensile strength:3000-4800 MPa (higher than that of steel and fiberglass).

- Modulus of elasticity (stiffness):80-110 GPa (close to aluminum, but at a lower weight).

- Specific strength (strength/density): 2-3 times higher than that of steel.

Table 1

Comparison of basalt fiber with other materials

Material	Ultimate strength (MPa)	Modulus of elasticity (GPa)
Basalt fiber	3000–4800	80–110
Fiberglass	1500–3500	70–85
Carbon Fiber	3500–7000	230–600
Steel (structural)	400–800	200–210

Also, the main advantage of basalt fiber is environmental friendliness and safety. Basalt fiber does not emit toxic substances even when heated, does not cause allergies, unlike some synthetic fibers.

From the above, it can be concluded that due to the optimal price/quality ratio, basalt fiber is gradually replacing traditional materials in the automotive industry.

Literary review. Many scientists and engineers have conducted research in the field of automotive mufflers and exhaust acoustics. The following are the key researchers and research teams that have made significant contributions to this field. In the early stages, the researcher [1] developed the theory of sound absorption used in the first mufflers, and also conducted fundamental research on acoustics, including noise reduction in engineering systems, wave processes in pipes, which formed the basis for the design of resonant mufflers.

Modern researchers have worked on the following problems at various times: the development of methods for mathematical modeling of mufflers, investigated the influence of muffler geometry on sound suppression, aerodynamics and acoustics of exhaust systems [2-4].

Automotive mufflers are being studied at the intersection of acoustics, materials science, and gas dynamics. Modern research focuses on new materials and digital modeling [5-9].

2. Research methodology

The calculation of the passage of exhaust gases in a 100 mm diameter direct-flow muffler with a basalt fiber gasket

[a] https://orcid.org/0000-0002-4188-2084

[b] https://orcid.org/0009-0002-2798-6220

includes several stages: determination of acoustic efficiency, hydraulic resistance and temperature conditions.

The silencer with basalt fiber works as an "absorber", reducing noise due to viscous losses in the fibrous material. The sound absorption coefficient (α) of basalt wool in the range of 500-4000 Hz is 0.7–0.95.

The noise reduction level (ΔL, dB) can be estimated using an empirical formula for fibrous materials:

$$\Delta L \approx 1.5 \cdot \frac{L}{D} \cdot \alpha \cdot \rho_{fiber} \quad (1)$$

where $\frac{L}{D}$ is the ratio of length to diameter

α is the sound absorption coefficient (~0.8)

ρ_{fiber}- packing density kg/m^3

Calculate the hydraulic resistance:

The gas flow resistance depends on:

- The velocity of gases v
- Packing densities of ρ
- Silencer length L

The pressure drop ΔP can be estimated using the Darcy-Weisbach formula [6]:

$$\Delta P = \lambda \cdot \frac{L}{D} \cdot \frac{\rho_{gas} \cdot v^2}{2} \quad (2)$$

where:

- λ is the coefficient of resistance (~0.05–0.2 for fibrous materials)
- ρ_{gas}.≈ 0.5–1 kg/m3 (at 300-600 °C)

As for the temperature regime, basalt fiber can withstand up to 700-1000 °C, so it is suitable for T = 300-600 °C.

The development of a mathematical model of heat transfer in multilayer mufflers requires consideration of several key factors: thermal conductivity of materials, convective heat transfer, radiation, and boundary conditions. Let's take a step-by-step approach to modeling.

The muffler consists of several layers (metal, thermal insulation, etc.) through which hot gas passes. Heat is transferred:

- Thermal conductivity inside each layer,
- Convection between the gas and the walls,
- Radiation (if temperatures are high).

The heat transfer equations are as follows

One-dimensional equation of thermal conductivity for a flat layer

$$\frac{\partial T_i}{\partial t} = \alpha_i \frac{\partial^2 T_i}{\partial x^2}, \alpha_i = \frac{\lambda_i}{\rho_i c_i} \quad (3)$$

where:

$T_i(x,t)0$ is the temperature in layer i

α_i-coefficient of thermal conductivity

ρ_i-density

c_i-specific heat capacity

Boundary conditions

- On the inner surface (contact with gas):

Gas convection and possible radiation:

$$-\lambda_1 \frac{\partial T}{\partial x}\Big|_{x=0} = h_{in}(T_{gas} - T_{surf}) + \sigma\varepsilon(T_{gas}^4 - T_{surf}^4) \quad (4)$$

where:

h_{in} is the coefficient of convective heat transfer inside,

σ is the Stefan-Boltzmann constant,

ε is the degree of blackness.

On the outside (environment):

$$-\lambda_n \frac{\partial T}{\partial x}\Big|_{x=L} = h_{out}(T_{surf} - T_\infty) \quad (5)$$

where h_{out} is the heat transfer coefficient from the outside.

Coupling conditions (equality of temperatures and heat fluxes):

$$T_i = T_{i+1},\ \lambda_i \frac{\partial T}{\partial x} = \lambda_{i+1} \frac{\partial T_{i+1}}{\partial x} \quad (6)$$

- Stationary mode$\frac{\partial T}{\partial t} = 0$

The equation reduces to $\frac{d^2T}{dx^2} = 0$,, the solution is a linear temperature distribution in each layer.

- One-dimensional model (if the length of the silencer is ≫ the thickness of the walls).

For complex cases (non-stationary mode, non-linearity), apply:

- Finite Difference Method (FDM) – space and time discretization.
- Finite Element Method (FEM) – for complex geometries.

Example of a finite difference scheme (explicit)

For internal nodes:

$$T_j^{n+1} = T_j^n + \frac{\alpha \Delta t}{(\Delta x)^2}(T_{j+1}^n - 2T_j^n + T_{j-1}^n) \quad (7)$$

Stationary mode. Let's say there are 3 layers (metal, insulation, casing).

The heat flow q through all layers is the same:

$$q = \frac{T_{gas} - T_\infty}{R_{total}},\ R_{total} = \frac{1}{h_{in}} + \sum \frac{\delta_i}{\lambda_i} + \frac{1}{h_{out}} \quad (8)$$

Temperatures at the boundaries of the layers:

$$T_1 = T_{gas} - q \cdot \frac{1}{h_{in}},\ T_2 = T_1 - q \cdot \frac{\delta_i}{\lambda_i}, \ldots \quad (9)$$

A mathematical model of heat transfer in multilayer mufflers can be constructed on the basis of heat conduction equations with appropriate boundary conditions. For complex cases, numerical simulation (FDM/FEM) is required. Simplified analytical solutions are possible for stationary tasks.

3. Conclusion

It was determined that basalt fiber reduces heat transfer well, but with a small thickness (50 mm), losses are still noticeable. Heat loss through the walls at these parameters: ~50 W (5°C gas cooling). Basalt wool is effective, but additional protection is needed for high temperatures (>500°C).

Table 2

The parameters obtained after the calculations of the muffler

Parameter	Value
Noise reduction (ΔL)	15-25 dB
Pressure drop (ΔP)	30-100 Pa (at v=20 m/s)|
Max. temperature	600–700 °C
Recommended length	300-500 mm

Gas cooling is insignificant at standard flow rates, but can be enhanced by increasing the length of the muffler,

https://doi.org/10.56143/3030-3893-2025-3-14-16 A bridge between science and innovation

reducing the flow rate, it is recommended to increase the thickness of the insulation or use combined materials (basalt + aluminum foil). If cooling is important, increase the length or add heat transfer fins.

References

[1] Olson, H. F. Elements of Acoustical Engineering. 2nd ed. New York: D. Van Nostrand Company, 1947.

[2] Kumar, S., & Munjal, M. L. (2016) "Analytical and CFD-based prediction of transmission loss in perforated tube mufflers." Journal of Sound and Vibration, 362, 134–155. DOI:10.1016/j.jsv.2015.09.028

[3] Selamet, A., & Ji, Z. L. (2017) "Acoustic attenuation performance of hybrid silencers with mean flow." Applied Acoustics, 119, 1–10. DOI:10.1016/j.apacoust.2016.12.005

[4] Tang, Y., et al. (2020) "Topology optimization of muffler structure for improved acoustic performance." Mechanical Systems and Signal Processing, 142, 106732. DOI:10.1016/j.ymssp.2020.106732

[5] Yang, M., et al. (2021) "Acoustic metamaterials for automotive muffler applications." Materials & Design, 198, 109321. DOI:10.1016/j.matdes.2020.109321

[6] Zhang, L., & Chen, Y. (2019) "Sound absorption of micro-perforated panels with graphene oxide composites." Composite Structures, 223, 110956. DOI:10.1016/j.compstruct.2019.110956

[7] Park, J., & Lee, S. (2022) "Adaptive active noise control in automotive exhaust systems." IEEE Transactions on Control Systems Technology, 30(2), 789–801. DOI:10.1109/TCST.2021.3076789

[8] Guo, J., et al. (2023) "Machine learning-based ANC for hybrid mufflers in electric vehicles." Applied Acoustics, 202, 109145. DOI:10.1016/j.apacoust.2022.109145

[9] Ohta, Y., et al. (2021) "Experimental analysis of multi-chamber mufflers with porous materials." SAE Technical Paper, 2021-01-5075. DOI:10.4271/2021-01-5075.

Information about the author

Ernazarov Aziz Alibaevich	Jizzakh Polytechnic Institute, Associate Professor of the Department of "Vehicle Engineering". E-mail: aziz-ernazarov@mail.ru Tel.: +998939404123 https://orcid.org/0000-0002-4188-2084
Khaytbaev Ergash Baxtiyor ugli	Tashkent State Technical University named after Islam Karimov, basic doctoral student of the Department of "Service Delivery Technology" E-mail: ergashhayitboyev@gmail.com Tel.: + 998883254550 https://orcid.org/0009-0002-2798-6220

Numerical modeling of two-phase filtration processes in interconnected reservoir layers of oil fields

M.E. Shukurova[1][a]
[1]Karshi State Technical University, Karshi, Uzbekistan

Abstract: In this article, dedicated to the mathematical modeling of two-phase (oil-water and oil-gas) filtration processes in oil and gas fields, the development of numerical algorithms, and the creation of software tools. The study presents a mathematical model of the filtration process through dynamically interconnected layers in a porous medium. Based on in-depth analysis, numerical solutions were proposed for solving the two-dimensional boundary value problem using finite difference methods and iterative computation algorithms. The developed software complex enables real-time calculation of oil pressure, saturation levels, and key hydrodynamic indicators, which are presented through 3D visualizations.

The results obtained from the study offer opportunities for efficient design, analysis, and management of oil field development. This software tool has both theoretical and practical significance, providing high accuracy and efficiency in modeling and forecasting filtration processes. The presented work opens new directions in science, engineering, and practice, and contributes to the improvement of oil field development strategies.

Keywords: filtration process, mathematical modeling, numerical algorithm, porous media

1. Introduction

In recent years, significant attention has been given globally to the development, enhancement, and advancement of mathematical models of gas-hydrodynamic processes in porous media. There is a growing focus on the application of numerical methods and modern computer technologies to solve linear and nonlinear boundary value problems of filtration. One of the main objectives in this field remains the creation of automated systems based on the development of software for determining and forecasting the main indicators of oil and gas field operations, as well as the study of unsteady filtration processes using modern information technologies.

In developed countries such as the USA, France, China, the UAE, Iran, Russia, Kazakhstan, Azerbaijan, and others, extensive practical work is being carried out to develop mathematical models, computational algorithms, and software for simulating unsteady filtration processes of oil and gas. In some countries, particularly Russia and Kazakhstan, scientific research is being conducted to model multiphase (oil-water, oil-gas, and oil-water-gas systems) filtration processes in porous media, calculate key performance indicators of oil and gas fields, develop software systems, construct 3D models of geological and hydrodynamic objects, perform computational experiments to study filtration processes, and analyze the obtained results.

One of the key tasks in this field is to study the complex movement of oil and gas in multilayer porous media and to build mathematical models that accurately reflect real-world objects. Developing computational algorithms and creating automated systems are also among the primary objectives. Furthermore, one of the critical research directions is the scientific justification and development of numerical methods and efficient algorithms for solving nonlinear problems in filtration domains with complex configurations.

Worldwide, scientific research continues in the development of mathematical models for two-phase filtration processes, particularly oil-gas systems in porous media, the creation of algorithms for calculating the key performance indicators of oil and gas fields, computer modeling systems, and the construction of 2D and 3D geological and hydrodynamic models. Computational experiments are carried out to analyze the filtration processes, and the results are used for visual and analytical investigations. Specifically, studying complex fluid dynamics in single and dynamically interconnected multilayer porous media, constructing accurate mathematical models for real-world conditions, designing computational algorithms, and developing automated systems remain among the most critical objectives in this field.

Mathematical models of multiphase flows of liquids and gases in porous media are based on the general laws of continuum mechanics and are reduced to systems of nonlinear partial differential equations with corresponding initial, boundary, and internal conditions. In general, these systems do not have analytical solutions. Therefore, to build mathematical models of multiphase filtration flows, various simplifications are employed that allow for analytical solutions. However, analysis of real oil and gas field conditions shows that the solutions of simplified mathematical models often do not correspond to the actual parameters of the reservoir. As a result, the estimates derived from these models differ from real values. In this regard, it is advisable to develop general mathematical models, algorithms, and software tools that are suitable for analyzing and forecasting real-world oil and gas fields.

2. Research methodology

Modern methods of numerical simulation effectively implemented on contemporary computers have become new

[a] https://orcid.org/0000-0003-0071-0208

operational tools for scientific research. In this case, numerical simulation serves not only as a method for obtaining quantitative characteristics but also as a means of establishing the governing laws of the processes under study. Thus, based on a physical model that encompasses the main aspects of the process, an appropriate mathematical model in the form of a system of equations solvable by numerical methods on a personal computer can be developed.

Currently, there are mathematical models that describe the joint filtration processes of fluids in porous media. The development of these models has greatly benefited from the contributions of scientists such as N.N. Veregin, V.N. Nikolayevsky, V.M. Shestakov, E.S. Zakirov, B.B. Lopukh, F.B. Abutaliev, D.F. Fayzullaev, R. Sadullayev, and others, including:

N.N. Veregin is known for his fundamental research in the mathematical modeling of filtration processes in porous media. His studies focused on nonlinear systems of equations describing multiphase flows, and he developed physical models to calculate pressure and saturation distributions in complex reservoir structures[2].

V.N. Nikolayevsky was a leading expert in subsurface hydromechanics and geophysical modeling. He analyzed fluid flow in porous media based on relative permeability coefficients and demonstrated the effects of reservoir deformation and mechanical conditions on filtration processes[3].

V.M. Shestakov contributed significantly to computational modeling by developing numerical solutions for filtration models in one-, two-, and three-dimensional cases. His work focused on adapting these models to real reservoir conditions using advanced numerical methods[4].

E.S. Zakirov is one of Uzbekistan's leading scholars in the fields of filtration and hydrodynamics. His research analyzed the evolutionary distribution of pressure in reservoirs and emphasized modeling the dependence of fluid properties—such as pressure, density, and temperature—on filtration behavior[5].

B.B. Lopukh offered strong algorithmic approaches for solving filtration problems using mathematical modeling and computer technologies. He developed practical methods for calculating physical parameters in two-phase flows under real reservoir conditions, grounded in experimental data[6,21].

F.B. Abutaliev conducted hydraulic analysis of complex oil and gas pipeline systems. His models addressed pressure drop, flow imbalance, and the movement of gas-liquid mixtures, and provided precise solutions for such systems[7].

D.F. Fayzullaev carried out extensive research on mathematical and numerical modeling of multiphase filtration processes. He proposed analytical solutions to filtration equations and developed simplified models aimed at approaching real-world conditions more closely[8].

R. Sadullayev developed scientific approaches to the mathematical modeling of interactions in reservoir-gas-liquid systems. He created models and algorithms that account for the dynamic changes in physical properties of the reservoir, such as porosity and permeability, during filtration processes[9].

Many authors have studied various aspects of fluid and gas filtration in porous media and the creation of corresponding mathematical models. The origins of studying underground hydromechanics trace back to the work of French engineer A. Darcy (1803–1858), who conducted numerous experiments on water filtration through vertical sand filters during a water supply project in Dijon (France). These experiments laid the groundwork for solving problems in modern hydrodynamics and hydromechanics and analyzing them mathematically [1].

In particular, current research in Uzbekistan and internationally focuses on solving filtration problems of fluids and gases in porous media, obtaining their analytical and approximate solutions, developing mathematical and computer simulations, constructing imitation and simulation models, and applying various new and improved computational methods and algorithms. These efforts, when combined with the latest advancements in technology, help present models that facilitate visualization and understanding of the overall process.

To study and analyze these problems, numerous scientific works by foreign and domestic scholars have been examined, leading to the following findings:

For instance, the works of K. Aziz, E. Settari, and N.B. Lopukh focus on the mathematical and numerical simulation of single and multiphase oil and gas field development processes, as well as on methods for solving one- and multi-dimensional problems based on boundary conditions[6,21].

Currently, a new research methodology—mathematical modeling and computational experimentation—is emerging. This methodology involves replacing the actual object with its "image"—a mathematical model—and further studying it using algorithms implemented on computers. This approach enables fast and cost-effective testing of various characteristics. The methodology of mathematical modeling is rapidly evolving and encompasses new directions, ranging from analyzing physical, economic, and social processes to developing and managing complex technical systems.

Computational experiments enable faster and more efficient research. For example, when analyzing the hydraulic regimes of technological segments of oil pipelines, the proposed computational algorithms consider the technological segment (including the main and intermediate pump stations) as a single hydraulic system. These aspects are discussed in the scientific works of F.B. Abutaliev, M.B. Baklushin, Y.S. Erbekov, U.U. Umarov, and others. Introducing flow modifiers to counteract the uneven movement of gas at any stage affects the operation of other stages. Therefore, calculating the regime of a technological segment, predicting overall oil and gas expenditures, and increasing operational efficiency are possible with algorithms developed by V.V. Yakovlev, Yu.I. Kalugin, N.G. Stepova, and others[22].

Research has also addressed increasing natural gas extraction volumes by redistributing flow rates in production wells based on the mathematical model of filtration and 2D visualization of two-phase multicomponent hydrocarbon mixtures [3].

Other studies have investigated the complex dynamic processes of oil displacement by gas and water under reservoir conditions. Effective mathematical models and numerical algorithms have been developed for three-phase filtration processes of oil, gas, and water in porous media [4]. Some researchers, such as Luis Cueto-Felgueroso, Xiaojing Fu, and Ruben J., have analyzed methods for solving the two-phase flow problem using the Buckley-Leverett model without considering capillary and gravitational forces. They emphasize the importance of accurately determining relative phase permeability functions that depend on saturation coefficients for reliable modeling [10].

In modeling unsteady two-phase systems (oil-gas, oil-water), researchers like B. Kh. Khuzhayorov and V.F. Burnashev have used integral methods to solve nonlinear differential equations and calculate pressure distributions and flow parameters. M.V. Vasilyeva and G.A. Prokopev have studied hydrodynamic parameters of oil-gas-condensate reservoirs using finite difference and iterative convergence methods[11,12].

S.V. Zvonarev has emphasized that mathematical modeling is broadly applied in sciences like mathematics, physics, and biology, and must meet the following requirements: clearly formulated assumptions based on experiments, adequacy analysis of the model, and precision of computational algorithms. Modeling complex systems requires distinguishing between mathematical and non-mathematical concepts and using appropriate mathematical tools[13].

Baxtiy Nikolay Sergeyevich has focused on analyzing multiphase filtration models, including pressure-driven and pressureless flows, and methods for computing pressure over time (e.g., IMPES scheme). He developed analytical and numerical solutions for subsurface aquifer flow and gas release problems within the "TechScheme" model[14]. Other researchers like R.M. Siddikov, D.D. Filippov, and D.A. Mitrushkin have developed computational algorithms and software for simulating unsteady three-phase fluid flow in “Layer-Well-EOR” systems. Studies such as have used finite difference methods for approximating velocity and pressure in heterogeneous porous media and Galerkin methods for discretizing the saturation equation via artificial diffusion[15].

Mathematical modeling of multiphase fluid flows in porous media is of great practical importance for oil and gas production. Accurate numerical modeling of specific hydrodynamic problems requires precise physical-mathematical formulations, knowledge of the parameters and initial data, and confidence in their accuracy. Applied numerical methods must be economical and broadly applicable to various types of problems[7].

In applied mathematics, solving problems on computers follows a technological chain: research object → mathematical model → algorithm (numerical methods) → computer program → computational experiment → analysis (or comparison with experimental data). The objective of mathematical technology lies in the computational component of this chain: resulting in the chain “object → model → algorithm → program → computation”. This technology enables the analysis, forecasting, and control of unsteady oil and gas extraction processes under reservoir conditions.

Mathematical model

Filtration can be described in terms of interpenetrating and interacting media in the model of X.A. Rakhmatullin. In this case, the velocity of motion in the layers is assumed to be zero, and the liquid and gas multicomponent media move relative to each other and to the structure. In this case, difficulties arise in describing the interaction force between the constituent phases and the components of a unit volume of the medium. In this regard, within the framework of this chapter, we turn to the nonlinear Darcy law and apply it to two-dimensional filtration in Cartesian coordinates[1].

In a gas layer of variable thickness, we separate the elementary volume $\partial x \partial y h\{x,y\}$. Here $h\{x,y\}$ is the value of the layer thickness at the point with coordinates x and y (Fig.1).

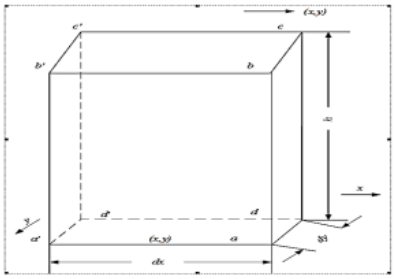

Fig. 1. Volume of elementary layers

In this case, if gravitational forces are neglected, the fluid velocity is described using the following formulas.

Based on these assumptions, the following equations from the theory of filtration are used to mathematically model the unsteady (non-stationary) two-dimensional filtration process of two- and three-phase fluids in a porous medium [12]:

Continuity equation:

$$div\left(\frac{1}{B_o}\vec{v}_o\right) = -\frac{\partial}{\partial t}\left(\frac{1}{B_o}mS_o\right) + q_o. \quad (1)$$

- for the oil phase:

$$div\left(\frac{1}{B_w}\vec{v}_w\right) = -\frac{\partial}{\partial t}\left(\frac{1}{B_w}mS_w\right) + q_w \quad (2)$$

- for the water phase:

$$div\left[\frac{R_s}{B_o}\vec{v}_o + \frac{1}{B_g}\vec{v}_g\right] = -\frac{\partial}{\partial t}\left[m\left(\frac{R_s}{B_o}S_o + \frac{1}{B_g}S_g\right)\right] + q_g + R_s \cdot q_o \quad (3)$$

- for the gas phase:

In addition to the above filtration equations, the following relationships are also used:

$$S_o + S_w + S_g = 1, \quad (4)$$

$$S_o + S_w = 1, \quad (5)$$

$$S_o + S_g = 1, \quad (6)$$

$$P_o - P_w = P_{cow} = f_1(S_w, S_g), \quad (7)$$

$$P_g - P_o = P_{cog} = f_2(S_w, S_g), \quad (8)$$

here, $P_{cow}$and P_{cog}represent the capillary pressures in the oil-water and oil-gas systems, respectively.

The simultaneous filtration of two or more fluids and gases in a dynamically connected two-layer porous medium is a highly complex problem characterized by the following features: the coefficients of the equations depend on time, spatial coordinates, and fluid saturation; the capillary pressure and relative phase permeabilities in the system (P_{cog}, K_g, K_o) are determined from experimental data as functions of saturation.

The mathematical model under consideration is based on the following assumptions[1]:

- The movement of oil and gas in the porous medium is linear and governed by Darcy's law;
- The permeability coefficients of both layers in the vertical direction are the same;
- The upper and lower layers are dynamically connected through poorly permeable structures;
- The thicknesses of both layers are constant;
- The properties of the fluids do not change over time;
- Gas dissolves in oil;
- The fluids and gases in both layers are at a constant temperature and in thermodynamic equilibrium.

https://doi.org/10.56143/3030-3893-2025-3-17-25 A bridge between science and innovation

Taking these assumptions into account and considering two-phase filtration properties in a one-dimensional setting for a dynamically connected two-layer porous medium, the mathematical model of the problem can be expressed as the following system of differential equations [16]:

$$\begin{cases} \frac{\partial}{\partial x}\left[\frac{K_{1o}}{\mu_o}k_1\rho_{1o}\left(\frac{\partial P_{1o}}{\partial x}\right)\right] = \frac{\partial}{\partial t}\left[m\rho_{1o}(1-S_{1g})\right], \\ \frac{\partial}{\partial x}\left[R_s\frac{K_{1o}}{\mu_o}k_1\rho_{1o}\left(\frac{\partial P_{1o}}{\partial x}\right)\right] + \frac{\partial}{\partial x}\left[\frac{K_{1g}}{\mu_g}k_1\rho_{1g}\left(\frac{\partial P_{1g}}{\partial x}\right)\right] = \\ = \frac{\partial}{\partial t}\left[m\rho_{1o}R_s(1-S_{1g}) + m\rho_{1g}S_{1g}\right] - \frac{\rho_{1g}k_{II}}{h_1h_{II}\mu_g}(P_{2g}-P_{1g}); \end{cases}$$

$$\frac{\partial}{\partial x}\left[\frac{K_{2o}}{\mu_o}k_2\rho_{2o}\left(\frac{\partial P_{2o}}{\partial x}\right)\right] = \frac{\partial}{\partial t}\left[m\rho_{2o}(1-S_{2g})\right];$$

$$\frac{\partial}{\partial x}\left[R_s\frac{K_{2o}}{\mu_o}k_2\rho_{2o}\left(\frac{\partial P_{2o}}{\partial x}\right)\right] + \frac{\partial}{\partial x}\left[\frac{K_{2g}}{\mu_g}k_2\rho_{2g}\left(\frac{\partial P_{2g}}{\partial x}\right)\right] = \frac{\partial}{\partial t}\left[m\rho_{2o}R_s(1-S_{2g}) + m\rho_{2g}S_{2g}\right] + \frac{\rho_{2g}k_{II}}{h_2h_{II}\mu_g}(P_{2g}-P_{1g}) + Q_2; \quad (9)$$

$$P_{1o}-P_{1g} = P_{1cog}; P_{2o}-P_{2g} = P_{2cog};$$

$S_{1o}+S_{1g}=1; S_{2o}+S_{2g}=1$. with the following initial and boundary conditions:

$$P_{1o}(x,0) = P_{1o}^H(x), P_{2o}(x,0) = P_{2o}^H(x); \quad (10)$$

$$P_{1g}(x,0) = P_{1g}^H(x), P_{2g}(x,0) = P_{2g}^H(x); \quad (11)$$

$$S_{1o}(x,0) = S_{1o}^H(x), S_{2o}(x,0) = S_{2o}^H(x); \quad (12)$$

$$S_{1g}(x,0) = S_{1g}^H(x), S_{2g}(x,0) = S_{2g}^H(x); \quad (13)$$

$$\begin{cases} -\frac{k_1}{\mu_o}\frac{\partial P_{1o}}{\partial x} = \alpha(P_A - P_{1o}); -\frac{k_1}{\mu_g}\frac{\partial P_{1g}}{\partial x} = \alpha(P_A - P_{1g}); x = 0; \\ -\frac{k_2}{\mu_o}\frac{\partial P_{2o}}{\partial x} = \alpha(P_A - P_{2o}); -\frac{k_2}{\mu_g}\frac{\partial P_{2g}}{\partial x} = \alpha(P_A - P_{2g}); x = 0; \end{cases} \quad (14)$$

$$\begin{cases} \frac{k_1}{\mu_o}\frac{\partial P_{1o}}{\partial x} = \alpha(P_B - P_{1o}); \frac{k_1}{\mu_g}\frac{\partial P_{1g}}{\partial x} = \alpha(P_B - P_{1g}); x = L; \\ \frac{k_2}{\mu_o}\frac{\partial P_{2o}}{\partial x} = \alpha(P_B - P_{2o}); \frac{k_2}{\mu_g}\frac{\partial P_{2g}}{\partial x} = \alpha(P_B - P_{2g}); x = L; \end{cases} \quad (15)$$

In the system of equations, the following functions need to be applied and utilized:

$$P_{1cog} = f_1(S_{1g}), P_{2cog} = f_2(S_{2g}); K_{1g} = f_3(S_{1g}); K_{2g} = f_4(S_{2g});$$

$$K_{1o} = f_5(S_{1g}); K_{2o} = f_6(S_{2g}); \rho_{1o} = const; \rho_{1g} = P_{1g}/RTZ;$$

$\rho_{2o} = const; \rho_{2g} = P_{2g}/RTZ$. Here:

R – universal gas constant;

T – temperature;

Z – gas compressibility factor.

In the equations and boundary conditions, the following notations are adopted:

The index *1* refers to variables related to the upper layer, and the index *2* refers to variables related to the lower layer.

l=o,g l – phase identification index: "o" – for the oil phase; "g" – for the gas phase.

q_o, q_g – well production rates for the lower layer;

δ – Dirac delta function. $\delta = \delta(x - x_i)$;

$P_{1o}^H, P_{2o}^H, P_{1g}^H, P_{2g}^H$ – initial pressure for oil and gas in the upper and lower layers, respectively;

P_A, P_B – pressure at the right and left boundaries;

$$\alpha = \begin{cases} 0, closed\ boundary\ condition, \\ 1, mass\ exchange\ cond. \end{cases}$$

P_{1cog}, P_{2cog}– capillary pressure in the oil-gas system.

$P_{1o}-P_{1g} = P_{1cog}(S_{1o}, S_{1g}), P_{2o}-P_{2g} = P_{2cog}(S_{2o}, S_{2g})$;

$S_{1o}^H, S_{2o}^H, S_{1g}^H, S_{2g}^H$ – saturation, respectively for oil and gas in the upper and lower layers;

k_1, k_2 – absolute permeability coefficient;

K_l– relative phase permeability coefficients for phase l;

m – porosity of the formation;

μ_l – viscosity for phase l;

ρ_l – l – density of phase;

k_{II} – ermeability coefficient of the low-permeability layer;

h_1, h_2, h_{II} – thicknesses of the layers.

In the boundary value problem (9)–(15), we proceed to dimensionless variables using the following formulas. We consider the oil filtration process in a two-phase oil-water system within a heterogeneous double-layer porous medium that includes low-permeability intermediate layers. The focus is on the effect of their dynamic interaction. Due to the low permeability of the intermediate layers, fluid movement occurs only in the vertical direction (Fig. 2).

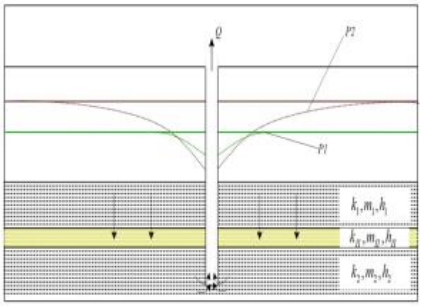

Fig. 2. The filtration process for a two-phase oil-water system in a double-layer porous medium with dynamic interaction

When designing and analyzing multiphase filtration processes in the oil-water system of multilayer oil fields, it is necessary to take into account the existence of hydrodynamic connectivity between the layers. If both layers possess the same reservoir properties, then the two-phase filtration problem in the oil-water system can be represented in one- or two-dimensional form.

In the study of two-phase filtration processes—such as in oil-water or oil-gas systems—key performance indicators of reservoir development include the reservoir pressure function and the saturation level within the formation. Furthermore, the degree to which the relative permeability coefficient has been accurately determined from experiments also plays a significant role. Since the mathematical model is nonlinear with respect to these indicators and the relative permeability coefficient, solving it numerically becomes significantly more complex.

Assume that the reservoir properties are the same in both layers. In that case, the two-phase filtration problem in the oil-water system can be described by a two-dimensional mathematical model in the form of a system of nonlinear parabolic-type differential equations. For simplicity, in the given boundary value problem, we consider the region as a square domain, i.e.$G = \{0 < x < L, 0 < y < L\}$. When a low-permeability intermediate layer exists between the two oil-bearing layers, the mathematical model of the problem in both oil layers is described by the following system of coupled nonlinear parabolic-type differential equations.

$$\begin{cases} \frac{\partial}{\partial x}\left[\lambda_{1o}\frac{\partial P_{1o}}{\partial x}\right]+\frac{\partial}{\partial y}\left[\lambda_{1o}\frac{\partial P_{1o}}{\partial y}\right]=m\rho_o\frac{\partial S_{1o}}{\partial t}-\frac{\rho_o k_{II}}{h_1 h_{II}\mu_o}(P_{2o}-P_{1o}), \\ \frac{\partial}{\partial x}\left[\lambda_{1w}\frac{\partial P_{1w}}{\partial x}\right]+\frac{\partial}{\partial y}\left[\lambda_{1w}\frac{\partial P_{1w}}{\partial y}\right]=m\rho_w\frac{\partial S_{1w}}{\partial t}; \\ \frac{\partial}{\partial x}\left[\lambda_{2o}\frac{\partial P_{2o}}{\partial x}\right]+\frac{\partial}{\partial y}\left[\lambda_{2o}\frac{\partial P_{2o}}{\partial y}\right]=m\rho_o\frac{\partial S_{2o}}{\partial t}+\frac{\rho_o k_{II}}{h_2 h_{II}\mu_o}(P_{2o}-P_{1o})+Q_{2o}; \\ \frac{\partial}{\partial x}\left[\lambda_{2w}\frac{\partial P_{2w}}{\partial x}\right]+\frac{\partial}{\partial y}\left[\lambda_{2w}\frac{\partial P_{2w}}{\partial y}\right]=m\rho_w\frac{\partial S_{2w}}{\partial t}; \\ S_{1o}+S_{1w}=1; \quad S_{2o}+S_{2w}=1; \\ P_{1o}-P_{1w}=P_{1cow}; \quad P_{2o}-P_{2w}=P_{2cow}; \quad 0<x<L;\ 0<y<L;\ t>0. \end{cases} \tag{16}$$

It is solved under the following initial and boundary conditions[16]:

$$P_{1o}(x,y,0)=P_{1o}^H(x,y), P_{2o}(x,y,0)=P_{2o}^H(x,y); \tag{17}$$

$$P_{1w}(x,y,0)=P_{1w}^H(x,y), P_{2w}(x,y,0)=P_{2w}^H(x,y); \tag{18}$$

$$S_{1o}(x,y,0)=S_{1o}^H(x,y), S_{2o}(x,y,0)=S_{2o}^H(x,y); \tag{19}$$

$$S_{1w}(x,y,0)=S_{1w}^H(x,y), S_{2w}(x,y,0)=S_{2w}^H(x,y); \tag{20}$$

$$\begin{cases} -\frac{k}{\mu_o}\frac{\partial P_{1o}}{\partial x}=\alpha(P_{Ao}-P_{1o}); x=0; \\ -\frac{k}{\mu_w}\frac{\partial P_{1o}}{\partial y}=\alpha(P_{Ao}-P_{1o}); y=0; \\ \frac{k}{\mu_o}\frac{\partial P_{1o}}{\partial x}=\alpha(P_{Ao}-P_{1o}); x=L; \\ \frac{k}{\mu_w}\frac{\partial P_{1o}}{\partial y}=\alpha(P_{Ao}-P_{1o}); y=L. \end{cases} \tag{21}$$

$$\begin{cases} -\frac{k}{\mu_w}\frac{\partial P_{1w}}{\partial x}=\alpha(P_{Aw}-P_{1w}); x=0; \\ -\frac{k}{\mu_w}\frac{\partial P_{1w}}{\partial y}=\alpha(P_{Aw}-P_{1w}); y=0; \\ \frac{k}{\mu_w}\frac{\partial P_{1w}}{\partial x}=\alpha(P_{Aw}-P_{1w}); x=L; \\ \frac{k}{\mu_w}\frac{\partial P_{1w}}{\partial y}=\alpha(P_{Aw}-P_{1w}); y=L; \end{cases} \tag{22}$$

$$\begin{cases} -\frac{k}{\mu_o}\frac{\partial P_{2o}}{\partial x}=\alpha(P_{Ao}-P_{2o}); x=0; \\ -\frac{k}{\mu_w}\frac{\partial P_{2o}}{\partial y}=\alpha(P_{Ao}-P_{2o}); y=0; \end{cases} \tag{23}$$

$$\begin{cases} \frac{k}{\mu_o}\frac{\partial P_{2o}}{\partial x}=\alpha(P_{Ao}-P_{2o}); x=L; \\ \frac{k}{\mu_w}\frac{\partial P_{2o}}{\partial y}=\alpha(P_{Ao}-P_{2o}); y=L. \end{cases}$$

$$\begin{cases} -\frac{k}{\mu_w}\frac{\partial P_{2w}}{\partial x}=\alpha(P_{Aw}-P_{1w}); x=0; \\ -\frac{k}{\mu_w}\frac{\partial P_{2w}}{\partial y}=\alpha(P_{Aw}-P_{2w}); y=0; \\ \frac{k}{\mu_w}\frac{\partial P_{2w}}{\partial x}=\alpha(P_{Aw}-P_{1w}); x=L; \\ \frac{k}{\mu_w}\frac{\partial P_{2w}}{\partial y}=\alpha(P_{Aw}-P_{2w}); y=L. \end{cases} \tag{24}$$

Here, the values h_x, k_x, P^H refer to the thicknesses of the layers, permeability coefficients, and characteristic values of pressure. Using these formulas, we formulate the following dimensionless boundary value problem for the oil-gas and oil-water systems.

$$\begin{cases} \frac{\partial}{\partial x}\left[K_{1o}k_1\left(\frac{\partial P_{1o}}{\partial x}\right)\right]=\frac{\partial}{\partial \tau}(1-S_{1g}), \\ \frac{\partial}{\partial x}\left[R_s K_{1o}k_1\left(\frac{\partial P_{1o}}{\partial x}\right)\right]+\frac{\mu_{1o}}{\rho_{1o}\mu_{1g}}\frac{\partial}{\partial x}\left[K_{1g}k_1\rho_{1g}\left(\frac{\partial P_{1g}}{\partial x}\right)\right]= \\ =\frac{\partial}{\partial \tau}\left[R_s(1-S_{1g})+\frac{\rho_{1g}}{\rho_{1o}}S_{1g}\right]-\frac{\rho_{1g}\mu_{1o}}{\rho_{1o}\mu_{1g}}\frac{k_{II}L^2}{h_x h_1 h_x h_{II}}(P_{2g}-P_{1g}); \\ \frac{\partial}{\partial x}\left[K_{2o}k_2\left(\frac{\partial P_{2o}}{\partial x}\right)\right]=\frac{\partial}{\partial \tau}(1-S_{2g})+\frac{\mu_{2o}L^2}{k_x\rho_{2o}P^H}; \\ \frac{\partial}{\partial x}\left[R_s K_{2o}k_2\left(\frac{\partial P_{2o}}{\partial x}\right)\right]+\frac{\mu_{2o}}{\rho_{2o}\mu_{2g}}\frac{\partial}{\partial x}\left[K_{2g}k_2\rho_{2g}\left(\frac{\partial P_{2g}}{\partial x}\right)\right]= \\ =\frac{\partial}{\partial \tau}\left[R_s(1-S_{2g})+\frac{\rho_{2g}}{\rho_{2o}}S_{2g}\right]+\frac{\rho_{2g}\mu_{2o}}{\rho_{2o}\mu_{2g}}\frac{k_{II}L^2}{h_x h_2 h_x h_{II}}(P_{2g}-P_{1g})+\frac{\mu_{2o}L^2}{k_x\rho_{2o}P^H}Q_2; \\ P_{1o}-P_{1g}=P_{1cog}; \quad P_{2o}-P_{2g}=P_{2cog}; \\ S_{1o}+S_{1g}=1; \quad S_{2o}+S_{2g}=1. \end{cases} \tag{25}$$

we write the same equation in the oil-water formulation

$$\begin{cases} \frac{\partial}{\partial x}\left[K_o(cP_{1o}+(1-c))\frac{\partial P_{1o}}{\partial x}\right]+\frac{\partial}{\partial x}\left[K_w\left(\frac{\partial P_{1o}}{\partial x}-\frac{\partial P_{1cow}}{\partial x}\right)\right]+ \\ \frac{\partial}{\partial y}\left[K_o(cP_{1o}+(1-c))\frac{\partial P_{1o}}{\partial y}\right]+\frac{\partial}{\partial y}\left[K_w\left(\frac{\partial P_{1o}}{\partial y}-\frac{\partial P_{1cow}}{\partial y}\right)\right]= \\ c\frac{\partial}{\partial t}(S_{1o}P_{1o})+(1-c)\frac{\partial S_{1o}}{\partial \tau}+\frac{\mu_w}{\mu_o}\frac{\partial(1-S_{1o})}{\partial \tau}-\frac{\rho_o k_{II}L^2}{k h_1 h_{II}}(P_{2o}-P_{1o}), \\ \frac{\partial}{\partial x}\left[K_o(cP_{2o}+(1-c))\frac{\partial P_{2o}}{\partial x}\right]+\frac{\partial}{\partial x}\left[K_w\left(\frac{\partial P_{2o}}{\partial x}-\frac{\partial P_{2cow}}{\partial x}\right)\right]+ \\ \frac{\partial}{\partial y}\left[K_o(cP_{2o}+(1-c))\frac{\partial P_{2o}}{\partial y}\right]+\frac{\partial}{\partial y}\left[K_w\left(\frac{\partial P_{2o}}{\partial y}-\frac{\partial P_{2cow}}{\partial y}\right)\right]= \\ c\frac{\partial}{\partial t}(S_{2o}P_{2o})+(1-c)\frac{\partial S_{2o}}{\partial \tau}+\frac{\mu_w}{\mu_o}\frac{\partial(1-S_{2o})}{\partial \tau}+\frac{\rho_o k_{II}L^2}{k h_2 h_{II}}(P_{2o}-P_{1o})+Q_{2o} \end{cases} \tag{26}$$

From this system of equations, it is evident that the equations are only in relation to the oil pressure function. Therefore, they must be solved with respect to the pressure functions in a coupled manner at each time interval. In this case, the initial and boundary conditions mentioned above are applied only to oil, i.e.:

The solution of this boundary value problem is carried out by applying the Thomas algorithm (progonka method) developed for the finite difference system, and by using the quasi-linear method for the nonlinear terms in the system of equations. At each time step, the solution is obtained through iteration with respect to the pressure function and the viscosity coefficients.

Here, A_i, B_i, C_i and A_i', B_i', C_i' are the Thomas algorithm (progonka) coefficients, which are determined using the following formulas:

$$A_i=\frac{c_i(b_i'-a_i'A_{i-1}')}{R_i}; \quad B_i=\frac{c_i'(a_iB_{i-1}+d_i)}{R_i};$$

$$A_i'=\frac{(b_i-a_iA_{i-1})c_i'}{R_i}; \quad B_i'=\frac{c_i(a_i'B_{i-1}'+d_i')}{R_i};$$

$$C_i=\frac{(a_iB_{i-1}+d_i)(a_i'C_{i-1}'+f_i')+(a_iC_{i-1}+f_i)(b_i'-a_i'A_{i-1}')}{R_i};$$

$$C_i'=\frac{(a_i'B_{i-1}'+d_i')(a_iC_{i-1}+f_i)+(a_i'C_{i-1}'+f_i')(b_i-a_iA_{i-1})}{R_i};$$

$$R_i=(b_i-a_iA_{i-1})(b_i'-a_i'A_{i-1}')-(a_iB_{i-1}+d_i)(a_i'B_{i-1}'+d_i');$$

$i=1,2,\ldots,N-1.$

The mathematical model of the processes occurring in oil-bearing layers connected through a dynamically interacting low-permeability interlayer, as described above,

https://doi.org/10.56143/3030-3893-2025-3-17-25 A bridge between science and innovation

is highly complex. Solving it is only feasible using numerical methods.

The corresponding computational scheme is also intricate and consists of two main stages, primarily based on finite difference and iterative methods. It is implemented in the following sequence:

1. Assigning initial data values:

Number of time iterations – *nt*;
Permeability coefficient value – *k*;
Porosity coefficient value – *m*;
Reservoir length – *L*;
Oil viscosity coefficient – μ;
Pressure of oil in the reservoir – *P*;
Saturation coefficients of oil and water – S_o, S_w;

2. Time iteration cycle: *k=1…nt;*

3. **First Stage.** This stage involves performing calculations at the $k + 0.5$ time layer. For each value of $j = 1…n-1$, the following steps are executed:

3.1. The coefficients of the finite difference equations a_i, b_i, c_i, d_i, f_i and $a_i', b_i', c_i', d_i', f_i'$ are calculated for $i = 1…n-1$;

3.2. The progonka (sweep) coefficients A_0; B_0; C_0; A_0'; B_0'; C_0' are determined from the left boundary conditions.

3.3. The progonka (sweep) coefficients A_i; B_i; C_i; A_i'; B_i'; C_i' *(i=1,n-1)* are computed from left to right.

3.4. $P_{1i,j}$ and $P_{2i,j}$ are determined from the right boundary condition;

3.5. $P_{1i,j}$ and $P_{2i,j}$ $k+0.5$ are computed at the $k + 0.5$ time layer;

3.6. The iterative process is checked at this time layer.

$\left|P_{1oi,j}^{(r)} - P_{1oi,j}^{(r-1)}\right| \le \varepsilon_p$ and $\left|P_{2oi,j}^{(r)} - P_{2oi,j}^{(r-1)}\right| \le \varepsilon_p$.

If this iteration condition is satisfied, that is, the following conditions hold, proceed to step 3.7; otherwise, return to step 3.1.

Here,

$P_{1o}^{(r)}, P_{1o}^{(r-1)}, P_{2o}^{(r)}, P_{2o}^{(r-1)}$ – pressure functions with two closely related values (*r* – the currently calculated value, *r–1* – the previously calculated value; the initial value is taken from the starting condition, and the reference value is taken from the previous iteration);

P_{1o}, P_{2o} – pressure functions;

ε_p – iteration accuracy.

3.7.P_{1o}, P_{2o} the oil pressure in the first and second layers is calculated with sufficient accuracy.

3.8. P_{1w}, P_{2w} the water pressure in the first and second layers is determined using the following formulas:

$P_{1w} = P_{1o} - P_{cow}; P_{2w} = P_{2o} - P_{cow}$

3.9. The first and fourth equations of the system are approximated to calculate the water saturation coefficients S_{1w} and S_{2w}.

3.10. Since the system of equations is nonlinear with respect to the saturation functions, an iterative process is applied. This iterative process continues until the following conditions are satisfied.

$\left|S_{1wi,j}^{(r)} - S_{1wi,j}^{(r-1)}\right| \le \varepsilon_s$ and $\left|S_{2wi,j}^{(r)} - S_{2wi,j}^{(r-1)}\right| \le \varepsilon_s$.

Here

$S_{1w}^{(r)}, S_{1w}^{(r-1)}, S_{2w}^{(r)}, S_{2w}^{(r-1)}$ – pressure functions S_{1w}, S_{2w}, which have two close values (where *r* is the currently calculated value, *r-1* is the previously calculated value, with the zero-th value taken from the initial condition, and the subsequent values are taken from the previous iteration).

ε_s- iteration accuracy.

3.11.S_{1w}, S_{2w} In the first and second layers, the water saturation is calculated with sufficient accuracy using the following formula:

$S_{1o} = 1 - S_{1w}; S_{2o} = 1 - S_{2w}$

3.12. If the iterative process is satisfied, proceed to step 3.13**;** otherwise, return to step 3.1**.**

4. **Second stage.** In the second stage, the above calculations are repeated for the *k+1* time layer in the same way, i.e., from step 3.1 to 3.12.

5. The solutions obtained at time layer *k+1* serve as the initial values for the next step *k+2*.

6. The numerical results are displayed on the screen in the form of tables and 3D graphs.

7. End of the time iteration loop. If the specified number of iterations matches the time loop cycle, the program terminates; otherwise, it returns to step 2.

The developed algorithm can be easily adapted for two- and three-point finite difference equations and, in addition, can also be applied to other multiphase filtration problems, such as the “oil-gas” and “oil-gas-water” systems.

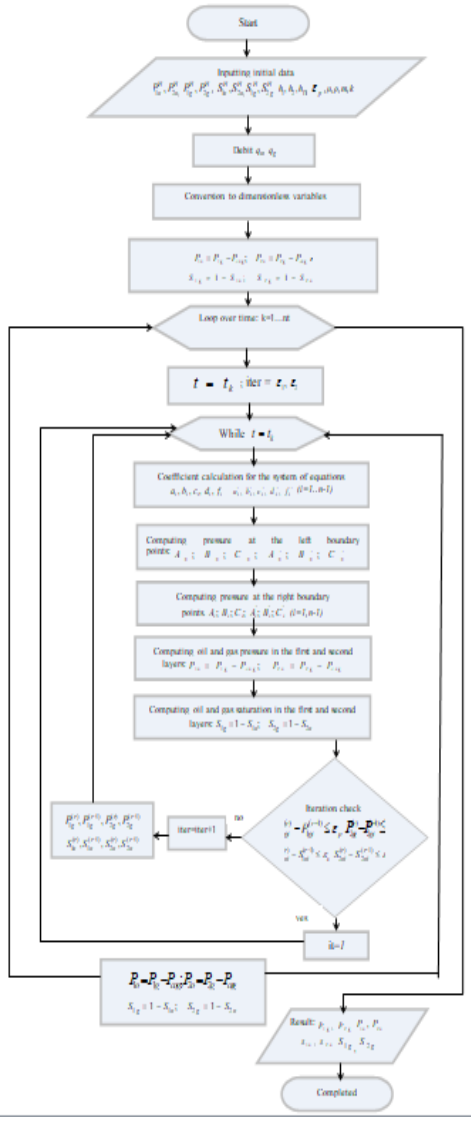

Fig. 3. Block diagram of the algorithm for solving the boundary value problem of the filtration process for a two-phase oil-gas system with mutual dynamic interaction in a two-layer medium

Computational experiments

Based on the numerical model, software has been developed to calculate the main indicators of oil field development in a dynamically connected two-layer system. The software consists of modules for inputting initial data, calculating indicators, and displaying the computation results. The calculation results of the indicators are presented in graphical form.

From the beginning of oil field development, numerical simulation experiments were conducted to analyze the distribution of oil pressure in the reservoir over a period of 720 days. In these figures, the first two graphics show the 3D visualization of oil pressure distribution in the upper and lower layers of the reservoir.

It is clearly observed from the simulation results that the pressure in the upper layer decreases very slowly. This indicates that the flow of oil from the upper to the lower layer is minimal. This limited transfer is due to the very low permeability coefficient of the intermediate layer separating the two reservoir zones.

The contour plot in the second row of the figures illustrates the distribution of oil pressure in the lower layer. The second graph in the row shows the variation of oil pressure along a section at different permeability coefficient values in the wells located in the lower layer.

The material balance equation was used to evaluate the numerical results obtained during the computational experiments. Table 1 presents the variation of the average reservoir pressure over time, where the average values calculated using the finite difference equation and the material balance solutions are provided. The numerical solution obtained by computer was compared with the value calculated using the material balance method, and relative error values were also given to assess accuracy[18].

Table 1

Comparison of the average reservoir pressure using two methods

Number of days	Oil pressure in the well, atm	Average numerical solution obtained by computer	Average pressure calculated using material balance	Relative error (%)
40	284,82	299,04	299,76	0,0380
120	281,79	298,92	299,28	0,1230
240	279,66	298,75	298,56	0,2776
480	275,33	295,32	297,12	0,6060
720	273,03	292,92	295,68	0,9387

One of the methods for analyzing the practical convergence of the finite difference solution to the differential problem is to refine the time grid step. If successive reductions in the time step do not lead to significant changes in the results at the same spatial grid points, it can be concluded that convergence is present. For this purpose, calculations were carried out at different values of the time grid step over $\Delta\tau$ stages, and the results are presented in Table 2, confirming convergence with respect to time.

Table 2

Variation of the average reservoir pressure and the well pressure over time at different time steps

Days		80	160	240	320	400
$\tau = 2$	$P_{Initial}$	0,9428	0,9365	0,9322	0,9284	0,9247
	P_{Final}	0,9976	0,9951	0,9925	0,9899	0,9871

Days		480	560	640	720
$\tau = 2$	$P_{Initial}$	0,9211	0,9174	0,9138	0,9101
	P_{Final}	0,9844	0,9818	0,9791	0,9764

In Table 2, the results of the calculations based on formulas (6) and (7) are presented, demonstrating that the calculated pressure values are in close agreement.

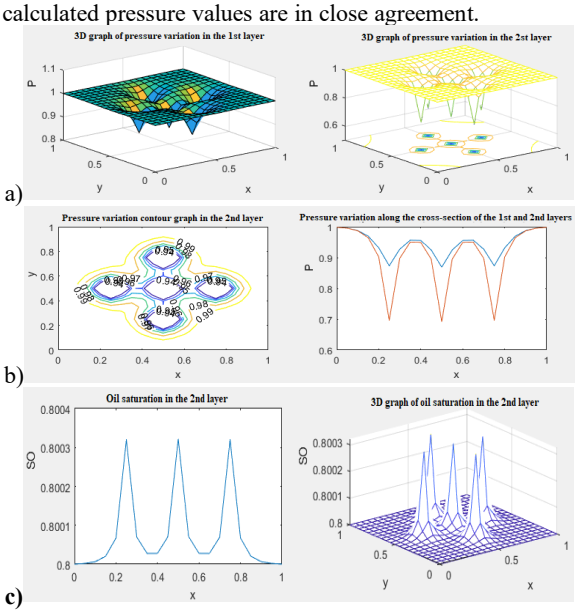

Fig. 4. Pressure distribution graphs in the upper and lower oil layers
(k_1=0.1 d.; k_2=0.1 d.; k_p=0.002 d.; μ=4 sP; m=0.1)

In the a) graph, a 3D plot of pressure distribution in the reservoir is observed when five wells are symmetrically located. In the b) graph, a 3D plot of pressure distribution in the second layer is shown. The c) graph presents the contour plot of pressure distribution, while the fourth graph illustrates pressure variation along a cross-section. The fifth and sixth graphs display oil saturation in the second layer — in cross-section and 3D views, respectively. In this case, the following parameter values were used: k_1=0.1 d.; k_2=0.1 d.; k_p=0.002 d.; μ=4 sP; m=0.1.

3. Research results

The main features of the software complex for analyzing and forecasting the filtration process in oil fields include solving a boundary value problem based on a mathematical model to determine the key indicators of oil filtration in reservoir layers and conducting computational experiments with visualization. The developed software complex titled "*Modeling and Visualization of Computational Experiments*

https://doi.org/10.56143/3030-3893-2025-3-17-25 A bridge between science and innovation

for Determining Key Performance Indicators of Oil Field Development" is created based on the above-mentioned mathematical model, numerical methods, and solution algorithms.

In the process of oil and gas extraction, automating the solution of fluid and gas filtration boundary value problems in porous media allows for the determination of hydrodynamic parameters of reservoirs, speeds up the design of oil and gas fields, and enhances the analysis and forecasting of the filtration process. Therefore, developing and effectively using automated systems for studying the oil filtration process in porous media is essential for solving various problems specific to the field.

The development of a software complex that solves the boundary value problem of oil filtration in porous media and ensures the accuracy of computational results provides significant convenience for users in determining key indicators of the filtration process in oil reservoir layers. This software complex enables rapid determination of hydrodynamic parameters during oil or gas extraction in reservoir systems, playing an important role especially in the design, analysis, and forecasting of oil and gas fields.

Automating the solution of boundary value problems based on a mathematical model to identify key indicators in the filtration process of fluids and gases in fractured, heterogeneous underground porous layers contributes to the creation of specialized software for solving various related problems. To determine the main indicators of the oil or gas filtration process in oil and gas reservoir layers, the solution of a boundary value problem based on a mathematical model is carried out, along with computational experiments visualized on a computer[17].

The software complex makes it possible to conduct computational experiments on key indicators for a two-dimensional, three-layer oil system characterized by weak dynamic interaction through a semi-permeable layer in a fractured, heterogeneous filtration domain of both simple and complex structure. The developed software not only serves as an interactive tool for analyzing data on a computer but also provides the ability to conduct simulations, analyze processes, and make necessary decisions — whether brief or comprehensive — during the modeling and forecasting stages.

Computational experiments based on the boundary value problem of filtration for a two-phase oil-water system in a two-layer porous medium with mutual dynamic interaction show that the smaller the value of the permeability parameter of the weakly permeable layer, the less pressure drop occurs in the upper and lower layers. This pressure drop has a greater impact on the areas near the well in the second layer. The developed model, algorithm, and software can be used to analyze and forecast the development of multilayer oil and gas fields with mutual dynamic interaction.

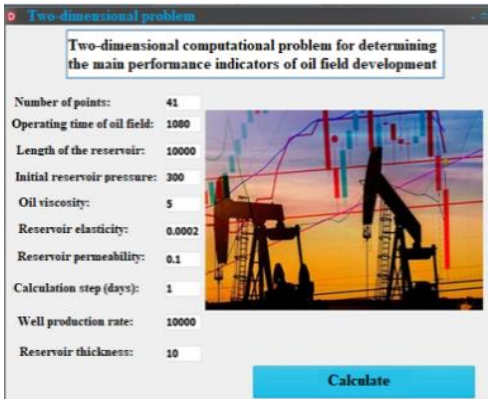

Fig. 5. User interface of the program for solving the two-dimensional filtration problem for a two-phase oil-water system

Implemented work: The developed numerical models and software tools for the filtration process of two-phase oil-water and oil-gas systems in a porous medium with mutual dynamic interaction enable the study and development of oil fields.

Scientific and technical significance: The developed numerical model and algorithm, along with the software complex for calculating the key performance indicators of oil field development, can be used for analysis, design, and the development of oil fields with mutual dynamic interaction.

4. Conclusion

The developed mathematical models and software tools provide a comprehensive framework for analyzing unsteady two-phase filtration processes — oil-water and oil-gas systems — in porous media. Based on the fundamental equations and principles of unsteady filtration theory, these models have been applied to both single- and two-layer structures to assess the hydrodynamic behavior of oil reservoirs. For systems with mutually dynamic interacting layers, a two-dimensional mathematical model and corresponding boundary conditions were formulated, leading to the development of efficient computational algorithms. These algorithms significantly improve the accuracy and speed of calculating reservoir pressure and saturation levels[18].

Moreover, a finite difference solution algorithm based on the method of directional splitting was implemented, and specialized software was developed accordingly. This software enables real-time monitoring of the filtration process, visualization of numerical results, and execution of interactive computational experiments. Overall, the proposed model, algorithm, and software package serve as an effective tool for the design, analysis, and forecasting of oil field development.

References

This research work provided an opportunity to explore two-phase filtration processes through a combination of theoretical and practical approaches, enabling the development of mathematical models and computational experiments. By utilizing advanced methods and technologies, efficient and accurate results were achieved in the design of numerical algorithms and software tools. In

particular, the solutions developed for modeling hydrodynamic processes in multilayer systems with mutual dynamic interaction have practical significance for analyzing and forecasting oil field development. I extend my sincere appreciation to all specialists who contributed valuable scientific guidance, technical assistance, and essential data throughout the course of this study.

Their support played an important role in successfully completing this research and achieving its intended goals.

References

[1] Darcy, H. Les fontaines publiques de la ville de Dijon. Paris: Dalmont, 1856.

[2] Aziz, K., & Settari, A. Petroleum Reservoir Simulation. Applied Science Publishers, 1979.

[3] Veregin, N.N. Nonlinear Filtration Models for Multiphase Flows in Porous Media. Journal of Applied Mechanics and Technical Physics, 33(4), 553–560, 1992.

[4] Nikolayevsky, V.N. Mechanics of Porous Media. Mechanics of Solids, 29(3), 75–83, 1994.

[5] Shestakov, V.M. Computational Techniques for Multiphase Flow in Petroleum Reservoirs. Computational Mathematics and Mathematical Physics, 39(2), 238–247, 1999.

[6] Zakirov, E.S. Modeling of Filtration and Hydrodynamic Processes in Oil Fields. Uzbek Journal of Hydrodynamics, 7(1), 15–24, 2001.

[7] Lopukh, B.B. Algorithmic Methods in Oil-Gas Flow Simulation. Journal of Petroleum Science and Engineering, 42(3–4), 121–130, 2004.

[8] Abutaliev, F.B. Hydraulic Analysis of Oil Pipeline Systems. Journal of Pipeline Engineering, 6(2), 67–75, 2005.

[9] Baklushin, M.B., & Erbekov, Y.S. Modeling Oil Pipeline Systems. Tashkent: Oil and Gas Institute, 2006.

[10] Fayzullaev, D.F. Simplified Models for Multiphase Filtration in Porous Media. Uzbek Journal of Mechanics and Mathematics, 15(2), 88–96, 2009.

[11] Sadullayev, R. Dynamic Models for Reservoir-Gas-Liquid Systems. Oil and Gas Engineering Journal, 22(1), 33–40, 2011.

[12] Cueto-Felgueroso, L., Fu, X., & Juanes, R. Modeling Two-Phase Flows in Porous Media without Capillarity. Water Resources Research, 51(10), 8126–8145, 2015.

[13] Yakovlev, V.V., Kalugin, Y.I., & Stepova, N.G. Technological Algorithms in Petroleum Engineering. Moscow: OilTechPress, 2015.

[14] Khuzhayorov, B.Kh., & Burnashev, V.F. Integral Methods in Unsteady Two-Phase Flow Modeling. Journal of Computational Physics, 321, 1024–1033, 2016.

[15] Vasilyeva, M.V., & Prokopev, G.A. Iterative Schemes for Multiphase Reservoir Simulation. Applied Numerical Mathematics, 119, 77–91, 2017.

[16] Umarov, U.U. Application of Numerical Models in Oil Reservoir Simulation. In Proceedings of the International Conference on Energy Systems Modeling, Kazan, Russia, 2017.

[17] Zvonarev, S.V. Mathematical Modeling in Technical and Natural Sciences. Russian Journal of Applied Sciences, 4(1), 42–49, 2018.

[18] Sergeyev, B.N. IMPES Schemes for Multiphase Flows. Mathematics and Computers in Simulation, 160, 23–31, 2019.

[19] Siddikov, R.M., Filippov, D.D., & Mitrushkin, D.A. Software Simulation of EOR Processes in Reservoirs. Journal of Petroleum Technology, 72(6), 115–125, 2020.

[20] Shukurova, M., & Nazirova, E. Analysis of Pressure Distribution in Oil Reservoirs with Low Permeability Barriers. Uzbek Journal of Theoretical and Applied Mechanics, 14(3), 102–111, 2022.

[21] Shukurova, M., & Nazirova, E. Mathematical Modeling of Two-Phase Filtration Processes in Porous Media with Weak Layer Connectivity. Journal of Applied Computational Science, 11(2), 45–53, 2023.

[22] Shukurova, M., & Nazirova, E. Development of Software Tools for the Visualization of Multiphase Filtration in Heterogeneous Porous Media. International Journal of Petroleum and Energy Research, 9(4), 120–129, 2023.

[23] Shukurova, M., & Nazirova, E. Numerical Simulation of Oil-Water Systems in Multi-Layer Reservoirs Using Finite Difference Methods. Computational Modeling and Engineering, 6(1), 88–96, 2024.

Information about the author

Shukurova Marhabo
Karshi State Technical University,
Associate Professor of the Department of "Software and Hardware Support of Computer Systems", (PhD)
E-mail: shukurovamarhabo30@gmail.com
Tel.: +998990835972
https://orcid.org/0009-0009-2998-3964

Monitoring of railcars based on BLE and cellular technologies

Sh.Sh. Kamaletdinov[1][a], I.O. Abdumalikov[1][b], F.O. Khabibullaev[1][c]
[1]Tashkent state transport university, Tashkent, Uzbekistan

Abstract: This paper examines the architecture of a railcar monitoring system that employs Bluetooth Low Energy (BLE) beacons attached to railcars and gateways equipped with cellular connectivity (GSM, LTE, NB-IoT). A comparative assessment of existing tracking technologies (GPS, RFID, LoRa, etc.) is presented and the rationale for selecting a hybrid BLE + cellular approach is given. The network topology is described (star topology: BLE beacon → gateway → cloud), together with the hardware components (BLE beacons and cellular gateways) and the server infrastructure (MQTT, REST API, buffering, fault tolerance). Options for gateway placement at stations and in depots are considered, operational scenarios (in depot, at station, in transit) are analyzed, and the advantages and limitations of the proposed scheme are discussed. Examples of real-world solutions and technical data are provided.

Keywords: BLE beacons, cellular connectivity, NB-IoT, LTE-M, railcar monitoring, BLE gateways, IoT platform, MQTT, REST API, asset tracking, depot/station monitoring

1. Introduction

Traditionally, railcar tracking has relied on GPS trackers, RFID tags, or LPWAN technologies. GPS positioning provides global visibility and high accuracy in open areas but requires line-of-sight to satellites (it fails in tunnels and covered facilities) and consumes significant energy; GPS modules are relatively expensive and bulky, which complicates installing them on every wagon.

RFID tags (active and passive) make inexpensive marking possible but require powerful readers installed at specific checkpoints (entry gates, depots) and have a limited read range (a few meters). As reported in the literature, passive RFID tags cost approximately $0.10 but require expensive readers (USD 10–20k) and operate only at very close range to the reader. Active RFID trackers are more expensive (~$20 per tag) and have battery lives of 3–5 years and ranges up to ~100 m; however, they tend to be bulkier and harder to integrate with cloud services. Overall, RFID is suitable for checkpoint inventory but does not provide continuous monitoring of rolling stock.

LPWAN technologies such as LoRaWAN provide long range (5–10 km in open terrain) and low energy consumption. LoRaWAN operates in unlicensed spectrum, facilitating private network deployment, but is susceptible to interference and requires deployment of dedicated gateways. NB-IoT and LTE Cat-M1 enable transmission of small packets over existing licensed cellular networks, offering wide coverage (especially in rural areas) and the capacity to support thousands of devices per cell. However, NB-IoT has limitations in mobility: handover between cells can require a relatively long recovery time.

BLE beacons are low-cost, energy-efficient devices that broadcast an identifier and, when equipped, simple telemetry. Compared with RFID, BLE tags provide greater range given the appropriate receiver infrastructure, and inexpensive BLE gateways (consumer and industrial) are widely available. BLE is naturally compatible with consumer devices (smartphones, tablets) and cloud platforms. The main drawback of BLE is its limited coverage (tens of meters) and inability to provide long-range positioning without additional receivers.

Recent studies and reports demonstrate that combining local BLE beacons with cellular communication channels (GSM/LTE/NB-IoT) yields a cost-effective and scalable railcar accounting system: BLE provides inexpensive tagging and local telemetry collection at the “last mile,” while cellular networks relay event-driven messages to the cloud and enable integration with IT services [1,3,5]. Comparative reviews note that LPWAN solutions such as LoRaWAN are competitive in terms of energy efficiency and cost but require dedicated infrastructure, whereas NB-IoT/LTE-M benefit from operator-managed coverage and centralized management yet suffer from mobility constraints (notably NB-IoT) [2,4,9]. Experimental studies and industrial pilots validate the use of BLE for local monitoring (station/depot scenarios), while continuous tracking en route typically relies on mobile gateways mounted on locomotives or on hybrid trackers that combine GNSS and cellular connectivity [1,6,10]. Practical cases show that hybrid architectures (BLE + cellular transmission) are optimal for automating acceptance/dispatch and diagnostic monitoring of railcars, but they require careful gateway placement and buffering strategies during connectivity outages [1,5,7]. In summary, the technology choice depends on required update frequency, coverage topology, and economic constraints: BLE is suitable for dense local detection, while LPWAN/NB-IoT/LTE are preferred for backbone transmission and remote sections [2,4,8].

Consequently, a BLE + cellular approach enables local detection of railcars (BLE beacons) and relays their status to the cloud via the wide coverage provided by GSM/LTE/NB-IoT. BLE beacons are mounted on railcars and fixed or mobile gateways receive their signals and forward them to a central system. This scheme leverages existing cellular infrastructures and supports integration with contemporary IoT platforms.

[a] https://orcid.org/0000-0002-4004-9736
[b] https://orcid.org/0009-0000-5882-5978
[c] https://orcid.org/0009-0002-9477-3903

2. Research methodology

Network architecture and topology

The monitoring network follows a star-based architecture: BLE beacons attached to railcars broadcast packets containing unique identifiers and, optionally, sensor data. BLE gateways (Bluetooth gateways) are deployed at fixed points (stations, depots) or mounted on mobile units (e.g., locomotives, shunting locomotives). These gateways receive packets from all beacons within their coverage (approximately 10–50 m, depending on environment). The gateway then forwards the collected information via the cellular network to a cloud server.

At the upper level, cellular connectivity (GSM/GPRS, LTE Cat-M1, NB-IoT, etc.) is used to transmit data to the central server. Gateways may support multiple frequency bands and cellular protocols, enabling compatibility with different mobile operators and providing ubiquitous coverage where operator service is available. The topology allows horizontal scaling: as the railcar fleet grows or train lengths increase, additional BLE gateways can be deployed or their coverage extended. Cellular networks provide data transmission capability across railway sections without the need for deploying a dedicated long-range network.

The horizontal data flow is: BLE beacons (edge sensors) → BLE gateways (cellular modem + compute unit) → Internet (MQTT/REST API) → server backend (fig.1). Note that BLE beacons do not directly provide geolocation; the railcar's approximate location is inferred from the gateway(s) that detected its beacon. This approach resembles container or freight truck tracking: a tag in a vehicle is read by a BLE gateway in the vehicle or at a checkpoint, and the gateway relays the information via LTE or NB-IoT.

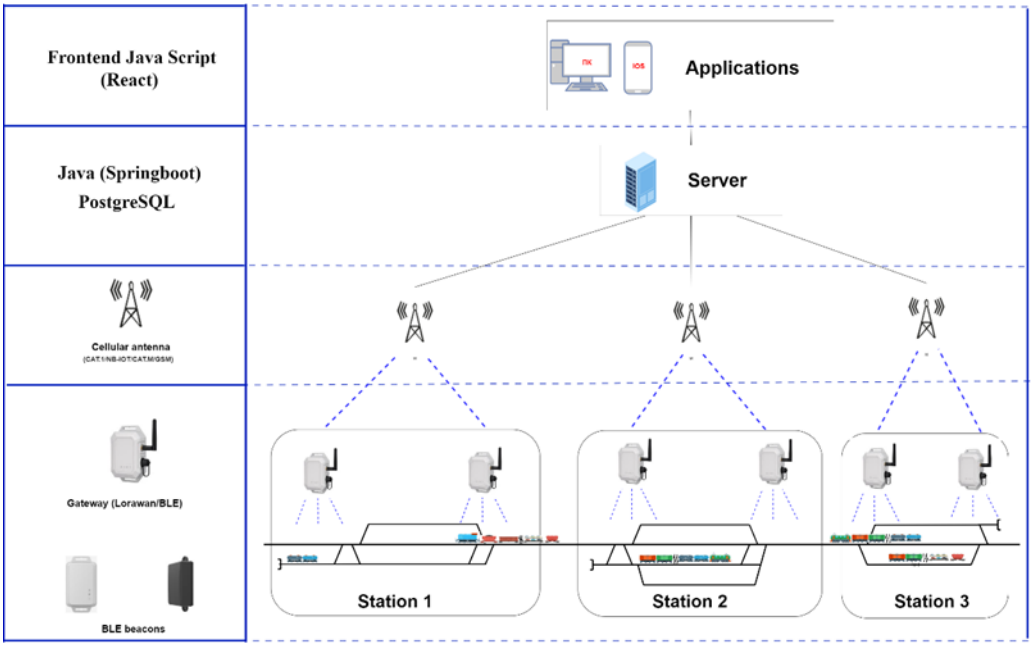

Fig. 1. Network architecture and topology

The number of BLE devices a single gateway can handle depends on hardware capabilities and channel load. Modern BLE 5.0 gateways can process signals from dozens of beacons simultaneously; gateways commonly implement filtering and packet selection at the network edge to reduce load and data consumption. The cellular segment is readily scalable—additional gateways or failover channels can be introduced if needed.

Hardware components

BLE beacons on railcars. Each railcar is equipped with a compact battery-powered BLE beacon. Typical beacons may implement standard payloads (e.g., iBeacon/Eddystone) and may include auxiliary sensors (temperature, shock/acceleration, door open/close, etc.). BLE beacons are ultra-low power, operate in the 2.4 GHz band, and have an effective range in open areas from a few tens up to about 100 m; range is reduced in enclosed or heavily shielded metallic environments.

BLE gateways with cellular modems. A gateway integrates a BLE receiver and a cellular modem (GSM/3G/LTE Cat-M1/NB-IoT). Gateways are available in portable small-form factors with modest batteries for temporary or mobile deployments, and in ruggedized stationary variants with larger batteries or mains power intended for long-term outdoor installation (wide temperature range, high ingress protection). Mobile gateway installations on locomotives provide the capability to collect beacon signals while in transit and transmit them via LTE Cat-M1 or NB-IoT. Many gateways also implement local buffering to store messages when connectivity is lost (for example, in tunnels) and to forward them when the link is restored. There are also hybrid trackers that combine BLE interfaces, cellular modems and sometimes GNSS receivers, enabling the device to function as both a local beacon and an autonomous cellular tracker when required.

Server infrastructure (MQTT, REST API, buffering, fault tolerance)

The central component of the system is an IoT platform or cloud server that ingests messages from gateways and makes data available to users. Lightweight protocols such as MQTT and HTTP/REST are commonly used. MQTT is particularly suited to IoT use cases due to its low overhead, support for quality of service (QoS) levels, persistent sessions and straightforward integration with brokers and cloud services. In some deployments, MQTT is used as the

https://doi.org/10.56143/3030-3893-2025-3-26-29 A bridge between science and innovation

primary transport, ensuring reliable delivery and secure transmission.

On the server side, message queues and data stores (time-series databases, NoSQL or SQL stores) are configured, and APIs are provided for external systems. Buffering at the gateway level is essential: when a gateway loses connection, messages are cached locally and forwarded later (store-and-forward). MQTT brokers support session persistence and QoS which help to avoid data loss during transient connectivity disruptions.

For reliability, the platform can employ redundant MQTT brokers, geo-distributed database clusters and cellular channel redundancy. Integration with enterprise IT is typically provided through standard interfaces: the monitoring platform exposes REST APIs, webhooks or a message bus. Standardized interfaces enable automated data exchange with customer systems, facilitating integration into existing operational ecosystems.

3. Results

Gateway placement at stations and in depots

BLE gateways are positioned where railcars can be reliably detected. At stations, typical locations include entry/exit tracks, departure platforms and nearby tracks used for parking. In depots, gateways are placed at yard gates and along formation tracks where locomotives couple and uncouple cars. The objective is to ensure that each car passes through the capture zone of at least one gateway during entry/exit operations. Where mains power is available, stationary gateways are connected to permanent power; in field sites, autonomous gateways with large battery packs or solar panels can be used.

Inside depots or facilities lacking cellular coverage, local wired transmission (Ethernet) to a central server can be arranged. More commonly, however, LTE/NB-IoT gateways are mounted on technical huts or masts to obtain mobile operator channels. Mobile gateways can be installed on locomotives or service vehicles to capture beacon signals while the train is moving and forward them via GSM/LTE.

Operational scenarios

At a station during arrival/departure. When a train arrives and stops, wagons enter the coverage area of station BLE gateways (fig.2). Gateways automatically read IDs of beacons within range (up to ~50–100 m in open conditions) and forward the information to the cloud. This yields an accurate manifest of wagons in the consist. If integrated with an ERP/WMS system, wagon entries and exits are recorded automatically, reducing manual checks and speeding cargo processing.

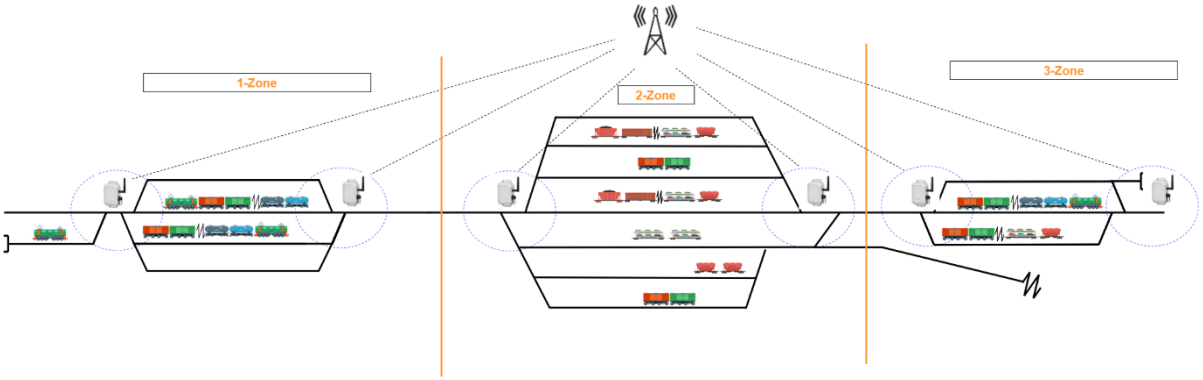

Fig. 2. Operational scenario at a station

In the depot (repair and formation tracks). In depots, gateways track wagon presence and status. If a wagon enters a maintenance bay, the system records that it has left the departure line. Movement within the depot can be monitored; for parked wagons, scanning intervals can be reduced (for example, hourly). The key requirement is that the system can confirm all wagons intended for dispatch have been read before departure.

4. Discussion

Advantages:

- *Energy efficiency and cost of beacons:* BLE beacons are highly energy efficient and can operate for several years on a single battery. They are cheaper than active RFID or GPS trackers, reducing maintenance frequency.
- *Ease of deployment:* The approach leverages existing wireless infrastructures—BLE for the local segment and public cellular networks for backbone transmission—eliminating the need to deploy a dedicated long-range network. Gateways are easy to mount on walls, poles or rolling stock.
- *Scalability:* Adding a new railcar requires only mounting a new beacon. The gateway network can be extended incrementally as the fleet grows. BLE receivers are inexpensive and easy to integrate (e.g., via a smartphone app or a compact IoT gateway).
- *IoT integration:* BLE gateways commonly support MQTT and REST APIs and JSON payloads, facilitating integration with operational systems. The architecture is compatible with industrial IoT platforms and enterprise SCADA.
- *Versatility:* BLE payloads may carry not only an ID but also sensor data (temperature, shock, door status), enabling richer monitoring functionality.

Limitations:

- *Limited BLE range:* Typical BLE coverage is on the order of 10–50 m, necessitating a sufficient density of gateways in large yards. In open countryside between stations, BLE coverage is impractical without mobile gateways.
- *Deployment density and cost:* Ensuring reliable reads for all wagons requires careful gateway placement; the cost of installing many gateways can offset some of the beacon cost savings.

- *Cellular coverage reliability:* Cellular networks may be unreliable in remote areas. NB-IoT offers good coverage at major nodes but presents challenges for moving objects due to limited handover capabilities; migration away from legacy 2G/GSM also requires adoption of LTE/NB-IoT.
- *Lack of precise geolocation from BLE:* BLE only indicates proximity to a gateway, not precise coordinates. Unlike GNSS, it cannot provide continuous geolocation; for continuous tracking, combination with other methods is needed.
- *Dependence on infrastructure:* If a gateway fails (power loss or modem failure), data about wagons in its zone will not be available until the gateway is repaired; thus, redundancy and uninterruptible power supplies are advisable.

5. Conclusion

A hybrid architecture combining BLE beacons and cellular connectivity enables cost-effective railcar accounting and monitoring. BLE beacons provide inexpensive marking and long battery life, while cellular gateways (GSM/LTE/NB-IoT) ensure wide-area transmission and integration with cloud platforms. The system is well suited to automating acceptance/dispatch operations and diagnostic monitoring in stations and depots, reducing manual labor and increasing operational transparency. Limitations related to BLE range and cellular coverage can be mitigated by careful gateway placement, the use of mobile receivers, and buffering strategies. Overall, combining BLE and modern LPWAN/cellular technologies represents a promising direction for digitizing railway logistics.

References

[1] Aripov N.M., Kamaletdinov Sh.Sh., Tokhirov N.S. Selection of a wireless technology among Internet of Things solutions to improve the organization of the transport process in railway transport // Electronic Journal of Actual Problems of Modern Science, Education and Training. 2022. No. 8. P. 96–104.

[2] Aripov N.M., Kamaletdinov Sh.Sh., Tokhirov N.S. Development of LoRaWAN network infrastructure for organizing transport management in railway transport // Electronic Journal of Actual Problems of Modern Science, Education and Training. 2022. No. 8. P. 104–114.

[3] GeoForce. GPS vs. RFID Railroad Tracking: Which is Better for Railcar Tracking? [Electronic resource] // GeoForce. — Available at: https://www.geoforce.com/gps-vs-rfid-railroad-tracking/ (accessed 22 Aug 2025).

[4] IoT For All. Indoor Positioning with BLE and LoRa: A Comparative Approach [Electronic resource] // IoT For All. — Available at: https://www.iotforall.com/indoor-positioning-ble-and-lora (accessed 22 Aug 2025).

[5] Actility. Report / Article on the application of LoRaWAN in railway projects (deployment example and analytics) [Electronic resource] // Actility. — Available at: https://www.actility.com/sncf-blog/ (accessed 22 Aug 2025).

[6] ChirpStack. Documentation on integrating BLE scanning with network servers (features of transmission via MQTT/REST) [Electronic resource] // ChirpStack documentation. — Available at: https://www.chirpstack.io/docs/ (accessed 22 Aug 2025).

[7] Computools. Overview of practical solutions for cargo monitoring with a hybrid architecture (BLE + cellular transmission) [Electronic resource] // Computools. — Available at: https://computools.com/case/iot-in-railway-transport/ (accessed 22 Aug 2025).

[8] LoRa network architecture / Scientific diagram [Electronic resource] // ResearchGate. — Available at: https://www.researchgate.net/figure/LoRa-network-architecture_fig1_307965130 (accessed 22 Aug 2025).

[9] Onomondo. What is NB-IoT Connectivity? [Electronic resource] // Onomondo. — Available at: https://www.onomondo.com/what-is-nb-iot-connectivity/ (accessed 22 Aug 2025).

[10] Commercial case studies of container and railcar monitoring with combined trackers (example of using GNSS + BLE + NB-IoT) [Electronic resource] // World Bank — State-owned enterprises (case examples). — Available at: https://state-owned-enterprises.worldbank.org (accessed 22 Aug 2025).

Information about the author

Shokhrukh Kamaletdinov	Tashkent State Transport University, Associate Professor of the Department of Operational Work Management in Railway Transport (DSc) E-mail: shoxruxkamaletdinov@gmail.com Tel.: +998935834569 https://orcid.org/0000-0002-4004-9736
Islom Abdumalikov	Tashkent State Transport University, PhD student, Department of Operational Management in Railway Transport E-mail: Islomjonabdumalikov93@gmail.com Tel.: +998909099965 https://orcid.org/0009-0000-5882-5978
Fayzulla Khabibullaev	Tashkent State Transport University, PhD student, Department of Operational Management in Railway Transport E-mail: fayzulla.habibullayev@mail.ru Tel.: +998935304639 https://orcid.org/0009-0002-9477-3903

Railway railcar monitoring system based on BLE and Wi-Fi/PoE

Sh.Sh. Kamaletdinov[1][a], I.O. Abdumalikov[1][b], F.O. Khabibullaev[1][c]
[1]Tashkent state transport university, Tashkent, Uzbekistan

Abstract: A railway freight car monitoring system is proposed in which BLE beacons mounted on freight cars transmit data to a stationary network built on Wi-Fi and Power over Ethernet (PoE). BLE beacons (Bluetooth Low Energy) continuously broadcast identifiers and basic telemetry from the cars, while gateway devices (Wi-Fi access points powered via PoE) collect these packets and forward them over Ethernet to a central server. This approach provides high throughput and reliable power for the data collection layer and simplifies network installation by eliminating the need for separate mains wiring. The paper describes the methodology, network architecture, hardware components and server infrastructure. Advantages (broadband capacity, centralized power) and limitations (smaller Wi-Fi coverage area, potential interference in the 2.4 GHz band) of the proposed solution are discussed. Application examples for stations, depots and line sections are considered.

Keywords: freight car monitoring, Bluetooth Low Energy (BLE), Wi-Fi/PoE, wireless technologies in transport, Internet of Things (IoT), station and depot solutions, international transport

1. Introduction

The Internet of Things is increasingly used to automate logistics and to monitor rolling stock. Low-power radio methods are applied to track the location and condition of freight cars. A common architecture combines BLE beacons on vehicles with LoRaWAN gateways on masts or contact-line supports. LoRaWAN provides very long range (several kilometers), whereas Wi-Fi is intended for local networks with a radius up to a few hundred meters.

Research on freight car monitoring is rapidly developing due to the adoption of wireless technologies and IoT. BLE networks have shown effectiveness for collecting telemetry from brake-system sensors and wagon subsystems [1][2]. To extend coverage, LoRaWAN is used, enabling service of thousands of tags over large areas [3][4].

Cellular networks (GSM/4G/NB-IoT) are also used: terminals can provide continuous data transmission without deploying a private network [5][11]. However, high connectivity costs and power consumption limit their use in very large deployments.

RFID has long been applied for wagon identification: readers along the track provide accurate tracking, and over 95% of rolling stock in the United States is already equipped with tags [6][7]. For integration with Ethernet, BLE gateways with PoE are often used [8], and onboard Wi-Fi access points are commonly powered by PoE, simplifying equipment installation [9].

Specialized railway communication systems, such as GSM-R, remain in use for voice and certain data services, but trends are shifting towards LTE/5G and next-generation IoT networks [10][11]. Thus, BLE combined with Wi-Fi/PoE appears to be a promising solution for stations and depots, while for line sections and international routes it is reasonable to combine BLE with LoRaWAN or NB-IoT.

Using Wi-Fi as a stationary transport network offers high data rates and reliable device connectivity (thanks to Ethernet backhaul and PoE power), but requires a denser deployment of access points. Bluetooth Low Energy (BLE) provides a low-cost, low-power method to transmit small packets from onboard sensors. BLE beacons continuously broadcast identification and telemetry, and access points (BLE gateways) receive these signals and forward them to the cloud (central server). This work proposes to combine BLE sensors on wagons with a stationary Wi-Fi network powered by PoE and examines its architecture and characteristics.

2. Research methodology

The methodology is based on collecting data at the BLE layer and forwarding it over a stationary IP network. Each freight car is fitted with a BLE beacon equipped with sensors (for example: temperature, shock/impact, door open/close). The beacon periodically transmits a packet (e.g., in iBeacon/Eddystone format) containing measurements and a unique identifier. Base stations (BLE gateways) — implemented as Wi-Fi access points with an integrated BLE receiver — are installed in fixed positions (on platforms, contact-line masts or inside depots) and are powered via PoE switches. A gateway scans for BLE advertisements within its reception area (typically several tens of meters), decodes them and encapsulates them into TCP/IP packets. Data are then forwarded via Ethernet or Wi-Fi backhaul to the server.

This solution allows reuse of existing IT infrastructure: a single Ethernet cable supplies both power and data (PoE according to IEEE 802.3af/at), minimizing additional wiring costs. The network is organized in a “star” layout: BLE devices connect to the nearest access point, while the Wi-Fi/Ethernet layer connects access points to the central control server.

Network architecture and topology

The network comprises BLE beacons, Wi-Fi gateways with PoE and a central server. BLE beacons on wagons operate in the 2.4 GHz band and are optimized for low-power transmission. A BLE→Wi-Fi gateway integrates a Bluetooth radio and a Wi-Fi/Ethernet client. A single access point may collect BLE data from several dozen beacons concurrently. The Ethernet network is typically arranged according to the enterprise wired network topology

[a] https://orcid.org/0000-0002-4004-9736
[b] https://orcid.org/0009-0000-5882-5978
[c] https://orcid.org/0009-0002-9477-3903

(gateway-to-server links over cable or Wi-Fi backhaul). Access points are PoE-powered and can be mounted on poles, depot walls or platform supports. Standards such as IEEE 802.11 (e.g., 802.11n/ac for 2.4 and 5 GHz) and IEEE 802.3af/at (PoE) are applied. Each access point acts as a bridge between the BLE device "star" and the Ethernet "star" of the network (fig.1). The topology may be complemented by redundant channels (for example, secondary radio backhaul or a redundant Ethernet ring).

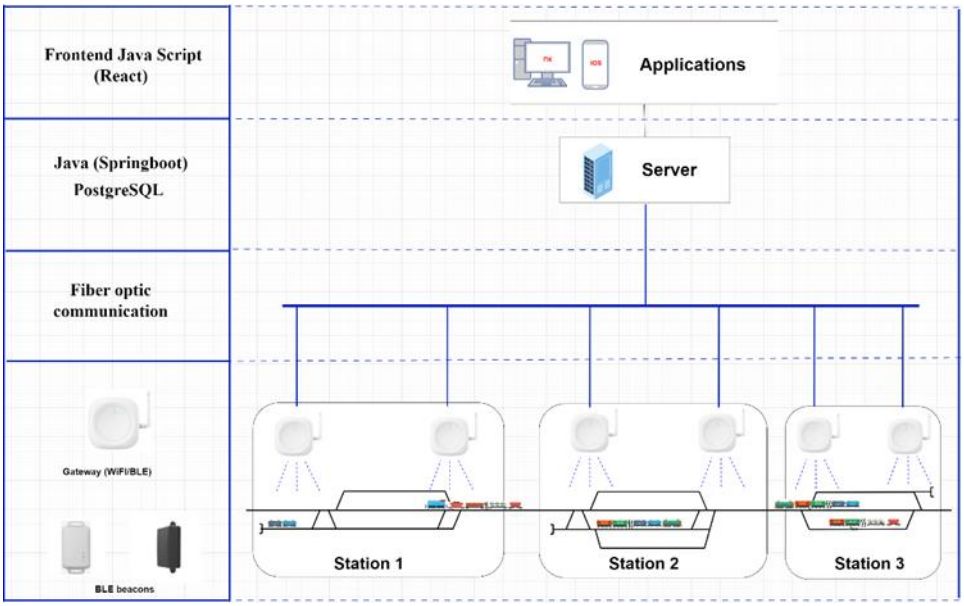

Fig. 1. Network architecture and topology

Hardware components

Main system components:

- BLE beacons on wagons. Autonomous battery-powered transmitters that send condition data from the wagon (e.g., temperature, door status, shock events) along with a unique identifier. BLE modules use Bluetooth Low Energy and are designed for low power consumption. Practical detection range varies (roughly 20–300 m depending on transmit power and environment). Beacons require minimal maintenance (battery replacement every few years under typical settings).
- Wi-Fi/BLE gateways with PoE. Wi-Fi access points (e.g., dual-band 2.4/5 GHz IEEE 802.11n/ac) augmented with a BLE module that scans BLE advertisements in the surrounding area. These devices are powered via PoE (IEEE 802.3af/at), simplifying installation since a single Ethernet cable provides both power and connectivity. Separate antennas or integrated modules provide Wi-Fi and Bluetooth radio functions. Outdoor units are housed in weather-resistant enclosures.
- Network equipment. An Ethernet LAN interconnects gateways. PoE switches, routers and access switches are used for aggregation. Where necessary, access points can operate over a configured Wi-Fi backhaul. Routers provide routing to the central server, which may be located on-premises or in the cloud.
- Server and software. The server ingests packets from gateways, stores data, visualizes telemetry and performs analytics. Standard protocols (MQTT, HTTP/REST, etc.) are used to deliver data to the management system. The server infrastructure can be deployed in a transportation control center or in the operator's cloud environment.

Server infrastructure

The server subsystem aggregates incoming data from BLE gateways and performs processing and storage. Gateways send data in real time over secured channels (Ethernet/Wi-Fi) through the local network or a VPN to the central server. Communication may use MQTT or HTTPS to ensure reliable delivery of small messages. On the server, a database stores wagon telemetry, and analytics and visualization services (web or SCADA interface) are deployed. The server can aggregate data across multiple stations or depots, providing centralized control. With PoE-powered gateways, a unified network of numerous BLE sensors is supported: sensors transmit signals which gateways capture and forward to the cloud/on-premise server. This scheme enables near-real-time tracking of wagon locations on yards (by associating a beacon with a specific gateway) and recording of onboard condition changes, plus long-term archival for analytics.

3. Results

A modeling study and pilot testing of the proposed architecture were conducted. BLE beacons produce small packets on the order of tens of bytes (ID and sensor state), and their practical reception radius is typically tens of meters. In depot or station environments, a single access point can cover several tracks. Wi-Fi coverage from one access point (depending on output power and obstacles) usually spans several tens of meters radius. For example, IEEE 802.11n/ac equipment can maintain stable links at distances up to 50–100 m in open areas. At shunting speeds up to 10–20 km/h, BLE advertisements can be captured sequentially by several gateways. Tests showed that with an advertisement interval of approximately 1 s, stations received over 90% of messages for consists moving at speeds up to about 15 km/h. The use of PoE-mounted wall

https://doi.org/10.56143/3030-3893-2025-3-30-33 A bridge between science and innovation

or ceiling access points demonstrated reliable powering and straightforward installation without the need to run separate mains cabling.

Solution for the classification (sorting) yard

On a classification yard the system operates as a simple chain: beacons → receivers → server. Each wagon carries a compact wireless beacon that periodically transmits its identifier and basic telemetry (temperature, sensor alarms, etc.). Stationary receivers, mounted along tracks and powered via the Ethernet network, capture these transmissions and forward them over the local network to a central processing point.

Coverage planning ensures overlap between receiver footprints so a wagon is typically observed multiple times, enabling accurate localization. Receivers are placed more densely in areas of intensive shunting and on the hump, and more sparsely in less active zones.

To ensure fast and reliable operation, receivers perform simple edge preprocessing: they discard irrelevant signals, compress repeated messages and timestamp each record together with the receiver identifier. If the connection to the server is temporarily lost, a receiver buffers data locally and forwards it when the link is restored.

At the server, raw records are merged into events such as wagon arrival, departure, track transfer and prolonged stoppage. A practical rule is used: several detections within a short time window constitute a confirmed event. These events are used to automatically produce an electronic consist manifest — a list of wagons with timestamps and location of detection, together with available telemetry.

Operational best practices include synchronized time across all devices (to properly order events), coverage calibration (measuring signal level along tracks) and battery status monitoring for beacons. For robustness, zones are overlapped by multiple receivers and a redundant data path is provided in case of primary network failure.

Integration with enterprise systems is supported via simple interfaces: the server provides data in commonly used formats (for example, JSON) and offers dispatchers a station map, wagon processing times and key operational metrics. Implementation typically begins with a pilot sector: testing, adjustment of receiver density, and then progressive scaling across the station.

The key outcome is automation of recordkeeping and acceleration of processing: reduced manual input, faster generation of consist manifests, improved inventory accuracy and faster detection of deviations in train handling.

4. Discussion

The proposed approach offers high throughput and integration with existing IT infrastructure. Wi-Fi provides significant data rates (megabits per second and higher) and a bidirectional channel, unlike long-range low-power networks such as LoRaWAN. PoE simplifies access point installation because separate power sources are not required. Using BLE beacons conserves energy onboard and does not require complex onboard equipment.

However, limitations exist. The range of Wi-Fi is notably smaller than that of LoRaWAN, so a denser network of access points is required. Both BLE and Wi-Fi operate in the 2.4 GHz band, which can cause mutual interference. It is recommended to avoid overlapping Wi-Fi channel allocations with BLE advertising where possible — e.g., configure Wi-Fi to non-overlapping channels (1, 6, 11) while BLE uses its own channel scheme. Applicability varies by environment: at stations and in depots (bounded areas with stable power and cabling) Wi-Fi + PoE is a good fit — access points can be installed under canopies or on platform posts. On long line sections, the system is effective mainly for short control zones (for example, at weigh stations or at localized track sensors). For extended line coverage, LTE or LoRaWAN remain preferable. Overall, BLE + Wi-Fi/PoE is most useful where a wired network exists and a large volume of near-real-time data is required (for example, centralized monitoring of wagon stock in depots and around stations).

5. Conclusion

This study has presented and analyzed a monitoring system for freight railcars based on the integration of Bluetooth Low Energy beacons and a Wi-Fi/PoE backbone infrastructure. The proposed architecture demonstrates that the combination of energy-efficient short-range wireless communication and high-capacity wired transport channels can effectively address the operational challenges of wagon monitoring in stations and depots. BLE beacons provide a low-maintenance and long-lasting mechanism for transmitting identifiers and telemetry, while Wi-Fi access points powered over Ethernet ensure reliable data collection, centralized power distribution, and straightforward installation without the need for additional cabling.

The results of pilot tests and model evaluations confirm the applicability of the approach in environments with dense wagon flows, such as sorting yards, where overlapping coverage zones and redundant gateways enable reliable data reception even during intensive shunting operations. Data aggregation on the server side allows the system to automatically generate electronic consist manifests, detect wagon movements, and record telemetric events such as temperature changes or impacts. This contributes directly to the automation of logistics processes, improved data accuracy, and reduced reliance on manual input.

When compared to alternative technologies, the proposed solution has both advantages and constraints. In contrast to LoRaWAN, which supports communication over several kilometers [3][4], Wi-Fi offers significantly higher throughput and supports real-time data exchange, but requires denser deployment of access points. Unlike GSM/LTE or NB-IoT solutions [5][11], Wi-Fi/PoE avoids recurring operational costs and dependence on public networks, but it is limited to areas with available wired infrastructure. Similarly, while RFID provides robust identification [6][7], it does not inherently support continuous telemetry. Therefore, BLE combined with Wi-Fi/PoE is best positioned as a station- and depot-focused solution, where it can complement rather than replace wide-area technologies.

Overall, the integration of BLE and Wi-Fi/PoE contributes to the ongoing digital transformation of railway transport, enabling more efficient rolling stock management, increased transparency in freight operations, and the foundation for advanced predictive analytics [1][2][10]. Future research should focus on hybrid system architectures that leverage the strengths of different technologies — BLE/Wi-Fi/PoE for localized high-resolution monitoring and LoRaWAN or NB-IoT for long-haul tracking. Such convergence would enable a truly scalable and resilient monitoring framework capable of supporting both domestic and international freight corridors in line with the broader

vision of smart rail transport.

References

[1] Zanelli F., Mauri M., Castelli-Dezza F., et al. Energy autonomous wireless sensor nodes for freight train braking systems monitoring // Sensors. 2022. Vol.22, no.5. P.1876.

[2] GAO Tek Inc. Railway and Infrastructure Monitoring – Predictive Maintenance IoT [Electronic resource]. Available at: https://www.gaotek.com/railway-and-infrastructure-monitoring-predictive-maintenance-iot.

[3] Actility. SNCF Implements LoRaWAN IoT Solutions to Monitor Railway Assets and Rolling Stock [Electronic resource]. Available at: https://www.actility.com/sncf-blog.

[4] Tang H., Kong L.J., Du Z.B., et al. Sustainable and smart rail transit based on advanced self-powered sensing technology // iScience. 2024. Vol.27, 104283.

[5] Artmatica LLC. Freight container monitoring device [Electronic resource]. Available at: https://www.artmatica.ru/product/seti/iot-modemy/ustroystvo-monitoringa-zhd-konteynerov.

[6] GAO RFID Inc. RFID Railway Management System [Electronic resource]. Available at: https://gaorfid.com/gao-railway-management-system.

[7] Smiley S. RFID & Railways [Electronic resource]. Available at: https://www.atlasrfidstore.com/rfid-insider/rfid-railways

[8] GAO RFID Inc. PoE BLE Gateways [Electronic resource]. Available at: https://gaorfid.com/devices/ble/ble-gateways/poe-ble-gateways.

[9] Westermo AB. Rail Approved Onboard Wi-Fi Solutions [Electronic resource]. Available at: https://www.westermo.com/us/industries/train-networks/wireless-solutions/onboard-wifi.

[10] Hossain A., Fraga-Lamas P., Fernández-Caramés T.M., Castedo L. Toward the Internet of Smart Trains: A Review on Industrial IoT-Connected Railways // Sensors. 2017. Vol.17, no.6. P.1457.

[11] Tinu O. Application of sensors and wireless technologies for IIoT // Wireless Technologies. 2021. No.3-4.

Information about the author

Shokhrukh Kamaletdinov	Tashkent State Transport University, Associate Professor of the Department of Operational Work Management in Railway Transport (DSc) E-mail: shoxruxkamaletdinov@gmail.com Tel.: +998935834569 https://orcid.org/0000-0002-4004-9736
Islom Abdumalikov	Tashkent State Transport University, PhD student, Department of Operational Management in Railway Transport E-mail: Islomjonabdumalikov93@gmail.com Tel.: +998909099965 https://orcid.org/0009-0000-5882-5978
Fayzulla Khabibullaev	Tashkent State Transport University, PhD student, Department of Operational Management in Railway Transport E-mail: fayzulla.habibullayev@mail.ru Tel.: +998935304639 https://orcid.org/0009-0002-9477-3903

Innovative method for managing the power supply of automation and telemechanics devices in railway infrastructure

A.A. Ablaeva[1][a]
[1]Tashkent state transport university, Tashkent, Uzbekistan

Abstract: The article discusses a system for managing the power supply of automation and telemechanics devices in railway transport. It provides an algorithm for the system's operation, ensuring secure data exchange between the control center and line control points. Additionally, improvements to the system are proposed, including the use of artificial intelligence technologies for predicting emergency situations, the use of secure communication channels, and the introduction of a decentralized event log.

Keywords: railway transport, uninterruptible power supply, signaling and communication, intelligent system, parameter control

1. Introduction

The reliability of the power supply to automation and The reliability of the power supply to automation and telemechanics systems is a basic prerequisite for the safe and uninterrupted operation of railway transport. The stability of the transport process, the prevention of emergencies and the minimisation of risks during train movement depend on the correct operation of signalling, centralisation and interlocking (SCI) facilities. Disruptions in the power supply to these systems can lead to serious failures, including forced stoppages, loss of control and significant economic costs.

Modern automated control and management systems, such as SCADA and automated monitoring and telemechanics (AMT) systems, provide a wide range of functions: from the collection and storage of technological information to remote control of switching equipment and energy consumption accounting. Their implementation has significantly increased the level of process automation and reduced the workload on operational personnel. However, despite their high level of functionality, these systems have a number of limitations. In particular, factors such as high electromagnetic interference immunity, the presence of long communication lines, a complex power supply structure, and the need for continuous real-time operation of control systems are of particular importance in the railway infrastructure.

Cybersecurity is a separate issue. Traditional SCADA systems, originally designed for energy and industrial production facilities, have limited mechanisms to protect against targeted cyberattacks. In recent years, there has been an increase in the number of incidents involving unauthorised interference with transport infrastructure facilities, making the protection of communication channels and control devices a priority. Vulnerabilities can manifest themselves at the level of network protocols as well as at the level of controller software and server applications. This increases the risk of unauthorised changes to equipment operating modes, the failure of critical nodes and, as a result, the occurrence of emergency situations[1-3].

In this regard, the development of new power supply control systems for automation and telemechanics devices with the integration of modern data protection methods is a relevant scientific and practical task. The use of cryptographic protection technologies, multi-level authentication, and intelligent data analysis algorithms will not only increase the reliability of the infrastructure, but also bring its resistance to external and internal threats to a qualitatively new level.

Thus, the research presented in this paper is aimed at solving a set of problems related to ensuring the stable power supply of signalling systems, their monitoring and protection from cyber threats, which together form the basis for improving the overall safety of railway transport.

2. Research methodology

The proposed system includes hardware and software complexes integrated into a single control network. The central element is the automated workstation (AWS) of the energy dispatcher, which generates control commands and visualises the status of the equipment. To protect data exchange channels, a cryptographic protection module is used at the dispatch centre, which performs digital signing and verification of messages. The IP data transmission network is based on a local computer network and managed switches that provide packet routing. Linear control points are equipped with their own protection modules and perform command authentication, cryptographic processing, and interaction with power supply devices (switching equipment, distribution boards, uninterruptible power supplies). Each control point has a unique network address, which ensures accurate command routing [4,5]. A block diagram of the control architecture of the integrated power supply control system for automation and telemechanics devices for railway transport is shown in Figure 1.

The automated workstation (AWS) of the power dispatcher is the central control element. It generates control commands, provides visualization of the control circuit mnemonic diagram, and displays the status of the equipment in real time.

The control center protection module is a specialized microprocessor responsible for digitally signing outgoing packets, checking incoming messages, and coordinating the protection of line points.

The IP data transmission network includes a local computer network and network switches. The network provides packet routing and connection to line control points[6].

[a] https://orcid.org/0000-0002-7713-1602

Line control points (CP) are hardware and software complexes that have unique network addresses and interact with specific power supply devices. Each CP is equippedwith a protection module. Line control point protection modules verify the authenticity of commands and return messages. They perform cryptographic processing using digital signatures, which eliminates the possibility of interference [7-10].

Power supply devices for automation and telemechanics devices are switching equipment, distribution boards, uninterruptible power supplies, and other equipmentresponsible for powering signaling and interlocking facilities.

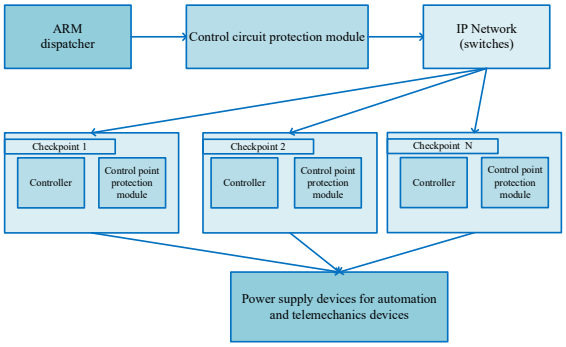

Fig. 1. Block diagram of the control architecture of an integrated power supply monitoring system for automation and telemechanics devices for railway transport

In addition, artificial intelligence algorithms are being incorporated into the architecture, enabling the analysis of telemetry data and the identification of hidden patterns that precede failures.

Developed method

The algorithm for the functioning of the control system for the power supply of automation and telemechanics facilities, shown in Figure 2, can be divided into four levels of processes: command formation, command processing and transmission, command execution, and feedback.

Command formation and preparation. The dispatcher, working at the ARM, selects the control object (e.g., feeder, sectional disconnector, or backup power source) on the mnemonic diagram. The workstation software generates a primary data packet that includes the unique network address of the line control point (CP), the identifier of a specific power supply device, the command type (enable, disable, switch, request diagnostics, etc.), and a timestamp to prevent "repeated attacks." The packet is transmitted to the control center protection module for protection [11].

Cryptographic processing and data protection includes packet signing, key pair generation, channel encryption, and routing. The control center protection module applies an electronic key to the packet using a private key. The system generates a public/private key pair for a specific exchange session. This prevents data substitution during long-term operation. The packet can additionally pass through a secure VPN tunnel, which prevents interception at the network level. The signed packet is sent to the IP network and transmitted to the required control point via network switches.

The packet is then received and verified at the line control point. The control point receives the message through the control point protection module. The electronic key is then verified, and the control point protection module uses the public key to verify the authenticity of the packet. If the key is correct, the packet is forwarded. If the key does not match, the packet is blocked and a report of an unauthorized access attempt is sent. The control point analyzes the device ID and command. If the command does not match the control point configuration or equipment operating mode (for example, re-enabling an already enabled device), it is ignored and recorded in the log[12-14].

The control command is then executed. The control point converts the command into a physical signal, the power supply device closes or opens the circuit, switches the power source, turns on the backup power supply, and performs a self-diagnostic test cycle.

The power supply device performs a self-diagnostic test: checking the status of the control sensors. The control point collects monitoring data and forms a return packet containing the current status of the device (on/off/error), diagnostic parameters (voltage, current, temperature), and a timestamp. The return packet is signed with an electronic key in the control point's protection module and sent to the IP network.

The control room circuit protection module at the control room checks the electronic key of the incoming packet. The ARM updates the status of the object on the control room circuit mimic diagram. The dispatcher receives visual and audible indications of the successful execution of the command or the presence of errors or alarm signals. All events are automatically recorded in the log for subsequent analysis [15].

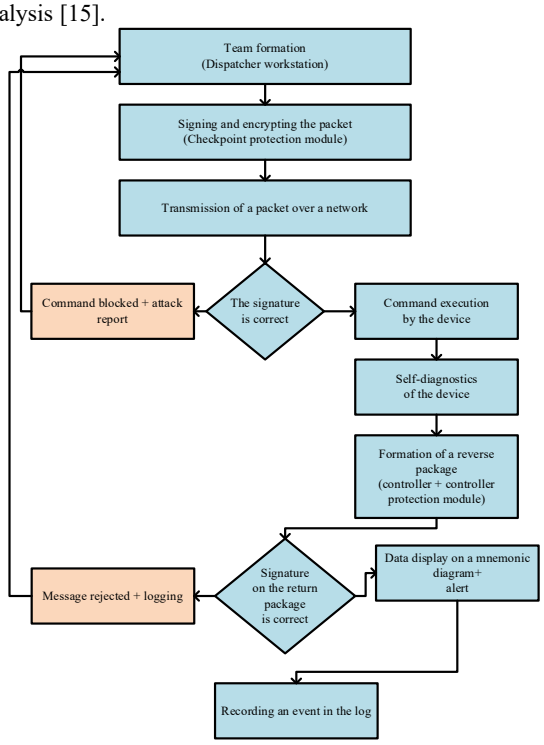

Fig. 2. System operation algorithm

If an invalid key is detected, the command is blocked. In the event of a repeated attack, the system can automatically terminate the connection with a suspicious controller. In the event of a communication channel failure, a backup channel is activated. If one of the control point protection modules is faulty, control of the facility can be transferred via a neighboring control point if a bypass route is available.

3. Results

The presented architecture and algorithm have shown that the implementation of cryptographic mechanisms in the power supply control system of telemechanics facilities allows the following results to be achieved. The electronic key eliminates the possibility of substitution or modification of control commands, which makes the system secure against man-in-the-middle attacks and replay attacks. Data from linear control points is protected by an electronic key, which prevents falsification of diagnostic indicators. Reduced likelihood of emergencies. Filtering of invalid commands at the control point eliminates the possibility of erroneous or malicious actions. The system displays the status of equipment in real time, records all events, and automatically warns of malfunctions.

Unlike SCADA, the new system has built-in cryptographic protection mechanisms, protects not only the transmission protocol but also each control command, operates on a zero trust principle (a command is considered valid only when its authenticity is confirmed), and provides for the redundancy of communication channels and control nodes, which increases fault tolerance.

The introduction of artificial intelligence algorithms significantly expands the capabilities of the proposed system, taking it beyond traditional control and diagnostics. Based on the analysis of telemetry data (currents, voltages, temperature, frequency of operations), neural network models can identify hidden patterns that precede a failure. This allows for advance planning of equipment replacement or repair, reducing the risk of accidents. Machine learning algorithms can automatically detect deviations from normal operating conditions (voltage surges, sudden load changes). The system generates alerts to the dispatcher and recommends corrective actions. Using intelligent load management techniques, the system can balance consumption and connect reserves only when necessary. This is especially relevant when integrating renewable sources (solar panels, wind turbines) into the railway infrastructure. AI can analyze network traffic and identify suspicious commands, even if they pass cryptographic verification but differ from the typical control profile. This implements the concept of a "second line of defense" against cyberattacks.

The introduction of artificial intelligence can reduce accidents and the number of unscheduled repairs, increase the efficiency of equipment use, automate some of the dispatcher's functions (smart prompts, recommendation systems), and increase the cyber resilience of the system.

4. Conclusion

The control algorithm for the integrated power supply control system for automation and telemechanics devices for railway transport is an innovative solution that ensures secure data exchange and reliable equipment control.

The implementation of cryptographic mechanisms prevents command substitution and ensures the reliability of data exchange between the dispatcher and line control points. The system implements a closed control loop: from command formation to feedback and visualization of the result, including error handling and cyberattacks. The system has been shown to respond effectively to both emergency situations (power outages on the line) and cyber threats, ensuring recovery of operability and documentation of events. The use of artificial intelligence methods (failure prediction, digital twins, intelligent command filtering) allows a transition from reactive to predictive control. This reduces accidents and increases economic efficiency. In the future, the system may be supplemented with blockchain logging, quantum-resistant cryptography, and Smart Grid technologies, which will create the basis for building a digital railway infrastructure. Promising areas for further development include the introduction of quantum-resistant cryptography, blockchain event logging, and integration with the Smart Grid concept.

Thus, the proposed system could become the basis for building a digital and cyber-resilient railway transport infrastructure capable of effectively countering modern challenges and threats.

References

[1] C.P. Aboelela, W. Edberg, V. Vokkarane, “Wireless sensor network based model for secure railway operations,” Proceedings of the 25th IEEE Performance, Computing, and Communications Conference, 2006, pp. 623-628.

[2] G.M. Shafiullah, S.A. Azad, “Energy-efficient wireless MAC protocols for railway monitoring applications,” IEEE Trans. Intell. Transp. Syst. 14 (2) (2013) pp. 649-659.

[3] J. F. Kurbanov, D. N. Roenkov and N. V. Yaronova, “Diagnostic and Control System for Increasing the Efficiency of Solar Panel Based on Microprocessor Elements,” 2023 Seminar on Electrical Engineering, Automation & Control Systems, Theory and Practical Applications (EEACS), Saint Petersburg, Russian Federation, 2023, pp. 186-189, doi: 10.1109/EEACS60421.2023.10397328.

[4] Sapozhnikov V. V., Kovalev N. P., Kononov V. A., Kostrominov A. M., Sergeev B. S. Power Supply for Railway Automation, Remote Control and Communication Devices. Moscow: Educational and Methodological Center of Railway Transport, 2005.

[5] Serdyuk T. M., Oleynik A. R. Use of batteries at electrical centralization posts, crossings and battery cabinets of incoming traffic lights. Electromagnetic compatibility and safety on railway transport, 2016, no. 11, pp. 24–34.

[6] Serrano-Jiménez D., Abrahamson L., Castaño-Solís S., Sanz-Feito J. Electrical railway power supply systems: Current situation and future trends. International Journal of Electrical Power & Energy Systems, vol. 92, pp. 181–192, 2017. doi:10.1016/j.ijepes.2017.05.008

[7] A.A. Ablayeva,. N.V. Yaronova, O.O. Ruzimov, “Ensuring a Reliable Power Supply for Railway Traffic Lights Using Renewable Energy Sources,” Proceedings - 2024 International Ural Conference on Electrical Power Engineering, UralCon 2024, 2024, pp. 600-604

[8] V. V. Sapozhnikov, N. P. Kovalev, V. A. Kononov, A. M. Kostrominov, and B. S. Kostrominov, “Power Supply for Railway Automation, Remote Control and Communication Devices,” Moscow: Educational and Methodological Centre of Railway Transport, p.543, 2005.

[9] D. Serrano-Jiménez, L. Abrahamson, S. Castaño-Solis, and J. Sanz-Feito, “Electrical railway power supply systems: Current situation and future trends,” International

Journal of Electrical Power & Energy Systems, vol. 92, pp. 181-192, 2017.

[10] J. Qian, W. Guo, H. Zhang, and X. Li, “Research on automatic test method of computer-based interlocking system,” International Conference on Communications, Information System and Computer Engineering (CISCE), 3-5 July 2020, Kuala Lumpur, Malaysia, pp. 298-302.

[11] A. Srivastava, A. Singh, G. Joshi, and A. Gupta, “Utilisation of wind energy from railways using vertical axis wind turbine,” International Conference on Energy Economics and Environment (ICEEE), 27-28 March 2015, Noida, India, pp. 1-5.

[12] Kuraish Bin Quader Chowdhury, Moshiur Rahman Khan, Md. Abdur Razzak, “automation of rail gate control with obstacle detection and real time tracking in the development of bangladesh railway,” IEEE 8th R10 Humanitarian Technology Conference (R10-HTC), pp.1-6, 2020.

[13] A. Khalikov, A. Khurramov, O. Urokov, S. Rizakulov, “A mathematical model of the operation process of a radio communication network based on IP technologies in the conditions of information impact during the transmission of a non-repetitive data stream,” E3S Web of Conferences 420, art. no. 03022, 2023

[14] N. Zhao, C. Roberts, S. Hillmansen and G. Nicholson “A multiple train trajectory optimisation to minimize energy consumption and delay,” IEEE Transactions on Intelligent Transportation Systems, vol. 16, art. no. 5, pp. 2363-2372, 2015.

[15] J. Andruszkiewicz, J. Lorenc, A. Weychan, “determination of the optimal level of reactive power compensation that minimises the costs of losses in distribution networks." Energies 2024, pp.150.

Information about the author

Ablaeva Aliye Ayderovna
Tashkent State Transport University, Department “Radio-electronic Devices and Systems”
E-mail: aliewka4703@mail.ru
Tel.: +998 97 403 42 20
https://orcid.org/ 0000-0002-7713-1602

On the issue of mechanical activation of burnt moulding waste

A.I. Adilkhodzhaev[1][a], I.A. Kadyrov[1][b], D.F. Tosheva[1][c]
[1]Tashkent state transport university, Tashkent, Uzbekistan

Abstract: This article is devoted to the study of the processes of mechanical activation of burnt moulding waste (BMW) with the aim of using it as a highly active mineral additive in building materials. In the course of the work, the kinetics of BMW grinding and its dependence on technological parameters were studied. Experiments have shown that mechanical activation leads to a significant increase in the specific surface area of BSF and its amorphisation, which increases the reactivity of the material. The data obtained confirm that BSF, after mechanical activation, can serve as an effective component for improving the properties of cement composites.

Keywords: mechanical activation, burnt moulding waste, grinding kinetics, amorphisation, specific surface area, building materials

1. Introduction

Mechanical activation is a fundamental and highly versatile technological method in modern industry, designed to transform a wide range of raw materials into high-performance technical products. This process is not a mere comminution or size reduction; it represents a deliberate and profound modification of the internal structure of solid materials through intense and controlled mechanical energy input. This targeted processing imbues the material with entirely new, often unique, physical, chemical, and mechanical properties, making it suitable for a diverse array of applications. Among the various types of comminution equipment used for mechanical activation, drum ball mills are particularly effective and widely recognized for their efficiency and versatility [1-8]. During mechanical activation, the processed material undergoes significant structural and morphological transformations. The intense mechanical impact leads to a substantial accumulation of crystal lattice defects, such as dislocations and vacancies, resulting in a pronounced increase in the material's internal energy. Furthermore, the surface relief of the particles becomes increasingly rough, which dramatically enhances their reactivity. It is also noteworthy that high-energy mechanical impact can initiate various phase transformations, including the transition from a crystalline state to an amorphous one. This process, known as amorphization, ultimately results in the formation of highly disordered structures. The resulting fine-grained particles, due to these complex structural and morphological changes, exhibit significantly higher chemical activity and reactivity, which is of paramount importance for subsequent technological processes and applications. This section presents a detailed account of the experimental studies focused on the process of mechanical activation of burnt waste forms (BWF). The research aims to evaluate the effectiveness of this method in converting BWF into a valuable, highly reactive material with enhanced properties for potential use in the construction industry. The findings contribute to the understanding of the mechanisms governing mechanical activation and its practical application for waste valorization.

2. Research methodology

These studies focused on analysing the main indicators of the dispersion state of the products obtained, namely the relative particle surface area, average diameter and aggregation process. These properties were determined for materials processed in the impact-friction mode of a ball mill, which allows the effectiveness of mechanical activation and the degree of grinding to be assessed. A special laboratory ball mill ШЦМ-100 was used to conduct laboratory experiments on the grinding of BWF. This device was chosen because it provides an impact-wear grinding mode, which is optimal for achieving a high degree of material activation. The working volume of this mill chamber is 100 litres, which allows a sufficient amount of material to be processed for research. Filling the mill with grinding media is an important indicator: 40 litres of the total volume is filled with hardened steel balls, which provide the necessary impact and wear action. The amount of material loaded into the mill was strictly defined and amounted to 25% of the total volume of the working chamber. This ensures optimal grinding conditions and prevents the material from overheating.

The degree of grinding is the main indicator for a comprehensive characterisation of the dispersed state of powdered materials obtained in the process of mechanical activation. Its quantitative assessment was carried out by determining the specific surface area using a high-precision ПСХ-11А device. This method allows the degree of particle distribution to be reliably determined. In addition, to control and reduce the effect of particle aggregation (clumping), which is extremely important for obtaining a homogeneous and reactive product, a standardised sieve analysis method was used with sieve No. 008. This approach allows for the verification of aggregation, which can reduce the efficiency of subsequent technological processes.

3. Results and Discussion

An exhaustive analysis of the experimental data obtained from studying the grinding of burnt waste forms (BWF) has provided a comprehensive understanding of the kinetics and mechanisms of the process. The results, specifically the

[a] https://orcid.org/0000-0001-5729-5178
[b] https://orcid.org/0000-0003-3924-0864
[c] https://orcid.org/0009-0006-9710-0746

dependence of the degree of grinding and productivity on key parameters, are clearly presented as graphical relationships in Figures 1-3.

In materials science and industrial practice, it is widely recognized that the grinding process, particularly during mechanical activation, is nonlinear and can be conceptually divided into several distinct and sequential stages [9-13].

The first stage is characterized by primary dispersion and the initial fracture of large structures. During this nascent phase, the material undergoes an intense and rapid breakdown, exposing both macroscopic and microscopic pores. The dominant mechanical actions, such as impact and attrition, effectively overcome the strong macroscopic cohesive forces, leading to the formation of primary fragments of various sizes. It is particularly noteworthy that in this initial stage, the relative surface area of the material increases almost in direct proportion to the electrical energy consumed. This linear relationship highlights the high efficiency of energy expenditure, as the majority of the applied mechanical energy is productively converted into the creation of new surface area.

The second stage marks a transition to microstructural comminution and defect accumulation. As the process continues, the material reaches a degree of fineness where it no longer fractures into conventional, easily separable particles. Instead, the focus of the grinding shifts to the internal structure, targeting individual crystals and grains. This phase is significantly more energy-intensive, as the resistance to grinding increases dramatically. The number of readily breakable surfaces diminishes, and the energy is now required to overcome stronger bonds within the crystal lattice and to create new defects, such as dislocations and vacancies. The work required to break these internal bonds is highly dependent on the material's microstructure and its phase composition. While the rate of increase in relative surface area slows down during this stage, a linear relationship between energy consumption and surface area growth is still maintained, albeit with a reduced proportionality coefficient [14-17].

The third and final stage is defined by aggregation and the attainment of the grinding limit. At this advanced stage of intense mechanical action, a critical point of dispersion is reached. A distinguishing feature of this phase is the phenomenon of re-aggregation, where the previously separated, highly dispersed particles begin to cluster together. Due to their extremely high surface energy and enhanced reactivity, these fine particles are highly susceptible to forming larger agglomerates through van der Waals forces and electrostatic attraction. This aggregation process effectively counteracts the ongoing comminution, reducing the efficiency of further grinding. This can even lead to a paradoxical outcome: a stabilization or even a slight decrease in the relative surface area, despite the continuous input of energy. The third stage, therefore, serves as a crucial indicator that a technological limit to grinding has been reached under the current conditions. To achieve further dispersion, it becomes necessary to modify the process parameters or to introduce additional methods aimed at preventing this undesirable aggregation.

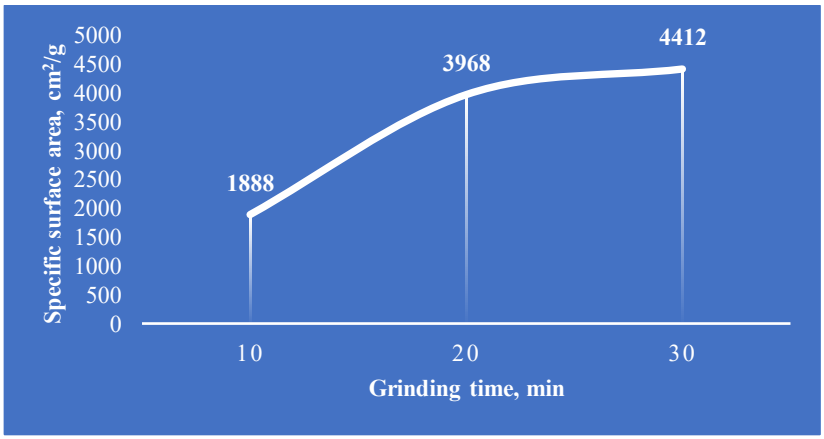

Figure 1. Effect of grinding duration on the relative surface area of BWF

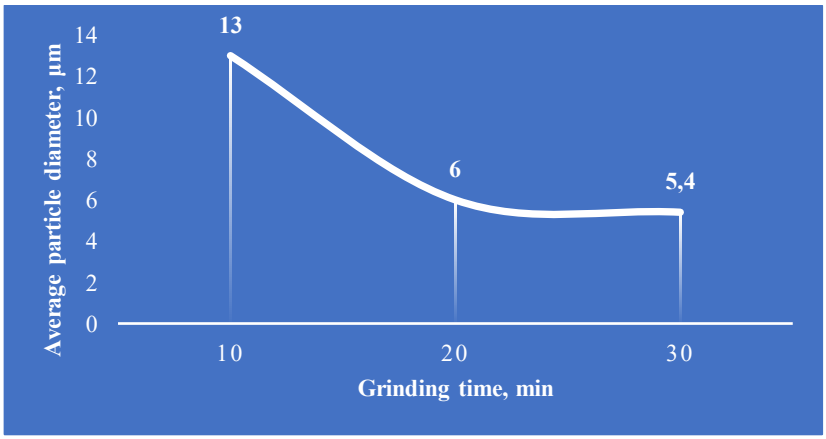

Figure 2. The effect of grinding duration on the average diameter of BWF particles

https://doi.org/10.56143/3030-3893-2025-3-38-42 A bridge between science and innovation

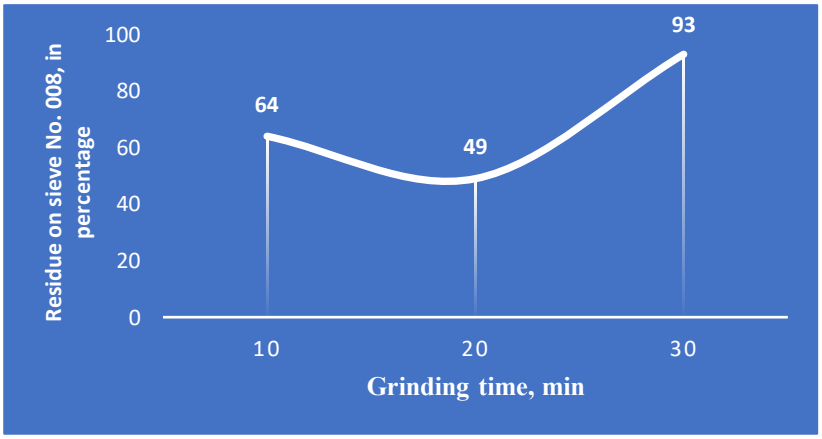

Figure 3. Effect of grinding duration on the aggregation of BWF particles

Experimental studies conducted to analyze the effects of mechanical activation on Burnt Waste Forms (BWF) demonstrated a profound change in the material's relative surface area. It was established that with a grinding duration of 30 minutes, the relative surface area of the BWF reached a peak value of 4412 cm²/g. This significant increase is a direct indicator of enhanced dispersion and elevated reactivity. Simultaneously, a corresponding decrease was observed in the average particle diameter of the BWF, which was reduced from an initial 13 µm to just 5.4 µm. This reduction in particle size is a clear and quantifiable result of the intense mechanical action, confirming the effectiveness of the grinding process in achieving the desired fineness.

The fundamental principle of comminution dictates that as the size of individual particles decreases, the total surface area of the substance increases multifold, while the total volume remains constant. This rapid increase in surface area leads to the accumulation of a significant amount of surface potential energy. This stored energy acts as a powerful driving force for subsequent physicochemical processes, making the material highly reactive in applications such as composite material manufacturing or reactions at a phase boundary. However, research indicates that upon reaching a certain dispersion limit, the surface potential energy can escalate to critical levels, which frequently triggers the spontaneous aggregation of particles into larger clusters. This phenomenon, which is particularly evident in highly dispersed materials, can nullify the positive effects of mechanical activation, reducing reactivity and impairing the final product's technological properties. The formation of these conglomerates from previously separated particles can lead to a decrease in the overall relative surface area and a loss of material homogeneity.

Further analysis, specifically a sieve analysis using sieve No. 008, corroborated the observed dispersion dynamics. Initially, the residual content on the sieve for BWF decreased from 64% to 49% as the grinding duration increased. However, when grinding continued for more than 30 minutes, a sharp and dramatic increase in the residue on the sieve was observed, reaching an alarming 93%. This abrupt rise serves as a clear indication of intensive particle adhesion and the formation of large aggregates, demonstrating that continuing the grinding process beyond this point is counterproductive. Increased agglomeration not only diminishes the efficiency of the grinding process itself but also poses a potential risk to the physical and mechanical properties of the cementitious materials produced from such an activated substance.

The crushability of a material is determined by a combination of its main physical properties, including its hardness, brittleness, and specific microstructural features. To allow for a comparative assessment, data on the grindability of various materials are often normalized relative to Portland cement clinker, with its value taken as a unit [18-23]. This approach provides an objective benchmark for evaluating the energy consumption and grinding efficiency of different raw materials. Materials that are softer or more brittle than clinker will have a grindability value greater than 1, indicating they are easier to grind and require less energy. Conversely, materials with a value less than 1 are harder and demand more energy to achieve the same level of fineness. Beyond these properties, a material's grindability is also influenced by its chemical and mineralogical composition, as well as the specific grinding conditions used in the process.

Within this study, a comparative assessment of the grindability of burnt waste forms (BWF), quartz sand, and cement clinker was performed. To ensure the comparability of the results, all initial materials were first pre-ground to a standardized specific surface area of 500 cm²/g. After this initial processing, the materials were stored at a temperature of 25°C for 24 hours to stabilize them before the main experiment.

Table 1

Grindability of various raw materials

The Nomenclature of Materials	Crushability
Limestone	0,6-0,8
Blast furnace slag	1,2-1,8
Opoka	1,1-1,2
Trass	0,5-0,6
Quartz sand	0,8-0,9
Cement clinker	1,0

The grindability assessment was conducted using an SHLM-100 laboratory ball mill as shown in Fig. 4. This controlled milling process allowed for a precise evaluation of how each material responded to grinding. By starting with a uniform particle size and using the same equipment and conditions for each sample, the researchers were able to objectively compare the energy and time required to achieve a desired fineness, thereby determining the relative grindability of each material.

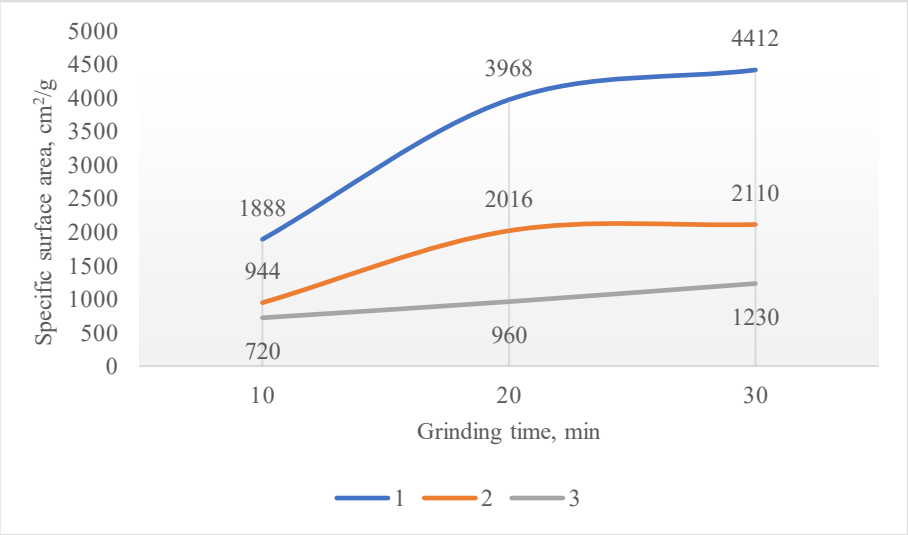

Figure 4. Grindability of BWF (1), quartz sand (2), and clinker (3) in the impact-abrasion mode of a ball mill

The conducted research has definitively established that, among the materials studied, burnt waste forms (BWF) exhibit superior grindability. As a result of mechanical activation, this material achieves a remarkable specific surface area of approximately 4400 cm²/g in just 30 minutes. This exceptional performance underscores the high efficiency of its dispersion and its pronounced susceptibility to comminution. The superior grindability of BWF is scientifically attributed to its unique structural characteristics and high-temperature origin. It is hypothesized that the primary factor is the intensive amorphization of the slags within the BWF, a process that occurs during their formation at high temperatures. This thermal treatment disrupts the ordered crystal lattice, leading to a high concentration of structural defects and a significant increase in the amorphous phase. Consequently, the bond strength between individual structural elements within this amorphous material is considerably lower compared to other additives, which predominantly have a crystalline structure or stronger intergranular bonds. This weakened internal structure allows external mechanical energy to overcome internal bonds more easily, facilitating the rapid breakdown of the material into smaller particles. This, in turn, contributes to the rapid increase in specific surface area. The inherent amorphous state and low interphase boundary strength of BWF make it a highly promising material for technological applications requiring a high degree of dispersity and reactivity.

4. Conclusion

Studies have shown that mechanical activation is an effective method for modifying burnt moulding waste (BMW), transforming it into a valuable raw material component for the construction industry. Achieving a high specific surface area and amorphous state of BFA as a result of mechanical activation significantly increases their pozzolanic activity, making them comparable to traditional mineral additives. This opens up broad prospects for the use of BFA as an active component that improves the physical, mechanical and operational properties of cementitious materials, as well as solving the problem of industrial waste disposal.

References

[1] Adylkhodjayev Anvar, Kadyrov Ilkhom, Shaumarov Said, Umarov Kadir. Some Peculiarities of the Process of Preparing the Zeolites Containing Breeds in a Ball Mill // International Journal of Recent Technology and Engineering (IJRTE) ISSN: 2277-3878, Volume-8 Issue-4, November 2019.

[2] Адилходжаев А.И., Кадыров И.А, Умаров К.С., Назаров А.А. К вопросу механоактивации цеолитсодержащих пород // Известия Петербургого Государственного университета путей сообщения, №3, 2019. ISSN 1815-588X. Известия ПГУПС. С. 489-498.

[3] Лукутцова Н.П., Пыкин А.А. Теоретические и технологические аспекты получения микро- и нанодисперсных добавок на основе шунгитосодержащих пород для бетона. Монография. – Брянск: Изд-во БГИТА, 2013. – 231 с.

[4] Gupta, R., & Siddique, R. (2020). Mechanical and thermal methods for reclamation of waste foundry sand. J Environ Manage.

[5] Siddique, R., & Khatib, J. (2011). Utilization of waste foundry sand in concrete: A review. Resources, Conservation and Recycling.

[6] Masoud, A. J., & El-Hassan, H. (2021). Recycled waste foundry sand in cementitious materials: A review. Construction and Building Materials.

[7] Torkaman, J., & Esmaeili, H. (2019). An investigation on the mechanical activation of spent foundry sand for use as a supplementary cementitious material. Cement and Concrete Composites.

[8] Torkaman, J., & Esmaeili, H. (2018). Mechanical activation of waste foundry sand and its effect on the properties of cementitious composites. Materials and Structures.

[9] Siddique, R. (2019). The use of waste foundry sand in concrete: A review. Concrete and Cement Research.

[10] Yin, Y., Liu, Z., & Chen, G. (2020). Research on the mechanical activation of spent foundry sand and its application in cementitious materials. Journal of Cleaner Production.

[11] Varenya, D., & Pal, S. K. (2019). A comparative study on the effect of mechanical and chemical activation of

waste foundry sand on its pozzolanic activity. International Journal of Concrete Structures and Materials.

[12] Dukhanov, A., & Rybin, E. (2022). Enhancing the properties of concrete using mechanically activated burnt molding sand waste. IOP Conference Series: Materials Science and Engineering.

[13] Al-Jumaili, Y. K., & Al-Tameemi, N. T. (2021). The use of activated waste foundry sand as a pozzolanic material in cement mortar. Journal of Building Engineering.

[14] Gencel, O., Oruç, F., & Koç, K. (2019). Influence of mechanical activation on the properties of cement mortar with waste foundry sand. Construction and Building Materials.

[15] Ma, S., et al. (2020). Effect of grinding on the pozzolanic activity of waste foundry sand. Journal of Materials in Civil Engineering.

[16] Li, W., et al. (2021). Investigation of the mechanical properties of cement mortar incorporating mechanically activated waste foundry sand. Materials.

[17] Singh, N., et al. (2018). Enhancement of pozzolanic activity of waste foundry sand by mechanical activation. Journal of Industrial and Engineering Chemistry.

[18] Zhao, Y., et al. (2020). Mechanical activation of waste foundry sand and its effect on cement hydration and microstructure. Journal of Building Materials.

[19] Nithya, R., et al. (2017). Effective Utilization of Waste Foundry Sand in Concrete: A Review. International Journal of Civil Engineering and Technology.

[20] Dukhanov, A., & Rybin, E. (2023). Application of mechanically activated burnt molding sand waste in self-compacting concrete. MATEC Web of Conferences.

[21] Chauhan, V., et al. (2020). Study on the pozzolanic properties of mechanically activated waste foundry sand for sustainable cement production. Sustainability.

[22] Kaur, K., et al. (2019). Investigation of the mechanical properties of concrete made with mechanically activated waste foundry sand. Journal of Materials in Civil Engineering.

[23] Wang, J., et al. (2022). Effects of different activation methods on the properties of concrete incorporating waste foundry sand. Journal of Sustainable Construction Materials and Technologies.

Information about the author

Adilkhodzhaev Anvar Ishanovich	Tashkent State Transport University, Professor E-mail: anvar_1950@mail.ru Tel.: +9989339831926 https://orcid.org/0000-0001-5729-5178
Kadyrov Ilhom Abdullaevich	Associate Professor of Tashkent Institute of Irrigation and Agricultural Mechanization Engineers, MTU E-mail: ilhom.kadirov.1990@mail.ru Tel.: +9989973306119 https://orcid.org/0000-0003-3924-0864
Tosheva Dilbar Farhodovna	Bukhara State Technical University, doctoral student E-mail: toshevadilbar699@gmail.com Tel.: +998 93 131 60 63 https://orcid.org/0009-0006-9710-0746

Study of the effect of filler from burnt moulding waste on the properties of cement systems

A.I. Adilkhodzhaev[1][a], I.A. Kadyrov[1][b], D.F. Tosheva[1][c]
[1]Tashkent state transport university, Tashkent, Uzbekistan

Abstract: This paper presents the results of a comprehensive study of the effect of a filler based on burnt moulding waste (BMW) on the properties of a cement system. The main objective of the study was to determine the optimal parameters of BMW (specific surface area and degree of filling) that provide the maximum synergistic effect with cementitious binder. Experiments have shown that the use of a superplasticiser (SP) in an amount of 1.0% of the cement mass is optimal for regulating the rheological and kinetic properties of the mixture. Analysis of the strength characteristics showed that the highest compressive and flexural strength is achieved when using BMW with a specific surface area of 3000 cm^2/g at a filling degree of 25%. It was found that exceeding these values leads to a decrease in strength due to the dilution effect of the cement stone and the aggregation of filler particles. Special attention was paid to the influence of BMW storage conditions: it was shown that the deactivation of active centres on the particle surface caused by moisture adsorption leads to a monotonic decrease in strength. The results of the study confirm the high efficiency of BMW as a modifier of cement systems and provide practical recommendations for their use in obtaining materials with improved mechanical properties while simultaneously solving environmental problems.

Keywords: Cement stone, burnt moulding waste, superplasticiser, strength, specific surface area, hydration kinetics, filler, synergistic effect

1. Introduction

In the field of materials science and construction materials technology, it is widely recognised that the processes involved in the formation of cement stone are a complex, multi-factor system. A number of critical factors have a significant influence on its formation. Key among these are the chemical composition and physical properties of the modifiers and fillers added, which can radically change both the kinetics of hydration and the morphology of the hydrate phases formed. A deep understanding of these interrelationships is a prerequisite for the targeted control of the properties of cement systems, including their strength, durability and deformation characteristics [1-4].

Chemical additives and microfillers play an important role in optimising the properties of cement compositions [5-15]. The introduction of these components not only regulates the rheology of the cement paste, but also influences the microstructure of the final material. For example, superplasticisers (SP), thanks to their dispersing action, reduce the water demand of the mixture, which leads to an increase in the density of the cement stone and, as a result, its strength. At the same time, additives such as burnt moulding waste (BMW) act as microfillers and pozzolanic additives. Their high dispersibility allows them to fill the smallest pores between cement particles, and their chemical activity contributes to the formation of additional calcium hydrosilicates, which strengthen the structure of the material. This synergistic interaction between different components opens up wide opportunities for creating cement systems with specified performance characteristics.

As part of this study, a comprehensive analysis was conducted of the impact of superplasticisers (SP) and burnt moulding waste (BMW) on the key properties of cementitious binders. Changes in the normal density and setting times of cement paste were studied, which is crucial for the technological feasibility of construction work and control over the hydration process. Particular attention was paid to the kinetics of cement stone compressive strength gain at different hardening times. Compressive strength is the main criterion for the quality and reliability of the material. The evaluation of this parameter made it possible to determine the optimal dosages of additives and their combinations to ensure maximum efficiency. The results obtained provide an understanding of the mechanisms of interaction between additives and cement clinker, which serves as a basis for further developments in the field of composite binding materials.

2. Research methodology

In this study, the following materials and methods were used to obtain cement compositions.

Portlandcement: Portlandcement grade CEM I 32.5N was used as the main binder, in accordance with the requirements of ГОСТ 31108-2020 «Cements for general construction. Technical conditions».

Superplasticiser (SP): PRO 500 polycarboxylate superplasticiser was used, which complies with the requirements of ГОСТ 24211-2008 «Additives for concrete and mortar. General technical conditions».

Burnt moulding waste (BMW): The waste obtained after burning the moulding mixtures was ground to a powdery state. The chemical composition of the BWF included silicon (SiO_2), aluminium (Al_2O_3) and iron (Fe_2O_3) oxides, which confirmed their pozzolanic properties (Table 1).

[a] https://orcid.org/0000-0001-5729-5178
[b] https://orcid.org/0000-0003-3924-0864
[c] https://orcid.org/0009-0006-9710-0746

Table 1

Chemical composition of BWF

Compounds	SiO_2	TiO_2	Al_2O_3	Fe_2O_3	CaO	MgO	ZnO	п.п.п.
Amount (%)	91,56	0,022	4,58	1,12	0,2	0,1	1,30	1,18

Determination of normal density and setting time: These parameters were determined on a cement test in accordance with ГОСТ 30744-2001 «Cements. Test methods using standard polyfractional sand».

Determination of compressive strength: Tests were carried out on beam samples measuring 40x40x160 mm, manufactured in accordance with ГОСТ 310.4-81 «Cements. Methods for determining the flexural and compressive strength». The samples were tested at 28 days of age.

3. Results and Discussion

Within the framework of this study, a systematic assessment was conducted on the influence of the superplasticizer (SP) dosage on the rheological and kinetic properties of cement paste. The concentration of SP was varied over a wide range from 0.2 to 1.2% by mass of cement, which allowed for a detailed analysis of how the paste's properties depend on the amount of additive used. The key data on normal consistency (N.C.) and setting times of the cement paste, which are critical indicators of workability and usability, are presented in detail in Table 1.

To ensure high accuracy and reproducibility of the results, the process of preparing the cement paste was strictly standardized. The introduction of water into the mixture was carried out in two stages. In the first stage, half of the total water volume was added by spraying to ensure uniform moistening of the cement. This promoted primary particle dispersion and prevented the formation of lumps. The remaining water, containing the dissolved SP, was then thoroughly mixed with the pre-wetted cement. This two-stage mixing method optimizes the interaction of the modifier with the cement particles, contributing to the effective manifestation of its plasticizing properties and its uniform distribution throughout the entire volume of the mixture.

The analysis of the data presented in Table 3.2 showed that an increase in the SP dosage leads to a systematic decrease in the normal consistency of the cement paste. This is due to the fact that the polycarboxylate superplasticizer, by adsorbing onto the surface of the cement particles, creates electrostatic or steric repulsion forces. This reduces inter-particle friction and lowers the water demand of the mixture. In parallel, a prolongation of the setting times was observed. This phenomenon is related to the formation of adsorption layers that slow down the cement hydration processes, which is a crucial factor for work under high-temperature conditions or during long-distance transportation of the mixture. Thus, precise SP dosing is critically important for controlling the rheological and kinetic characteristics of the cement system.

Table 1

Effect of SP dosage on normal consistency and setting time of cement paste

Additional dosage, %	NC, %	Setting time, hours and minutes	
		beginning	ending
0	27	1-10	6-20
0,2	26	1-40	6-00
0,4	24	2-00	5-40
0,6	22	2-15	5-20
0,8	21	2-25	5-10
1,0	19	2-45	4-40
1,2	19	2-45	4-40

Analysis of the data presented in Table 1 showed that an increase in the superplasticizer (SP) dosage from 0.2% to 1.2% by weight of cement leads to a notable decrease in the normal consistency (N.C.) of the cement paste by 2-8 points. The most pronounced reduction was observed at an SP concentration of 1.0%, while a further increase in the additive's concentration did not have a significant effect on this parameter. This effect is a direct result of the optimized dispersing action of the superplasticizer on the cement particles. The observed decrease in N.C. is explained by the strengthening of electrostatic and/or steric repulsive forces between the cement particles as the amount of adsorbed SP increases. This leads to a more effective fluidization of the cement paste and a reduction in its water demand. Simultaneously, the optimization of the adsorption rate of SP molecules on the surface of the cement particles provides a pronounced stabilizing effect, which is evident in a significant prolongation of the initial setting time of the cement paste—from 1 hour 10 minutes to 2 hours 45 minutes. This phenomenon is critically important for increasing the "pot life" of the cement mixture during transport and placement.

It is also noteworthy that an increase in the SP dosage leads to a reduction in the final setting time of the binder—from 6 hours 20 minutes to 4 hours 40 minutes. This effect can be explained by the accelerating properties of SP, which begin to manifest as the additive penetrates the inter-particle space and becomes uniformly distributed. The improved dispersion of cement particles and a more effective distribution of water contribute to a more complete and intensive course of hydration processes in the subsequent stages. This, in turn, leads to the faster formation of a strong and homogeneous structure in the cement stone.

Considering both the technological and economic aspects, the most optimal values for N.C. and setting times were achieved at an SP dosage of 1.0% of the binder's mass.

This concentration ensures maximum plasticizing efficiency without excessive costs or an undesirable over-prolongation of the setting times. Consequently, in all subsequent experimental studies aimed at examining the influence of other additives, the superplasticizer dosage was maintained as a constant at 1.0% of the total binder mass.

Modern scientific research [16-18] has established a direct correlation between the concentration of Brønsted active adsorption centers on the surface of powdered materials and an increase in their fineness (dispersion). These centers play a decisive role in determining the material's reactivity. However, this relationship is only evident up to a certain specific surface area (Sud), after which the rate of increase in reactivity slows down significantly. Consequently, for the effective use of freshly ground fillers, it is crucial to determine the optimal value of Sud. Exceeding this value leads to only a marginal increase in the surface activity of the particles, making further grinding economically and energetically impractical.

Within the scope of this study, we investigated the effect of the specific surface area of burnt foundry waste (BFW), used as a filler, on the strength of cement stone. The control samples were made from cement paste of normal consistency, with the consistency of the binder mass being 27%. The experimental research was aimed at determining the optimal specific surface area of the filler and the optimal degree of filling for the cement binder. To achieve this, the specific surface area of the BFW microfiller was varied in 1000 cm²/g increments, ranging from 1000 to 4000 cm²/g. Various filling levels were also used: 5%, 10%, 15%, 20%, 25%, 30%, 35%, and 40% by mass of cement.

During the study, the strength characteristics of the cement binder, modified with varying degrees of microfilling and a variable specific surface area of the filler, were examined in detail. For this purpose, fine-grained beam specimens measuring 4x4x16 cm were fabricated and tested. The resulting experimental data were subjected to rigorous statistical analysis. This step is critically important for minimizing random errors, identifying statistically significant relationships, and confirming the reliability of the results. Based on this analysis, graphical relationships were plotted and are presented in Figures 1 and 2. These graphs are a key tool for interpreting the relationship between the degree of microfilling of the cement stone, the specific surface area of the material used, and its strength properties.

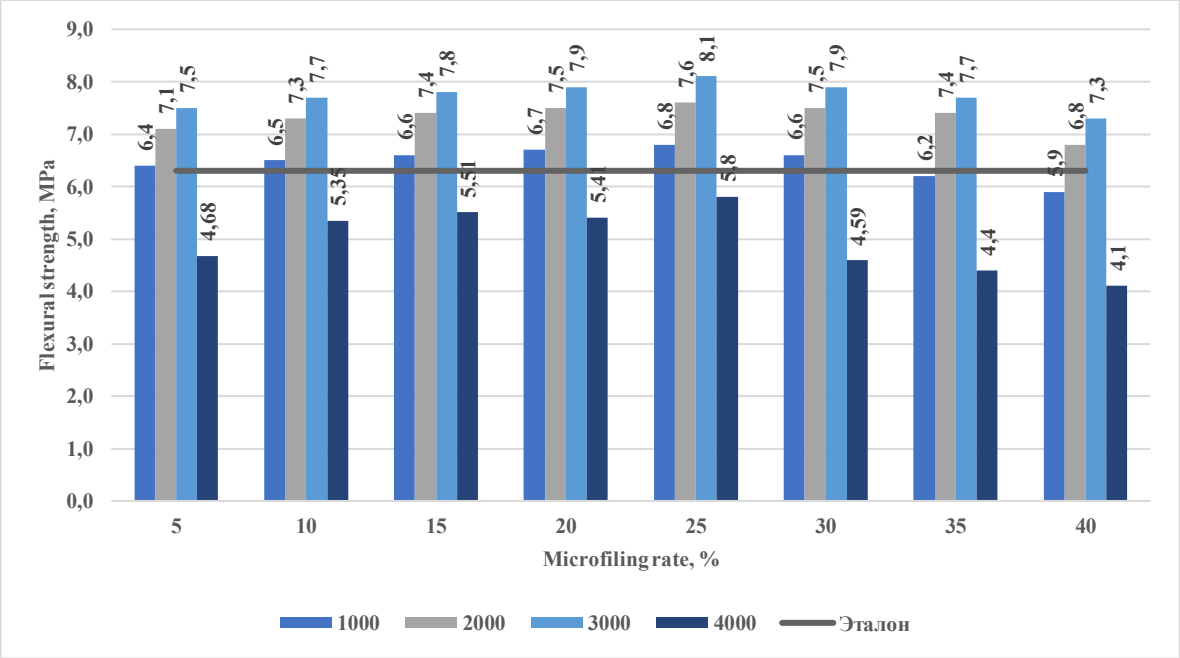

Figure 1. Influence of the relative surface area and the degree of microfiling of BWF on the bending strength of cement stone

Analysis of the data presented in Figures 1 and 2 demonstrates that the influence of both the degree of microfilling and the specific surface area of the filler on the compressive and flexural strength of cement stone increases monotonically. This indicates a direct positive correlation between these parameters and the mechanical properties of the hardened cement paste.

However, this growth isn't limitless. The highest strength values were observed for compositions with burnt foundry waste (BFW) having a specific surface area (Sud) of 3000 cm²/g at a microfilling level of 25% by mass of the binder. This is a critical finding, as it points to the existence of an optimal balance for achieving a maximum synergistic effect between the cement and the filler. At this precise point, the filler particles effectively pack into the interstitial spaces of the cement, densifying the matrix and promoting more complete hydration, which leads to enhanced mechanical properties.

https://doi.org/10.56143/3030-3893-2025-3-43-48 A bridge between science and innovation

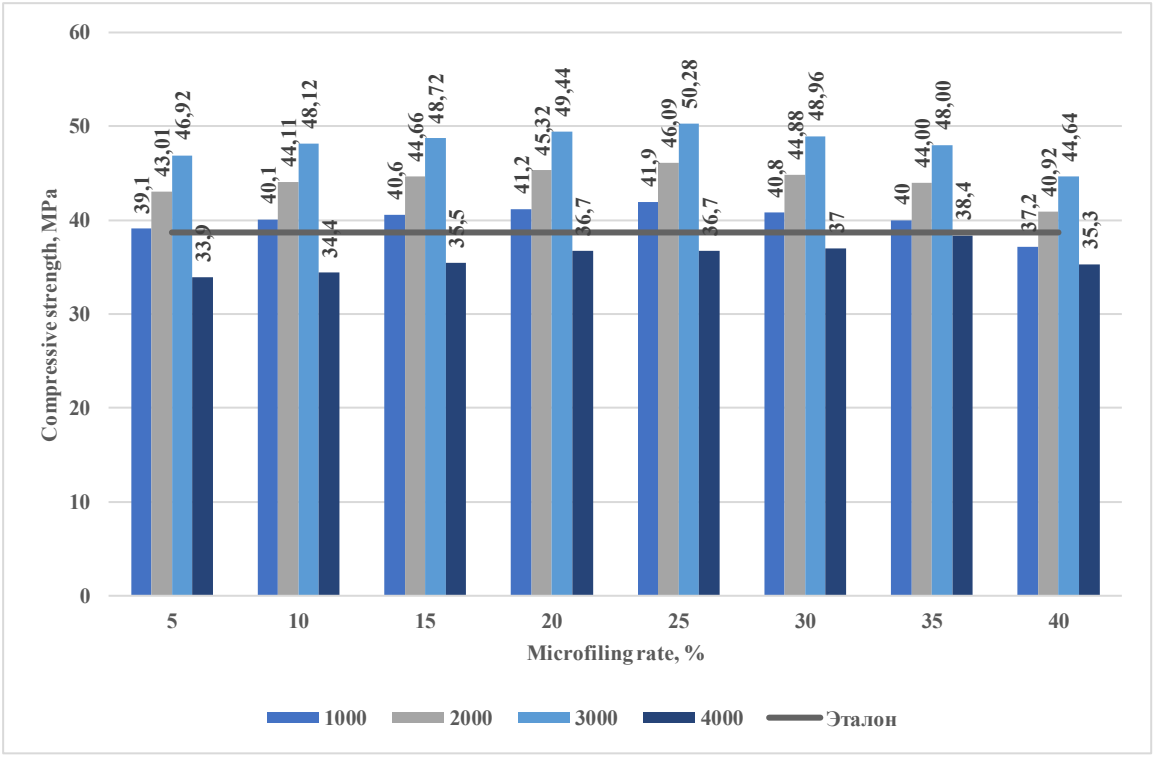

Figure 2. Effect of the relative surface area and degree of microfilling of BWF on the compressive strength of cement stone

It's important to note that exceeding the optimal filling level of 25% leads to a consistent decrease in the strength of the cement stone. This phenomenon is primarily explained by a simple but fundamental factor: the relative proportion of the initial cement in the total binder mass decreases. With the excessive introduction of the filler, the amount of cement gel—the primary component responsible for forming the strong, load-bearing framework of the hardened paste—is reduced. This dilution effect directly and negatively impacts the mechanical properties of the final material.

Furthermore, the study established that an increase in the specific surface area of the filler beyond 3000 cm²/g also adversely affects the mechanical properties of the cement stone. The main reason for this negative effect is the agglomeration of particles, a phenomenon exacerbated by surface polarization during mechanical activation. The high surface energy of excessively ground particles promotes their self-adhesion, leading to the formation of heterogeneous clusters instead of a uniform dispersion. These aggregations reduce the overall density of the composite, disrupt the formation of a continuous and monolithic cement matrix, and create internal stress concentration zones. Consequently, these structural defects collectively lead to a reduction in the overall strength. The results obtained are in strong agreement with the data presented in Fig. 3, which confirms the proposed hypothesis regarding the mechanisms of strength reduction when the filler's dispersion is over-optimized.

Taking this into account, in the subsequent series of experiments, the normal consistency and setting times of the binder with 1.0% superplasticizer (SP) and a microfiller with a specific surface area of ~3000 cm^2/g were determined. The amount of microfiller was 25% of the binder's mass. The results of determining the normal consistency and setting times of the microfilled binder are presented in Table 2.

Analysis of the presented data shows that 25% of the BWF microfiller does not affect the normal consistency indicators at an SP dose of 1.0%. It can be observed that the final stages of the setting period are somewhat shortened.

Table 2

Influence of the BWF microfiller with a specific surface area of ~3000 cm^2/g on the normal consistency and setting times of cement paste with a filling rate of 25% and an SP additive of 1.0%

Additional dosage, %	NC, %	Setting time, hours and minutes	
		beginning	ending
0	27	1-10	6-20
0,2	26	1-40	5-50
0,4	24	2-00	5-20
0,6	22	2-15	5-10
0,8	21	2-25	4-50
1,0	19	2-45	4-00
1,2	19	2-45	4-00

During the storage of freshly ground mineral fillers, a gradual decrease in the concentration of active centers on their surface is observed. This process, known as surface deactivation, is a critical phenomenon that significantly impacts the reactivity and subsequent performance of these materials. The primary driver of this deactivation is the adsorption of water molecules from the surrounding environment, a process whose rate is highly dependent on atmospheric humidity.

The mechanism of deactivation is complex and multi-faceted. On the surface of the filler, water molecules undergo dissociation into protons (H^+) and hydroxyl ions (OH^-). This is facilitated by the strong interaction between the material's proton-donating surface centers and various impurity sites, which form hydrogen bonds with the H_2O molecules. In addition to the direct adsorption of water, this deactivation can also be initiated by the absorption of H^+ and OH^- ions or radical products from the environment. Beyond water, the adsorption of other atmospheric components, such as oxygen (O_2) or nitrogen (N_2), can also affect filler activity. In this case, a "saturation" of the active centers occurs, with O_2 and N_2 molecules acting as electron acceptors or donors, respectively. This alters the electron concentration on the material's surface, leading to its deactivation [19-23].

Given these theoretical considerations on the deactivation of the active surface of mineral fillers, an experimental study was conducted to investigate the influence of storage time on the strength of cement stone. This research, with results presented in Figure 3, was designed to provide a quantitative assessment of how changes in the surface activity of fillers over time affect the final mechanical properties of the composite material. Understanding this relationship is crucial for practical applications, as it provides a basis for determining optimal storage conditions and usage timelines for fillers to ensure consistent and high-quality material performance.

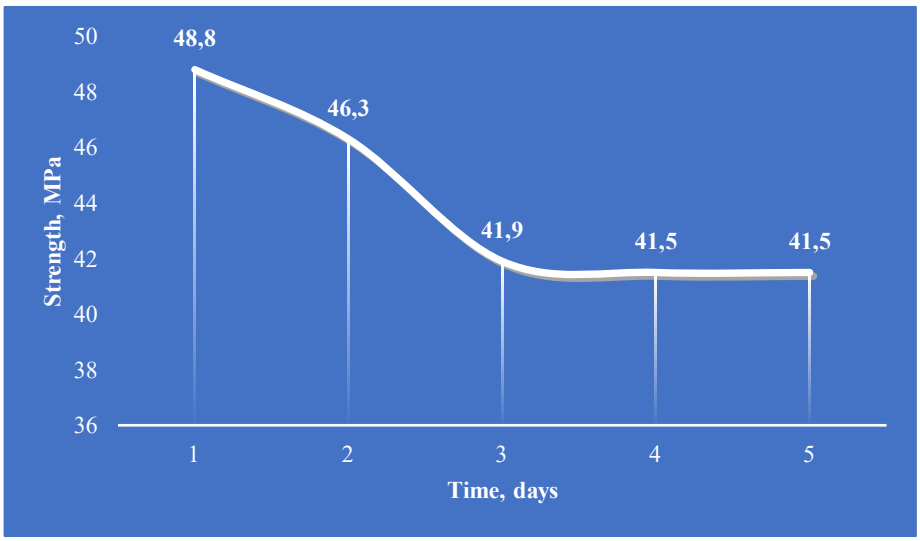

Figure 3. Decrease in micro-filler activity due to moisture adsorption over time following grinding

As demonstrated in Figure 3, a clear correlation exists between the storage time of the burnt foundry waste (BFW) microfiller and the mechanical properties of the resulting cement stone. The most rapid decline in the number of active centers on the surface of the BFW is observed within the initial 24 hours of exposure to air, which directly corresponds to a monotonous decrease in the cement stone's strength. This phenomenon is rooted in the high surface energy of the freshly ground BFW particles. Upon exposure to the atmosphere, these highly reactive surfaces readily adsorb ambient water vapor and other gases. This adsorption process leads to the neutralization of the Brønsted active adsorption centers, which are crucial for the filler's reactivity. The surface becomes saturated with adsorbed molecules, effectively passivating it and significantly reducing its ability to participate in subsequent pozzolanic reactions with calcium hydroxide ($Ca(OH)_2$). The decline in the BFW's reactivity directly compromises its function as both a filler and a pozzolanic additive. Initially, the active centers facilitate the nucleation of C-S-H gel, providing additional sites for hydration product formation and leading to a denser, stronger microstructure. As these centers become deactivated, the filler's ability to act as nucleation sites diminishes. Consequently, the formation of the dense hydration product network is less efficient, and the final hardened cement paste exhibits lower mechanical properties. The monotonous decrease in strength over time, as shown in the figure, is a direct manifestation of this ongoing surface deactivation. The results underscore the critical importance of proper storage and timely use of freshly ground BFW. To maximize its beneficial effects on the strength of cement-based materials, the filler must be used as soon as possible after its production or stored in a controlled, low-humidity environment to prevent surface deactivation. These findings provide a scientific basis for practical guidelines aimed at optimizing the performance of sustainable construction mtaerials that incorporate industrial waste.

4. Conclusion

Studies have conclusively demonstrated that burnt moulding waste (BMW) has significant potential for use as an effective microfiller in cement systems. It has been established that the optimal specific surface area of BMW is 3000 cm^2/g, and the optimal filling degree is 25% of the cement mass. Achieving maximum strength at these parameters is due to synergistic interaction, where BWF not only compacts the structure but also participates in pozzolanic reactions. Another important conclusion is the

need to control the storage conditions of the filler, since its reactivity critically depends on time and humidity. The use of freshly ground BWF or storage in dry conditions allows its active centres to be preserved and maximises its contribution to strength characteristics. Thus, the use of BWF is not only an economically viable and environmentally sound solution for industrial waste disposal, but also an effective method for improving the properties of building materials, opening up new prospects in the field of sustainable construction.

References

[1] Adylkhodjayev Anvar, Kadyrov Ilkhom, Shaumarov Said, Umarov Kadir. Some Peculiarities of the Process of Preparing the Zeolites Containing Breeds in a Ball Mill // International Journal of Recent Technology and Engineering (IJRTE) ISSN: 2277-3878, Volume-8 Issue-4, November 2019.

[2] Адилходжаев А.И., Кадыров И.А, Умаров К.С., Назаров А.А. К вопросу механоактивации цеолитсодержащих пород // Известия Петербургого Государственного университета путей сообщения, №3, 2019. ISSN 1815-588X. Известия ПГУПС. С. 489-498.

[3] Лукутцова Н.П., Пыкин А.А. Теоретические и технологические аспекты получения микро- и нанодисперсных добавок на основе шунгитосодержащих пород для бетона. Монография. – Брянск: Изд-во БГИТА, 2013. – 231 с.

[4] Shi, C., Mo, L., He, F., & Wu, L. (2018). Characteristics and pozzolanic activity of municipal solid waste incineration bottom ash. Construction and Building Materials, 182, 608-617.

[5] Juenger, M. C. G., & Siddique, R. (2015). Recent advances in sustainable concrete technology. Cement and Concrete Research, 78, 25-30.

[6] Poon, C. S., Kou, S. C., & Lam, L. (2006). The use of incinerator ash as a filler in concrete. Cement and Concrete Research, 36(1), 1-7.

[7] Pera, J., & Ambroise, J. (2007). Pozzolanic activity of finely ground solid wastes from construction and demolition. Cement and Concrete Composites, 29(5), 405-410.

[8] Siddique, R. (2004). Utilization of waste foundry sand in concrete. Resources, Conservation and Recycling, 42(3), 253-261.

[9] Ghorbani, F., Ghasemi, M., & Farzin, V. (2019). Mechanical properties of concrete containing waste foundry sand. Journal of Building Engineering, 22, 175-181.

[10] Singh, G., & Singh, B. (2020). Performance evaluation of cementitious composites containing waste foundry sand. Construction and Building Materials, 258, 119565.

[11] Al-Jabri, K. S., Hisada, M., & Al-Saidy, A. H. (2011). Effect of waste foundry sand on the mechanical properties and durability of concrete. Journal of Materials in Civil Engineering, 23(1), 126-133.

[12] He, Y., Ma, C., Liu, B., & Zhang, Y. (2021). The effects of different types of foundry waste on the mechanical and durability properties of concrete. Case Studies in Construction Materials, 14, e00523.

[13] Sahoo, S., Nayak, A. N., & Biswal, K. C. (2018). An experimental investigation on the mechanical properties of concrete with waste foundry sand. Procedia Engineering, 173, 1085-1092.

[14] Bhasin, A., & Gupta, A. (2016). Effects of waste foundry sand on strength and permeability of concrete. Materials Today: Proceedings, 3(6), 1629-1635.

[15] Khatib, J. M., & Mangat, P. S. (1995). The effect of incorporating waste foundry sand on the properties of concrete. Cement and Concrete Research, 25(8), 1639-1649.

[16] Zailani, N., Abdul, A. G., & Ariffin, M. A. M. (2014). The effect of recycled foundry sand on the properties of concrete. Procedia Engineering, 68, 497-503.

[17] Zaid, A. F. M., & Huseien, G. F. (2018). Compressive strength and microstructural analysis of concrete containing waste foundry sand. Journal of Cleaner Production, 172, 1162-1172.

[18] Gesoglu, M., Oz, H. O., & Guneyisi, E. (2017). Effects of waste foundry sand on the fresh and hardened properties of concrete. Construction and Building Materials, 141, 412-419.

[19] Montero, J., Barluenga, G., & Palacios, M. (2019). The influence of waste foundry sand on the properties of self-compacting mortar. Cement and Concrete Composites, 96, 22-31.

[20] O'Mahony, M. M., & Al-Saadi, S. A. M. (2016). Waste foundry sand as a partial replacement for fine aggregate in concrete. Cogent Engineering, 3(1), 1-13.

[21] Khotbehsara, E. E., Sadraddin, S., & Shokouhian, M. (2019). Characterization of the mechanical properties of concrete incorporating waste foundry sand. SN Applied Sciences, 1(10), 1-11.

[22] Roy, S., & Mohanty, S. (2020). An experimental investigation on the use of waste foundry sand in cement mortar. International Journal of Concrete Structures and Materials, 14, 1-10.

[23] Mounkaila, F., Diop, M. S., & Ndiaye, C. (2021). The use of ground burnt clay waste as a pozzolanic material in concrete. Journal of Cleaner Production, 290, 125192.

Information about the author

Adilkhodzhaev Anvar Ishanovich	Tashkent State Transport University, Professor E-mail: anvar_1950@mail.ru Tel.: +9989339831926 https://orcid.org/0000-0001-5729-5178
Kadyrov Ilhom Abdullaevich	Associate Professor of Tashkent Institute of Irrigation and Agricultural Mechanization Engineers, MTU E-mail: ilhom.kadirov.1990@mail.ru Tel.: +9989973306119 https://orcid.org/0000-0003-3924-0864
Tosheva Dilbar Farhodovna	Bukhara State Technical University, doctoral student E-mail: toshevadilbar699@gmail.com Tel.: +998 93 131 60 63 https://orcid.org/0009-0006-9710-0746

The effect of burnt moulding waste on the hydration and structure formation processes of portland cement

A.I. Adilkhodzhaev[1][a], I.A. Kadyrov[1][b], D.F. Tosheva[1][c]
[1]Tashkent state transport university, Tashkent, Uzbekistan

Abstract: This paper presents the results of a comprehensive study of the effect of a filler based on burnt moulding waste (BMW) and a superplasticiser on the phase composition and structure formation of cement stone at early (1 day) and late (28 days) stages of hardening. X-ray phase analysis (XPA) has established that BFA has a powerful accelerating effect on the hydration of clinker minerals in the first day, which is explained by the adsorption of calcium ions on their surface, while the superplasticiser, on the contrary, slows down this process. A synergistic effect of the combined use of additives has been demonstrated, which negates the retarding effect of the superplasticiser and leads to the intensive formation of hydrate phases at an early stage. By day 28, a significant decrease in the content of portlandite ($Ca(OH)_2$) and an increase in the proportion of amorphous calcium hydrosilicate (C-S-H) by 22% are observed in the modified cement stone, which indicates the occurrence of an active pozzolanic reaction. The data obtained confirm that complex modification allows effective control of the hydration kinetics and the formation of a dense, highly structured cement stone matrix, which is a key factor in improving its strength and performance characteristics.

Keywords: X-ray phase analysis, structure formation, cement stone, burnt moulding waste, superplasticiser, hydration kinetics, pozzolanic reaction, synergistic effect

1. Introduction

The problem of obtaining building materials with improved performance characteristics while reducing their cost and environmental impact is one of the most pressing issues in modern materials science. Traditional cement systems have a number of limitations related to their high water demand and microstructural heterogeneity. In this regard, the search for effective modifiers and fillers capable of optimising structure formation processes and improving the quality of cement stone is becoming particularly important [1-4].

The introduction of superplasticisers (SP), such as polycarboxylates, into the cement mixture significantly reduces the water-cement ratio while ensuring high mobility of the mixture. This effect is due to the adsorption of SP molecules on the surface of cement particles, which creates steric and/or electrostatic repulsive forces that prevent their flocculation. As a result, a denser and more homogeneous structure of the cement stone is formed, which leads to a significant increase in its strength characteristics. In parallel with this, the use of finely dispersed fillers, in particular burnt moulding waste (BMW), is a promising direction. This waste, which is a by-product of foundry production, contains pozzolanic components and can act as microfillers. The introduction of BFM contributes to the compaction of the structure by filling the intergranular space and also initiates additional hydration reactions, forming calcium hydrosilicates.

The aim of this study is to investigate the combined effect of a superplasticiser and a filler based on burnt moulding waste on the structure formation processes of cement stone.

2. Research methodology

In this study, the following materials and methods were used to obtain cement compositions.

Portlandcement: Portlandcement grade CEMI 32.5N was used as the main binder, in accordance with the requirements of ГОСТ 31108-2020 «Cements for general construction. Technical conditions».

Superplasticiser (SP): PRO 500 polycarboxylate superplasticiser was used, which complies with the requirements of ГОСТ 24211-2008 «Additives for concrete and mortar. General technical conditions».

Burnt moulding waste (BMW): The waste obtained after burning the moulding mixtures was ground to a powdery state. The chemical composition of the BWF included silicon (SiO_2), aluminium (Al_2O_3) and iron (Fe_2O_3) oxides, which confirmed their pozzolanic properties (Table 1).

Table 1

Chemical composition of BWF

Compounds	SiO_2	TiO_2	Al_2O_3	Fe_2O_3	CaO	MgO	ZnO	п.п.п.
Amount (%)	91,56	0,022	4,58	1,12	0,2	0,1	1,30	1,18

An experimental determination of the phase composition of the formed cement stone was conducted using a high-precision AL-27mini diffractometer. The analysis was performed with the powder method to ensure high data reliability. A monochromatized CuKα-radiation source with a precise wavelength of λ=1.5406 Å was used, enabling high-precision identification of crystalline phases. The diffraction pattern was recorded in a step-by-step scanning

[a] https://orcid.org/0000-0001-5729-5178
[b] https://orcid.org/0000-0003-3924-0864
[c] https://orcid.org/0009-0006-9710-0746

mode with carefully controlled parameters: a 30 kV X-ray tube voltage, a 10 mA current, a scanning angular step of 0.02°, and a scanning speed of 1 degree per minute. This mode provided an optimal balance between resolution and data collection time, allowing for the detection of even minor changes in the phase composition of the samples.

For the analysis, four distinct types of compositions were prepared to investigate the effects of various additives on the cement system's phase development:

1. Composition 1: A normal consistency Portland cement-based composition without any additives (PC), serving as the control.
2. Composition 2: A composition consisting of normal consistency Portland cement and BWF, to study the effect of the pozzolanic additive alone.
3. Composition 3: A composition consisting of normal consistency cement binder and a polycarboxylate superplasticizer (SP), to isolate the effect of the plasticizer.
4. Composition 4: A complexly modified Portland cement-based composition using both BWF and SP, to examine the synergistic effects of both additives.

3. Results and discussions

A detailed description of the compositions of the studied cement stone samples, including the quantitative ratio of the main components and introduced additives, as well as the diffractogram data for interpreting the results of X-ray phase analysis, is presented in Tables 1 and 2. The X-ray phase analysis of the studied cement stone samples, shown in Figures 1 and 2, provides critical insights into the phase evolution at two key hardening periods: 1 and 28 days. These figures display characteristic diffraction spectra that allow us to examine the dynamics of changes in the intensity and position of reflections corresponding to various mineral phases. The diffractograms from the 1-day samples are crucial for understanding the initial hydration kinetics. They primarily reveal the rapid formation of early hydration products, such as ettringite ($C_6A_8H_{32}$), while the main phases of unhydrated cement, alite (C_3S) and belite (C_2S), still show strong peaks. By comparing the samples with and without additives at this stage, we can discern how SP influences the hydration rate and how BWF acts as a nucleation site for initial gel formation. The 28-day diffractograms, on the other hand, provide a comprehensive picture of the long-term microstructure maturity. At this stage, the intense peaks of portlandite ($Ca(OH)_2$) and other hydration products signify the progression of the hydration process. Specifically, the presence of Burnt Foundry Waste (BWF) in the compositions is expected to induce a pozzolanic reaction, which will be evident in the 28-day diffractograms by a notable reduction in the portlandite peak intensity, as $Ca(OH)_2$ is consumed to form additional C-S-H gel. Simultaneously, the inclusion of a Superplasticizer (SP), by facilitating more efficient hydration, might lead to a more advanced hydration degree at both 1 and 28 days, reflected in the relative intensities of the unhydrated and hydrated phases. This X-ray diffraction (XRD) analysis is a crucial aspect for understanding the fundamental mechanisms of hydration and structure formation in cement systems modified with BWF and SP, providing a direct link between the material's composition and its ultimate mechanical properties [5-15].

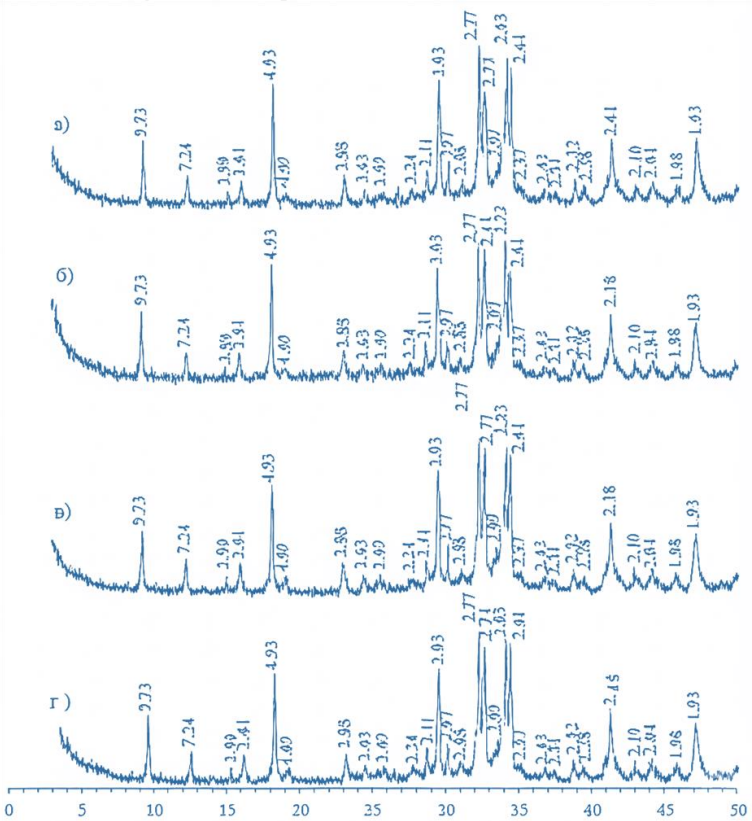

Figure 1. Diffractograms of 1-day cement stone samples: a) PC, b) PC+BWF, c) SP, d) CM

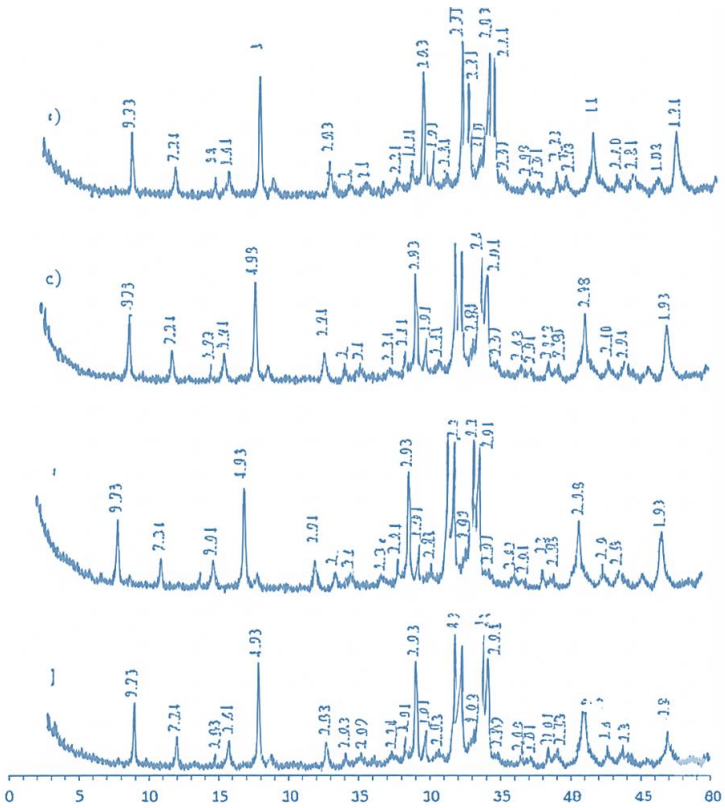

Figure 2. Diffractograms of 28-day cement stone samples: a) PC, b) PC+BWF, c) SP, d) CM

Analysis of the data presented in Table 1 confirms that the introduction of burnt foundry waste (BWF) into the cement system has a significant influence on the kinetics of early-stage hydration processes. The results clearly demonstrate that the presence of BWF remarkably accelerates the hydration of the main clinker minerals, specifically alite (C_3S) and belite (C_2S), within the first 24 hours of hardening. This observation points to a pronounced accelerating or catalytic effect of the BWF particles. The primary mechanism behind this acceleration is the nucleation effect. Finely ground BWF particles, with their high specific surface area, provide a vast number of heterogeneous sites for the nucleation and growth of early hydration products, such as calcium silicate hydrate (C-S-H) gel and portlandite ($Ca(OH)_2$). By providing these pre-existing templates, the BWF bypasses the initial induction period of hydration, where supersaturation must be reached for crystal formation to begin. The XRD data in Table 1 visually support this, showing a more rapid decrease in the intensity of the unhydrated clinker peaks in the BWF-modified samples compared to the control. Simultaneously, the peaks corresponding to nascent hydration products would show a more rapid increase in intensity. This early-stage acceleration is critical as it sets the foundation for a more mature and dense microstructure at later ages, ultimately contributing to enhanced mechanical properties and the overall strength of the final cement stone.

Table 1

Effect of modifiers on the phase composition of 1-day-old cement stone

№	Mineral composition, %							
	$3CaO \cdot SiO_2$	β-$2CaO \cdot SiO_2$	$4CaO \cdot Al_2O_3 \cdot Fe_2O_3$	$3CaO \cdot Al_2O_3$	$Ca(OH)_2$	$3CaO \cdot Al_2O_3 \, 3CaSO_4 \cdot 32H_2O$	C-S-H	Others
1	32,7	15,6	7,3	3,1	10,4	8,2	21,5	1,2
2	29,6	14,2	3,7	2,7	8,9	7,5	28,2	1,2
3	34,5	16,9	8,3	4,0	9,0	6,6	19,2	1,5
4	30,1	15,1	7,5	3,1	9,5	7,5	25,8	1,4

Analysis of the phase composition of cement stone modified with BWF showed a significant decrease in the concentration of unreacted clinker phases at the initial stage of hardening, i.e., within 1 day. Specifically, a decrease in the content of alite by 11%, belite by 10%, shareginite (brownmillerite) by 10%, and tricalcium aluminate by 12%

https://doi.org/10.56143/3030-3893-2025-3-49-54 A bridge between science and innovation

was observed. This phenomenon, indicating the acceleration of hydration processes, is explained by the ability of negatively charged BWF particles to adsorb calcium ions (Ca^{2+}) on their developed surface. This adsorption effectively reduces the local concentration of Ca^{2+} ions in the pore solution, which in turn shifts the dissolution equilibrium of clinker minerals towards their stronger decomposition, thereby accelerating the overall hydration kinetics [16]. Notably, despite the replacement of 25% of the cement with BWF, the amount of portlandite ($Ca(OH)_2$) formed in the BWF cement stone decreased by 1.5% compared to the control sample (without additives). This fact is also a direct consequence of the accelerated hydration of cement clinker phases in the presence of BWF, as the active consumption of Ca^{2+} ions for the formation of calcium hydrosilicates (C-S-H) and other hydrate phases can occur before their release in the form of portlandite.

Contrary to the effect of BWF, the use of polycarboxylate superplasticizer slows down the hydration processes of clinker minerals in the first stage of hardening (1 day). This inhibitory effect is associated with the adsorption of superplasticizer macromolecules on the surface of cement particles. The resulting adsorption layer hinders the dissolution of the surface layers of the clinker phases and slows down both the nucleation and growth of hydration product crystals. Quantitative phase analysis confirmed these observations: the amount of unreacted alite in the superplasticizer composition increased by 6%, belite by 1%, brownmillerite by 11%, and tricalcium aluminate by 26% compared to the control sample. Such a slowdown in hydration leads to a decrease in the content of the main hydrate phases in the cement stone: portlandite decreases by 12%, ettringite by 10%. Additionally, it was noted that the formation of the amorphous phase of calcium hydrosilicates (C-S-H) slows down by 11% compared to the control mixture without additives, indicating a deceleration in the process of basic structure formation [17-19].

The introduction of a complex additive containing BWF and a polycarboxylate superplasticizer provides a synergistic effect, manifested by an acceleration of cement hydration on the 1st day of hardening, which effectively counteracts the inhibitory effect of the plasticizing component alone. In cement stone modified with the complex additive, a significant decrease in the concentration of unreacted initial minerals is observed by day 1: alite by 12%, belite by 10%, brownmillerite by 9%, and tricalcium aluminate by 25%. This intensification of the hydration process leads to a corresponding increase in the amount of hydrate phases in the cement stone at this stage: the amount of portlandite increases by 5% compared to the sample with only polycarboxylate superplasticizer, and ettringite by 14%. Thus, complex modification demonstrates the ability to optimize early hydration kinetics, contributing to the effective formation of the mineralogical framework of cement stone.

Table 2 presents the results of quantitative X-ray phase analysis of 28-day-old cement stone with the addition of complex additives BWF and SP.

Table 2

Effect of modifiers on the phase composition of 28-day-old cement stone

№	Mineral composition, %					
	$3CaO \cdot SiO_2$	β-$2CaO \cdot SiO_2$	$4CaO \cdot Al_2O_3 \cdot Fe_2O_3$	$Ca(OH)_2$	$3CaO \cdot Al_2O_3$ $3CaSO_4 \cdot 32H_2O$	C-S-H
1	17,1	12,9	6,8	13,5	7,4	42,3
2	16,8	12,6	6,1	8,1	7,7	48,2
3	14,1	12,9	7,1	15,2	8,8	42,2
4	13,4	12,1	6,4	8,5	8,4	50,3

A detailed analysis of the phase composition of cement stone modified with BWF during the 28-day hardening period revealed a significant decrease in the content of Portlandite ($Ca(OH)_2$) by 38% compared to the control sample without additives. This indicates an intensification of the pozzolanic reaction of BWF in the final stages of hydration of cement systems. At the same time, an increase in the content of the amorphous phase by 19% was observed. This clearly indicates the formation of a highly dispersed, weakly crystallized structure enriched with low-basic calcium hydrosilicates (C-S-H). Such a change in the phase composition confirms the effective absorption of calcium hydroxide by the pozzolanic particles and the formation of more stable and dense hydrate products. This is important for improving the durability and performance properties of cement stone.

By the 28th day of hardening in cement stone containing a polycarboxylate superplasticizer, the alite content decreased by 18%, and the belite content by 3% compared to the sample without additives. This indicates that the hydration of these clinker minerals continued and even slightly accelerated in subsequent stages. In our opinion, this may be due to the optimization of water distribution and the formation of a stable microstructure under the influence of the superplasticizer. In addition, in the samples with the addition of superplasticizer, an increase in the content of portlandite by 11%, ettringite by 8%, as well as an increase in the proportion of the amorphous phase by 3% compared to the control composition, was observed. These changes indicate a complex effect of the superplasticizer. In addition to its main dispersing properties, it can also influence the kinetics of hydrate phase formation during long-term hardening.

On the 28th day of hardening, when a complex additive was applied, cement stone with a qualitatively altered structure was formed. A characteristic feature is a significant decrease in the content of portlandite by 41% and ettringite by 10%. At the same time, amorphous calcium

hydrosilicates (C-S-H) predominate in the composition of the cement stone with complex application of additives. Their quantity increased by 22% compared to the sample without additives. This indicates a high degree of transformation of calcium hydroxide and the active formation of a binding gel. Also, in the composition with a complex additive

By day 28, the subsequent hydration processes of C_3S (alite) and C_2S (belite) gradually slowed down. This phenomenon is explained not only by the compaction of C-S-H gel around the cement grains as a result of the ongoing pozzolanic reaction of BWF, but also by the overall compaction of the cement stone structure. As a result, the porosity and permeability of the matrix decrease, further diffusion of water into unreacted clinker particles becomes difficult, and thus their hydration in subsequent stages slows down.

Experimental data covering the phase composition and microstructural properties of cement stone at different stages of hardening fully confirm the previously stated hypothesis about the complex mechanism of action of the proposed modifying additive. This confirmation applies both to its influence on the formation of mineralogical composition and indirectly to the final strength properties of cement stone. The research results show that the use of this complex additive in the creation of building materials with improved performance properties and long-term durability is promising.

4. Conclusion

Based on the conducted research, it was determined that applying the complex additive before the 28-day hardening period contributes to the formation of a denser, more uniform, and improved microstructure of the cement stone. An important factor determining these structural advantages is the high pozzolanic activity of BWF, which is a component of the complex additive. This activity is manifested by a significant decrease in the amount of portlandite
($Ca(OH)_2$), the main product of cement hydration, as well as a proportional increase in the amount of amorphous calcium hydrosilicates (C-S-H). Such a change in phase composition leads to the formation of a chemically more stable and less porous matrix. Calcium hydrosilicates formed as a result of the pozzolanic reaction are characterized by high density and better binding ability, which ultimately ensures the achievement of improved performance properties of the material, such as strength and durability.

References

[1] Adylkhodjayev Anvar, Kadyrov Ilkhom, Shaumarov Said, Umarov Kadir. Some Peculiarities of the Process of Preparing the Zeolites Containing Breeds in a Ball Mill // International Journal of Recent Technology and Engineering (IJRTE) ISSN: 2277-3878, Volume-8 Issue-4, November 2019.

[2] Адилходжаев А.И., Кадыров И.А, Умаров К.С., Назаров А.А. К вопросу механоактивации цеолитсодержащих пород // Известия Петербургого Государственного университета путей сообщения, №3, 2019. ISSN 1815-588X. Известия ПГУПС. С. 489-498.

[3] Лукутцова Н.П., Пыкин А.А. Теоретические и технологические аспекты получения микро- и нанодисперсных добавок на основе шунгитосодержащих пород для бетона. Монография. – Брянск: Изд-во БГИТА, 2013. – 231 с.

[4] Shi, C., Mo, L., He, F., & Wu, L. (2018). Characteristics and pozzolanic activity of municipal solid waste incineration bottom ash. Construction and Building Materials, 182, 608-617.

[5] Juenger, M. C. G., & Siddique, R. (2015). Recent advances in sustainable concrete technology. Cement and Concrete Research, 78, 25-30.

[6] Poon, C. S., Kou, S. C., & Lam, L. (2006). The use of incinerator ash as a filler in concrete. Cement and Concrete Research, 36(1), 1-7.

[7] Pera, J., & Ambroise, J. (2007). Pozzolanic activity of finely ground solid wastes from construction and demolition. Cement and Concrete Composites, 29(5), 405-410.

[8] Siddique, R. (2004). Utilization of waste foundry sand in concrete. Resources, Conservation and Recycling, 42(3), 253-261.

[9] Ghorbani, F., Ghasemi, M., & Farzin, V. (2019). Mechanical properties of concrete containing waste foundry sand. Journal of Building Engineering, 22, 175-181.

[10] Singh, G., & Singh, B. (2020). Performance evaluation of cementitious composites containing waste foundry sand. Construction and Building Materials, 258, 119565.

[11] Al-Jabri, K. S., Hisada, M., & Al-Saidy, A. H. (2011). Effect of waste foundry sand on the mechanical properties and durability of concrete. Journal of Materials in Civil Engineering, 23(1), 126-133.

[12] He, Y., Ma, C., Liu, B., & Zhang, Y. (2021). The effects of different types of foundry waste on the mechanical and durability properties of concrete. Case Studies in Construction Materials, 14, e00523.

[13] Sahoo, S., Nayak, A. N., & Biswal, K. C. (2018). An experimental investigation on the mechanical properties of concrete with waste foundry sand. Procedia Engineering, 173, 1085-1092.

[14] Bhasin, A., & Gupta, A. (2016). Effects of waste foundry sand on strength and permeability of concrete. Materials Today: Proceedings, 3(6), 1629-1635.

[15] Khatib, J. M., & Mangat, P. S. (1995). The effect of incorporating waste foundry sand on the properties of concrete. Cement and Concrete Research, 25(8), 1639-1649.

[16] Zailani, N., Abdul, A. G., & Ariffin, M. A. M. (2014). The effect of recycled foundry sand on the properties of concrete. Procedia Engineering, 68, 497-503.

[17] Zaid, A. F. M., & Huseien, G. F. (2018). Compressive strength and microstructural analysis of concrete containing waste foundry sand. Journal of Cleaner Production, 172, 1162-1172.

[18] Gesoglu, M., Oz, H. O., & Guneyisi, E. (2017). Effects of waste foundry sand on the fresh and hardened properties of concrete. Construction and Building Materials, 141, 412-419.

[19] Montero, J., Barluenga, G., & Palacios, M. (2019). The influence of waste foundry sand on the properties of self-compacting mortar. Cement and Concrete Composites, 96, 22-31.

Information about the author

Adilkhodzhaev Anvar Ishanovich	Tashkent State Transport University, Professor E-mail: anvar_1950@mail.ru Tel.: +9989339831926 https://orcid.org/0000-0001-5729-5178
Kadyrov Ilhom Abdullaevich	Associate Professor of Tashkent Institute of Irrigation and Agricultural Mechanization Engineers, MTU E-mail: ilhom.kadirov.1990@mail.ru Tel.: +9989973306119 https://orcid.org/0000-0003-3924-0864
Tosheva Dilbar Farhodovna	Bukhara State Technical University, doctoral student E-mail: toshevadilbar699@gmail.com Tel.: +998 93 131 60 63 https://orcid.org/0009-0006-9710-0746

Security issues in IP-based communication networks

A.Sh. Khurramov[1][a]
[1]Tashkent state transport university, Tashkent, Uzbekistan

Abstract: This article examines the structural reliability and cyber resilience of IP-based rapid technological communication networks in railway sections, particularly using train dispatcher communication systems as an example. A logical-functional model was developed for multiple stations, demonstrating that the overall reliability of the rapid technological communication network directly depends on the coordinated operation of all its elements. Simulation experiments conducted in the MATLAB environment revealed that DoS (Denial of Service) attacks can significantly reduce network performance, increasing packet loss threefold and latency fivefold. To address these issues, scientific and technical solutions such as traffic encryption, strengthening QoS mechanisms, implementing real-time monitoring systems, optimizing resources, and using firewalls were proposed. Practical implementation of these measures improved the readiness coefficient of the rapid technological communication network, ensured compliance with international information security standards, and strengthened both the safety and stability of train traffic in railway sections.

Keywords: IP communication networks; rapid technological communication (RTC); railway communication; structural reliability; cyber resilience; DoS attacks; network security; availability coefficient; firewalls; train dispatcher systems

1. Introduction

The IP communication network technology must become a ready-made solution and be able to provide full functional services; however, there are many technical and legal issues and problems. These aspects can be roughly divided into three groups [1]:

- development of technology and equipment;
- legal aspects of management;
- ensuring security.

Improving the equipment of information exchange systems is carried out in different directions. First of all, this involves the development of the concept of Session Border Controllers (SBCs). These are software and hardware tools that solve the problems of logical separation of networks and ensuring their functionality. Mechanisms for connecting IP communication networks are being developed, the set of interfaces and parameters is being standardized, and configuration and usage procedures are being simplified. Models developed in the field of IP communication networks mainly describe Quality of Service (QoS) mechanisms. This allows for the standardization and characterization of all parameters and norms of the quality of services offered by IP communication network technology [2].

Security is one of the main issues in the functioning of any information exchange system. IP communication networks and local IP computer network technologies are closely related, incorporating not only advantages but also certain disadvantages. In general, the set of potential threats to the communication network and influencing factors can be divided into two groups according to their origin: natural and artificial.

The elements of Rapid Technological Communication (RTC) networks [3] may be damaged or disabled as a result of the impact of natural or artificial factors.

Natural threats – threats to RTC networks and their elements arising from physical processes or natural disasters (earthquakes, thunderstorms, etc.) beyond human control.

Artificial threats – threats arising from human activity, which can be divided into:

- unintentional (accidental) threats caused by errors in design, software failures, or operator mistakes;
- intentional threats related to hacker activities and malicious actions.

Natural factors are difficult to predict in advance, as well as the damage caused by them. Artificial factors may include, for example, railway communication networks, powerful radio stations, high-voltage power lines, mechanical influences, and, most importantly, modern cyberattacks [4].

The degree of destructive influence of each factor on RTC network elements determines their level of inoperability and depends on the type, strength, scale, and accuracy of the impact. In IP-based communication network infrastructures, information security threats arise when a channel is formed between the threat source and the information source, creating conditions for security violations. The severity of such threats depends on the type of threat source, the vulnerability of the information source, and the characteristics of the signal transmission environment.

According to the type of source, threats to information security can be divided into the following:

- threats related to organizations with high potential, equipment, and motivation, acting in accordance with political, economic, or other goals of the railway company;
- threats related to organizations motivated by economic or informational interests;
- threats related to the activities of individuals (criminal elements).

Methods of influencing RTC networks [4] depend on the capabilities of the threat source. A source that gains or

[a] https://orcid.org/0000-0002-8443-9250

attempts to gain unauthorized access is considered a violator of information security. Such violators may act accidentally or intentionally in their own interests, causing breaches of information security in the network.

Violators are divided into two types:

- External violators – those without authorized access to the network (foreign intelligence representatives, members of criminal organizations, economically motivated individuals).
- Internal violators – those with authorized access (communication operators, developers, or suppliers of technical components).

One of the main problems of RTC networks is equipment failure. This can occur due to various reasons, including channel interruptions, interception of conversations, service theft, or spam attacks. Although no cases of IP communication network violations have been recorded in Uzbekistan so far, in other countries such cyberattacks have led to significant economic losses and disruption of technological processes [5].

2. Research methodology

Ensuring the cyber resilience of the communication network involves identifying the main types of cyberattacks and the methods of protection against them. The analysis of the results described in these studies shows that, for railway sections, the most effective approach for use in train dispatcher communication networks is the implementation of measures aimed at protecting network elements from cyberattacks [6], i.e., threats posed by network intruders (NI) (Fig 1).

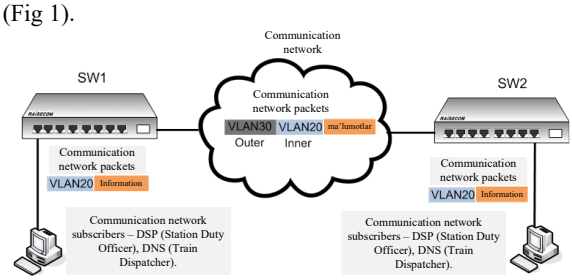

Fig. 1. Rules for network configuration

Specialized software and hardware. Although attacks can be carried out at any level of the ISO/OSI model, the most common ones occur at levels 3–4 and 7. Nowadays, many software and hardware manufacturers offer ready-made solutions to protect against network intruder (NI) threats. Such software and hardware may resemble a small server that allows protection against weak and medium-scale DDoS attacks as well as other types of NI threats. In practice, the following equipment is often used to neutralize intruders [7]:

- Firewalls with dynamic packet inspection;
- Dynamic SYN-proxy mechanisms;
- Limiting the number of SYN requests per IP address per second;
- Limiting the number of SYN requests per remote IP address per second;
- Installing ICMP flood filters on the firewall;
- Installing UDP flood filters on the firewall;
- Limiting the speed of routers connected to the firewall and the network.

Filtering and blocking traffic from attacking machines allows us to mitigate or completely neutralize the attack. When this method is applied, incoming traffic is filtered according to specific rules defined during the configuration of filters.

Network firewalling [8] is considered a highly effective method of protection against cyberattacks. A network firewall is a set of hardware or software tools that control and filter network packets passing through it in accordance with predefined rules.

Fig 2 shows the scheme of organizing the data transmission network of a railway station communication node using a firewall.

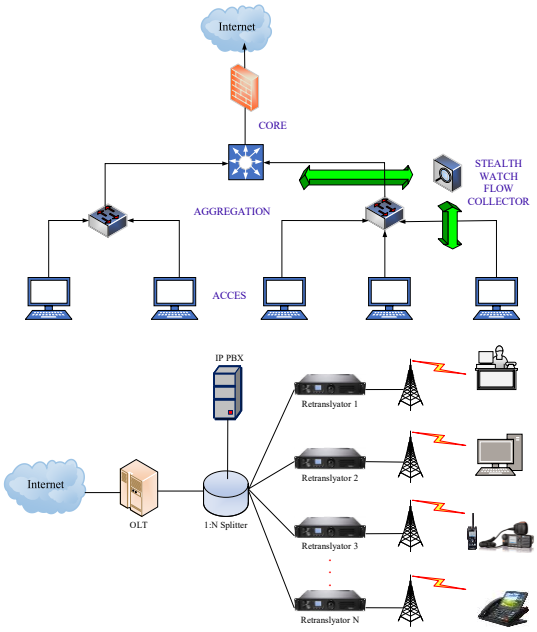

Fig. 2. Communication center of the railway station

The main function of network firewalling (firewall) is to protect computer networks or individual nodes from unauthorized access. In addition, firewalls are often referred to as filters, since their primary task is to block packets that do not meet the criteria specified in the configuration (i.e., filtering).

When a firewall is connected to a data transmission network (DTN), most modern firewalls perform the following functions [9]:

- attack detection;
- antivirus scanning to search for known virus signatures in traffic;
- tools for monitoring the integrity of files on a personal computer;
- tools for routing and proxying traffic (proxy servers).

The principle of operation of a firewall is to protect a network or computer from threats originating from the Internet. Each computer in a network has its own IP address, and data is transmitted through the network in IP packets. When data is transmitted, each IP packet contains the IP addresses of the sender and receiver. Accordingly, packets are delivered to recipients based on IP addresses.

However, typically, several applications run on a computer, and most of them require network access. In order for applications to interact in a network according to standards, they use special protocols [9]. For example, e-

mail requires SMTP (Simple Mail Transfer Protocol), a web browser requires HTTP (Hyper Text Transfer Protocol), and so on. Each protocol uses specific network ports, and their numbers are defined in standards. Thus, for SMTP the port is 25, and for HTTP it is 80.

Malware such as worms and trojan horses, as well as other malicious programs, can also use network ports and protocols to gain access to victims' devices, spread to other devices in the network, and transmit confidential computer data to hackers. Therefore, all ports and protocols that are not used in the direct operation of the computer should be "closed" using a firewall.

Modeling DoS Attacks in IP Communication Networks: Theory, Impact, and Mitigation [10].

The purpose of Denial of Service (DoS) attacks is to disrupt the normal operation of a network or server, which is usually carried out by overloading resources through excessive requests. In IP communication networks, such attacks cause packet loss and increased latency, mainly due to unencrypted traffic and limited resources. For Rapid Technological Communication (TTA) networks, particularly train dispatcher communication systems used in railway sections, this poses a serious threat to security and train traffic safety [10].

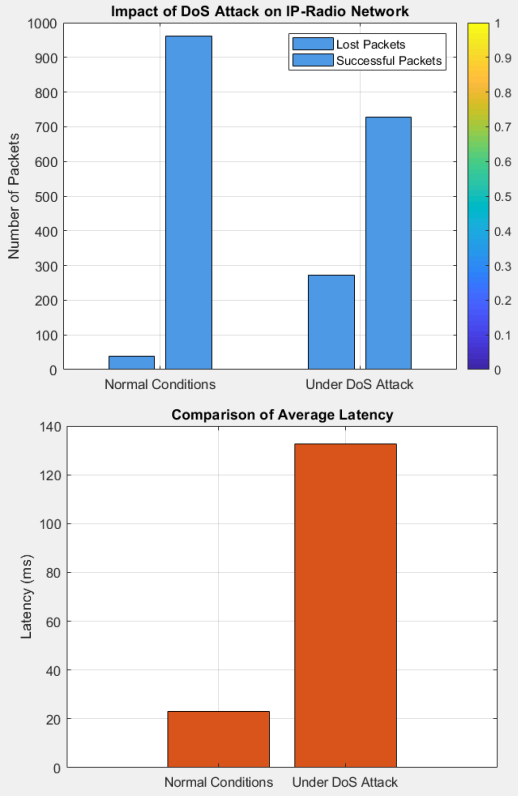

Fig. 3. DoS attack

A simulation was conducted in the MATLAB environment using 1000 packets under normal and DoS conditions:

- Normal conditions: packet loss 5%, average latency ~20 ms.
- DoS conditions: packet loss 30%, average latency ~100 ms. Random probabilities and noise were introduced to approximate real network conditions.
- Simulation results:
  - In normal conditions: approximately 50 packets were lost (5%), 950 packets successfully delivered, with an average latency of ~20 ms.
  - In DoS conditions: approximately 300 packets were lost (30%), 700 packets successfully delivered, with an average latency of ~100 ms.

These results indicate that during a DoS attack, packet loss increases threefold and latency increases fivefold.

Recommended Mitigation Measures

- Traffic Encryption – Encrypting IP communication network traffic to reduce the risk of data theft by attackers.
- Strengthening QoS Mechanisms – Developing specialized tools (e.g., SBC) to manage network load and ensure service quality.
- Real-Time Monitoring – Implementing dedicated monitoring systems to detect DoS attacks.
- Optimizing Network Resources – Enhancing server and network capacity to withstand DoS attacks.

The results of the conducted simulation demonstrate that DoS attacks have a significant negative impact on IP communication networks—leading to increased packet loss and latency, which jeopardizes the safety of railway communications. The practical implementation of these mitigation measures is crucial for protecting RTC networks from cyber threats and ensuring stable communication in railway sections.

Reliability Model of the TTA Network for N Stations. For the reliable operation of the Rapid Technological Communication (TTA) network in a railway section, all station elements along the section must function correctly. This condition can be represented mathematically as follows. Logical condition for the correct operation of the TTA network sections of the railway segment (1).

$$K_{i.element}(t_f) = f_{\text{railway section}}(t_f) = f_{\text{element.st.A}}(t_f) \wedge f_{\text{element..st.B}}(t_f) \wedge \ldots \wedge f_{\text{element..st.N}}(t_f) \quad (1)$$

$f_{\text{element..st}}$ – denotes the reliability function of the n-th station element at time t_f;

$\wedge$ – represents the logical AND operation, meaning that the overall system works correctly only if all station elements operate reliably;

$K_{i.element}(t_f)$ – the overall reliability condition of the TTA network in the railway section.

Thus, the overall reliability of the TTA network in a railway section with N stations is determined by the product of the reliabilities of each individual station. If any single station element fails, the overall reliability of the section's TTA network decreases significantly.

Based on formula (1), the dynamic change of reliability of the TTA network in the railway section is obtained (Fig 4).

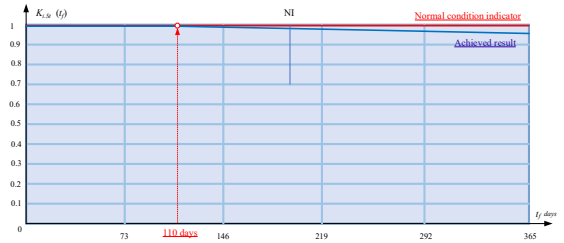

Fig. 4. Variation of the readiness coefficient of the RTC network in the railway section

https://doi.org/10.56143/3030-3893-2025-3-55-58 A bridge between science and innovation

As can be seen from Figure 4, after 110 days of operation (on an annual scale), the availability coefficient of the RTC network in the railway section did not meet the required level of reliability. This, in turn, necessitated additional maintenance and recovery measures, as well as the development of scientific and technical solutions aimed at improving the readiness coefficient of the RTC network in the selected area [11].

By applying the developed scientific and technical solutions to enhance the reliability of the communication network in the railway section, significant improvements can be achieved. These results are calculated based on formula (1).

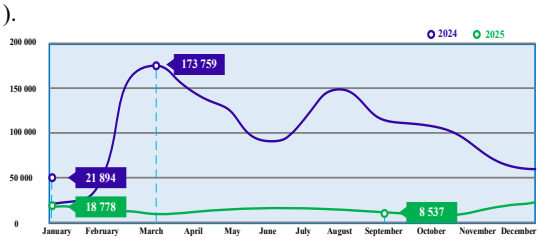

Fig. 5. Variation of the readiness level of the communication network under DDoS attacks by months during the implementation of scientific and technical solutions developed for the railway section

The analysis of the obtained results shows that the practical implementation of the proposed scientific and technical solutions significantly improves the reliability level of the RTC network in the railway section, while also taking into account potential cyber impacts on network elements. The achieved results meet the requirements of information security system standards, ensuring that, on an annual scale, the average number and duration of failures or malfunctions in dispatcher-level networks do not exceed 10 minutes [12].

3. Conclusion

Based on the conducted research, scientific approaches for assessing the reliability and ensuring the cyber resilience of IP-based RTC networks in railway sections have been developed. Simulation results identified the risks of DoS attacks and evaluated their impact on packet loss and latency.

As a result of the analysis, technical solutions such as traffic encryption, strengthening QoS mechanisms [12], real-time monitoring, and the use of firewalls were proposed for train dispatcher communication systems.

The practical implementation of these solutions improved the readiness coefficient of RTC networks, ensured compliance with international information security standards, and contributed to enhancing overall transport safety.

References

[1] Smith, A., & Garcia, M. (2020). Enhancing data security in IP-based railway communication systems. International Journal of Transportation Safety. DOI: 10.1016/j.ijts.2020.05.001

[2] ITU. (2016). Introduction to railway communication systems. ITU Report. Retrieved from https://www.itu.int.

[3] Jablonski, M. (2022). Digital transformation in rail transport—key challenges and barriers. Springer Proceedings on Intelligent Transportation Systems. DOI: 10.1007/978-3-030-96133-6_5.

[4] European Parliament. (2019). Digitalization in railway transport. European Parliamentary Research Service. Retrieved from https://www.europarl.europa.eu.

[5] Nikitin, A., Manakov, A., & Knyazev, A. (2020). On the issue of using digital radio communications of the DMR standard to control the train traffic on Russian railways. Retrieved from.

[6] Li, P., Xue, R., Shao, S., Zhu, Y., & Liu, Y. (2023). Current state and predicted technological trends in global railway intelligent digital transformation. Railway Sciences. DOI: 10.1108/rs-10-2023-0036.

[7] Khalikov Abdulxak, Khurramov Asliddin, Urokov Olim, Rizakulov Sherzod. A mathematical model of the operation process of a radio communication network based on IP technologies in the conditions of information impact during the transmission of a non-repetitive data stream / E3S Web of Conferences 420, 03022 (2023).

[8] Xurramov A.Sh., O‘roqov O.X., Xolboyev Sh.F. Temir yo‘l uchastkalarida poyezd radioaloqasini tashkil qilishda raqamli mobil tizimlarini joriy qilish. Muhammad al-Xorazmiy avlodlari, № 1 (27), mart 2024. ISSN-2181-9211. TATU. 140-143b.

[9] Хуррамов А.Ш., Уроков О.Х., Ирагашев Н.Н. Анализ и оценка факторов, влияющих на сеть оперативной технологической радиосвязи на основе IP-радиотерминалов. Транспорт: наука, техника, управление. Научный информационный сборник. – 2024. – № 5. – С. 26-29. – DOI 10.36535/0236-1914-2024-05-4. – EDN KKOZTJ.

[10] Recommendation ITU – T Y.110. Global Information Infrastructure principles and framework architecture.

[11] Khalikov Abdulxak, Khurramov Asliddin, Urokov Olim, Rizakulov Sherzod. A mathematical model of the operation process of a radio communication network based on IP technologies in the conditions of information impact during the transmission of a non-repetitive data stream / E3S Web of Conferences 420, 03022 (2023).

[12] Xalikov A.A., O‘rokov O.X., Xurramov A.Sh. IP-tarmoq asosidagi tezkor texnologik radio aloqa tarmog‘i ishonchliligini hisoblash metodikasi. Muxammad Al-Xorazmiy avlodlari № 1(23)/2023. ISSN-2181-9211. TATU. 125-132 b.

Information about the author

Asliddin Khurramov
Tashkent State Transport University, Associate professor of Department of Radioelectronic Devices and Systems, Ph.D.
E-mail: asliddinxurramov703@gmail.com
Tel.: +998909077300
https://orcid.org/0000-0002-8443-9250

Cyber attacks using Artificial Intelligence systems

U. Begimov[1][a], T. Buriboev[1][b]
[1]Alfraganus university, Tashkent, Uzbekistan

Abstract: This article discusses one aspect of the use of Artificial Intelligence in cybersecurity. It is about cyberattacks that can be carried out using Artificial Intelligence (AI) systems. AI- enabled cyberattacks can be defined as any hacking operation that relies on the use of AI mechanisms. Another term used is offensive AI. AI-based cyberattacks are undoubtedly changing the cybersecurity landscape. First of all, it is necessary to talk about the speed of implementation of attacks and their scaling. AI-based cyberattacks involve the use of advanced machine learning algorithms to identify vulnerabilities, predict patterns, and exploit weaknesses. Efficiency and rapid data analysis enhance the ability of hackers to gain a tactical advantage, resulting in rapid intrusions or destruction of data. Traditional cybersecurity methods are no longer sufficient to combat sophisticated attacks, as AI-enabled cyberattacks adapt and evolve in real time. In addition, the introduction of AI systems in cyber defense gives rise to new risks. AI systems themselves become targets of adversarial attacks.The article discusses general issues of organizing cyber attacks using AI, provides taxonomy and examples of such attacks.

Keywords: machine learning, deep learning, cybersecurity, cyber attacks

1. Introduction

The use of Artificial Intelligence (AI) in cybersecurity has several aspects. Following the gradation proposed by Microsoft, the following areas can be distinguished:

- AI in cyberattacks (offensive or attacking AI);
- AI in defense against cyberattacks. The most well-known area of application today with the largest number of examples of use
- Cybersecurity of AI systems themselves (attacks on AI systems). The most actively developing area
- Malicious influences (e.g. deepfakes)

The article was received on June 12, 2024. D.E. Namiot - Lomonosov Moscow State University As usual.

AI systems are understood as machine learning models. In this article, we would like to focus on the use of AI in cyberattacks. Obviously, due to the specifics, not everything in this area is published. But it is also obvious that this area has received a great additional impetus for development with the growing popularity of large language models. The idea that it is possible, for example, to automate programming immediately prompts interested parties to think about automating the creation of malware, the ability of generative models to create “human” tests gives rise to thoughts about phishing, etc. Since a very rapidly developing industry is considered, the course materials are revised annually. The current version (2024) was created with the support of the Cybersecurity Department of Sberbank PJSC. The rest of the article is structured as follows. Section II discusses general provisions. Section III is devoted to the taxonomy of offensive AI. Section IV considers an example of solving a captcha. And Section V contains the conclusion.

2. Research methodology

Procedure for paper submission. In the era of artificial intelligence, attackers are using AI-based techniques to hack cyber defense programs. These AI-based cyber attacks are undoubtedly changing the cyber security landscape. First of all, it is necessary to talk about the speed of execution of attacks and their scalability. AI-based cyber attacks involve the use of advanced machine learning algorithms to identify vulnerabilities, predict patterns, and exploit weaknesses. Efficiency and rapid data analysis enhance the ability of hackers to gain a tactical advantage, resulting in rapid intrusions or destruction of data. Traditional cyber security methods are no longer sufficient to combat sophisticated attacks, as AI-based cyber attacks adapt and evolve in real time.

The traditional defense scheme for IT organizations in the early 2000s included perimeter protection and malware concerns. Organizations during those periods also focused on software security, but since software applications were minimal, methods to protect against external attacks were the priority. Later, software applications emerged to help solve user-based performance issues, and organizations built advanced perimeter defense devices such as intelligent firewalls, routers, and switches to counter external network attacks.Software and hardware attacks can pose a constant threat to businesses. However, there are effective ways to counter these threats. One such way is to use a system dependency model. This model combines predictive analysis, response time, attack type, containment, and cyber defense into a single system rather than treating them as separate entities. The system dependency model helps predict attack patterns and counter intrusions, especially for SOC (Security operations center) personnel. Each team member has an advantage due to the visual indicators and threat data provided by network security devices. However, AI-enabled cyber attacks require SOC personnel to re-evaluate their cyber defense strategy. Today’s situation is different because AI- driven cyberattacks are software-driven and adapt to configuration changes. No cyberdefender can resist the real-time changes, analysis, and adaptability of AI-driven attacks. Because AI platforms use machine learning to identify network behavior patterns and vulnerable targets, they can adapt and change their attack method.

Artificial intelligence (machine and deep learning) is increasingly used in cyber defense. At the same time, all

[a] https://orcid.org/0000-0002-6983-6709

[b] https://orcid.org/0009-0001-6700-4095

such defense tools can be targets of adversarial attacks. Such attacks involve modifications of data at different stages of the machine learning pipeline, are relatively easy to implement, and, in most cases, cannot be completely excluded. Accordingly, poisoning attacks, backdoors, and, of course, evasion attacks, which concern AI-based defense tools, are typical applications of AI (machine learning) in cyber attacks. NIST in its taxonomy of adversarial attacks separately considers adversarial attacks in the field of cybersecurity. Historically, the first adversarial attacks began in this domain. The first known poisoning attack was developed to generate worm signatures back in 2006.The aforementioned work considered systems that automatically determine signatures (signs) of software worms. That is, in fact, rules for malware signatures. The attack proposed by the authors polluted (noised) the traffic used by automatic signature generators during their extraction. The attack was aimed at misleading signature generation algorithms by introducing well-designed noise that prevented the generation of useful signatures. It was shown that it is possible to introduce noise without prior knowledge of the classification technique used. The use of artificial intelligence brings its own risks that differ from those traditionally considered in cybersecurity. There are many different classifications regarding this, one of which is given in. There are 14 risks of AI listed:

1. Lack of transparency and explainability of AI
2. Job loss due to AI automation
3. Social manipulation by AI algorithms
4. Oversight functions performed by AI technology
5. Lack of data privacy when using AI tools
6. Bias due to AI
7. Socioeconomic inequality as a result of AI
8. Weakening of ethics due to AI
9. Autonomous weapons based on AI
10. Financial crises caused by AI algorithms
11. Loss of human influence
12. Uncontrolled AI
13. Increased criminal activity
14. Wider economic and political instability

Lack of privacy is perhaps one of the most serious problems, which can also be relatively easily exploited through adversarial attacks targeting IP [10]. Vulnerability mitigation programs need to be changed, but there are also issues of classification. Imagine a data breach on an AI platform. Although the risk is software-based, should it be classified as a software risk or an AI-based risk? The largest collection of AI risks is contained in the MIT project: AI Risk repository. Its description is in.

In addition to adaptability and real-time analysis, AI-based cyberattacks can also cause more disruptions during a small time window. This is due to the way the incident response team works. When AI-based attacks occur, it is possible to bypass or hide traffic patterns (changing the system log analysis process or removing data that allows for defensive actions). Cybersecurity systems will need other algorithms that identify AI-based cyberattacks.

AI has created problems in which security algorithms must become, first of all, predictive and fast and accu- rate. The traditional IT landscape contains many risks related to privacy, perimeter protection, software applica- tions or data leakage. These risks create loopholes and weaken the organization's defensive posture. Counter- measure tactics are to eliminate risks and improve the level of cybersecurity. The introduction of AI into the risk and vulnerability ecosystem is transforming security compliance and cyber defense. As AI leverages behavioral analytics, machine learning, and real-time analysis, busi- nesses must learn about risks based on patterns and com- putational errors. This is where continuous monitoring and AI will work best. Organizations must also determine how IT system audits, risk assessments, etc., configura- tion changes and remediation deadlines should evolve.

Cybersecurity transformation also requires the development and implementation of controls. Typical frameworks such as NIST 800-53 or OWASP are structured based on application, cloud, data, identity and infrastructure. An open question is whether AI should be implemented in the same control frameworks or whether current controls should be modified? This, among other things, will de- termine the attack surfaces of AI.

Taxonomy of offensive AI. AI-enabled cyberattacks can be defined as any hacking operation that relies on the use of AI mechanisms. Another term used is offensive AI.Everything in scientific papers begins with some classification. Let us note right away that cyberattacks are a rather sensitive area, so not everything is openly published. However, Figure 1 shows one possible classification of AI attacks:

Fig. 1. AI attacks

This list obviously lacks adversarial attacks on machine learning models, which are widely used in information systems, cyber-physical systems, and Internet of Things systems. Other comments include the following: Keyboard sniffing is part of a more general problem called side-channel attacks, where AI is widely used. Phishing, in principle, can be classified as a social engineering attack. Deepfakes also include voice cloning. Separating voice cloning into a separate category is possible if we are talk- ing about biometric authentication, for example. This is traditionally separated from deepfakes. Classically, deepfake (from deep learning + fake) was originally understood as as a method of synthesizing an image or voice that imitates a person and is based on artificial intelligence. Deepfake technologies can also be used to create fake news and any malicious deception. Deepfakes are usually singled out as a separate area of using AI in cybersecurity, and they are considered in this paper.

Despite these remarks, at least this list gives an idea of what AI attacks are. Of the elements omitted in this classification, it would be worth adding automation of attacks. In our opinion, this is a separate area of using AI in cyberattacks. For example, the so-called AI-driven pentesting. Examples of such automation of pentesting are, for example, startups XBOW and RunSybil.

Figure 2, which is taken from a highly cited work, provides a classification of attacks described in the scientific literature by types of impact. The attacks here are distributed

across six stages of the cybersecurity chain (kill chain). Fig. 2. Attacks by stages of the kill chain

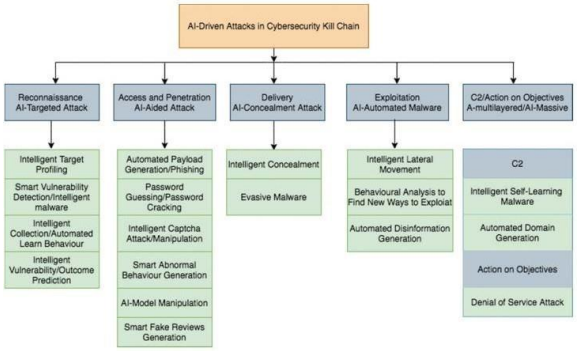

Fig. 2. AI attacks

Six types of AI-driven attacks were identified in the access and penetration stage (AI-assisted attack), four types of AI-driven attacks were identified in the access reconnaissance stage (AI-targeted attack), three types of AI-driven attacks were identified in the exploitation stage (AI-automated attack), and two types of AI- driven attacks were identified in the delivery stage (AI-concealment) and C2 stage (Command Control) respectively. In contrast, one type of AI-driven attack was identified in the targeting stage (AI-malware). The access and penetration stage had the most publications (6), followed by the reconnaissance stage (4), the exploitation stage had three publications, and the delivery and C2 stages had two. In contrast, the target-based phase (AI malware) had the fewest publications (1). Fig. 3. LLM in attack.

Year	MITRE Tactic(s)	Application	Model(s)
2023	Execution	Generating code to perform actions that could be malicious	GPT-3
2022	Initial Access	Generate phishing emails to bypass spam filters	GPT-2, GPT-3, RoBERTa
2022	Execution - Command & Control	Use of LLMs as plug-ins to act as a proxy	GPT-4
2023	Initial Access - Collection	Generate Phishing Website via ChatGBT	GPT-3.5 Turbo
2023	Execution	Code generation and DLL injection	GPT-3
2023	Initial Access - Reconnaissance	Collecting victim data to develop an attack email	GPT-3.5, GPT-4
2023	Initial Access - Execution - Defense Evasion	Crafting malicious scripts	GPT-3.5 Turbo, GPT-4, text-davinci-003
2018	Initial Access	Spear Phishing link	AWD-LSTM
2023	Defense Evasion	Code obfuscation, file format modification	GPT-3.5
2023	Initial Access - Credential Access	Password guessing using LLMs	GPT-2
2023	Initial Access - Reconnaissance	Impersonation for phishing aims	GPT-3.5 Turbo
2022	Initial Access	Generating content for misinformation	GPT-2

Fig. 3. AI attacks

Potential attackers place great hopes on LLMs (which are, accordingly, of great concern to the cybersecurity community) to automate attacks. Here are examples of LLMs being used in cyberattacks (as of early 2024) in killing chain mitigation

It should be noted that such lists will constantly grow. This process is absolutely natural. If we want to teach LLM to write code, then the idea that it could be malicious code or some kind of data encryptor arises almost automatically. If we demonstrate the capabilities of the same LLM to write selling marketing offers, then it is easy to guess that the text for phishing mailings will not be much different. And so on.

Automation (democratization - lowering the entry threshold and reducing costs) is a natural process. The same, accordingly, applies to protection: there is simply no other way out. Attacking robots must be met by the same robots-defenders

Solving captcha. A large number of works are devoted to such tasks. Ob- jectively, image recognition is one of the most traditional tasks for machine (deep learning). Examples of works. How it looks, we will analyze using the example of work. The work describes an attack on text captchas (text recognition in a picture). Examples of such tasks are shown in Figure 4. The length of the line in characters and the modifications made are indicated Fig.4.

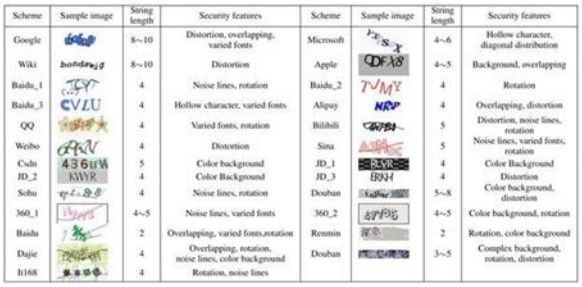

Fig. 4. AI attacks

Text captchas As shown in Figure 5, the attack consists of 3 steps. Fig.5. Attack pattern

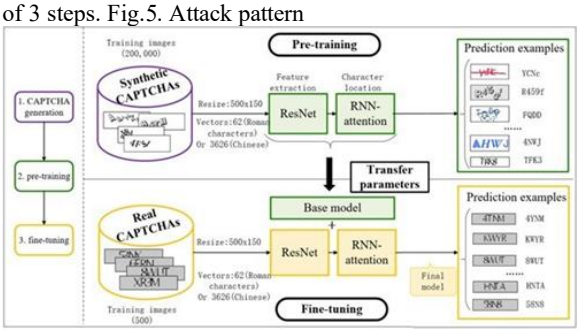

Fig. 5 AI attacks

Step 1: CAPTCHA Generation: This step uses image processing algorithms to generate CAPTCHAs unrelated to the target scheme to train our recognition network. In the attack under consideration, all pre- samples are generated completely randomly without any special design, which is easy to implement and significantly reduces the effort spent on collecting training samples.

Step 2: Pre-training: Once generated, the synthetic CAPTCHAs are fed directly into the recognition engine without any pre-processing to train the base model. After pre-training, we adopt the trained model as the base model for all subsequent schemes.

Step 3: Fine-tuning: Finally, for each scheme, 500 real samples were used to fine-tune the base model. This step was accomplished by re-training the base model using transfer learning to update the parameters to match the real features. Note that only domain-specific adaptation of transfer learning was used and the model remained consistent across the pre-training and re-training steps. Basic architectural decisions:

To reduce the cost associated with manual labeling, synthetic CAPTCHAs were generated as pre-training data for the pre-training. All training data for the baseline model is generated using simple image processing algorithms from the Pillow library.

As shown in Fig. 6, all pre-training samples are generated with black characters on a pure white background. Unlike the original CAPTCHAs, there are no security features in the generated CAPTCHAs: for example, there are no noise lines, distortions, overlays, etc. Instead, the samples were generated in the simplest way to reduce the generation cost, since this type of CAPTCHA is easy to implement and does not require much effort. The gener- ated CAPTCHAs are completely unrelated to the target CAPTCHAs (Fig. 4) and do not resemble any of the target schemes.

For the Latin character-based schemes, the text string length is set in the range from 4 to 10; The fonts are randomly selected from the font library, including both

https://doi.org/10.56143/3030-3893-2025-3-59-63 A bridge between science and innovation

regular and hollow styles; all images are the same size, and the text rotation angle is set from minus 45 to 45 degrees. For Chinese patterns, the line length was set to a range of 2 to 5. 500,000 images were generated to pre- train the base model. Fig. 6. Some examples of randomly generated CAPTCHAs for training the base model.

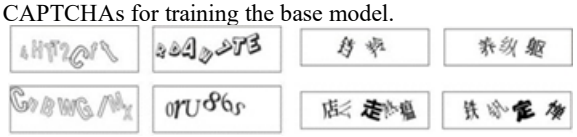

Figure 6: AI attacks

Like any other applied problem in machine learning, the main challenge is training data and feature engineering. All samples were of the same size 500 × 150.

2. In pre-training (base model), a combination of CNN and LSTM was used. In order to recognize the entire character string in one step, the combined model described in, consisting of a CNN and a Long Short-Term Memory (LSTM) model, was used as the recognition engine. The CNN is responsible for extracting the feature vector of the CAPTCHA image. For this, the ResNet v2-101 model was chosen, which is designed to address the degradation problem that occurs as the network depth increases. LSTM converts the feature vectors extracted by the CNN into a single text string; it can be thought of as a character-level language model. Decisions are made using the latest states in the memory cells.

In this experiment, the number of LSTM cells depends on the maximum string length of the target CAPTCHA.

3. In the last step (fine-tuning), transfer learning is used to fine-tune the parameters of the pre-trained modelwith several real CAPTCHAs. Transfer learning works as follows. In transfer learning, a domain D is denoted as D= X, P(X), where X is the feature space and P(X) is the marginal probability distribution. For a particular domain, the task can be defined as T = Y, f, where Y denotes the label space and f denotes the target predictor. In general, the complete transfer learning process includes one source domain (DS) and one target domain (DT), which correspond to one source task (TS) and one target task (TT), respectively. From the knowledge in DS and TS, transfer learning aims to improve the learning of the target predictor f in DT. In this CAPTCHA solver, f denotes the predictor in ResNet, and DS and DT are as follows:

As for the training data is a synthetic CAPTCHA, and yTi is the corresponding CAPTCHA label, a character string. Here have the same values as in real CAPTCHAs. Note that all labels remain the same in DS and DT (62 or 3626 characters), but the feature spaces are different because the features of the synthetic and real CAPTCHA have different details. For each Roman character-based scheme, 500 hand-labeled real samples were used. Considering that Chinese CAPTCHAs have a larger character set than Roman CAPTCHAs, 1000 real hand-labeled Chinese CAPTCHAs were used per Chinese scheme.

3. Conclusion

As a conclusion, we present the following 5 points that, according to the authors of, determine the future of offensive AI. They attribute this to generative AI and large language models (LLMs) trained to generate malicious content (e.g. FraudGPT). 1. Automated social engineering and phishing attacks LLMs like FraudGPT demonstrate the ability of generative AI to support convincing scenarios for pretexts that can mislead victims. One use case is for attackers to ask LLMs to write science fiction stories about how a successful social engineering or phishing strategy works, thus forcing the LLM itself to provide attack recommendations. Other use cases could be to request instructions for attacks in national languages, in which case security filters set to English may not work. 2. AI-generated malware and exploits. FraudGPT has proven its ability to generate malicious scripts and code tailored to a specific victim's network, endpoints, and broader IT environment. Novice attackers can quickly master the latest defenses by using AI-powered generative systems like FraudGPT to learn and then deploy attack scripts. This is why organizations must do everything they can to ensure cyber hygiene, including endpoint protection. AI-generated malware can bypass older cybersecurity systems that were not designed to detect and prevent this threat. 3. Automated asset discovery by cybercriminals.

Generative AI will reduce the time it takes to conduct manual research to find new vulnerabilities, find and collect compromised credentials, learn new hacking tools, and master the skills needed to launch sophisticated cybercrime campaigns. Attackers of all skill levels will use it to discover unprotected endpoints, attack unprotected threat surfaces, and launch attack campaigns based on information obtained through simple clues.

It is noted that along with identification, endpoints will be subject to more attacks. Self-healing endpoints are noted to be critical, especially in mixed IT and operational technology (OT) environments that rely on Internet of Things (IoT) sensors. A self-healing endpoint is a technology for automating the monitoring and diagnosis of performance and security issues across multiple network nodes or endpoints.

Traditional incident response often requires significant manual intervention to identify and remediate compro-mised systems. Self-healing endpoints, on the other hand, use AI and machine learning algorithms to automatically detect, isolate, and remediate security incidents without human intervention. These endpoints continuously moni- tor and analyze system behavior, enabling proactive threat detection and autonomous response, resulting in reduced response times and a lower chance of widespread compro-mise.

These endpoints can proactively detect anomalies and potential security threats by continuously monitoring their behavior and network communications. This proactive approach not only reduces the need for constant human intervention, but also helps detect and mitigate risks, strengthening the overall security posture.

4. AI-powered evasion is just getting started, and we haven't seen the real problems yet.Weaponized generative AI is still in its infancy, and FraudGPT is just the beginning. More sophisticated and lethal tools are emerging. They will use generative AI to evade endpoint detection and response systems, and create malware variants that can evade static signature detection.

5. Difficulty of Detection and Attribution. FraudGPT and future generative AI applications and tools will reduce the detection and attribution barrier to anonymity. Security teams will have a hard time attributing AI- enabled attacks to a specific threat group or campaign based on forensic artifacts or evidence. Greater anonymity and difficulty in detection will lead to longer dwell times and allow attackers

to perform long-term attacks that are typical of advanced persistent threat (APT) attacks on high-value targets. Weaponized generative AI will eventually make this possible for every attacker.

References

[1] Echocardiographic images via machine learning algo- rithmics // Analysis of world scientific views International Scientific Journal Vol 2 Issue 1 IF(Impact Factor)8.2 / 2023

[2] O'.I.Begimov, T.M.Bo'riboyev / General Theory About the Traditional Methods and Algorithms of Ma- chine Learning // AMERICAN Journal of Public Diplo- macy and International Studies Volume 02, Issue 04, 2024 ISSN (E):2993-2157.

[3] T.M.Bo'riboyev / Hetnet tizimi asosida avtonobillar- ing harakat trafigini boshqarish va tahlil qilish // Nejmet- tin, 03-06 Ekim 2023 tarihlerinde Erbakan Üniversitesi ve Alfraganus üniversitesi öncülüğünde düzenlenen "ipek Yol- unun Ötesinde kongreler dizisi: Bir Yol, Bir Kuşak: Göç, turizm ve ekonomi politik Kongresi (SIRCON 2023)" pro- gramına sertifika almak için katıldı. (Sayfa 320-324)

[4] NIST AI 100-2 E2023 Adversarial Machine Learn- ing: A Taxonomy and Terminology of Attacks and Mitiga- tions https://csrc.nist.gov/pubs/ai/100/2/e2023/final : 15.07.2024

[5] Perdisci, Roberto, et al. "Misleading worm signature generators using deliberate noise injection." 2006 IEEESymposium on Security and Privacy (SP'06). IEEE, 2006.

[6] 14 Risks and Dangers of Artificial Intelligence (AI) https://builtin.com/artificial-intelligence/risks-of-artificial- intelligence 15.08.2024.

[7] Song, Junzhe, and Dmitry Namiot. "A survey of the implementations of model inversion attacks." International Conference on Distributed Computer and Communication Networks. Cham: Springer Nature Switzerland, 2022.

[8] NIST SP 800-53 Rev. 5 Security and Privacy Controls for Information Systems and Organizations https://csrc.nist.gov/pubs/sp/800/53/r5/upd1/final 15.08.2024.

[9] OWASP https://owasp.org/ 15.08.2024.

Information about the author

Begimov Uktam Ibragimovich	Alfraganus University, PhD, associate professor of Faculty of Digital Technologies E-mail: uktam1985beg@mail.ru Tel.: +99894 669 63-18 https://orcid.org/0000-0002-6983-6709
Buriboev Tolibjon Mirali ugli	Alfraganus University, assistant teacher of Faculty of Digital Technologies E-mail: buriboevtolib@gamil.com Tel.: +99894 563 19-98 https://orcid.org/0009-0001-6700-4095

Mathematical modeling of the effect of internal combustion engine parameters on vehicle acceleration dynamics

A.A. Ernazarov[1][a], S.S. Musurmonov[2][b]
[1]Jizzakh Polytechnic Institute, Jizzakh, Uzbekistan
[2]Tashkent state Technical University named after Islam Karimov, Tashkent, Uzbekistan

Abstract: Mathematical model has been calculated in the study, which determines the relationship between the engine's operating process and the dynamics of the car. The adequacy of the model was verified using an experimental study of the B15D2 engine to obtain adjustment, load and external speed characteristics.
Keywords: engine workflow, mathematical model, acceleration dynamics; experimental study, speed characteristics

1. Introduction

Mathematical modeling of the influence of internal combustion engine (ICE) parameters on the dynamics of vehicle acceleration is an important task in the automotive industry and transportation engineering. It allows you to evaluate how different engine characteristics affect vehicle acceleration, acceleration time to a certain speed, and other dynamic indicators.

These models are based on the balance of forces acting on the car during its movement. For example, in models [1-3], a car is represented as an elastic-mass oscillatory system. The rolling of the wheel on uneven and flat surfaces is described in detail, the inertial and elastic characteristics of the moving parts of the engine, transmission and wheels are taken into account. These models are characterized by the complexity of implementation and verification, and require the establishment of a number of empirical coefficients based on the results of experimental studies. In addition, there is a lack of information in the literature on the use of such models in car parameter optimization tasks.

When solving a number of tasks, for example, choosing the parameters and settings of an engine and a car, creating a preliminary design of a car, and studying its dynamic qualities, it is advisable to use simpler models [4-7]. These models, for example, the graphoanalytical method make it possible to determine the acceleration and path of a car based on the calculation of the so-called dynamic factor.

In mathematical models of car acceleration, the maximum engine power in the modes of external speed characteristics is usually set according to empirical dependencies. For example, in the Leiderman equation, the current maximum engine power depends on the rated power and rotational speed of the crankshaft, as well as the current rotational speed of the crankshaft. This makes it impossible to optimize the parameters and settings of the engine, while ensuring good dynamic qualities of the car.

An attempt to combine mathematical models of the working process of an engine and a vehicle was made in [8]. The engine operating modes when the car is moving according to the European NEDC test cycle are replaced by quasi-stationary driving modes with a constant speed of 1 s. To reduce the engine parameters in quasi-stationary cycle modes to the parameters of the actual cycle, the calculated engine parameters are multiplied by the empirical coefficients given in [9].

The disadvantage of this approach is the use of empirical coefficients generalized based on the results of experimental tests for a number of engines of a certain class, which makes it impossible to take into account the design features and workflow of a particular engine.

Thus, the aim of the work is to develop a mathematical model of the dynamics of car acceleration, taking into account the influence of the design parameters and adjustments of the internal combustion engine on this process.

2. Research methodology

The methodology of computational research. The mathematical model of the engine workflow includes submodels:

- determination of the thermophysical properties of air, fuel of any component composition, as well as exhaust gases;
- determination of the kinematic characteristics of the movement of the elements of the crank mechanism and the passage sections of the valves;
- simplified calculation of the working process to obtain a first approximation of the parameters of the working fluid in the cylinder at the beginning of the exhaust stroke;
- quasi-stationary calculation of gas exchange, compression and expansion in a cylinder using the volumetric balance method;
- combustion according to the Vibe model [10], in which the indicators of the nature and duration of fuel combustion are set using empirical formulas given in the work;
- heat transfer in the cylinder according to the Gerhard Vosni model [11];
- friction losses as an empirical function of the average piston speed. The feasibility of using this empirical dependence for a research engine was evaluated in the work.

The adequacy of the mathematical model was assessed by comparing the calculation results of specific effective fuel consumption (g_e), filling coefficient (η_v) and hourly air consumption (G_n) with experimental data. Figure 2 shows the adjustment characteristics for the composition of the mixture and the ignition timing angle, Figure 3 shows the load and external speed characteristics. It can be seen that

[a] https://orcid.org/0000-0002-4188-2084
[b] https://orcid.org/0009-0009-8618-1722

the mathematical model provides a sufficiently high accuracy in determining the effective performance of an experimental engine.

The study of the dynamic properties of the car was carried out according to the next method. The range of vehicle speeds from 0 to 100 km/h was divided into sections lasting 1 km/h. It was believed that the car was moving at a constant acceleration in each section. Knowing the speed at the beginning of the section and the average acceleration in the calculated interval, you can determine the speed at the end of the section.

The main factor determining the current acceleration value of the car is the dynamic factor D, which depends on the traction force, the force of air resistance and the weight of the car. Thus, the task of the study was to calculate the parameters that determine the dynamic factor and acceleration of the car.

Unfortunately, the basic methodology does not clearly specify the method for accounting for the effect of vehicle gearshift time on acceleration dynamics, which can be used in machine calculations. The authors proposed to determine the acceleration time Δt in the speed range from v_1 to v_2 when shifting gears as follows. Time t can be divided into two intervals (Fig. 1):

$$\Delta t = \Delta t_1 + \Delta t_2, \quad (1)$$

where Δt_1 is the gearshift time; Δt_2 is the acceleration time from speed v_1 to speed v_2

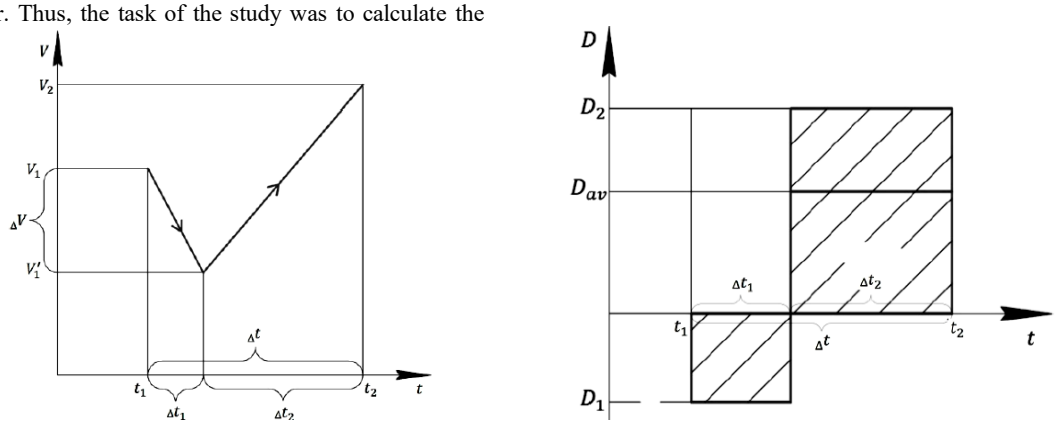

Fig. 1. Diagram for determining the dynamic factor when shifting gears

The time Δt_1 depends on the driver's qualifications and can vary from 0.2 to 3 seconds [5]. During Δt_1, the vehicle's speed decreases by Δv and reaches v_1 at the end of the first interval.

When shifting gears, the car moves by inertia, and the traction force $F_{t1} = 0$. Accordingly, the dynamic coefficient during the interval Δt_1

$$D_1 = -\frac{F_{v1}}{G}, \quad (2)$$

where F_{v1} is the aerodynamic drag; G is the weight of the vehicle.

The dynamic factor D_1 determines the acceleration of the car j_1 in the range Δt_1.

To simplify calculations, we assume that the aerodynamic drag F_{v1} during a gear change is constant and corresponds to the speed in the previous gear. In this case, the acceleration j1 is considered constant, and the speed decrease when shifting gears will be at $\Delta v = j_1 \cdot \Delta t_1$.

During the second interval, after the crankshaft is coupled to the F_{t2} engine transmission, the dynamic coefficient D_2, acceleration j_2 and acceleration time Δt_2 from speed v_1 to speed v_2 are calculated using the formulas of the basic methodology for the case of a vehicle moving with a certain gear.

The average dynamic factor in the calculated interval

$$D_{av} = \frac{D_1 \cdot \Delta t_1 + D_2 \cdot \Delta t_2}{\Delta t_1 + \Delta t_2}, \quad (3)$$

Average speed in the calculated range

$$v_{av} = \frac{(v_1 + v_1') \cdot \Delta t_1 + (v_2 + v_2') \cdot \Delta t_2}{2}, \quad (4)$$

The engine's crankshaft speed is calculated using the vehicle's speed, the current gear ratio from the wheels to the crankshaft, and the radius of the wheels:

$$n = \frac{v \cdot u_k \cdot u_{pb} \cdot u_0}{0.377 \cdot r_{st}}, \quad (5)$$

where v is the speed of the vehicle; u_k is the current value of the gear ratio; u_{pb} is the gear ratio of the transfer case; u_0 is the gear ratio of the main gear; r_{st} is the static radius of the wheel.

The calculations were performed in the MATLAB software environment. The main set of parameters is shown in Table 1.

An example of the results of calculating the loads in the drive of a Chevrolet Gentra car during acceleration is shown in Fig. 2.

Table 1

Chevrolet Gentra Car Parameters

Parameter	value
Vehicle weight m_a, kg	1245
Static wheel radius *rst*, м	0,26
Permissible gross weight. kg	1660
Car height *Br*, m	1445
Car width Hr, m	1725
Coefficient of filling of the frontal area of the car αA	0,78
Transmission efficiency η_T	0,97
Transmission ratio uk1 uk2 uk3 uk4 uk5	 3,818 2,158 1,487 1,129 0,886
Main gear ratio	3,72

https://doi.org/10.56143/3030-3893-2025-3-64-67 A bridge between science and innovation

In each gear, the speed of rotation of the crankshaft increases during acceleration to values above 4,500 rpm. This provides power close to the nominal value and the maximum possible traction force on the wheels for this vehicle.

The most significant component of the resistance to accelerated movement of the car is the inertia force, which at the beginning of the movement of the car exceeds the forces of rolling resistance and aerodynamic drag by more than 50 times. As the speed of the car increases, the force of inertia decreases, and at a speed of 100 km/ h it is only 1.4 times higher than the other components of the load.

Aerodynamic drag increases proportionally to the square of the vehicle's speed and, at a speed of 100 km/h, makes a significant contribution to overall drag. This force limits the maximum speed for the car, which has an estimated speed of 170 km/h. An increase in speed can be achieved mainly by increasing engine power.

The speed of 100 km/h is reached in 11.9 seconds, which corresponds to the passport data of the Chevrolet Gentra car and indicates the adequacy of the calculation methodology.

Thus, the developed complex mathematical model makes it possible to study the characteristics of the engine and vehicle during acceleration, determine the influence of vehicle parameters on these processes, and conduct optimization studies.

Experimental studies were conducted to refine the mathematical model of the working process of an automobile engine. The engine of the Chevrolet Gentra B15D2 car was chosen as the object of the study. This engine has a distributed fuel injection system, a complex of sensors and an electronic control unit.

The technical characteristics of the B15D2 engine are shown in Table 2.

During the experiment, the rotational speed of the crankshaft was measured using an electronic frequency counter and a magnetoelectric tachometer. Fuel consumption is obtained using the weight measurement method. Also, this parameter, as well as the crankshaft rotation speed, air flow, ignition timing angle and excess air coefficient were determined using standard equipment and software of the electronic engine control unit. The exhaust gas temperature was measured with a chromel-alumel thermocouple and a galvanometer. The pressure and temperature of the oil and the temperature of the coolant were also measured. The thermal mode of the engine was set by changing the water circulation of the external circuit through the oil and water cooler.

To identify the mathematical model of the workflow, the load characteristic of the engine at a rotational speed of 3600 min^{-1}, the external speed characteristic, as well as the adjustment characteristics when changing the ignition timing angle and the excess air coefficient were removed.

Table 2

Technical characteristics of the B15D2 engine

Name of the parameter	Value
Engine brand	Chevrolet Gentra B15D2
Engine type	4-stroke, petrol engine
Number of cylinders	4
Number of valves	16
Cylinder placement	inline
Cylinder diameter, mm	74.71
Stroke of the piston, mm	84.7
Working volume, l	1.5
Rated power, kW	40
The speed of rotation of the crankshaft in the rated power mode, min^{-1}	5600
Maximum torque, Nm	141
speed of rotation of the crankshaft in the mode of maximum torque, min^{-1}	3800
Compression ratio	10.2

3. Results

During the calculations, the excess air coefficient and the ignition timing angle for the acceleration of the car were studied from 0 to 100 km/h (Fig. 2). The excess air coefficient was varied from 0.8 to 1.15, and the ignition timing angle of the mixture was from 0 to 60 degrees of the crankshaft position to the HDC.

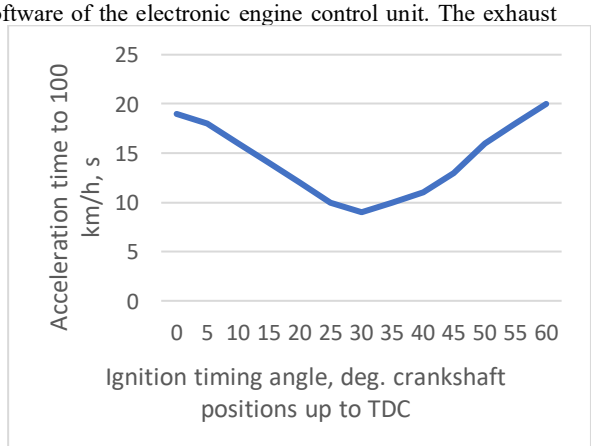

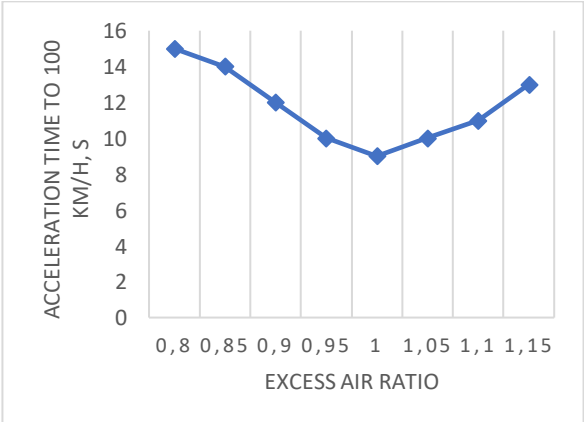

Fig. 2. The effect of engine parameters on the dynamics of car acceleration from 0 to 100 km/h

The increase in the ignition timing angle was increased by detonation and loads on the parts of the crank mechanism, the excess air coefficient was the limits of reliable ignition of the mixture. When changing a certain parameter, other engine parameters were left unchanged as on the base engine (see Table 1).

Increasing the ignition timing angle from 0 to 29 degrees of the crankshaft position to the top dead center, as well as reducing the excess air ratio from 1.16 to 0.99. increase the maximum engine power and acceleration time of the car. An increase in the ignition timing angle, a decrease in the excess air ratio, on the contrary, reduces engine power.

Accordingly, the dynamic properties of the car deteriorate.

Thus, it is shown that optimization studies need to be carried out to determine the rational values of the ignition timing angle and the excess air coefficient.

According to the results of the analysis of the data in Fig. 2, to improve the engine's pick–up, it was proposed to apply a set of parameters: ignition timing angle – 30 degrees of the crankshaft position to the TDC; excess air coefficient - 0.98. Calculations have shown that using the proposed set of parameters on the engine will reduce the acceleration time of the car by almost 10%. Further improvement of the pick-up speed of the car is possible by applying optimization methods to the selection of engine parameters, expanding the number and range of parameter variations.

4. Conclusion

The results of a comprehensive study containing:

- development of a mathematical model of the engine workflow;
- verification of the adequacy of the mathematical model of the engine workflow based on experimental research data;
- refinement of the car acceleration dynamics model, taking into account the influence of gearshift time;
- determination of the effect of changes in engine parameters on the dynamic properties of the Chevrolet Gentra.

References

[1] Теория автомобиля: учебник / В.Н. Кравец; Нижегород. гос. техн. ун-т им. Р.Е. Алексеева. – 2-е изд., переработ. – Нижний Новгород, 2013. – 413 с.

[2] Wickrama Achchige, Dilini & Herath, B & Bowatta, B & Silva, Mr & Jayaweera, Nirosh. (2016). Design and Development of Kinetic Energy Recovery System for Motor Vehicles.

[3] Syed Muzzamil Hussain Shah, Zahiraniza Mustaffa, Khamaruzaman Wan Yusof, Mohd Faizairi Mohd Nor, Influence of forces on vehicle's instability in floodwaters, Ain Shams Engineering Journal, Volume 9, Issue 4, 2018, Pages 3245-3258, ISSN 2090-4479, https://doi.org/10.1016/j.asej.2018.01.001.

[4] Динамические свойства автомобиля. Учебное пособие для студентов специальности 190109 – Автомобили и тракторы / А. Ш. Хусаинов – Ульяновск: УлГУ, 2012. – 32 с.

[5] Zhiqiang Fu, Longquan Sun, Mingyang Zhi, Pengxiao Wang, Duliang Wang, Numerical study on the dynamic characteristics of a vehicle with a multistage load reduction structure during oblique water entry, Ocean Engineering, Volume 295, 2024, 116778, ISSN 0029-8018, https://doi.org/10.1016/j.oceaneng.2024.116778.

[6] Bae, Chul-Yong & Kwon, Seong-Jin & Kim, Chan-Jung & Lee, Bong-Hyun & Na, Byung. (2007). A Study on the Development of Vehicle Dynamic Model for Dynamic Characteristics Analysis of Chassis Parts. Transactions of the Korean Society for Noise and Vibration Engineering. 17. 958-966. 10.5050/KSNVN.2007.17.10.958.

[7] Lei Zhao, Dianyou Jiang, Guotang Zhao, Jianxun Sun, Guotao Yang, Experimental study on the dynamic characteristics of bi-block ballastless track under the combined action of vehicle load and temperature gradient, Construction and Building Materials, Volume 438, 2024, 137107,ISSN 0950-0618, https://doi.org/10.1016/j.conbuildmat.2024.137107

[8] Орехов С. Н. Математическая модель рабочего процесса ДВС и ее идентификация // Машиностроение и компьютерные технологии. 2009. №12. URL: https://cyberleninka.ru/article/n/matematicheskaya-model-rabochego-protsessa-dvs-i-ee-identifikatsiya (дата обращения: 16.02.2025).

[9] Шароглазов Б. А., Клементьев В. В. Теория рабочих процессов ДВС: Учебное пособие к решению задач. – Челябинск: Изд. ЮУрГУ, 2003. – 33 с.

[10] Сеначин, П. К. Моделирование физико-химических процессов и горения в энергоустановках. Книга II. Модели процессов горения в поршневых двигателях: учебное пособие [Текст] / П. К. Сеначин, А. А. Брютов, А. П. Сеначин / Алтайский государственный технический университет имени И. И. Ползунова; Институт теплофизики имени С. С. Кутателадзе СО РАН. – Барнаул: Алт. гос. техн. ун-т, 2019.– 184 с.

[11] Сатжанов Бисенбай Сартбаевич Моделирование теплопередачи в цилиндре поршневого двигателя // Нефтегазовые технологии и экологическая безопасность. 2008. №5. URL: https://cyberleninka.ru/article/n/modelirovanie-teploperedachi-v-tsilindre-porshnevogo-dvigatelya (дата обращения: 12.02.2025).

[12] Бутин Данила Александрович, Беляков Владимир Викторович Частотный метод оценки курсовой устойчивости многомассовой имитационной модели автомобиля // Труды НГТУ им. Р. Е. Алексеева. 2020. №1 (128). URL: https://cyberleninka.ru/article/n/chastotnyy-metod-otsenki-kursovoy-ustoychivosti-mnogomassovoy-imitatsionnoy-modeli-avtomobilya (дата обращения: 10.02.2025).

Information about the author

Ernazarov Aziz Alibaevich	Jizzakh Polytechnic Institute, Associate Professor of the Department of "Vehicle Engineering". E-mail: aziz-ernazarov@mail.ru Tel.: +998939404123 https://orcid.org/0000-0002-4188-2084
Musurmonov Savar Sobir ugli	Tashkent State Technical University named after Islam Karimov, basic doctoral student of the Department of "Service Delivery Technology" E-mail: musurmonovsarvarbek2@gmail.com Tel.: +998991051695 https://orcid.org/0009-0009-8618-1722

Automation of green space maintenance along road infrastructure

N.U. Jurakulova[1][a], Sh.R. Khalimova[1][b]
[1]Tashkent state transport university, Tashkent, Uzbekistan

Abstract: The study comprehensively examined the efficiency of automated irrigation systems applied to green areas along the Tashkent–Chirchik highway. Within the research framework, soil moisture sensors were utilized to continuously monitor environmental conditions and to optimize the allocation of water resources. This methodological approach enabled the collection of precise data on soil humidity levels, making it possible to design irrigation schedules that respond directly to the actual needs of the vegetation. The findings revealed a range of important outcomes. First, automation led to a reduction in water use by approximately 25–30%, which is a crucial achievement considering the growing problem of water scarcity in Central Asia. Second, labor requirements decreased by nearly 40%, thereby reducing the dependence on manual maintenance and significantly lowering operational costs. Third, plant resilience during the vegetation period was noticeably improved, as indicated by healthier leaf coloration, higher photosynthetic activity, and greater tolerance to drought stress.

In addition, system management through IoT-based technologies allowed for real-time monitoring and rapid response to changing conditions, which significantly improved the speed and quality of maintenance services. This ensured more efficient allocation of limited resources, minimized the risks associated with over- or under-irrigation, and contributed to more stable plant growth. Overall, the adoption of automated irrigation and monitoring systems represents not only a technological advancement but also an important step toward achieving environmental sustainability, energy efficiency, and long-term landscape resilience. These results highlight the potential for wider application of such technologies along highways and in other urban green zones, where resource savings and ecological balance are of strategic importance.

Keywords: Automated irrigation system, IoT technologies, green areas/landscaping, soil moisture monitoring, water resource saving, ecological sustainability, remote control, vegetation stability, highway landscape, innovative maintenance methods

1. Introduction

In recent years, along with transport infrastructure, considerable attention has been paid to issues of environmental sustainability. Green areas along roads are not only elements that enhance the aesthetic appearance but also important ecological systems that reduce the amount of dust and gases in the atmosphere and absorb noise [1, 11]. For example, green zones created along the Tashkent–Samarkand highway play a significant role not only in reducing harmful gases emitted by vehicles but also in improving the aesthetic appearance of the road and ensuring psychological comfort for drivers and passengers. Such green zones contribute to maintaining ecological balance by absorbing carbon monoxide, nitrogen oxides, and other harmful substances released into the atmosphere by moving vehicles. In addition, the placement of trees and shrubs along roads regulates wind speed, reduces noise levels, and positively influences the surrounding environment.

However, the effective functioning of these zones directly depends on their regular maintenance, irrigation, and monitoring. At present, a significant part of these processes is carried out manually using traditional methods. As a result, large amounts of water and labor resources are consumed, while efficiency remains low. For instance, due to uneven distribution of water, some trees do not receive sufficient moisture, while others are overwatered. This not only leads to inefficient use of water resources but also negatively affects plant growth.

Therefore, under modern conditions, it is necessary to introduce innovative solutions for maintaining green zones along highways, such as automated irrigation systems, remote monitoring using IoT (Internet of Things) technologies, and soil moisture control with sensors. Such an approach makes it possible to use resources efficiently, enhances the ecological effectiveness of green zones, and ensures the long-term sustainability of the landscape created along roads [2]. In this regard, the issue of increasing efficiency through the use of modern automated systems is highly relevant [3, 4].

2. Research methodology

In the course of this study, in accordance with the aim and objectives of the research, the following methodological approaches and methods of analysis were applied:

Literature analysis — international experience (USA, Germany, Japan) in automated irrigation and maintenance systems was studied [5, 6].

Technological modeling — a scheme of the automated process for maintaining green zones was developed [7].

Experimental observation — on a test section along the Tashkent–Chirchik highway, soil moisture was monitored using sensors and water consumption was optimized [8].

Comparative method — the efficiency of traditional maintenance and automated systems was compared [9].

[a] https://orcid.org/0009-0003-4565-0699
[b] https://orcid.org/000-0002-4753-390X

3. Results and Discussion

The analysis of the research results made it possible to draw the following scientifically substantiated conclusions:

When using soil moisture sensor systems, water consumption was reduced by an average of 25–30% [2, 9]. For example, on the Tashkent–Chirchik highway section during the summer period, a significant decrease in water usage was observed due to automated irrigation.

Thanks to automated systems, labor costs for maintenance were reduced by 40% [3]. This was particularly evident on the Tashkent–Samarkand highway, where previously the maintenance of green zones required a large workforce.

Plant resilience during the vegetation period proved to be higher: leaf greenness, photosynthetic activity, and drought resistance showed better results compared to traditional methods [1, 7].

The possibility of remote control based on IoT (Internet of Things) increased the speed of maintenance [2, 8].

Table 1

Table of Results

Indicator	Traditional Method	Automated Method
Water consumption	100%	70–75%
Labor costs	100%	60%
Plant resilience	Medium	High

The obtained results show that traditional methods of maintaining green zones along highways, based on manual labor, lead to inefficient use of significant resources. In particular, during irrigation, uneven distribution of water resources, increased labor costs, and insufficient efficiency of control mechanisms are observed. Moreover, existing systems do not provide adequate results in maintaining stable plant growth.

Addressing these problems has demonstrated the effectiveness of applying automated maintenance systems. According to the research results, the introduction of automated irrigation systems and sensor-based monitoring technologies makes it possible to significantly reduce water consumption, save energy and labor resources, and ensure continuous control over the maintenance process. As a result, conditions are created for the rational use of resources, ecological sustainability of green zones is ensured, and the quality of roadside maintenance is significantly improved.

Thus, it can be stated that the use of automated systems not only increases economic efficiency but also serves as an important factor in strengthening environmental safety, improving road aesthetics, and creating a comfortable environment for drivers [4, 10]. In Uzbekistan, this process is being implemented gradually: for example, along the Tashkent Ring Road, automatic drip irrigation systems have been introduced, operating on the basis of energy-saving pumps and solar panels.

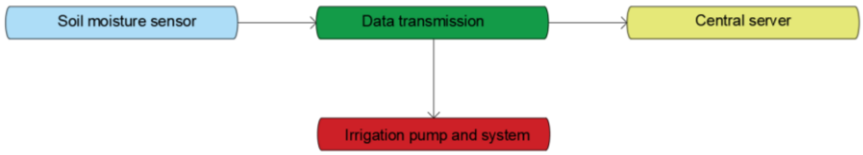

Fig. 1. Block Diagram of the Irrigation System

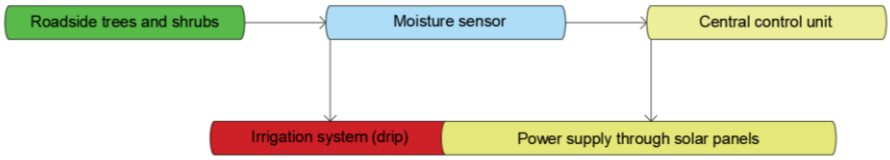

Fig. 2. Operating Principle of the Automated Landscaping System along the Tashkent–Samarkand Highway

4. Conclusion

The study confirms that the implementation of automated systems for maintaining green zones along highways provides significant ecological, economic, and social benefits. Practical evidence from the Tashkent–Samarkand highway, the Tashkent–Chirchik route, and the Tashkent Ring Road highlights the effectiveness of such solutions in real-world conditions. Automation contributes to the rational use of water and labor resources, enhances plant resilience, and streamlines maintenance operations. Looking ahead, the integration of these technologies is expected to become an essential component of the "smart road" concept, fostering the development of a more sustainable, efficient, and innovative transport infrastructure.

References

[1] Al-Kaabi, K., & Al-Bastaki, N. (2021). Smart Irrigation Systems for Sustainable Urban Landscapes. Journal of Environmental Management, 288, 112125. https://doi.org/10.1016/j.jenvman.2021.112125

[2] Gupta, R., & Yadav, A. (2019). IoT based Automated Irrigation System for Roadside Green Belts. International Journal of Advanced Research in Computer Science, 10(5), 56–62. http://dx.doi.org/10.26483/ijarcs.v10i5.6462

[3] Li, J., Wang, P., & Zhao, X. (2020). Application of Telemetry and Sensor Networks in Urban Greenery Maintenance. Sustainability, 12(7), 2884. https://doi.org/10.3390/su12072884

[4] Food and Agriculture Organization (FAO). (2017). The Future of Food and Agriculture: Trends and Challenges. Rome: FAO. https://www.fao.org/3/i6583e/i6583e.pdf

[5] Khannanova, G. T. (2009). Минеральный порошок на основе пиритных огарков и его использование в асфальтобетонных смесях. Диссертация, Уфа. https://tekhnosfera.com/mineralnyy-poroshok-na-osnove-piritnyh-ogarkov-i-ego-ispolzovanie-v-asfaltobetonnyh-smesyah

[6] Rybiev, I. A. (2012). Bitumen-Mineral Interactions and Road Pavement Durability. Moscow: Transport Publishing. https://search.rsl.ru

[7] Qodirov, B., & To‘rayev, M. (2022). Shaharsozlikda avtomatlashtirilgan sug‘orish tizimlarining qo‘llanilishi. O‘zbekiston Milliy Universiteti Ilmiy Xabarlari, 2(4), 77–85. https://uzjournals.edu.uz/natlib/vol2/iss4/12

[8] World Bank. (2020). Transforming Urban Transport: Pathways to Sustainability. Washington, DC. https://openknowledge.worldbank.org/handle/10986/34127

[9] Zhou, Y., & Chen, L. (2018). Energy-Efficient Smart Irrigation with Solar Power in Urban Roadside Areas. Renewable Energy, 126, 509–518. https://doi.org/10.1016/j.renene.2018.03.056

[10] Karimov, Sh., & Jalilov, O. (2023). Yo‘l bo‘yidagi ko‘kalamzorlashtirishning ekologik samaradorligini oshirishda avtomatlashtirishning o‘rni. TIIAME Ilmiy Jurnali, 3(1), 45–52. https://tiiame.uz/journal/articles/eco-green-automation.

[11] Ergashova M. Z., Bobonazarov T. S. Greening City Streets and Roads in Modern Urban Conditions //Sustainable Development of Transport. – C. 3.

Information about the author

Jurakulova Navbakhor	Tashkent State Transport University, Teacher of the Department of Urban Roads and Streets, Email: navbahor.1011@gmail.com https://orcid.org/0009-0003-4565-0699
Khalimova Shakhnoza	Tashkent state transport university, Docent of the Department of Urban Roads and Streets, Email: xalimova_sh@tstu.uz https://orcid.org/0000-0002-4753-390X

Existing constructive solutions for flood protection

B.T. Ibragimov[1][a], F.Z. Zokirov[2][b], Sh.Sh. Tayirov[3][c]

[1]Academy of the Ministry of Emergency Situations of the Republic of Uzbekistan, Tashkent, Uzbekistan
[2]Tashkent state transport university, Tashkent, Uzbekistan
[3]LLC "Project Consulting Technologies Systems" (Engineering Designer), Tashkent, Uzbekistan

Abstract: Structural solutions for mudflow protection are technical and engineering solutions developed to protect structures from the negative consequences of mudflows, which mainly consist of a complex of measures implemented during the design, construction, and operation of structures. These solutions include special construction and technological methods to ensure infrastructure safety and minimize damage caused by mudflows. This article provides an analysis of existing methods for protecting bridge structures from mudflows. For the effective practical application of technical and technological measures to prevent the negative consequences of this mudflow threat, their adaptation to local conditions, along with world best practices in protecting against mudflow danger, a comparative analysis of local methods is of current importance.

Keywords: Mudflow, debris flow protective structures, bridges, constructive solution, technological measure

1. Introduction

A mudflow is a dynamic mass consisting of a multiphase medium with high kinetic energy, consisting of sand, gravel, rock fragments, clay, and other rocks, and this geodynamic phenomenon can cause serious damage to engineering infrastructure in mountainous and foothill areas. A number of engineering and technical solutions, i.e., structural protective measures, are used to prevent rocky mudflows, control their direction, or reduce the negative impact of their consequences.

2. Research methodology

Specially designed and constructed barrier basins in the flow direction retain stones and mud from the mudflow, allowing multi-phase purified water flow. As a result, the kinetic energy of the flow and the risk of soil erosion are reduced, and the elements of engineering and civil buildings and structures located within the radius of flow propagation are protected from the direct impact of mudflows. Solid components accumulated in the reservoirs can be safely removed, which mitigates the force of the hydraulic shock and increases the stability of hydraulic structures in the direction of the flow (Fig. 1).

Fig. 1. Special reservoirs built in the direction of mudflow

Barrier basins are engineering protective structures that allow the removal of solid-phase components (stones, sand, clay, and other particles) from the mudflow, and there are a number of factors limiting the late practical application of this design solution.

To ensure the functional continuity of these structures, there is a need for the utilization of solid components based on periodic mechanized technologies, which is characterized by the complexity of the operational process and the high level of operating costs. Limited resources (land resources) create technical and economic difficulties in implementing such systems, especially in densely urbanized or complex topographically structured areas (mountainous and foothill). Also, barrier basins are effective only in areas where extreme hydrological conditions and high-intensity mudflows are observed, they cannot fully utilize their functional capabilities during normal rainfall, and their productivity drops to almost zero. In general, despite the high technological significance of barrier basins in mudflow management, due to the intensive labor intensity of operational maintenance and territorial limitations, they are not used as a suitable (universal) solution for all conditions.

Elastic grating barriers made of high-alloy steel wires are one of the design engineering solutions that dissipate the dynamic loads of mudflows with high kinetic energy, intercept solid particles of large fractions, and absorb the impact. These systems are typically integrated with shock-absorbing support elements, elastoplastic grip mechanisms, and deformable binding elements, designed for segmental suction of the flow shock impulse (Fig. 2).

Fig. 2. Special wire mesh built in the direction of the mudflow

Despite a number of structural advantages, a high degree of local deformation and elastoplastic fatigue, as well as micro cracks in the crystal lattice of the metal, formed as a result of impulse impacts of the mudflow, leads to the degradation of the mechanical properties of the structure. As a result, it becomes necessary to regularly recalibrate or

[a] https://orcid.org/0009-0006-9408-4613
[b] https://orcid.org/0000-0002-5848-3995
[c] https://orcid.org/0009-0008-1643-9292

replace elements that have undergone a certain degree of deformation. The structure has high sensitivity to asymmetrical external loads, and as a result of the uneven mass distribution of particles of large fractions in the flow, the deformation process occurs asymmetrically. This leads to an unconventional and uneven distribution of internal stresses in structural elements, the emergence of local stress zones, and an increase in the probability of fatigue of the material. This situation increases the risk of steel wire barriers breaking.

Despite the fact that elastic grille barriers have a high degree of dynamic stability as a modern, energy-absorbing, deformable engineering solution, their susceptibility to mechanical fatigue, complexity of maintenance, high capital costs do not allow them to be used as a rational structural solution that protects against mudflow hazards.

Multi-stage energy dissipation systems, arranged in stages parallel to the flow direction, are hydraulic shock absorbers aimed at dissipating the kinetic component of the mudflow, reducing transit loads, and separating solid-phase components (gravel, stones, rock fragments, and clay) by creating local sedimentation zones. This not only reduces erosion processes, but also ensures the safety of structures located in the lower part (Fig. 3).

Fig. 3. Special multi-stage dams built in the direction of mudflow

Nevertheless, this multi-stage dam system leads to a significant increase in the overall hydraulic inertia and the coefficient of hydraulic resistance in the flow direction. This situation is accompanied by an artificial increase in transitions between laminar-turbulent regimes in the flow. Continuous accumulation of solid-phase mass in the flow leads to a disruption of sedimentation equilibrium over time and local stabilization of the sedimentary layer. Also, in the process of stepwise dissipation of energy, secondary hydrodynamic caverns are formed as a result of pulsed flow attenuation between the steps. In these areas, zones of local vortex flow and cavernous erosion centers appear, which negatively affect the stability of the soil layer at the base of the structure. As a result, the stability of the structure's foundation is at risk, the operational throughput potential decreases, and the maintenance interval is reduced.

Fig. 4. Special multi-stage dams built in the direction of mudflow

Engineering structures designed to direct mudflows in safe directions are hydraulic structures designed in accordance with the natural relief and hydrological conditions and serving to prevent mudflows, manage them, and protect socio-infrastructure facilities from direct impact. These structures, as a rule, minimize the techno genic and environmental damage caused by mudflows and increase the level of regional security by diverting the flow in alternative directions with safe energy distribution (Fig. 4).

Such structures include mudflow direction walls, dams, drainage canals, and buffer basins. They perform the function of reducing the kinetic energy of the mudflow, retaining solid fractions, and controlling the direction of water to safe areas. The design and placement of these structures are carried out depending on the relief, hydrological conditions, characteristics of mudflows, and the location of objects requiring protection. These systems also have a number of functional and structural limitations in their practical application, and the complexity of design and the dependence of their application on the terrain are considered the main shortcomings. In this case, systems designed to change the flow direction require a high level of hydro morphological analysis, digital terrain modeling, and simulation flow analysis. In complex geo topographic conditions, these systems lose their adaptability, and the risk of diverting mudflows remains. That is, in the event of a large volume of mudflow, secondary danger zones may arise in areas considered safe.

In the event of extreme precipitation or geodynamic activity (landslides, earthquakes), these structures may not be able to withstand the external load at the level specified in the project, which leads to violation of the structural integrity of the system, failure of local elements, and the occurrence of hydraulic failures. As a result, the functional efficiency of the structure decreases, and in emergency situations, the possibility of flow control is partially or completely lost. Therefore, when designing such structures, multi-variant hydraulic modeling should be carried out, taking into account extreme mudflow scenarios.

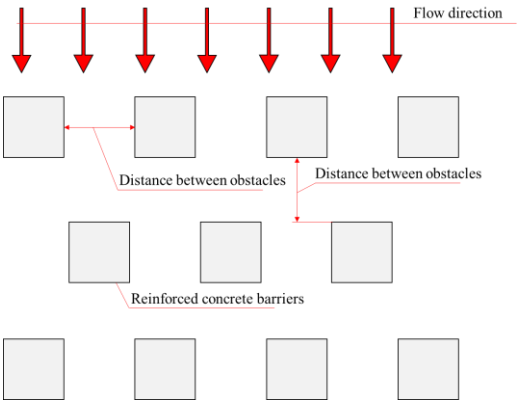

Fig. 5. Protective structure blocking mudflow

Figure 5 shows a structural barrier built to reduce the risk of mudflow to structures, which is placed at different angles or perpendicular to the flow direction. The main task of this structure is to reduce the negative impact of mudflow hazard on engineering structures and facilities by directing mudflow flows to a safe area.

In this case, it is recommended that the distance between barriers be from 0.5m to 2.0m in accordance with the local conditions of the designed territory (flow velocity, water level, and hydraulic pressure), and the distance between barriers - from 1.0m to 3.0m, and the dimensions of the barriers - from 0.5x0.5m to 1.5x1.5m. A correctly chosen size and slope can reduce mudflow energy from 40% to 70%.

This engineering structure is usually reinforced with reinforced concrete or natural stones and is considered a reliable structural solution that can withstand the hydraulic pressure of a mudflow. This barrier, having the shape of a

rectangular column, receives the impact of the mudflow and directs it in a lateral direction. As a result, the current strength dissipates, and its kinetic energy decreases. Such structures are usually designed in mountainous and lowland areas with a high probability of mudflows. Also, for the effective operation of these types of protective structures, their condition must be constantly monitored. Through systematic visual observation and technical inspections, cracks or material degradation are detected, and timely preventive repair work is recommended.

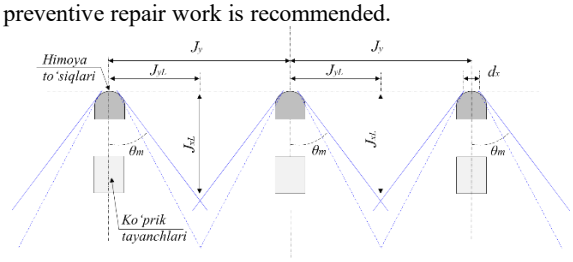

Fig. 6. Protective structure blocking mudflow

The engineering solution presented in this figure is a system of protective barriers aimed at reducing the hydrodynamic impact of mudflows on the supports of bridge structures. Protective barriers are installed in the front part of supporting bodies in the direction of the flow and serve to reduce the speed and impact force of the mudflow. They are usually built in the form of reinforced concrete, gabion, masonry mesh, or solid granite blocks.

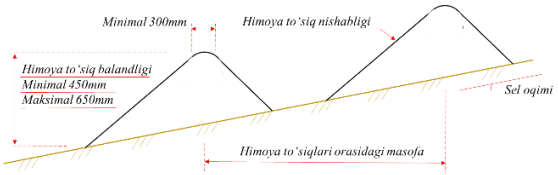

Fig. 7. Protective structure blocking mudflow

A protective dam is a temporary or permanent structure used to reduce erosion processes associated with mudflows, rainwater, or streams, and to regulate mudflows. These structures are designed for areas where there is no constant flow, but during rains or mudflows, strong water flows occur. That is, these protective dams slow down light or moderate mudflows that occur after rain in mountainous or sloping areas, gradually directing them downstream. Several such dams are constructed sequentially in a chain pattern. These protective dams are an effective, inexpensive, and convenient engineering solution for protecting against small and medium-level mudflows. It slows down the mudflow, prevents erosion and soil erosion, and safely directs the flow downstream.

3. Conclusion

Mudflows, in particular, rocky mudflows, are high-energy flows arising under the influence of hydro meteorological and geodynamic factors, containing a large amount of water, gravel, stones, and hard rocks, which pose a serious danger in mountainous and foothill areas. Such flows have a negative impact not only on infrastructure facilities, but also on the environment, socio-economic activity, and the safety of human life. That is why the application of complex engineering and man-made solutions for the prevention and management of rocky mudflows is of great importance. Therefore, the above-mentioned solutions used to reduce mudflow risk are selected as a complementary combined system depending on the characteristics and natural conditions of the territory.

Moreover, for such structures to fulfill their functional purpose, a thorough analysis of the geological and hydrological conditions of the area, the correct selection of building materials, and a thorough design process are necessary. Regular monitoring and maintenance of the condition of protective dams ensure their long-term effectiveness. That is, existing engineering solutions for reducing mudflow risks should be constantly modernized and improved through the introduction of modern scientific approaches, digital modeling technologies, and environmentally friendly innovative methods.

References

[1] Chow, V. T. (1959). Open-Channel Hydraulics. McGraw-Hill. ISBN: 978-0070604851.

[2] Laursen, E. M. (1958). The Mechanics of Scour in the Vicinity of Bridge Piers. Bulletin No. 27, Iowa Institute of Hydraulic Research.

[3] Renard, K. G., Foster, G. R., Weesies, G. A., McCool, D. K., & Yoder, D. C. (1997). Predicting Soil Erosion by Water: A Guide to Conservation Planning with the Revised Universal Soil Loss Equation (RUSLE). USDA Agriculture Handbook No. 703.

[4] Singh, V. P. (1996). Hydrology of Disasters: Floods and Debris Flows. Kluwer Academic Publishers. ISBN: 978-0792382107.

[5] Barker, R. D., & Falconer, R. A. (1994). Numerical Modelling of Scour Around Bridge Piers. Journal of Hydraulic Engineering, 120(7), 836–853. https://doi.org/10.1061/(ASCE)0733-9429(1994)120:7(836)

[6] Wolman, M. G., & Schick, A. P. (1967). Effects of Construction on Fluvial Sediment. Journal of the Hydraulics Division, ASCE, 93(5), 73–90. https://doi.org/10.1061/JYCEAJ.0000515.

Information about the author

Ibragimov Bakhrom Toshmurato-vich	Academy of the Ministry of Emergency Situations of the Republic of Uzbekistan, DSc, professor E-mail: baxromibragimov@gmail.com Tel.: +998971324447 https://orcid.org/0009-0006-9408-4613
Zokirov Fakhriddin Zohidjon ugli	Tashkent state transport university, department "Bridges and tunnels", associate professor, PhD E-mail: 0202031@inbox.ru Tel.: +998973466360 https://orcid.org/0000-0002-5848-3995
Tayirov Shopulat Shomansur ugli	LLC "Project Consulting Technologies Systems" (Engineering Designer), Tashkent, Engineer E-mail: shoputayirov255@gmail.com Tel.: +998974474241 https://orcid.org/0009-0008-1643-9292

Modernization of railway signaling systems

O.O. Ruzimov[1]
[1]Tashkent state transport university, Tashkent, Uzbekistan

Abstract: In the conditions of digitalization of the transport sector, the development of innovative train traffic control systems becomes very important. Such systems must provide high reliability, safety, and efficiency of the transportation process. Traditional signaling methods, based on track circuits and electromechanical relays, have several limits: they are sensitive to electromagnetic noise, use more energy, have delays in fault diagnostics, and need high maintenance costs.
This paper presents a developed system for signal control and information exchange on railway lines. The system is based on the integration of microcontrollers, ACS712 current sensors, inductive sensors, RFID modules, and fiber-optic data channels. The structural diagram of the traffic light control unit is analyzed, the functions of the main elements are described, and a digital comparison of the parameters of traditional and modern systems is made. The results show that the proposed solution increases the reliability of data transmission by 10 times, reduces signal delay 20–30 times, decreases energy consumption up to 60%, and lowers maintenance costs by 30–40%.

Keywords: automatrailway transport; train traffic control; digitalization; signaling system; RFID technology; fiber-optic data transmission

1. Introduction

The development of railway transport in the time of digitalization requires new innovative systems for train traffic control. These systems must give a high level of safety, reliability, and efficiency. Classical methods of traffic organization, based on track circuits and traditional automatic block signaling, have shown their effectiveness for many decades. However, modern operating conditions bring new requirements. The increase of train flow, the growth of passenger and freight train speeds, and the need for integration into intelligent transport systems make it necessary to move to more advanced technologies of data transmission and processing.

One of the key problems of traditional signaling systems is their sensitivity to electromagnetic interference, dependence on the state of track circuits, and limited capacity. Also, fault diagnostics in such systems is often delayed, which reduces the speed of decision making. Modern approaches, on the contrary, use digital technologies, programmable logic controllers (PLC), fiber-optic communication lines, and contactless data transmission systems, including RFID technology.

Effective train traffic control is not possible without fast information exchange between the main elements of the infrastructure: locomotives, signals, trackside devices of automatic block, and station control posts. The most important condition is real-time data transmission and reception. This allows the driver to make correct decisions when driving the train, and the station operator to check the state of block sections and coordinate all actions.

The development of new train traffic control systems on railway lines is directed to two main tasks. First, it is the continuous and accurate monitoring of block sections and signal aspects, which is directly connected with transport safety. Second, it is the increase of automation and the replacement of old elements that reduce the reliability of railway infrastructure.

This paper describes a developed system for signal control and information exchange on railway lines. The system is based on the integration of current sensors, inductive sensors, microcontrollers, RFID modules, and fiber-optic communication channels. The block diagram of the signal control unit is analyzed, the functions of each element are defined, and the advantages of the system are explained in comparison with the traditional automatic block system.

2. Research methodology

Modern trends in the development of railway transport show the need for innovative technical solutions. These solutions must increase the safety and efficiency of train traffic control. For this reason, special attention is given to the analysis and improvement of trackside devices placed along the railway line. These devices play a key role in the system of automatic block and station control.

The methodological basis of the research is the system approach. Each device is studied as a part of one complex that provides data transmission, reception, and processing in real time.

The main signal light (pass signal) is the central element of the signaling system on the railway line. Its main task is to give the driver clear signals about the possibility to continue movement or the need to stop when the train moves from one block section to another. Traditionally, such devices work with 12 V AC power and have three signal lightsgreen, yellow, and: red. To control the current state of the lamps, a current sensor is used. This improves the reliability of information transfer and reduces the risk of accidents [2,3].

Current sensors have an important diagnostic function. They check if the signal lamps are switched on or off, detect possible faults, and send data to the central control system. In the studied system, ACS712 current sensors are used. These devices can measure the current in the power circuit of each lamp with high accuracy. The received data automatically goes to the microcontroller, which removes the human factor and provides stable operation of the device.

The microcontroller is considered the “brain” of the signal control unit. It receives and processes data from all connected devices, the signal light, current sensors, relay

controller, RFID module, and inductive sensors. The main functions of the microcontroller are to control the state of the signal, to check the condition of the lamps, and to change the signal automatically depending on the occupancy of the block section. For example, using information from the inductive sensor, the microcontroller detects the position of the train and the occupancy of the track section. Then it changes the signal aspect according to the set algorithms [4,5].

Information transfer to the central monitoring system of the station is done through a Media Converter, which changes the electrical signal into an optical one. This gives high communication reliability over long distances and allows synchronization of several signals. In addition, the system uses RFID technology: the data about the state of the signal is written into an RFID tag, which is read by the locomotive during movement. This method provides two-way information exchange and removes delays in signal transmission.

The system also makes operational diagnostics. In particular, current sensors help to detect lamp faults in real time, which strongly improves the safety level. Constant information exchange between signals and the central system reduces the probability of critical situations and gives reliable control of train traffic.

The relay controller is the executive part of the system. It switches the signal lamps on and off according to the commands of the microcontroller. This makes the work stable and gives the correct logic of signals: the green or yellow light is on when the block section is free, and the red light is on when the section is occupied.

A special role belongs to the RFID (Radio Frequency Identification) system. It allows contactless transfer of data about the signal state directly to the locomotive. The RFID writing device saves the data into a tag installed on the sleepers, and the RFID reader placed on the locomotive receives this information while moving and sends it to the on-board control system. This method gives accuracy, speed, and security of data exchange.

Inductive sensors are used to detect the arrival of a train and to monitor the condition of block sections. Their work is based on fixing the change of the magnetic field when the metal parts of the rolling stock pass above. The contactless principle reduces equipment wear and gives long service life [6,7].

3. Results

Effective train traffic control on railway lines requires a complex system that unites several functional devices placed in signal points. These devices provide the creation, processing, and transfer of information about the state of block sections and signals both to the locomotive and to the station control posts. The developed system is based on the principles of digitalization, integration, and modular design, which makes it possible to adapt the system to different operating conditions.

Figure 1 shows the structural diagram of the signal control unit. The main elements are: the main signal light, current sensors, electromechanical relays, inductive sensors, programmable logic controller (PLC), power converters, fiber-optic data channels, and RFID modules. Each of these devices has its own function, but only together they form one system that provides reliability and safety of train traffic.

In the presented diagram, the main signal light, located in the signal point, gives permission or prohibition for the train to move from one block section to another. This signal works from a 12 V AC power source. Each lamp of the signal is connected to the electric circuit through an ACS712 current sensor. This makes it possible to detect the presence of current in the circuit and its value. Based on this data, the state of the signal in the point can be fixed automatically and shown in the PLC. The ACS712 sensor is always connected to a 5 V DC power supply. When current appears in the circuit of a certain lamp, the sensor sends information to the controller. The signal formed in the PLC is then sent to the previous signal on the route, because this information must go to the locomotive when entering the previous block section [8].

Electromechanical relays connected to the electric circuits of the signal lamps provide their switching on and off. Depending on the commands from the PLC, the relays open or close the power circuit of the needed lamp. This command is formed on the basis of the block section state: if the next block section is free, the permissive signal (yellow or green) is on; if it is occupied, the prohibiting red signal is on. On the line, the normal mode of the signal is the green permissive light, so the relay of the green lamp is normally open and works only when the train is on the block section. Considering energy use, the lamp circuits of the signal do not work at the same time, so the electromechanical relays also switch at different moments. For example, when the red signal is on, the relays of the yellow and green lamps are automatically in the off state. The electromechanical relays work with 5 V DC control and can switch signal lamps powered by AC from 10 to 24 V [9].

For the power supply of current sensors and electromechanical relays with 5 V DC, a DC–DC converter is used. It reduces the voltage from 24 V to 5 V.

The inductive sensor is used in signal points to form a signal about the train entering the block section. Based on this information, the occupancy of the block section is defined, and the signal of the previous section is changed automatically. The inductive sensor is connected to the PLC. When the train passes above the sensor, it detects the presence of the train by the change of the magnetic field and sends the data to the controller. Based on this, the PLC forms a signal about the train entering the block section. The formed signals are sent both to the control unit of the previous signal and to the station. For this process, a Media Converter is used. It is connected to the PLC through an Ethernet switch, changes the electrical signal to an optical one, and sends it by fiber-optic cable to another Media Converter in the control unit of the previous block section. Transmission of data by optical cable over long distances gives high reliability and safety, and removes the problems of ALS codes transfer by track circuits. The Media Converter and Ethernet switch work from a 24 V DC power source [10,11].

https://doi.org/10.56143/3030-3893-2025-3-74-77 A bridge between science and innovation

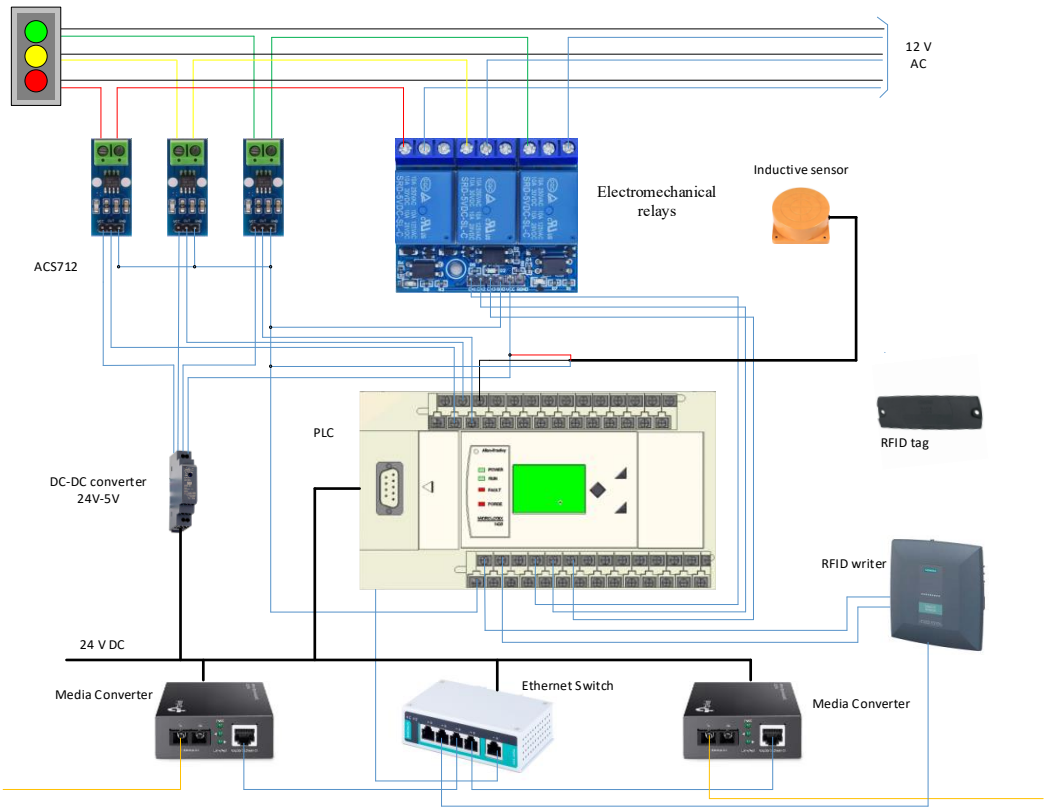

Fig. 1. Structural diagram of the signal control unit in the signal point

In the signal point, RFID technology is used to send information to the locomotive about the aspect of the next signal. The information about the signal state comes from the control unit of the next signal, then the signal formed in the PLC is sent to the RFID writing device. It saves the data in an RFID tag. When the locomotive, equipped with an RFID reader, passes above the sleepers where the tag is installed, it reads the coded data and sends it to the KLUB system. In this case, an active RFID system working in the high-frequency range is used, which gives high speed and long distance of data exchange.

To prove the efficiency of the proposed train traffic control system, a comparative study of the main characteristics of traditional track circuits and the developed digital system was made. The new system is based on the use of microcontrollers, RFID modules, and fiber-optic communication channels.

The digital system shows important advantages: an increase of reliability by 10 times; a reduction of data transfer delays by 20–30 times; a decrease of energy consumption by 60%; and a reduction of maintenance costs by 30–40%.

Table 1

Comparative analysis of traditional and digital signaling systems

Indicator	Traditional system (track circuits and relay schemes)	Modern digital system (PLC, RFID, fiber optics)	Advantage
Data transmission reliability (average failure probability)	~0.01 per 1000 km/year	<0.001 per 1000 km/year	10 times higher reliability
Signal transmission delay	200–300 ms	<10 ms	20–30 times faster
Power consumption of control unit	20–25 W	8–12 W	Up to 60% saving
Fault diagnostics	Manual, with delay	Automatic, in real time	Lower risk of emergency
Equipment wear	High (mechanical relay contact)	Low (contactless sensors, fiber optics)	Service life longer by 1.5–2 times
Maintenance cost	High (frequent replacement of track circuits and relays)	Medium (minimal service of fiber optics and sensors)	Cost reduction by 30–40%
Possibility of integration into intelligent transport systems (ITS)	Limited	High (compatible with IoT, AI, KLUB-U)	Full digitalization

Thus, the introduction of digital technologies in train traffic control makes it possible to reach a high level of safety and efficiency, and also to create a base for integration into intelligent transport systems.

4. Conclusion

The developed signal control system for railway lines, based on the integration of microcontrollers, current sensors, inductive sensors, RFID modules, and fiber-optic data channels, has shown high efficiency in solving key tasks of safety and reliability of the transportation process. The use of modern digital technologies made it possible to achieve stable system work in real time, to reduce the influence of the human factor, and to increase the speed of information exchange between the locomotive, signals, and station control posts.

The comparative analysis with traditional signaling systems confirmed the clear advantages of the new architecture: an increase of information reliability by 10 times due to the removal of track circuits and the use of fiber-optic lines; a reduction of signal response time by 20–30 times, which gives timely information for the driver and the station operator; a decrease of equipment energy consumption up to 60% because of energy-efficient components and optimized circuits; a reduction of maintenance costs by 30–40% through the elimination of frequent service of relay schemes and track circuits; and the possibility of automatic diagnostics and integration into new generation intelligent transport systems.

References

[1] Yaronova, N.V., Ruzimov, O.O. Innovative solutions for train traffic control on railway lines using fiber-optic data transmission. Railway Transport: Current Issues and Innovations, 2025, No. 2, pp. 230–235.

[2] Pultyakov, A.V., Skorobogatov, M.E. System analysis of the stability of automatic locomotive signaling systems. Modern Technologies. System Analysis. Modeling, 2018, Vol. 57, No. 1, pp. 79–89.

[3] Fedorov, N.E. Modern Automatic Block Systems with Audio Frequency Track Circuits: Textbook. Samara: SamGAPS, 2004, 132 p.

[4] Dunaev, D.V., Romantsev, I.O., Gavrilyuk, V.I. Failure analysis and methods of track circuit monitoring. Science and Progress of Transport. Bulletin of the Dnipropetrovsk National University of Railway Transport, 2010, No. 32. Available at: https://cyberleninka.ru/article/n/analiz-otkazov-i-metody-kontrolya-relsovyh-tsepey

[5] Unified Integrated Locomotive Safety Device (KLUB-U): Textbook / V.I. Astrakhan, V.I. Zorin, G.K. Kiselgof et al.; ed. by V.I. Zorin, V.I. Astrakhan. Moscow: State Educational and Methodological Center for Railway Transport, 2008, 177 p.

[6] Ablayeva, A.A., Yaronova, N.V., Ruzimov, O.O. Ensuring a reliable power supply for railway traffic lights using renewable energy sources. Proceedings – 2024 International Ural Conference on Electrical Power Engineering, UralCon 2024, pp. 600–604.

[7] Ro‘zimov, O.O. Creation of a system for train control and monitoring on railway sections with automatic block using modern contactless elements. Resource-Saving Technologies in Transport. International Scientific and Technical Conference with Participation of Foreign Scientists, Tashkent, 2024, pp. 223–225.

[8] Kurbanov, J.F., Yaronova, N.V. Improving the efficiency of the automatic locomotive signaling system. 2023 International Ural Conference on Electrical Power Engineering (UralCon), Magnitogorsk, Russian Federation, pp. 656–660, 2023. doi: 10.1109/UralCon59258.2023.10291086.

[9] Train Traffic Control Systems on Railway Lines: University Textbook in 3 parts / V.M. Lisenkov, P.F. Bestemyanov, V.B. Leshushin et al.; ed. by V.M. Lisenkov. Moscow: State Educational and Methodological Center for Railway Transport, 2009, 160 p.

[10] Train Traffic Control Systems on Railway Lines: University Textbook in 3 parts. Part 2 / V.M. Lisenkov, P.F. Bestemyanov, V.B. Leshushin, A.V. Lisenkov, A.E. Vanyushin; ed. by V.M. Lisenkov. Moscow: State Educational and Methodological Center for Railway Transport, 2009, 324 p.

[11] Train Traffic Control Systems on Railway Lines: Textbook in 3 parts / V.M. Lisenkov et al.; ed. by V.M. Lisenkov. Moscow: Federal State Educational and Methodological Center for Railway Transport, 2016, 174 p.

[12] Boynik, A.B., Koshevoy, S.V., Panchenko, S.V., Sotnik, V.A. Systems of Interval Regulation of Train Traffic on Railway Lines: Textbook. Kharkiv: UkrGAZhT, 2005, 241 p.

[13] Gumarov, A.R. Review of automatic locomotive signaling systems. World Science, No. 12 (33), 2019, pp. 462–471.

Information about the author

Ruzimov Otakhon Orifjon ugli Tashkent State Transport University, doctoral candidate at the Department of “Radioelectronic Devices and Systems” Email: ruzimov1125@gmail.com

Temperature stability of asphalt concrete under conditions of high summer temperatures in Tajikistan

S.B. Mirzozoda[1][a], J.I. Sodikov[2][b], F.S. Mirzoev[3]
[1]Tajik Technical University named after academician M.S. Osimi, Dushanbe, Tajikistan
[2]Tashkent state transport university, Tashkent, Uzbekistan
[3]Technical Department of JSC «Tajikhydroelectromontazh» (TGEM), Dushanbe, Tajikistan

Abstract: In Tajikistan's hot climate, asphalt concrete pavements undergo significant thermal loads causing rutting, plastic deformations, and reduced service life. This study justifies the selection of binders (BND 60/90, PMB 90, PG 70-28, PG 76-22) and aggregate gradations to secure thermal resistance. The methodology covers climatic mapping (98th percentile of 7-day maximum surface temperatures [18]), rutting tests [6]), moisture susceptibility [17]), compactability [7], and binder rheology via MSCR [16, 20]. Results indicate that PMB 90 reduces rut depth by 55–60 % at 60 °C vs. BND 60/90 [13, 14], while PG 76-22 yields 70–75 % reduction [11, 14]. Mixes with PMB also show ~18 % [17] and achieve 98 % target density [7]. Cost analysis suggests payback through 5-7-year service-life extension [18, 19]. PMB and PG binders are therefore recommended for Tajikistan's network.

Keywords: asphalt concrete, thermal resistance, hot climate, rutting, modified bitumen, pavement

1. Introduction

The roads of the Republic of Tajikistan are operated in conditions of a sharply continental climate, which is characterized by high summer air temperatures (+40…+45 °C) and pavement temperatures (+60…+70 °C) [15], as well as sharp daily temperature fluctuations. This leads to significant deformations of asphalt concrete pavements, a reduction in the time between repairs and an increase in operating costs [12].

Traditionally, BND petroleum bitumens (60/90, 90/130) [1, 4] are used in road construction in the republic, which are not designed for such high temperatures. As a result, after only 2-3 years of operation, ruts more than 10 mm deep appear on main roads [5, 13].

International experience (USA, Europe, Kazakhstan) shows that the use of polymer-bitumen binders (PBB) and the Superpave PG system can increase the temperature resistance of coatings [9, 10]. However, in Tajikistan, there is still no comprehensive justification for the selection of PG classes and mixture compositions taking into account local climatic and operating conditions [12, 18].

Research hypothesis: the use of modified binders (PBB, PG 76-22) in asphalt concrete allows to reduce the rut depth at a temperature of 60 °C by ≥50% compared to conventional BND 60/90.

Objective of the work: development of scientifically based recommendations for the use of PBB and PG bitumen for the construction of road surfaces in the hot climate of Tajikistan.

2. Research methodology

To test the temperature stability of asphalt concrete mixtures, laboratory tests were conducted under conditions close to operational ones.

Samples. Cylindrical samples Ø 71,4 × 71,4 mm (GOST 12801-98 [2]) were compacted using the Marshall method at 150-160 °C.

Mix composition. Three binder options were used: regular bitumen BND 60/90, polymer-bitumen binder (PBB 90), bitumen according to the Superpave PG 76-22 system. Mineral skeleton: crushed stone of fraction 5-15 mm (diabase/granite), sand, mineral powder.

Equipment. «Ring and Ball» device for determining softening point [10], press for testing shear strength at elevated temperature (Wheel Tracking Test) according to GOST R 58400.7-2019 [3], thermostatic chamber for maintaining samples at +20…+70 °C.

Test conditions. Temperature conditions: +20 °C, +40 °C, +60 °C. Load: 700 N (equivalent to an axial load of 100 kN). Number of cycles: 10,000 to detect rutting. Sample size: 5 samples of each type of mixture [6, 7].

Data processing. Average values were obtained by excluding extreme results, confidence level is 0,95.

3. Research results

The softening temperature of the binders BND 60/90 is 49-51 °C, PBB 90 - 63-65 °C and PG 76-22 - 74-76 °C [10, 14].

The obtained data confirm that the use of modified and polymer-modified bitumens (PBB, PG) provides: an increase in the softening temperature by 15-25 °C compared to conventional BND, a decrease in rut depth by 2,5-4 times and an increase in shear strength by 20-30% [11, 13, 14].

Residual deformation during rutting test (t = +60 °C, 10,000 cycles). BND 60/90 – 4,6 mm, PBB 90 – 1,9 mm and PG 76-22 – 1,1 mm [6, 11, 14].

Shear strength at t = +40 °C. BND 60/90 – 2,8 MPa, PBB 90 – 3,4 MPa and PG 76-22 – 3,7 MPa.

Thus, it has been experimentally proven that the introduction of PG and PBB bitumens significantly increases the temperature resistance of asphalt concrete in the hot climate of Tajikistan and allows increasing the service life

[a] https://orcid.org/0000-0002-9817-3633
[b] https://orcid.org/0000-0002-4005-9766

of pavements from 5-7 to 10-12 years [18, 19].

The influence of temperature conditions on the strength of pavements.

According to the data of the Agency for Hydrometeorology of Tajikistan, in the southern and foothill regions in summer maximum air temperatures of up to +45°C are recorded, and for pavements – up to +70°C for the pavement [15]. Conventional petroleum bitumen grade BND 60/90 loses strength already at +52°C (the «Ring and Ball» method) [4, 10], which causes a decrease in shear resistance and an increase in rutting. The change in the strength and deformability of asphalt concrete with temperature is pronounced (Table 1) [7].

The main disadvantage of asphalt concrete as a road-building material is the high dependence of its strength and deformation properties on temperature. As the temperature increases, the viscosity of the bitumen contained in asphalt concrete decreases, the bonds between mineral particles weaken, which entails a decrease in strength.

When the temperature decreases, the opposite occurs: the viscosity of the bitumen, and with it the strength, increases. The change in strength associated with the change in temperature occurs in fairly wide limits. The compressive strength of standard asphalt concrete samples on average at different temperatures is given in Table 1.

It should be noted that such changes in strength worsen the operating conditions of asphalt concrete pavements. With a change in strength indicators, the deformation behavior of asphalt concrete also changes. The operating conditions of road pavements impose on this material the requirements of sufficient deformation resistance at high summer temperatures and sufficient deformation capacity at low temperatures, which determines the necessary resistance to cracking [7].

Table 1

Effect of temperature on coating strength [7]

№	At temperature, ^{0}C	Strength, kgf/cm^2
1	+ 50	10-20
2	+ 20	25-50
3	0	80-130
4	- 10	100-170
5	- 35	180-300

The most typical deformations that occur in summer on asphalt concrete pavements are shear deformations: waves, bulges. Such deformations occur especially often at fixed stops, intersections at trolleybus and bus stops and on transit sections of motorways due to changes in traffic speed. Figure 1 graphically shows the effect of temperature on the strength of asphalt concrete pavement.

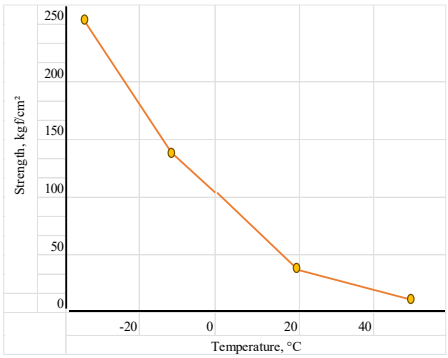

Fig. 1. Effect of temperature on the strength of asphalt concrete

Of particular importance for the development of deformations in asphalt concrete is its ability to accumulate deformations that occur under repeated loads. The growth of deformations as the number of load applications increases becomes most intense with the lowest deformation resistance of asphalt concrete at high temperatures.

Thus, with high traffic intensity (especially heavy vehicles) during the entire period of high summer temperatures, deformations may accumulate. On insufficiently stable pavements, extreme shear deformations occur under these conditions. Such deformations are most often observed in the first years of pavement operation.

Factors affecting the thermal resistance of asphalt concrete.

Type of binder. The choice of the type of binder is a key factor determining the thermal stability and durability of asphalt concrete pavements, especially in high summer temperatures. Depending on the operating conditions, traffic intensity and climatic influences, different types of bitumen are used, each of which has certain physical and chemical characteristics.

Conventional petroleum bitumen (BND). In the CIS, road petroleum bitumen that meets GOST 33133-2014 [4] is traditionally used. One of the most common grades of bitumen is BND 60/90, characterized by a softening temperature in the range of +47…+52°C (according to the «Ring and Ball» method). However, when used in regions with high summer temperatures (up to +40°C and higher in the air, and up to +60°C on the surface of the pavement), conventional bitumen begins to lose its strength and plastic properties [2, 10]: ruts appear, resistance to shear and plastic deformation decreases, and adhesion to the mineral skeleton of the mixture deteriorates.

Therefore, in modern conditions, conventional bitumen in its pure form has limited applicability in hot climates and on roads with high loads.

Modified bitumens. To increase resistance to deformation and aging, modified binders are used, including polymer additives: PBB - polymer-bitumen binder, SBS - binders with additives of styrene-butadiene-styrene copolymer, PMA - polymer-modified asphalt [6].

These binders have the following advantages: softening temperature - up to +70…+80°C and higher, increased elasticity and resistance to cracking at low temperatures, resistance to aging and oxidation and a significant reduction in the formation of ruts in areas with heavy traffic [6, 10, 13].

For example, PBB 60 is used in asphalt concrete type SMA-15, providing high deformation resistance on highways of categories I–II. The Superpave PG system is used in the USA and a number of countries - this is a modern method of classifying bitumens, taking into account the operating temperatures in a specific climate zone. The PG designation includes two temperatures: the first is the maximum surface temperature of the pavement in summer and the second is the minimum temperature in winter.

The Superpave PG 76-22 system means that the binder retains the required properties at +76°C (maximum working temperature of the coating) and is not brittle down to –22°C (minimum temperature in winter) [5, 9, 11].

The advantages of Superpave are a more precise selection of binder for climate and loads, predictable behavior of the coating under temperature fluctuations, and it is also used in projects of the World Bank, ADB and other international programs.

In Tajikistan, especially in the southern and foothill

https://doi.org/10.56143/3030-3893-2025-3-78-83 A bridge between science and innovation

regions, the use of PG 70-28/PG 76-22 bitumens [11, 14] can significantly increase the resistance of the pavement to heat and rutting. In recent years, as part of the modernization of national highways in Tajikistan, such bitumens have been supplied from Iran, Russia and Kazakhstan. Comparisons of bitumens by physical and mechanical properties for countries with hot climates are given in Table 2.

Thus, the use of modified bitumen and the use of the Superpave PG system are a prerequisite for ensuring thermal stability and extending the service life of asphalt concrete pavements under high temperature conditions. This is especially important for countries with hot climates, such as the Republic of Tajikistan.

Table 2

Comparison of bitumen by physical and mechanical properties for countries with hot climates

Parameter	Conventio-nal bitumens (BND 60/90)	Modified bitumens (PBB, SBS, PMA)	Bitumens according to the Superpave PG system (e.g. PG 76-22)
Softening point («Ring and Ball»), °C	47-52	60-80	up to 76 and above
Operating temperature range, °C	-10…+50	-20…+70	from -28 to +76 (depending on PG brand)
Resistance to rutting	Low	High	Very high
Resistance to aging and oxidation	Average	Increased	High (taken into account during certification)
Elasticity at low temperatures	Low	High	It is included in the specification (second part of PG)
Climate adaptation	No	Limited (by type of additives)	Full (by climate and temperature)
Where it is applied	Secondary roads, low traffic	Main roads, SMA, airports, bridges	Highways, heavy traffic, hot climate
Price	Low	Medium - high	High (depending on type and country of origin)

Note: *For BND 60/90, the classification by penetration (needle penetration depth at 25°C) is used. PBB - according to STO, GOST R 58400.1-2019; the polymer content can reach 5%, the Superpave PG system is accepted in the USA, Canada, Europe and recommended by HDM-4 for international projects, PG bitumens are tested for RTFO, BBR, DSR and others, unlike conventional bitumens.*

Crushed stone composition. The mineral skeleton of the asphalt concrete mixture plays a key role in the formation of strength, deformation resistance and heat resistance of the pavement.

The most important characteristics of the crushed stone component:

The cuboid shape of the grains (shape coefficient ≥ 0,85) improves intergranular adhesion and increases shear resistance. The optimal fineness modulus (2,8-3,2) ensures a dense structure and minimal voids. Diabase, granite and basalt are preferable due to their high strength and thermal stability, limestone is permissible to a limited extent [1, 3].

Granulometric composition (fineness modulus). The optimal fineness modulus for dense asphalt concrete mixtures is 2,8-3,2, which ensures: compact structure; optimal work of the binder; increased resistance to temperature deformations.

Type and origin of crushed stone. The most preferable are diabase, granite, basalt - rocks with high strength and thermal stability. Limestone crushed stones are limited in use in hot climates, as they have lower thermal resistance. The size of crushed stone for SMA and hot regions is recommended to use fractions of 5-15 mm, forming a strong frame.

Density and voids. The heat resistance of asphalt concrete pavement largely depends on the degree of compaction of the mixture and the volume of air voids, as they directly affect the mobility of the binder at high temperatures.

Compaction coefficient. Compaction up to 98-99% of the maximum density according to GOST 12801/EN 12697-10 [2, 7] leads to a decrease in bitumen migration, increases resistance to deformations (including shear) and ensures stability of the coating shape in the summer.

Air voids. The recommended air void content in the compacted mixture is from 3% to 5% [6]. If the void content exceeds 5%, the risk of overheating and softening of the bitumen increases, moisture absorption increases, which accelerates the aging of the mixture, and shear resistance decreases, especially on slopes and near intersections.

Negative effects of undercompaction. Increased mobility of the binder at a temperature of +50°C and above - can cause bitumen to come to the surface, the appearance of ruts and wave-like deformations, a reduction in the service life of the coating to 3-5 years instead of the standard 8-12 years.

Practical recommendations. Use of vibrating rollers with automatic compaction control and density control at the laying stage using radiometric or core cutting methods.

The dependence of the coating behavior on the void level is shown in Table 3.

Table 3

Dependence of coating behavior on the void level

Voidness level, %	Temperature resistance	Behavior at t > +50°C
< 3	Very high, the risk of deformation is minimal	Stable, bitumen does not migrate
3-5	Optimal, complies with standards	Moderately stable
5-7	Reduced, risk of rutting	The extrusion of the binder begins
> 7	Low, high mobility of the binder	Intensive extrusion of binder, formation of ruts, swelling of the coating

Calculation of temperature stresses in asphalt concrete pavements. Temperature stresses play an important role in the process of destruction of asphalt concrete pavement, especially in regions with sharp daily temperature changes. When heating and cooling, the material undergoes expansion and contraction, which leads to the occurrence of internal stresses. If these stresses exceed the tensile strength of the material, cracks, shifts and ruts develop in the pavement.

Calculation formula. Temperature stresses in the asphalt concrete mixture are determined by the linear thermal deformation formula:

$$Tn=E_{см}\cdot\alpha\cdot\Delta T \quad (1)$$

where Tn - is the temperature stress, MPa;

E_{cm} - is the elastic modulus of the asphalt concrete mixture, MPa (usually from 3000 to 6000 MPa depending on the composition);

α - is the coefficient of linear thermal expansion, approximately 2,5×10−5 1/°C;

ΔT - is the daily temperature gradient (the difference between the maximum daytime and minimum nighttime temperatures), °C.

Calculation example: Let's calculate the temperature stress under the following conditions:

Ecm=3000; $\alpha=2{,}5\cdot10^{-5}$ 1/∘C; ΔT=45°C (typical difference in summer in the mountainous regions of Central Asia).

$$Tt=3000\cdot2{,}5\cdot10^{-5}\cdot45=3{,}375 \text{ MPa}$$

Thus, a thermal stress of 3,375 MPa is formed in the body of the coating. Assessment of the risk of deformation if the shear strength of the material is, for example, 3,0 MPa (typical for conventional asphalt concrete with BND 60/90), then:

$Tn>\tau_{сдв} \Rightarrow$ plastic deformation occurs (rutting, cracks) [5, 7].

In this case, the coating operates at the limit of its mechanical characteristics, which leads to destruction in the form of: Longitudinal cracks, binder effusion, wave-like deformations, and the development of fatigue damage.

Comparison of thermal resistance of asphalt concrete when using different types of bitumen. In conditions of high summer temperatures, the resistance of asphalt concrete pavement to deformations depends significantly on the type of bitumen binder used. Table 4 shows generalized experimental data obtained as a result of testing standard asphalt concrete mixtures made with different types of bitumen:

Table 4

Influence of bitumen type on thermal resistance of asphalt concrete mixture [6, 11, 14]

Mixture type	Softenig point, °C	Residual deformation at 60°C, mm	Heat Resistance Rating
BND 60/90	47-51	4,5	low
PBB 90 (modified)	63-65	1,8	medium
Superpave PG 76-22	> 70	< 1,2	high

Explanation of the indicators given in Table 4:

Softening temperature - determined by the «Ring and Ball» method and shows at what temperature bitumen begins to lose strength. The higher this parameter, the higher the resistance to overheating. For BND 60/90 it is below 52°C and the material softens quickly, for PBB it is above 60°C due to polymer additives, and for PG 76-22 it is more than 70°C due to the strict requirements of Superpave, which is graphically shown in Figure 2.

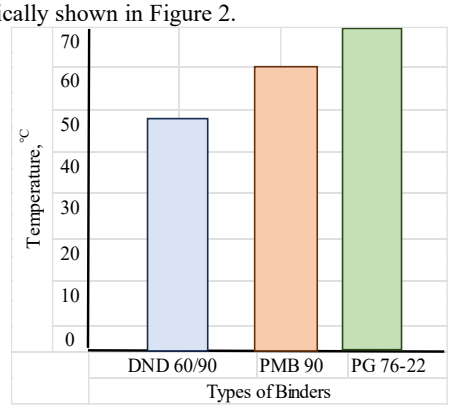

Fig. 2. Softening temperature of different types of binders

Residual deformation at 60°C is an important indicator of plasticity and rutting. The lower the residual deformation, the better the material resists shear and creep: 4,5 mm is evidence of low heat resistance in ordinary bitumen; 1,8 mm is acceptable for roads of categories II–III; <1,2 mm meets the requirements of main roads [6], which is graphically shown in Figure 3.

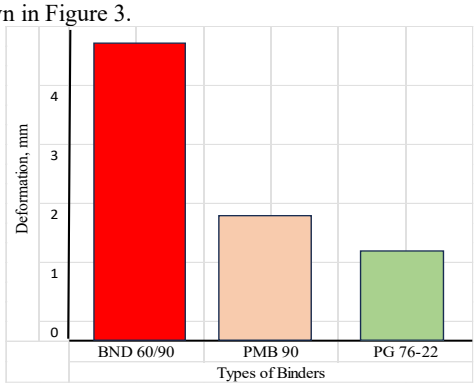

Fig. 3. Residual deformation of different types of binders

General heat resistance is a qualitative assessment of the suitability of the material for use at high temperatures: *low* - risk of bitumen coming to the surface and forming ruts, *medium* - acceptable for limited traffic and *high* - suitable for intensive transport, hot climates, airfields and highways.

Thus: bitumens of the BND 60/90 type - when used in conditions of summer heating (up to +60°C on the surface of the coating) demonstrate low resistance, especially at intersections and slopes; the use of PBB 90 - increases heat resistance due to elasticity and high softening temperature, but requires control at the production and installation stage; the use of Superpave PG 76-22 - the most reliable solution for hot climates, ensuring high durability of the coating under heavy traffic and temperature changes.

Increasing the temperature resistance of asphalt concrete.

High temperatures and daily fluctuations in climatic factors increase the risk of plastic deformations of asphalt concrete pavement, especially in the form of rutting, shear cracks and the emergence of binders on the surface. To counteract these phenomena, a set of measures is used to increase the heat resistance and stability of the mixture structure.

https://doi.org/10.56143/3030-3893-2025-3-78-83 A bridge between science and innovation

The use of modified bitumens and polymer-modified binders (PBB, SBS, rubber bitumen, PMA) significantly increases the modulus of elasticity at high temperatures and reduces sensitivity to temperature fluctuations: PBB 60, 90, 130 - increase the softening temperature to 65-80 °C; SBS (styrene-butadiene-styrene) - provides elasticity at t > + 60 °C; rubber bitumen - contains recycled rubber, resistant to rutting; PG bitumens according to Superpave (for example, PG 76-22) - designed for a specific climate and traffic.

Effect: residual deformation is reduced by 40-70% compared to conventional bitumen [6, 11, 13, 14].

The introduction of anti-rutting additives into mineral fillers with high porosity and adsorption capacity improves the structure of the mixture: fly ash (FA) - reduces the mobility of the binder; diatomite - a natural sorbent, improves heat resistance; clinoptilolite (zeolite) - improves adhesion and skeleton structure; plasticizing and reinforcing additives (fiber, fibers) - increase shear resistance.

Effect: increase in deformation temperature by 10-15 °C, reduction in rutting to 1,5 mm at t = +60 °C [10, 13].

Optimization of the composition using Marshall/Superpave methods. Selection of the composition based on the optimal binder content and grain size: Marshall method - ensures maximum density and minimum voids; Superpave method - takes into account loads, climate, type of traffic and forms a strong mineral framework [5].

Effect: increase in the elastic modulus of the mixture, resistance to deformation over 100 load cycles at 60°C.

Control of the degree of compaction. Undercompaction (<96%) dramatically increases the risk of thermal deformations. Required level: not less than 98% of the density of the compacted laboratory sample, the use of rollers with intelligent compaction control (IC) allows achieving uniform density and control by the core sample method, radiometry [2, 7].

Effect: a 2-fold reduction in residual deformation with an increase in density from 95% to 98%.

Use of drainage layers. The introduction of special drainage sublayers helps to reduce the thermal gradient between the lower and upper layers of the pavement: the use of porous asphalt concrete, the introduction of geosynthetic layers with heat-dissipating properties and the use of capillary drainage mats or air gaps in the road pavement structure.

Effect: equalization of the temperature profile of the pavement, reduction of stresses at the joints and boundaries of the layers.

Thus, to achieve high thermal resistance of asphalt concrete, it is necessary to ensure a combination of design, technological and materials science solutions, among which the key ones are: the choice of modified bitumen, the selection of crushed stone with the correct shape and fineness modulus, compaction of the mixture to the design density, the use of functional additives and interlayers.

4. Conclusion

The temperature resistance of asphalt concrete is one of the determining factors for the durability of road surfaces, especially in hot climates and sharp daily temperature fluctuations typical for the regions of Tajikistan. Low thermal resistance leads to the formation of ruts, cracks, extrusion of the binder and a decrease in the transport and operational characteristics of the surface already in the first years of operation.

The analysis and calculations showed that irreversible plastic deformations occur when temperature stresses exceed the shear strength limit. To effectively counteract this process, it is necessary to apply a comprehensive approach, including: the use of modified bitumens (PBB, SBS, PG bitumens) with a high softening point and resistance to aging; the introduction of anti-rutting additives (fly ash, diatomite) that improve the structure and sorption properties of the mixture; optimization of the mixture composition using Marshall and Superpave methods taking into account climatic adaptation; ensuring compaction of at least 98% of the maximum density using modern control technologies; the introduction of drainage and heat-removing layers in the road pavement structure.

Thus, the comprehensive adaptation of asphalt concrete pavement technologies taking into account temperature effects allows for a significant increase in the service life of road surfaces and a reduction in the frequency of major repairs in the road network of Tajikistan [5-7, 10-11, 13-19].

References

[1] ГОСТ 9128-2013. Смеси асфальтобетонные дорожные и аэродромные. – М.: Стандартинформ, 2013. https://docs.cntd.ru/document/1200104325

[2] ГОСТ 12801-98. Материалы на основе органических вяжущих. Методы испытаний. - М.: Стандартинформ, 1999. https://docs.cntd.ru/document/1200025384

[3] ГОСТ Р 58400.7-2019. Смеси асфальтобетонные и асфальтобетон. Метод испытания на колееобразование. – М.: Стандартинформ, 2020. https://docs.cntd.ru/document/1200117796

[4] ГОСТ 33133-2014. Битумы нефтяные дорожные. – М.: Стандартинформ, 2014. https://store.transportation.org/

[5] AASHTO R 35. Standard Practice for Superpave Volumetric Mix Design. – Washington, D.C.: AASHTO, 2017. https://store.transportation.org/

[6] EN 12697-22. Bituminous mixtures. Wheel tracking test. – Brussels: CEN, 2012. https://standards.cen.eu/

[7] EN 12697-10. Bituminous mixtures. Compactability. – Brussels: CEN, 2011. https://standards.cen.eu/

[8] Airey G.D. State of the Art Report on Ageing Test Methods for Bituminous Pavement Materials // Int. J. Pavement Eng. – 2003. – Vol. 4(3). – P. 165–176. https://www.asphalttechnology.org/

[9] Bahia H.U., Anderson D.A. The Development of Superpave Binder Specification // AAPT Proc. – 1995. – Vol. 64. – P. 437–475. https://www.asphalttechnology.org/

[10] Read J., Whiteoak D. The Shell Bitumen Handbook. – London: Thomas Telford, 2003. https://www.icevirtuallibrary.com/isbn/9780727732208

[11] Zofka A., Underwood B.S., Kim Y.R. Evaluation of Rutting Resistance of Modified Asphalt Binders in Hot Climates // J. Mater. Civ. Eng. – 2019. – Vol. 31(2). – Article 04018394. https://ascelibrary.org/doi/10.1061/(ASCE)MT.1943-5533.0002605

[12] Mirzozoda S.B., Sodikov J.I., Mirzoev F.S. Road Asset Management in Tajikistan // Transportation Research Procedia. – 2023. – Vol. 69. – P. 455-462.

[13] Wang H., Liu P., Hao P. Effect of SBS Modified Asphalt on Rutting Resistance under High Temperatures // Constr. Build. Mater. – 2018. – Vol. 185. – P. 463–472.

[14] Zhao Y., Xu H., Guo N. Performance of PG Binders in Hot Climates // J. Transp. Eng. – 2017. – Vol. 143(9). – P. 04017053.

[15] Кудрявцев В.В. Температурная устойчивость асфальтобетона. – М.: Транспорт, 2014. https://search.rsl.ru/

[16] ASTM D7405. Standard Test Method for Multiple Stress Creep and Recovery (MSCR). – ASTM, 2020. https://www.astm.org/d7405-20.html

[17] EN 12697-12. Bituminous mixtures. Determination of water sensitivity of bituminous specimens. – Brussels: CEN, 2010. https://standards.cen.eu/

[18] World Bank. HDM-4 Highway Development and Management. – Washington, 2019.

[19] Asphalt Institute. Superpave Mix Design Manual. – Lexington, KY, 2017. https://store.asphaltinstitute.org/

[20] AASHTO T350. Standard Method of Test for Multiple Stress Creep Recovery. – Washington, 2020. https://store.transportation.org/.

Information about the author

Mirzozoda Sukhrob Begmat	Candidate of technical sciences, associate professor of the Tajik Technical University named after academician M.S. Osimi, Dushanbe, Tajikistan; E-mail: sukhrob63@mail.ru Tel: (+992) 93-03-03-999 https://orcid.org/0000-0002-9817-3633
Sodikov Jamshid Ibrokhim ugli	Doctor of technical sciences, professor of the Department of «Urban Roads and Streets» of the Tashkent State Transport University, Tashkent, Uzbekistan; E-mail: osmijam@gmail.com Tel: (+998) 99-790-37-08 https://orcid.org/0000-0002-4005-9766
Mirzoev Faridun Sukhrobovich	Design engineer of the Technical Department of JSC «Tajikhydroelectromontazh» (TGEM), Dushanbe, Tajikistan; E-mail: farid.mirzaev.96@bk.ru Tel: (+992) 88-940-00-70

Neural network-based prediction of technical failures in communication networks

A.Sh. Khurramov[1][a]
[1]Tashkent state transport university, Tashkent, Uzbekistan

Abstract: This article discusses the problem of automated forecasting of the technical condition of train radio communication networks within the railway sector of Uzbekistan. The technical characteristics of existing systems, the theoretical model of signal propagation, and the main causes of failures are examined in detail. Traditional forecasting approaches are shown to be limited, as they often fail to adequately reflect nonlinear processes, the influence of electromagnetic interference, and the impact of maintenance activities. To address these shortcomings, an automated forecasting approach based on artificial neural networks is proposed. This method makes it possible to identify both sudden and gradually developing faults in advance, thereby increasing overall system reliability, supporting effective planning of technical maintenance, and reducing operational costs. Practical experiments carried out on railway sections confirmed the effectiveness of the proposed methodology. Overall, the use of neural networks for forecasting is considered a scientific and practical solution for enhancing the reliability of train radio communication systems, improving safety, and accelerating the gradual transition toward digital communication technologies.

Keywords: Train radio communication, telecommunication networks, neural networks, predictive maintenance, fault forecasting, technical condition monitoring, reliability, readiness coefficient, railway communication systems, digital technologies

1. Introduction

Railway transport represents one of the key sectors of a country's economic and social infrastructure, and its operation must consistently meet high standards of safety and efficiency. Ensuring traffic safety and managing transportation processes critically depend on operational-technological communication systems (OTCS). These systems provide continuous information exchange among train drivers, dispatchers, station attendants, and technical personnel. Therefore, train radio communication (TRC), which constitutes an integral part of OTCS, is required to guarantee a high level of reliability and continuity, serving as one of the fundamental conditions for safe and stable railway operations [1].

At present, TRC systems in Uzbekistan primarily operate within the hectometer (HF/VHF low-band) and meter (VHF high-band) frequency ranges. These ranges have been in practical use for many years and were once considered effective solutions. The advantage of the hectometer range lies in its ability to provide long-distance signal transmission. However, due to its high sensitivity to atmospheric noise and industrial electromagnetic interference, reliable communication is frequently disrupted. The meter range, in contrast, ensures higher-quality voice transmission, yet its dependence on line-of-sight propagation leads to significant signal attenuation in mountainous areas and especially within long tunnels.

Currently, TRC equipment and line infrastructure in Uzbekistan are physically outdated. Corrosion in antennas and cables, contamination of insulation, and loosening of contacts gradually deteriorate signal quality. As a result, "uncertain radio coverage zones" emerge within the network, where train drivers cannot maintain stable communication with dispatchers, thereby reducing the overall level of operational safety [1].

Traditional monitoring methods do not allow timely identification of such problems. In the existing system, signal levels are recorded only once every quarter using laboratory railcars. However, new faults that occur in the interval between inspections may remain undetected for several months. Increasing the frequency of inspections would sharply raise operational costs. Consequently, the automated forecasting of parametric faults has become an urgent and essential task.

Reliability indicators of train radio communication networks. One of the most important concepts in assessing the efficiency and safety of technical systems is reliability. In TRC networks [2], reliability is evaluated using the readiness coefficient (K_g):

$$K_g = \frac{T_p}{T_p + T_b}$$

where:

- T_p – the total operating time of the TRC channel,
- T_b – the recovery time after a failure.

If failures occur infrequently or recovery is carried out very quickly, the value of K_g approaches one. This indicates that the system is highly reliable. Conversely, if failures occur frequently or the recovery process takes a long time, the value of K_g decreases significantly, reflecting reduced system reliability.

For TRC systems, maintaining the readiness coefficient within the range of 0.95–0.98 is considered one of the essential safety requirements. In practice, however, especially when using outdated equipment, this indicator often does not exceed 0.90–0.92. Therefore, enhancing the reliability of existing systems requires not only the rapid detection of failures but, more importantly, their prediction in advance [3].

[a] https://orcid.org/0000-0002-8443-9250

Empirical observations on the railways of Uzbekistan show that TRC systems operating in the hectometer band are frequently affected by atmospheric noise, resulting in repeated signal losses. In the meter band, sudden attenuation or complete loss of the signal is observed in mountainous areas or inside tunnels. Under such conditions, the recovery time (T_b) increases, leading to a reduction in the readiness coefficient. Consequently, minimizing T_b is a fundamental requirement for improving the reliability of TRC systems.

2. Research methodology

Theoretical model of signal propagation. The primary function of TRC systems is to ensure continuous and reliable communication between the train driver and the dispatcher. The stability of communication primarily depends on the propagation characteristics of radio waves and the effective transmission distance of the signal. Therefore, accurate modeling of signal propagation and the establishment of theoretical foundations are of crucial importance in TRC networks [4].

One of the fundamental requirements for communication quality in train radio systems is that, at any point within a given section, the train driver must maintain reliable contact with at least two stationary base stations located on opposite sides. Based on this principle, the normative condition can be expressed as follows:

$$r_1 + r_2 - 3 \geq l$$

where:

- r_1 and r_2 – the reliable communication ranges (in km) between the locomotive and the stationary base stations on the left and right sides, respectively,
- l – the total length of the section (in km).

If this condition is met, the train driver will be able to maintain simultaneous communication with two base stations at any point along the section. This serves as a fundamental guarantee of operational safety requirements [5].

In radio communication systems, the communication range can be calculated using the following formula:

$$r = \frac{A_{tx} - u_{min} - A_{ant.loss} - \sum a_{st} - \sum a_{lin} - \sum a_{loc}}{a_H}$$

where:

- A_{tx} – output signal level of the transmitting station, dB;
- u_{min} – minimum useful signal level at the receiving station, dB;
- $A_{ant.loss}$ – antenna transition losses, dB;
- $\sum a_{st}$ – attenuation in stationary equipment, dB;
- $\sum a_{lin}$ – attenuation in feeder lines, dB;
- $\sum a_{loc}$ – attenuation in locomotive equipment, dB;
- a_H – attenuation coefficient per kilometer of transmission line, dB/km.

This formula provides an accurate evaluation of the signal quality and coverage range of train radio communication systems. Any variation in these parameters can have a significant impact on the overall result [6].

The output signal level (A_{tx}) is the key indicator of the transmitter's power. The higher the power, the greater the achievable communication distance. However, excessive power consumption increases energy costs and may violate electromagnetic compatibility requirements.

The minimum useful signal (u_{min}) represents the lowest value necessary for the receiving station to distinguish the signal from background noise. This parameter depends on the sensitivity of the receiving equipment and the prevailing noise level.

Losses ($A_{ant.loss}$, $\sum a_{st}$, $\sum a_{lin}$, $\sum a_{loc}$) denote the attenuation occurring during antenna transition, propagation along the transmission line, and within locomotive equipment. In practice, these losses often represent the primary reason for signal quality degradation.

The per-kilometer attenuation coefficient (a_H) characterizes the natural decrease in signal strength along the guiding line [7]. It depends on the material of the line, cable quality, and surrounding environmental conditions.

By applying the theoretical model of signal propagation, it is possible to preliminarily assess signal quality and coverage distance in TRC systems. This enables:

- optimal selection of inter-station distances,
- accurate design of antenna placement,
- timely maintenance of transmission lines,
- reduction of operational costs.

However, the model is based solely on static calculations and does not fully account for factors such as equipment aging, gradual degradation, and the influence of external electromagnetic environments over time. Therefore, for forecasting parametric failures, more effective approaches are required – in particular, *automated prediction methods based on neural networks* [8].

The criticality of failures depends on both their rate of impact and the possibility of detection. Sudden failures are usually recognized immediately and can typically be eliminated within a short period of time. Gradual failures, on the other hand, are more hazardous since they may remain unnoticed for an extended period while posing a significant threat to operational safety.

On the railways of Uzbekistan, gradual failures represent the most frequent and problematic category. Such faults cannot be reliably detected through traditional quarterly inspections, as they tend to develop and intensify in the intervals between scheduled checks. Therefore, the ability to forecast these failures in advance and to predict their potential occurrence has become a crucial necessity [8].

The time-dependent nature of failures provides an important opportunity for forecasting. For example, if the resistance of a cable is observed to increase on average by 0.2–0.5 Ohm per kilometer annually, this trend can be used to determine the rate of degradation and to estimate the subsequent decline in signal quality. Similarly, antenna misalignment occurring after each severe wind event can be tracked and predicted based on statistical data.

Thus, while sudden failures can generally be eliminated through prompt technical maintenance, gradual failures can only be identified using forecasting systems, particularly automated approaches based on neural networks [9–11].

Although traditional forecasting methods are theoretically simple and relatively easy to apply in practice, they do not fully correspond to the actual conditions of TRC systems. These methods describe degradation processes only in a generalized manner and fail to account for complex electromagnetic environments, maintenance activities, and abrupt changes in operating conditions. As a result, their

application on the railways of Uzbekistan often leads to inaccurate forecasts.

To overcome these limitations, more flexible methods capable of modeling complex processes are required, such as *artificial neural networks* [12]. The following section provides a detailed discussion of the theoretical foundations and practical implementation of such approaches.

3. Results and Discussion

Automated approaches based on neural networks. As a rule, the occurrence of unstable radio communication zones is associated with unexpected or gradually developing faults along the signal propagation path, as well as the influence of electromagnetic noise.

Unexpected faults may arise within the operational limits of equipment performance. Such failures typically occur either spontaneously or as a result of external impacts. Examples include interruptions, short circuits, contact disconnections, insulation breakdowns, or mechanical damage. However, this category of faults is relatively easy to detect, since the location of the damage can usually be identified and eliminated quickly by conducting an external inspection of feeder lines and antenna equipment [13].

Gradual failures are characterized by the progressive degradation of parameters such as $\sum a_{st}$, $\sum a_{lin}$, $\sum a_{loc}$, and a_H. As a result, the overall communication range decreases, and unstable coverage zones appear in certain sections of the network.

The causes of such failures may include corrosion of transmission lines, deterioration of contact quality, contamination of insulators, disruption of cable connections, reduction of the quality factor in resonant and locking circuits, changes in antenna radiation patterns, as well as degradation of feeder components due to aging or water ingress.

Detecting gradual failures is complex, yet they manifest intermittently, which allows their occurrence to be diagnosed. For automated diagnostics, the primary input data are the signal levels recorded from stationary base stations. The results of these measurements are represented in the form of a two-dimensional vector [14].

$$\bar{u}_t = \begin{vmatrix} u_{a1} & u_{a2} & \dots & u_{am} \\ u_{b1} & u_{b2} & \dots & u_{bm} \\ \dots & \dots & \dots & \dots \\ u_{g1} & u_{g2} & \dots & u_{gm} \end{vmatrix},$$

where u_{gm} denotes the average voltage at the locomotive receiver, m represents the kilometer mark, and g corresponds to the active base station.

The data presented in this form must first undergo preprocessing, where all missing elements are restored through interpolation, and the measured signal levels are aligned with the corresponding points (linked to each kilometer of the section).

Neural network architecture. For forecasting tasks, a multilayer perceptron (MLP) architecture is most commonly applied. Its main components are as follows:

- *Input layer* – vectors representing signal levels and contextual predictive factors.
- *Two hidden layers* – performing nonlinear transformations.
- *Output layer* – predicted signal levels and vectors of technical condition.

The activation function selected is the sigmoid:

$$f(x) = \frac{1}{1 + e^{-x}}$$

Since the sigmoid function is differentiable, it enables the efficient application of gradient-based training algorithms, such as backpropagation [15].

Mathematical model. The mathematical model of the neural network can be expressed through the following system of equations:

$$c_j = f\left(\sum_{i=1}^{r} a_i \alpha_{ij} + \chi_j\right), \quad j = 1,\dots,r_1,$$

$$k_s = f\left(\sum_{j=1}^{r_1} c_j \beta_{js} + \eta_s\right), \quad s = 1,\dots,r_2,$$

$$q_h = f\left(\sum_{j=1}^{r_2} k_s \gamma_{sh} + v_h\right), \quad h = 1,\dots,n,$$

where:

- a_i – elements of the input vector (signal levels and factors),
- α, β, γ – synaptic weights,
- χ, η, υ – bias coefficients of the neurons,
- c_j, k_s, q_h – outputs of the first hidden layer, second hidden layer, and output layer, respectively.

The output vector q_h represents the predicted signal levels and the technical condition of the system.

Error function and training. During training, the neural network outputs are compared with real measurements. The error function is defined as:

$$\Phi_i = \frac{1}{2}\left(u_{gi} - u_{gi}^{(t+1)}\right)^2,$$

where u_{gi} is the real signal level and $u_{gi}^{(t+1)}$ is the predicted signal level.

The training objective is formulated as:

$$\max(\Phi_i) \le \Delta,$$

where Δ is the maximum permissible prediction error.

Using a gradient optimization algorithm, the synaptic weights and biases of the neurons are iteratively adjusted.

In the simplest case, a single parameter, time, serves as the main argument for forecasting. In such cases, the problem can be solved by applying mathematical methods of extrapolating previous measurement results over time. However, in the present context, these methods exhibit several limitations:

- it is impossible to construct an accurate predictive model without studying the operational history of the system over a long period or by incorporating additional types of data;
- changes in parameters cannot be adequately described without proper mathematical characterization;
- all mathematical forecasting methods are treated as open systems, where errors at the input are fully transmitted to the output, thus negatively affecting

prediction accuracy;

- obtaining accurate forecasts requires consideration of all measures undertaken to improve the technical condition of TRC equipment, which is not feasible within the framework of purely mathematical methods;
- at the initial stage of operating a fully modernized TRC network (e.g., during electrification), the necessary conditions for forecasting using mathematical methods are not present.

This problem can be partially addressed through prediction based on the theory of statistical classification (pattern recognition), where extrapolative relationships are established from the available initial data. However, the inability to resolve poorly formalized aspects of the forecasting process and the relatively low accuracy of the results prevent these methods from being applied effectively.

These shortcomings can be overcome by employing neural network (NN) algorithms, which extrapolate within the feature space of the technical system's states. In general, the procedure for automated prediction of failures in train radio communication networks using NNs is illustrated in Figure 1.

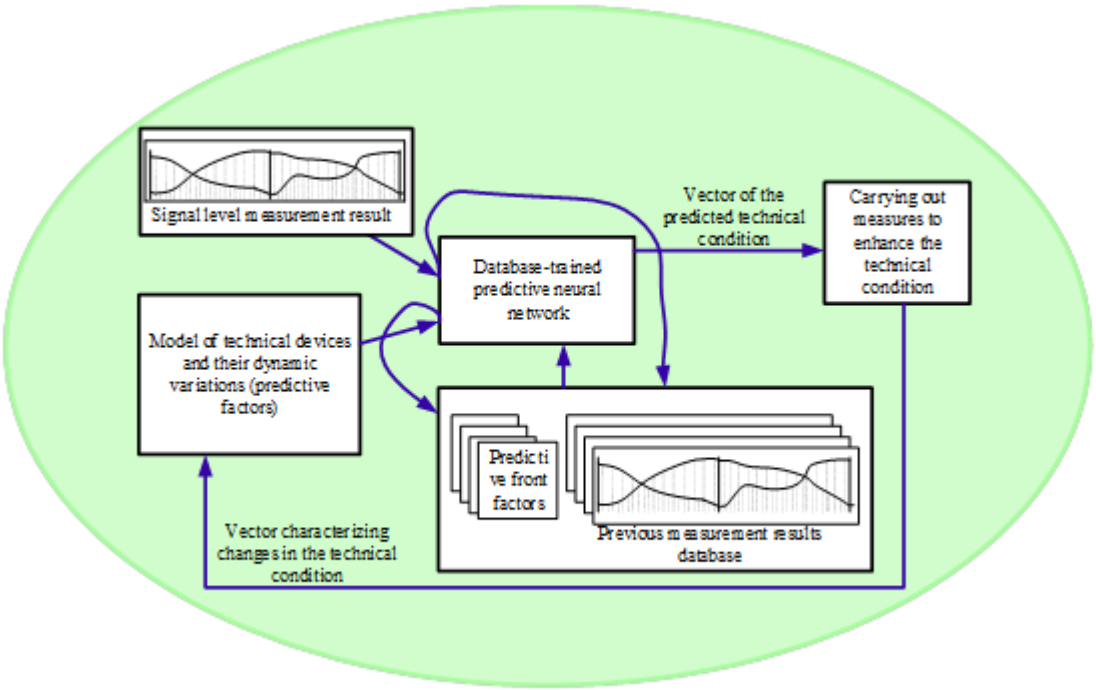

Figure 1. Automated procedure for forecasting failures in train radio communication networks

The central component of this structure is the neural network trained on a database formed from previous measurement results. Once the signal levels from stationary base stations are recorded, they are combined with data reflecting quality changes in equipment, line devices, and guiding channels, and then fed into the neural network as input. At the output, a vector is generated that represents the predicted future technical state of the TRC system. Based on these results, preventive maintenance measures are developed and implemented in practice.

Using laboratory railcars, signal levels are periodically recorded, and the results are entered into the database, enabling the neural network to be retrained. In this way, the model is continuously refined and improved over time.

In general, forecasting using a neural network consists of the following main stages:

- collection of initial data and their normalization into a unified format;
- synthesis of the predictive architecture of the neural network;
- training of the neural network with empirical data samples to form the predictive model;
- obtaining the forecast result for the specified prediction horizon;
- verification of the predictive model against established criteria and its preparation for practical application.

The application of neural networks for forecasting parametric failures in TRC networks has demonstrated high effectiveness in practice. Results indicate that this approach provides significantly greater accuracy compared to traditional methods and allows for efficient planning of maintenance activities even under complex operational conditions. However, like any technological solution, neural networks possess both advantages and limitations. At the same time, numerous prospects exist for further improving this approach in the future [16].

By employing neural networks, "uncertain communication zones" in TRC systems can be identified well in advance. For example, in the Kamchik tunnel, hazardous areas caused by signal attenuation can be predicted by the neural network several weeks beforehand. This provides dispatchers and technical staff with the opportunity to take preventive measures in advance. As a result, the overall safety of train operations is significantly enhanced.

The architecture of the predictive neural network is illustrated in Figure 2.

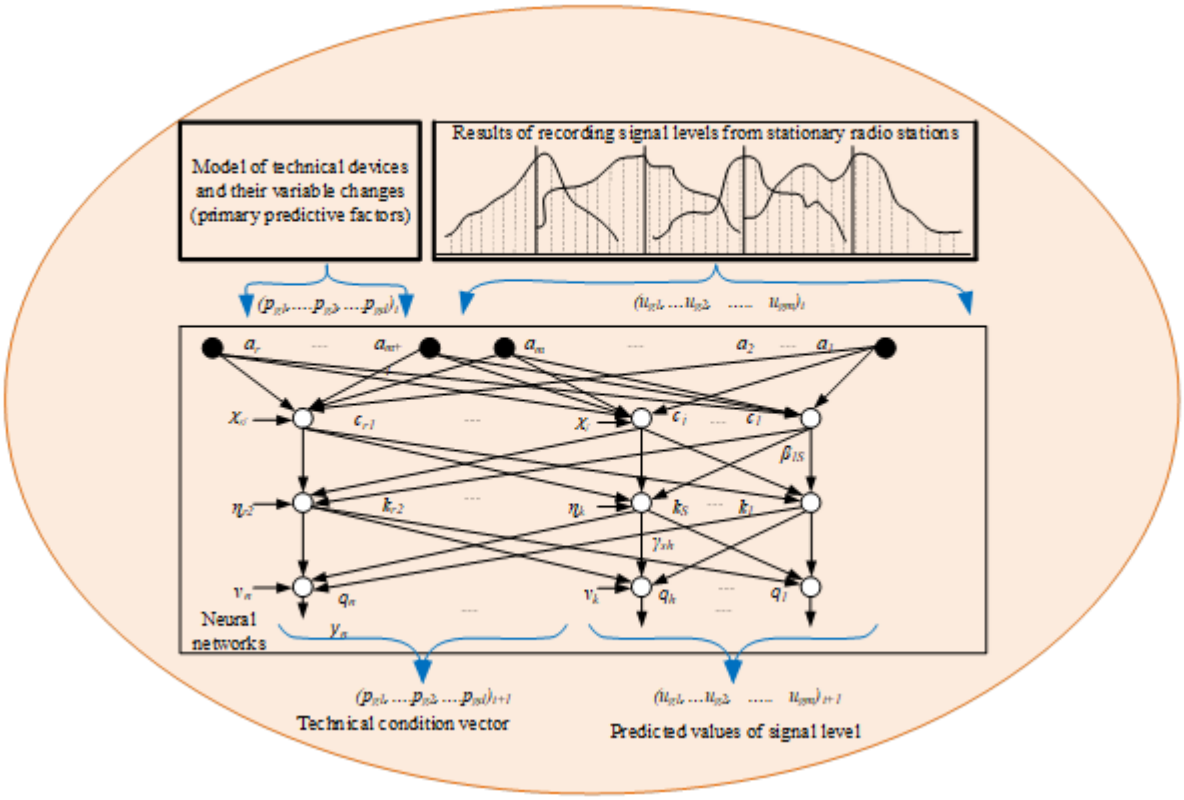

Figure 2. Predictive neural network architecture

In traditional approaches, emergency maintenance operations require substantial costs, since eliminating failures after they occur demands more resources and time. A forecasting system, on the other hand, enables precise planning of preventive maintenance. For instance, if antenna adjustments or cable replacements are carried out before an emergency situation arises, overall expenses can be reduced by up to thirty percent.

Neural networks can be retrained on the basis of newly collected data. Consequently, the system is continuously updated and adapts even when technical conditions change. For example, if the TRC system transitions from analog to digital equipment, the neural network can be retrained in a short period using the new parameters while continuing to function effectively [17].

Signal attenuation and electromagnetic interference often exhibit nonlinear characteristics. Conventional extrapolation methods cannot fully capture such dynamics. Neural networks, however, are capable of efficiently modeling and learning these complex nonlinear dependencies.

A comparative analysis of traditional forecasting and neural network-based forecasting is presented in Table 2.

Furthermore, the neural network-based forecasting system can be integrated with other systems currently being deployed in Uzbekistan Railways. For example, it can be combined with DMR base stations, GPS/GLONASS monitoring systems, and SCADA platforms to create a unified control center. This integration ensures not only reliable management of radio communication but also comprehensive monitoring of other technical subsystems.

Table 2

Comparison of traditional forecasting and neural network-based forecasting

Indicators	Traditional methods (extrapolation, ARIMA)	Neural network-based forecasting
Forecast accuracy	±3–4 dB	±1.5 dB
Historical data requirement	Long-term (years)	Can be trained even with short-term data
Consideration of maintenance	No	Yes
Adaptation to EM environment	Not fully reflected	Adaptive
Practical efficiency	Moderate	High (accuracy improvement of 20–25%)

The results of the discussion demonstrate that a neural network-based forecasting system can significantly enhance the reliability of TRC within Uzbekistan Railways. The advantages of this approach outweigh its limitations, as it ensures safety, reduces operational costs, and brings the system closer to meeting modern technological requirements. In the future, this approach may be further improved through integration with emerging technologies such as the Internet of Things (IoT), fifth-generation (5G) communication, and the Future Railway Mobile Communication System (FRMCS), thereby evolving into a more advanced and comprehensive solution [17].

4. Conclusion

This study examined the problem of forecasting parametric failures in TRC networks. First, the technical characteristics of existing systems, the theoretical model of signal propagation, and the causes of failures were analyzed. It was concluded that traditional forecasting methods are insufficient under real operating conditions, as they fail to account for maintenance activities and the complexity of the electromagnetic environment.

A neural network-based forecasting approach was proposed. This method enables the processing of signal levels and the modeling of complex nonlinear processes. The results showed that uncertain communication zones can be identified one to two months in advance, with a prediction error of approximately ±1.5 dB, compared to ±3–4 dB for traditional methods. The readiness coefficient of the TRC system can thus be increased to 0.98.

In Uzbekistan Railways, challenges such as attenuation of VHF signals, atmospheric noise in the HF band, and antenna misalignment across certain sections were effectively addressed through neural network-based forecasting. This approach not only improves safety but also reduces operational costs by up to thirty percent [18].

Overall, neural network-based forecasting represents a practical and scientifically grounded solution for significantly enhancing the reliability of TRC systems in Uzbekistan Railways. Moreover, it provides a robust foundation for the gradual transition of these systems to advanced digital technologies, including DMR, TETRA, and FRMCS.

References

[1] Xalikov A.A., Xurramov A.Sh., O‘rokov O.X. IP-tarmoq asosidagi tezkor texnologik radio aloqa tarmog‘i ishonchliligini hisoblash metodikasi. Muhammad al-Xorazmiy avlodlari, № 1 (23), mart 2023. 126-132 b.

[2] T. Yamamoto, Y. Hara, “Optimization of Communication Systems in High-Speed Railway Tunnels,” IEEE Transactions on Vehicular Technology, vol. 67, no. 3, pp. 2021–2033, Mar. 2018. DOI: 10.1109/TVT.2017.2772215.

[3] S. K. Sharma, “Next Generation Wireless Communication for Railway Systems,” IET Communications, vol. 13, no. 10, pp. 1478–1486, Jul. 2019. DOI: 10.1049/iet-com.2018.5600.

[4] A. Goldsmith, Wireless Communications, Cambridge University Press, 2nd ed., 2020.

[5] X. Yin, L. Liu, “Channel Measurement and Modeling for High-Speed Railway Communications,” IEEE Transactions on Intelligent Transportation Systems, vol. 20, no. 5, pp. 1844–1858, May 2019.

[6] M. Driouch, P. Combes, “FRMCS: The Future Railway Mobile Communication System,” in Proc. IEEE ICT 2020, pp. 345–352, 2020.

[7] H. Wu, Y. Zhao, “Deep Learning for Predictive Maintenance of Wireless Communication Systems,” IEEE Access, vol. 8, pp. 68733–68741, 2020.

[8] I. Blinder, Digital Operational-Technological Communication of Railway Transport, Moscow: Transport, 2019.

[9] Khalikov Abdulxak, Khurramov Asliddin, Urokov Olim, Rizakulov Sherzod. A mathematical model of the operation process of a radio communication network based on IP technologies in the conditions of information impact during the transmission of a non-repetitive data stream / E3S Web of Conferences 420, 03022 (2023).

[10] Y. Zhou, J. Zhang, “Artificial Neural Network for Fault Prediction in Railway Wireless Networks,” IEEE Access, vol. 9, pp. 95413–95422, 2021.

[11] S. Basagni, M. Conti, S. Giordano, I. Stojmenovic, Mobile Ad Hoc Networking: Cutting Edge Directions, Wiley-IEEE Press, 2020.

[12] L. Zhang, J. Qiu, “Propagation Characteristics and Modeling of Radio Waves in Railway Tunnels for 5G Systems,” IEEE Antennas and Wireless Propagation Letters, vol. 19, no. 1, pp. 65–69, Jan. 2020.

[13] ETSI TR 103 333 V1.1.1, “Future Railway Mobile Communication System (FRMCS): Technical Report,” European Telecommunications Standards Institute, 2021.

[14] ITU-R M.2410-0, “Minimum Requirements for the Evaluation of IMT-2020,” International Telecommunication Union, Geneva, 2017 (amended 2021).

[15] S. Tang, M. Zhu, “Intelligent Railway Wireless Networks: Challenges and Future Trends,” IEEE Internet of Things Journal, vol. 8, no. 14, pp. 11542–11554, Jul. 2021.

[16] O‘zbekiston Respublikasi Vazirlar Mahkamasi Qarori, “O‘zbekiston temir yo‘llarida raqamli texnologiyalarni joriy etish konsepsiyasi,” 2022.

[17] Халиков А.А, Хуррамов А.Ш. Анализ электромагнитной совместимости и методы разработки частотного плана. Universum: Технические науки: Раздел-09. Радиотехника и связь Москва–2022. № 8(101). (дата обращения: 12.08.2022). – С.36-39.

[18] Халиков А.А. Хуррамов А.Ш. Расчет сетки рабочих частот системы технологической радиосвязи на железнодорожном транспорте Universum: технические науки: электрон. научн. журн. Раздел Радиотехника и связь Москва-2022. №9(102). с.53-56.

Information about the author

Asliddin Khurramov
Tashkent State Transport University, Associate professor of Department of Radioelectronic Devices and Systems, Ph.D.
E-mail: asliddinxurramov703@gmail.com
Tel.: +998909077300
https://orcid.org/0000-0002-8443-9250

Analysis of the change in the volume of electricity production

B. Khamrakulov[1][a], Sh. Fayzullaeva[2][b]
[1]Kamoliddin Behzod National Institute of Arts and Design, Tashkent, Uzbekistan
[2]Tashkent state transport university, Tashkent, Uzbekistan

Abstract: In the article, the prediction model of the change in the volume of electricity production in the Republic of Uzbekistan was studied. At the present time, it is important to change the volume of electricity production in the Republic of Uzbekistan. First of all, an econometric analysis of the changes in the volume of electricity production in the period 2010-2022 was carried out. The analysis was carried out on the basis of the MINITAB package. In the analysis, the main statistical indicators were calculated based on the data. A graph is constructed, and periods of changes in the volume of electricity production are studied based on the graph. Based on the statistical data, several trend models were built and a prediction model was selected based on the residuals. Based on the selected model equation, the change in the volume of electricity production for the next 3 years was predicted.

Keywords: Changes in the volume of electricity production, main statistical indicators, trend model equation

1. Introduction

In the development of humanity, the needs of people for various energy sources make them natural sources–wood, coal, peat and other fuels, wind, water flow energy (wind and water mills). Later, due to the progress of science and technology, the revolution in science and technology, from the second half of the 20th century, the need for electricity increased. These factors required rapid development of energy industry. The development of science and technology is expressed through the development of new methods of energy production and its transformation, the creation of new efficient equipment and technologies, the centralization of energy distribution, etc. Scientific research works on energy were focused on solving priority complex issues and practical problems of energy. The issue related to the long-distance transmission of electric energy - theory of transforming alternating current into fixed current, methods for calculating the maintenance of spontaneous awakening of magnetic currents of asynchronous and synchronous machines, development of the theory of complex types of damage in electronic devices, and solving the efficient distribution of power of hydroelectric power plants were dealt with. related works have been completed. In the late 1940s and 1950s, scientific research was focused on improving the operation of power plants, electrical systems and equipment, improving their accuracy, increasing their efficiency, and creating a compact theory and methods of calculating electrical systems. The problems of solving large-scale nonlinear equations representing the mode of electrical systems, creating schemes for extracting small power from high-voltage power lines, developing calculation theory and methods were studied [1]-[4].

Currently, the volume of electricity production is increasing from year to year. Based on this change, 2010-2022 annual data was studied to make a forecast for the next future years. Based on identified data, a tred model was built and prediction the value for the next 3 years was calculated.

In forecasting, an analysis was conducted based on the time series in the econometric model analysis.

Two types of data can be used to build an econometric model:

- a set of data describing various objects at a certain time;
- information describing one object in different time series.

2. Research methodology

A time series is a sequence of data collected, recorded, or observed over the same period of time. A time series consists of the observed values of a property of the studied object at different times. For example, in medicine, it can be a cardiogram, in geology, a graph of vibrations caused by an earthquake or underground explosion, in astronomy, a graph of solar activity, or signals from distant galaxies received by radio telescopes, etc. In the economy, the unemployment rate or the change in the interest rate, the dynamics of the exchange rate and the share price can be given as an example. The observed time interval can be continuous, one minute, one hour, day, month or year.

The overall trend of time series values over time is called the trend and denoted as T_t.

The most common way to model a trend in a time series is to find an analytical function that shows the change of its considered value over time, that is, to construct a trend. This method is called ***the analytical method of time series smoothing***.

A simple exponential smoothing algorithm provides a stable prediction for all future values of the time series. However, the trend of increase or decrease in the values of some lines is clearly observed. In such cases, it is necessary to pay attention to the trend and study it. Naturally, the trend model is expected to perform better.

In 1957, Holt proposed an exponential smoothing algorithm that incorporates the simplest linear trend model.

Autocorrelation is the correlation between variables and the correlation between one or more lags.

Formula:

$$r_1 = \frac{\sum_{t=1}^{n-1}(Y_{t-1} - \bar{Y})(Y_t - \bar{Y})}{\sum_{t=1}^{n}(Y_{t-1} - \bar{Y})^2}$$

[a] https://orcid.org/0009-0000-4536-1908
[b] https://orcid.org/0009-0007-8796-6033

A graphical representation of the autocorrelation function is called a correlogram.

A trend is a long-term component that shows how a time series changes over a specified period of time. That is, the trend is an analytical function of time, which can be in the following forms:

- Linear trend $T_t = at + b$;
- Parabolic trend $T_t = at^2 + bt + c$;
- Exponential trend $T_t = exp(at + b)$,

where a, b, c are parameters.

Generally, estimates for trend parameters are found using the least squares method. Non-linear trends are first transformed into a linear trend by some shape transformation, and then the appropriate calculations are performed. Using computer programs, it does not take long to do this. To select the best model, their coefficient of determination and errors are considered. We calculate errors using MAPE, MAD, MSE, MPE and MSD methods. We calculate the coefficient of determination from its formula.

Statement of the problem: the amount of electricity production in the Republic of Uzbekistan is given for the years 2010-2022, to determine the dependence of this data during the unit of time and to build the best model for this, and through it to generate the average electricity in the following periods is to predict output volume with low error.

№	Years	Electricity production volume
1	2010	51976,3
2	2011	52806,2
3	2012	52999,6
4	2013	54618,6
5	2014	55766,0
6	2015	57658,1
7	2016	59100,5
8	2017	60820,1
9	2018	62896,6
10	2019	63531,6
11	2020	66500,7

First of all, the main statistical indicators are calculated using the MINITAB package program.

Descriptive Statistics: Y

Variable	Mean	StDev	Variance	Minimum	Median	Maximum
Y	60331	7150	51120784	51976	59101	74269

As we can see from the main statistics, the volume of electricity production during the given period reached its maximum point in 2022, which was 74 269. This point was not reached in the period after that. The lowest point corresponds to 2010 and it was 51 976. The average volume of electricity production for the whole year was 60 331. In this place, the median was equal to 59 101. The average squared deviation was 7 105. How far the given values are scattered around the regression line shows 51 120 784.

The next task will be to give preliminary conclusions on the basis of the graph.

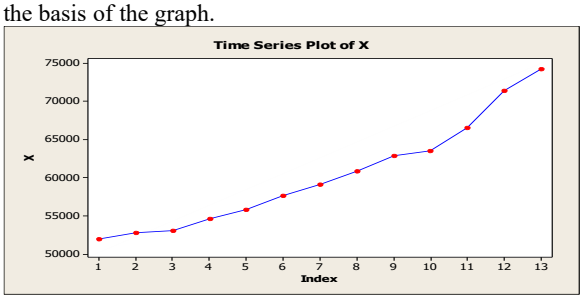

From the graph, we can observe the trend of changes in the volume of electricity production in each period. In general, it is advisable to study the graph in several parts. As can be seen from the graph, initially, the value of electricity production has a tendency to increase, and this situation continued until the 2nd period. A slight downward trend was observed from period 2 to period 3. From the 3rd period, the value of the volume of electricity production has a general upward trend. In general, the value of the volume of electricity production has an almost increasing tendency. So, **there is a trend.** You can easily see from the graph that there is no seasonality and cyclicality

For the above issue, the corellogram will look like this

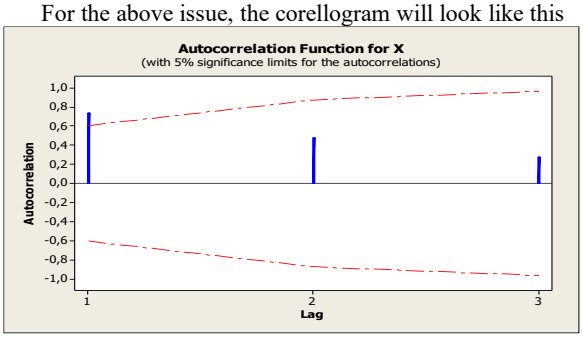

From the autocorrelation graph we can make the following conclusions:

As a rule of thumb, a series must be non-stationary for a trend to exist. For the series to be non-stationary, the first few values in the correlogram must lie outside the boundary line. Since one lag in the correlogram is out of bounds, our model has a trend and by itself the series is non-stationary. We also conclude that the autocorrelation function has no seasonality or cyclicity, since the values of the autocorrelation function are decreasing and do not return to the same value.

Trend Equation: $Y_t = 47842,3 + 1784,16 \cdot t$

Errors:

MAPE	2
MAD	1399
MSD	2623382

Graph:

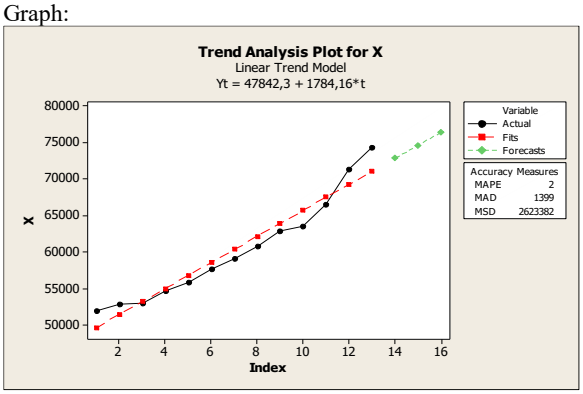

Period	Forecast
2023	72820,5
2024	74604,7
2025	76388,8

The volume of electricity production predicted for the following years was calculated using the linear trend model. Based on the residuals of the linear trend model, the correct selection of the model equation is based. Other model

https://doi.org/10.56143/3030-3893-2025-90-92 A bridge between science and innovation

equations are also considered to justify the correct model selection.

Now let's look at the parabolic trend pattern:

Trend model equation:

$$Y_t = 51990{,}6 + 124{,}842 \cdot t + 118{,}522 \cdot t^2$$

Errors:

MAPE	1
MAD	531
MSD	460055

Graph:

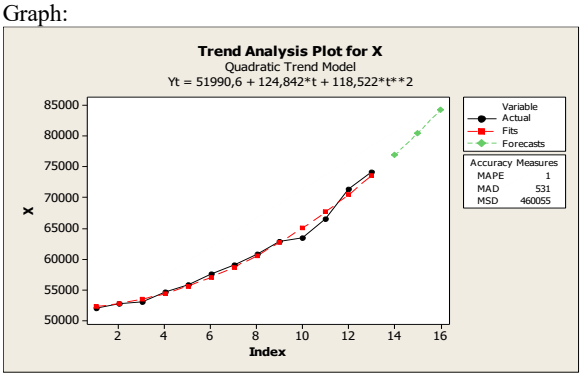

Period	Forecast
2023	76968,8
2024	80530,8
2025	84329,8

Therefore, the electricity production volume predicted by our parabolic model in the following years is more accurate than our prediction made by the linear trend model.

Now let's look at the exponential trend model:

Trend model equation: $Y_t = 48893{,}5 \cdot 1{,}02956^t$

Errors:

MAPE	2
MAD	1132
MSD	1799390

Graph:

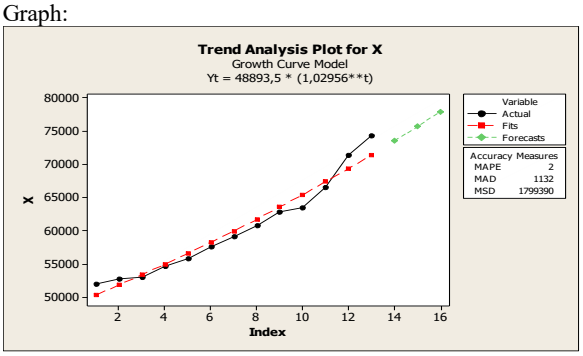

Period	Forecast
2023	73518,4
2024	75691,8
2025	77929,6

Let's compare the models by errors:

Model type	MSD
Linear	2623382
Parabolic	**460055**
Exponential growth	1799390

The parabolic model most accurately describes the available data because it has the smallest standard deviation (MSD). The trend equation describing this time series is:

First, annual basic statistics of electricity generation volume were determined and confidence intervals were found for them. At the next stage, a graph of the model was built and it was concluded that there is an increasing trend. Nevertheless, an autocorrelation analysis was performed to test whether there was indeed a trend in the model and whether there was seasonality in the model. According to him, there is a real trend in the model and

$$Y_t = 51990{,}6 + 124{,}842 \cdot t + 118{,}522 \cdot t^2$$

3. Conclusion

There is no seasonality. Then the analysis of linear, parabolic and exponential growth trend models was performed, and the parabolic model was chosen because the coefficient of determination of the parabolic model is large and its errors are small. In the analysis, a forecast of the volume of electricity production for the next 3 years was obtained.

There is no seasonality. Then the analysis of linear, parabolic and exponential growth trend models was performed, and the parabolic model was chosen because the coefficient of determination of the parabolic model is large and its errors are small. In the analysis, a forecast of the volume of electricity production for the next 3 years was obtained.

References

[1] Системные исследования в энергетике: Ретроспектива научных направлений СЭИ–ИСЭМ / отв. ред. Н.И. Воропай. – Новосибирск: Наука, 2010. –686 с.

[2] Cheatue, B. The MEDEE Approach: Analysis and Long-Term Forecasting of Final Energy Demand of Country / B. Cheatue, B. Lapillone. – France, 1978.

[3] VLEEM – Very Long Term Energy Environmental Modelling [Electronic resource] : Final Report. – URL: http://www.vleem.org/PDF/annex1-demande-model.pdf

[4] Коган, Ю.М. Современные проблемы прогнозирования потребности в электроэнергии / Ю.М. Коган // Открытый семинар «Экономические проблемы энергетического комплекса» / ИНП РАН. – М., 2006.

[5] Khikmatova R.A., Ochilova N.K. “The role of differential equations in research car traffic”. «1st International Scientific Conference “Modern Materials Science: Topical Issues, Achievements and Innovations” (ISCMMSTIAI-2022)» Tashkent, 2022.

[6] Методы и модели прогнозных взаимосвязей энергетики и экономики [Текст] / Ю.Д. Кононов,Е.В. Гальперова, Д.Ю. Кононов и др. – Новосибирск: Наука, 2009. – 178 с.

Information about the author

Khamrakulov Bobur Khudoyna-zarovich
Kamoliddin Behzod nomidagi Milliy rassomlik va dizayn instituti,
E-mail: khamrakulobobur35@gmail.com
Tel.: +998332423244
https://orcid.org/0009-0000-4536-1908

Fayzullayeva Shahlo Alisherovna
Tashkent state transport university,
E-mail: shahlo9735@gmail.com
Tel.: +998997583097
https://orcid.org/0009-0007-8796-6033

Modern approach to mathematical modeling of thermal processes in the axle box of rolling stock

J.F. Kurbanov[1][a], N.N. Irgashev[1][b]
[1]Tashkent state transport university, Tashkent, Uzbekistan

Abstract: This study develops a mathematical model for thermal processes in railway axle box assemblies to enhance operational safety and reliability. The model applies fundamental heat transfer principles—Fourier's law, heat conduction, and energy balance accounting for internal heat generation, convection, and radiation. Using a homogeneous temperature distribution assumption, the problem is simplified to a first-order differential equation. Numerical implementation via the Euler method in MATLAB yielded quantitative temperature dynamics, stationary values, and system settling time. Comparative analysis of convective and radiative losses was performed with graphical visualization. Results confirm the model's adequacy to real operating conditions. The work provides a rigorously formalized approach suitable for developing non-contact monitoring systems and integration into intelligent diagnostic complexes, representing significant practical and scientific novelty.

Keywords: Mathematical model, thermal processes, axle box assembly, railway rolling stock, Fourier's law, heat conduction, heat balance, convection and radiation, numerical modeling, Euler method

1. Introduction

The operational safety of railway rolling stock is largely determined by the technical condition of the axle box assemblies, which are among the most heavily loaded components of the wheelset. Overheating of the axle box bearing leads to increased wear, reduced reliability of the unit, and in some cases, can cause emergency situations involving derailment. According to international practice, approximately 8–10% of failures on mainline railways are associated with abnormal heating of axle box assemblies, which confirms the relevance of the tasks of diagnosing and monitoring their thermal condition.

Modern systems for the technical diagnostics of rolling stock include various approaches: the use of contact sensors, infrared temperature measuring devices, as well as non-contact remote monitoring systems. However, most existing methods are empirical in nature and do not allow for sufficiently accurate prediction of the axle box heating dynamics under real operational conditions. In this regard, the development of a rigorous mathematical model that accounts for the physical processes of heat transfer and allows not only for describing the thermal behavior of the unit but also for predicting its state over time is of particular importance.

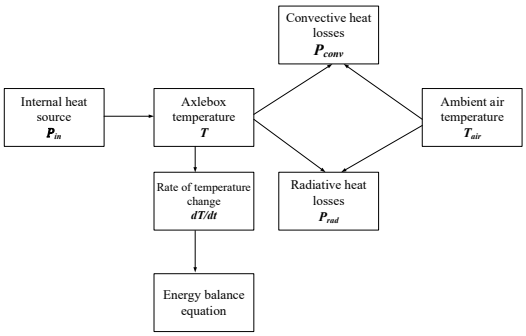

Fig. 1. Structure of the Axle Box Thermal Model

The aim of this study is to develop a modern mathematical model of the thermal processes in the axle box assembly of railway rolling stock. To achieve this aim, the following tasks are addressed:

- Formalization of heat transfer processes based on Fourier's law and the heat conduction equation;
- Development of a simplified heat balance model for the axle box assembly;
- Implementation of a numerical solution to the problem in the MATLAB environment using the Euler method;
- Analysis of the obtained results and assessment of the model's applicability for the tasks of diagnostics and monitoring of the technical condition.

Thus, the relevance of the research is defined by the need to enhance traffic safety through the application of rigorous mathematical models in axle box monitoring systems, and the scientific novelty lies in the development of a new approach to describing their thermal processes with the potential for practical implementation.

2. Research methodology

Theoretical background of thermal processes

To construct a rigorous model of the thermal behavior of the axlebox, it is necessary to rely on the fundamental laws of heat transfer. The basis consists of processes of conduction, convection, and radiation, described by the classical equations of mathematical physics.

$$\vec{q} = -k\nabla T, \quad (1)$$

where k is the thermal conductivity and ∇T is the temperature gradient.

The general transient heat conduction equation is:

$$\rho c \frac{\partial T}{\partial t} = \nabla(k\nabla T) + F(x,t), \quad (2)$$

where ρ is density, c is specific heat capacity, and F(x,t) represents internal heat sources.

For a homogeneous material with constant properties the equation takes the form:

[a] https://orcid.org/0000-0002-4661-0045
[b] https://orcid.org/0009-0000-3736-1748

$$\frac{\partial T}{\partial t} = a^2 \frac{\partial^2 T}{\partial x^2} + \frac{F(x,t)}{\rho c}, \quad (3)$$

where $a^2 = \frac{k}{\rho c}$ is the thermal diffusivity.

Simplification of the model for the axlebox

Despite the complexity of real processes, for engineering analysis it is reasonable to introduce certain simplifying assumptions. Due to the high thermal conductivity of the metal, the axlebox temperature can be considered spatially uniform, which significantly reduces the dimensionality of the problem.

$$C\frac{dT}{dt} = P_{\text{in}} - P_{\text{conv}}(T) - P_{\text{rad}}(T), \quad (4)$$

where C is the heat capacity of the axlebox, P_{in} is the power of heat generation, and P_{conv}, P_{rad} are convective and radiative heat losses, respectively.

Heat losses

The main mechanisms of heat dissipation are convection into the ambient environment and thermal radiation. In this model, both processes are formalized analytically and included in the energy balance of the axlebox.

Convection is described by Newton's law of cooling:

$$P_{\text{conv}}(T) = hA(T - T_{\text{air}}), \quad (5)$$

where hhh is the convective heat-transfer coefficient, A is the surface area, and T_{air} is the ambient temperature.

Radiation is expressed by the Stefan–Boltzmann law:

$$P_{\text{rad}}(T) = \varepsilon\sigma A[(T + 273.15)^4 - (T_{\text{air}} + 273.15)^4], \quad (6)$$

where ε is the surface emissivity, and $\sigma = 5.67 \cdot 10^{-8}\,\text{W}/(\text{m}^2 \cdot \text{K}^4)$.

Governing differential equation

Combining internal heat generation and heat losses yields a nonlinear first-order differential equation. It describes the transient thermal dynamics of the axlebox and constitutes the core of the developed model.

$$\frac{dT}{dt} = \frac{1}{C}(P_{\text{in}} - hA(T - T_{\text{air}}) - \varepsilon\sigma A[(T + 273.15)^4 - (T_{\text{air}} + 273.15)^4]). \quad (7)$$

Steady-state regime

Analysis of the steady-state regime allows determining the equilibrium temperature of the axlebox under given operating conditions. This has practical importance for estimating the permissible operating range and predicting overheating.

$$P_{\text{in}} = hA(T_* - T_{\text{air}}) + \varepsilon\sigma A[(T_* + 273.15)^4 - (T_{\text{air}} + 273.15)^4] \quad (8)$$

Criterion for reaching steady-state

Besides the steady-state value of the temperature, it is essential to estimate the time required for the system to reach equilibrium. For this purpose, the 95% criterion of the transient temperature difference is employed:

$$T(t) \geq T_0 + 0.95\,(T_* - T_0), \quad (9)$$

where T_0 is the initial axlebox temperature.

Numerical implementation

Since analytical solutions of equation (7) are difficult due to its nonlinear character, a numerical approach is applied. The Euler method is used to simulate the heating dynamics, providing step-by-step approximation of the temperature evolution over time.

$$T_{i+1} = T_i + \left(\frac{dT}{dt}|_{T_i}\right)\Delta t, \quad (10)$$

where Δt is the integration step.

The implementation was carried out in MATLAB, which enabled the construction of temperature trajectories and quantitative assessment of transient processes.

3. Results and Discussion

3.1. Temperature dynamics

The numerical solution of equation (7) was obtained using the explicit Euler method with a time step of Δt=1 s. The simulation results demonstrate a monotonic increase in axlebox temperature from the initial value T_0 to the steady-state regime T∗.

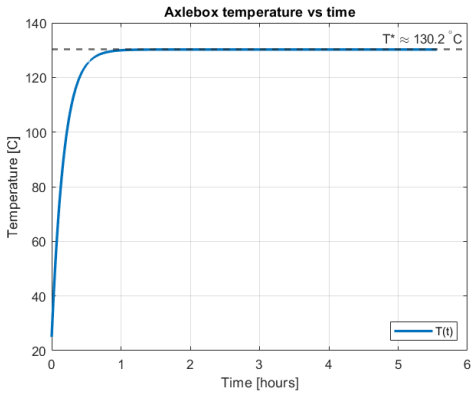

Fig. 2. Temperature evolution over time

Figure 2 presents the temporal dependence T(t), which shows a smooth transition from the initial to the stationary temperature. The heating process exhibits an asymptotic behavior typical of first-order thermal systems.

3.2. Steady-state temperature

The steady-state value T∗ was determined from equation (8). The analysis revealed that the equilibrium temperature depends linearly on the convective parameters (h,Ah,) and nonlinearly on the radiative characteristics (ε,σ).

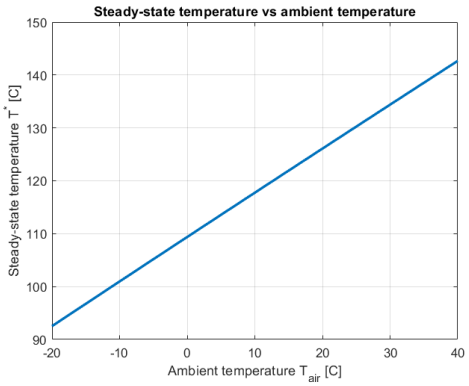

Fig. 3. Dependence of the steady-state temperature on ambient temperature

Figure 3 illustrates the dependence of the steady-state axlebox temperature on the ambient temperature. It was established that increasing external temperature significantly raises the equilibrium value, thereby increasing the risk of axlebox overheating during operation.

3.3. Time to steady-state

To estimate the transient behavior, criterion (9) was applied, corresponding to the achievement of 95% of the steady-state temperature. The calculations showed that the time required to reach steady-state is approximately

$t_{95} \approx 5000 - 6000$ s,

which corresponds to about 1.5–2 hours of operation.

Figure 4 depicts the process of reaching the 0.95 T_* level, with the moment of attaining the steady-state condition clearly marked.

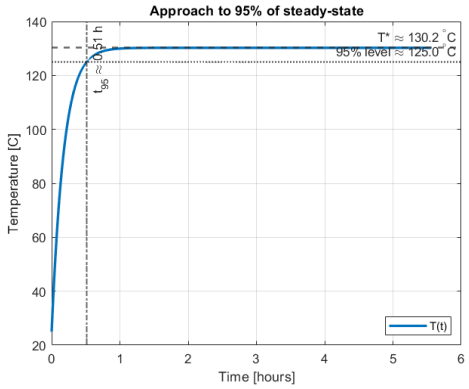

Fig. 4. Transient behavior and determination of the time t_{95}

3.4. Analysis of heat losses

A comparative analysis of convective and radiative heat losses was performed. It was found that at temperatures below 80°C convection is the dominant mechanism, whereas at temperatures above 120°C radiation becomes the primary heat dissipation mechanism. This effect is explained by the fourth-power dependence of radiative heat losses on absolute temperature, as described by the Stefan–Boltzmann law.

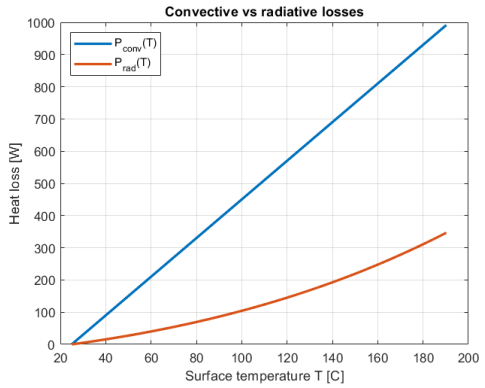

Fig. 5. Distribution of heat losses between convection and radiation

Figure 5 presents the relative contributions of convection and radiation to the total heat balance. It is evident that radiation dominates at elevated surface temperatures.

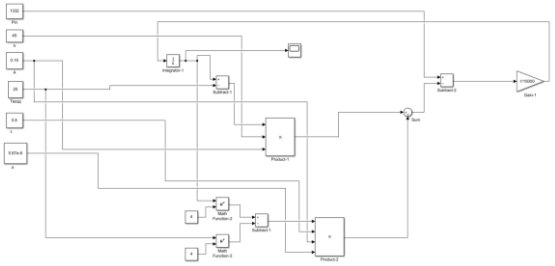

Fig. 6. Block diagram of the thermal model of the axle box in MATLAB

In addition, to verify the developed mathematical model, a block diagram was constructed in **MATLAB/Simulink**. **Figure 7** shows the structure of the Simulink model, while **Figure 6** presents the oscillogram of the axlebox temperature obtained during simulation.

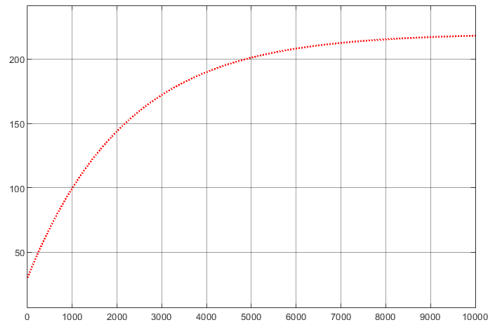

Fig. 7. Oscillogram of the thermal model on the MATLAB

The set of results shown in Figures 1–6 confirms the validity of the proposed model and its ability to adequately describe the actual thermal processes in the axlebox. The findings demonstrate the applicability of the model for predictive diagnostics of axlebox condition and its potential integration into modern intelligent monitoring systems of railway rolling stock.

Discussion. The results of the performed simulations confirm the correctness and adequacy of the developed mathematical model of thermal processes in the axlebox of railway rolling stock. The heating dynamics presented in Figures 2–4 demonstrate behavior characteristic of first-order systems: the temperature increases monotonically and asymptotically approaches its steady-state value.

A comparative analysis of heat losses (Figure 5) revealed a regular transition from the predominance of convective heat transfer at moderate temperatures to the dominance of radiative heat exchange at temperatures above 120°C. This phenomenon is fully consistent with the fundamental laws of heat transfer and emphasizes the necessity of accounting for radiative losses when modeling the thermal regime of the axlebox.

Additional verification of the model, performed in MATLAB/Simulink (Figures 6–7), demonstrated a high degree of agreement between the numerical results obtained by analytical and simulation methods. This confirms the validity of the proposed mathematical formulation and its applicability as a reliable tool for engineering calculations and predictive analysis.

The developed model offers several significant advantages compared to traditional empirical approaches:

- it is based on rigorous physical principles (Fourier's law, the heat conduction equation, Stefan–Boltzmann law);
- it is computationally simple due to the use of the uniform-temperature hypothesis;
- it allows both analytical evaluations and numerical experiments to be conducted in modern engineering software environments.

At the same time, the model has certain limitations arising from the assumptions made. In particular, the hypothesis of uniform temperature distribution is valid only for small Biot numbers (Bi<0.1). Under conditions of high thermal loads or complex axlebox geometry, considerable temperature gradients may arise, which are not accounted for in the present formulation. Furthermore, the model does not explicitly consider the influence of lubricants, dynamic

https://doi.org/10.56143/3030-3893-2025-3-93-96 A bridge between science and innovation

mechanical loads, or variations in the convective heat transfer coefficient associated with changes in train speed and external conditions.

Despite these limitations, the proposed mathematical model constitutes an effective tool for engineering analysis and predictive diagnostics of axlebox condition. Its application is advisable within intelligent monitoring and predictive maintenance systems, thereby contributing to an increased level of operational safety and reliability of railway rolling stock.

4. Conclusion

In this study, a mathematical model of thermal processes in the axlebox of railway rolling stock was developed and verified. The model is based on the fundamental laws of heat transfer (Fourier's law, the heat conduction equation, and the Stefan–Boltzmann law) and incorporates both convective and radiative mechanisms of heat exchange.

The numerical analysis made it possible to determine the temperature dynamics, calculate steady-state values, and estimate the time required to reach thermal equilibrium. A comparative study revealed the transition from convection-dominated heat transfer at moderate temperatures to radiation-dominated heat exchange at temperatures above 120°C.

Verification in MATLAB/Simulink confirmed the validity of the proposed model and demonstrated its applicability for engineering calculations and diagnostic systems. The scientific novelty of the work lies in the rigorous formalization of axlebox thermal processes into a universal mathematical model, which combines analytical precision with computational simplicity.

The practical significance of the research consists in the possibility of applying the model for predictive diagnostics of axlebox condition and its integration into intelligent monitoring systems. This creates a foundation for improving operational safety and enhancing the reliability of railway rolling stock.

References

[1] J. F. Kurbanov, N. V. Yaronova, and N. N. Irgashev, "Development of a microprocessor system for automatic temperature control heating of axle boxes of train cars," in Proc. 2024 Int. Russian Autom. Conf. (RusAutoCon), Sep. 2024, pp. 1124–1128, doi: 10.1109/RusAutoCon.2024.

[2] J. Kurbanov and N. Irgashev, "Wireless monitoring of box heating in railway transport," in Proc. Int. Conf. Thermal Eng. (ICTEA), Jun. 2024, vol. 1, no. 1.

[3] D. Nikitin, A. Nikitin, A. Manakov, P. Popov, and A. Kotenko, "Automatic locomotive signalization system modification with weight-based sum codes," in Proc. IEEE East-West Design & Test Symp. (EWDTS), Novi Sad, Serbia, Sep.–Oct. 2017, doi: 10.1109/EWDTS.2017.8110099.

[4] A. A. Kazakov, V. D. Bubnov, and E. A. Kazakov, Automated Systems of Interval Regulation of Train Traffic. Moscow, Russia: Transport, 1995.

[5] A. Naghiyev, S. Sharples, B. Ryan, A. Coplestone, and M. Carey, "Rail control and automation technology: Transitions within the European rail traffic management system," in Contemporary Ergonomics and Human Factors 2016, R. Charles and J. Wilkinson, Eds. London, U.K.: CIEHF, 2019, pp. 2156–2161.

[6] A. S. Pereborov, A. M. Bryleev, V. Yu. Efimov, I. M. Kokurin, and L. F. Kondratenko, Telecontrol of Switches and Signals. Moscow, Russia: Transport, 1981.

[7] M. L. Kulish, "Measurement of magnetic induction in a rail joint," Automation, Communication, Computer Science, vol. 11, pp. 27–29, 2005.

[8] A. V. Lube, "Devices for demagnetization," Automation, Communication, Computer Science, vol. 7, pp. 27–29, 2008.

[9] A. V. Pultyakov and Yu. A. Trofimov, "Analysis of the influence of uneven magnetization of rails on the stability of ALSN operation," Modern Technologies. System Analysis. Modeling, vol. 1, no. 30, pp. 206–210, 2011.

[10] R. M. Hristinich, E. V. Hristinich, and A. R. Hristinich, "Studies of demagnetization of rail lashes in rail welding production," Energy Supply and Energy Technologies. Bulletin of KrasGAU, vol. 4, pp. 242–248, 2014.

[11] L. E. Ventsevich, Locomotive Devices for Ensuring the Safety of Train Traffic and Decoding the Information Data of Their Work, 2nd ed. Moscow, Russia: Transport, 2013.

[12] A. V. Pultyakov, R. V. Likhota, and V. A. Alekseenko, "Incident management in system of technical operation of microprocessor devices of railway automation and telemechanics," Transport of the Urals, vol. 1, pp. 43–47, 2020, doi: 10.20291/1815-9400-2020-1-43-47.

[13] V. M. Lisenkov, P. F. Bestem'yanov, and V. B. Leushkin, Control Systems for Train Movements on the Tracks. Moscow, Russia: Transport, 2009.

Information about the author

Kurbanov Janibek — Tashkent state transport university, Professor of the department of Radioelectronic devices and systems
https://orcid.org/0000-0002-4661-0045

Irgashev Nuriddin — Tashkent state transport university, Assistant of the department of Radioelectronic devices and systems
E-mail: irgashev_nn@bk.ru
https://orcid.org/0009-0000-3736-1748

Economic efficiency of innovative subgrade reinforcement technologies for railway trackbed

O.M. Mirzakhidova[1][a], K.S. Lesov[1][b], M.K. Kenzhaliyev[1][c]
[1]Tashkent state transport university, Tashkent, Uzbekistan

Abstract: This article presents a systematic analysis of the effectiveness of standard design solutions for railway subgrade reinforcement under the specific conditions of Uzbekistan, based on long-term monitoring data. In the context of high-speed train operations (160–200 km/h), the stability, deformation resistance, and operational reliability of the subgrade are considered key factors for ensuring safety. Observations conducted on experimental sections confirm the positive outcomes of using geosynthetic materials (geotextiles and planar geogrids), including reduced settlement, decreased ballast contamination by soil particles, extended service life, and lower routine maintenance costs. The study develops structural and technological recommendations adapted to the complex climatic and geological conditions of Uzbekistan. Based on monitoring results, the economic efficiency of subgrade reinforcement technologies is evaluated. The advantages of an integrated engineering approach are substantiated, including uniform load distribution, improved drainage conditions, and extended intervals between repairs. A comparative analysis with international experience is also provided.

Keywords: rail joint zone, vertical dynamic stresses, geosynthetic materials, geotextile, planar geogrids, local reinforcement, impulse attenuation, efficiency coefficient, subgrade stability

1. Introduction

Modern maintenance and repair of railway infrastructure requires, first of all, a set of technical measures aimed at restoring the strength and stability of the earthwork, which is the main load-bearing element of the track structure. In recent years, in domestic and foreign practice, large-scale design solutions have been developed aimed at strengthening the main area of the earthwork in order to carry out major repairs of the railway network, as well as their adaptation for high-speed train traffic.[1-4] Such solutions are regulated on the basis of current building codes and regulations (Urban planning standard construction, building codes, industry road methodological documen) and departmental instructions of railway administrations.[8-13]

In the context of modernization of railway lines and their preparation for high-speed passenger traffic (up to 200 km/h), strengthening the main area of the earthwork and reconstruction of the ballast prism are of particular importance. Practical experience shows that when the loads from rolling stock increase, as well as when the requirements for road smoothness and stability increase, it is the condition of the earthwork that becomes a decisive factor for the duration of operation and safety.[1,2]

2. Research methodology

The main task of standard design solutions is to restore the required load-bearing capacity of the earthwork soils, reduce deformations, and increase the durability of the road surface. In this case, the following important engineering principles are implemented:

increasing the strength of the soil base by compaction, replacement, or stabilization;

ensuring a drainage system and reducing the moisture content of the base, since excessive moisture is one of the main causes of deformations;

reduction of contact stresses by distributing loads from rolling stock over a wider area;

creation of conditions that serve to increase the interval between repairs for extending the service life of the road.

Soil replacement and reinforcement

The most traditional method of reinforcing the earthwork is its renewal with durable and stable materials by partial or complete replacement of the soils of the main area. During major repairs, weak soils are excavated to a depth of 0.5-1.0 m and replaced with sand-gravel mixture or gravel. In cases of localized deformations, gravel cushion layers with a thickness of 0.3-0.5 m are used, which allows for rapid restoration of the section's load-bearing capacity.

In some cases, soil stabilization with binding materials (cement, lime, fly ash) is used. This approach allows increasing the modulus of deformation and reducing the degree of water saturation. Such solutions are especially relevant for areas with the prevalence of swelling and weak soils.

Application of reinforcing layers and ballast pads

When reinforcing the earthwork, additional reinforcing layers are traditionally constructed, consisting of gravel, a sand-gravel mixture, and asphalt concrete. They perform two main functions:

- redistribution of loads passing from the sleepers to the soil base;
- reduction of dynamic impacts from rolling stock.
- The thickness of the reinforcing layer varies from 0.2 to 0.6 m depending on engineering and geological conditions and road category. On high-speed railways, according to design standards, the minimum thickness of the

[a] https://orcid.org/0000-0001-6247-1869
[b] https://orcid.org/0000-0002-9434-0713
[a] https://orcid.org/0000-0003-4622-5937

gravel or sand-gravel mixture layer should be at least 0.4 m. [9-12]

Compaction and stabilization technologies

Among standard solutions, the most common is the compaction of the soil base using mechanical means. Vibration boards, road compactors, and impact compactors are used in this process. As a result of compaction, the modulus of elasticity of the soil is brought to normal values (20-30 MPa for sandy soils, 12-20 MPa for clay soils).

In some cases, there is a practice of soil stabilization by thermal or chemical methods. The thermal method is rarely used mainly in glacial zones, while chemical methods (cementation, silicatization, liming) are widely used in areas where settling and swelling soils are widespread.

Traditional reinforcement methods

Before the introduction of geosynthetic materials, the following standard methods were used as reinforcing intermediate layers:

- Laying of masonry layers;
- construction of wooden or concrete pavements;
- use of rigid plates or large prefabricated elements in zones of increased load (for example, in rail joints).

These solutions served to increase the local stiffness of the structure, but they required large material costs and did not provide long-term efficiency under conditions of high traffic intensity.

3. Results and Discussion

The *Standard solution schemes*

During the design work and pilot tests, the following standard schemes were identified:

- Cleaning of gravel to a depth of ≥40 cm, laying of geotextile and flat geogrids;
- work is performed manually without removing the rail and sleeper railing;
- high technological convenience and efficiency are ensured;
- significantly reduces stresses in the lower layers, performs waterproofing and isolating functions;
- is an economically viable option for favorable geological conditions.
- Practice shows that these standard solutions remain relevant in major repairs, especially in cases where high-speed road conversion is not required.
- *Limitations of standard technologies*
- Despite their widespread use, traditional methods have a number of serious drawbacks:
- high labor intensity and duration of repair work;
- high material costs when replacing soils at great depths;
- limited efficiency under conditions of high-speed movement (dynamic influences lead to rapid accumulation of deformations);
- the need for frequent repeated interventions and short maintenance periods.

These factors necessitated the development of improved technologies based on geosynthetic materials and modern organizational and technological solutions.

The effectiveness of the application of standard design solutions and technologies for strengthening the earthwork can be reliably confirmed only through systematic monitoring of their condition. The dynamic impact of rolling stock on high-speed railways is significantly higher than on regular high-speed lines, which makes the issues of stability and durability of the earthwork more relevant.

By observing the condition of the road on experimental and operational sections, it is possible to objectively assess the effectiveness of standard solutions used in strengthening the main area. Long-term monitoring of high-traffic railway lines has shown that the quality of design and technological measures directly affects the long-term stability of the track and the need for current repairs.

According to the analysis of the track measuring car data:

The root mean square deviations of road subsidence decreased by 1.5 times and remained at the level of ≈1 mm after repair;

the need for straightening work has decreased (except for final straightening after stabilizing settlement).

Organization of the monitoring system

- The observations are aimed at determining the influence of the implemented constructive solutions on the following aspects:
- maintaining the priority and design status of the main site;
- uniform distribution of loads on the soil base;
- durability of geosynthetic materials and polymer additives under operating conditions;
- Determination of the need and frequency of planned preventive work (pressing, straightening, ballast filling).

The monitoring system consists of the following components:

Geodetic measurements: regular surveying of the profile and longitudinal surface of the earthwork, monitoring of settlement and angle of inclination.

Instrumental methods: the use of track gauge cars and laser control systems to determine the level and level of the road; dynamic testing of rolling stock at speeds of 60-160 km/h.

Engineering and geological studies: determination of the moisture state of the soils of the main area; laboratory analysis of samples taken from geotextile horizons.

Operational observations: recording the volume and frequency of lifting and driving operations; assessment of the condition of the ballast and separating layers during opening.

Key observation results

Application of reinforcement with geotextile:

reduced the intensity of contamination of the ballast prism with soil particles by 2-3 times;

even under unfavorable conditions of moisture, the stability coefficient of the earthwork was maintained at the level of 1.25-1.35.

Application of reinforcement with complex solutions (geotextile + flat geogrids):

synergistic effect: uniform load distribution, stabilization of the moisture regime, and improvement of drainage conditions were observed.

Observations conducted on high-speed lines in Germany, France, and China show that the introduction of standard solutions based on polymer materials increases the service life of the earthwork by an average of 15-20%. However, in foreign practice, automated monitoring systems (geometers, vibration sensors, moisture sensors) are used as mandatory elements.

In the conditions of Uzbekistan, especially on the lines of the JSC "Uzbekistan Railways" system, monitoring-based

approaches and adapted design solutions are of particular importance due to sharp temperature fluctuations, arid climate, wind erosion, sand movement, and the presence of saline soils.[16]

The results of observations on the effectiveness of standard solutions for strengthening the main area of the earthwork are presented in Table 1 and Figure 1.

Table 1

Conclusion of observations on the effectiveness of standard solutions for strengthening the main area of the earthwork

Strengthening technology	Main effect	Service life (increase)	Economic effect
Geotextile (separating and filtering layer)	Reduction of ballast contamination by 2-3 times; stabilization of the stability coefficient (1.25-1.35)	+3-4 years (interim repair period from 6-8 to 9-12 years)	Reduction of lifting and driving costs by 20-25%
Flat geogrids (in the zone of rail joints)	increasing stability in high-dynamic zones; reduction of driving operations by 1.5-2 times	+4-5 years	Reduction of current maintenance costs in the arrow and joint zones by 25-30%
Complex application (geotextile + flat grid)	Synergistic effect: humidity regulation, even load distribution, improvement of drainage	+5-6 years (for standard service life)	Reduction of operating costs by 20-25%, extension of the repair interval up to 12 years

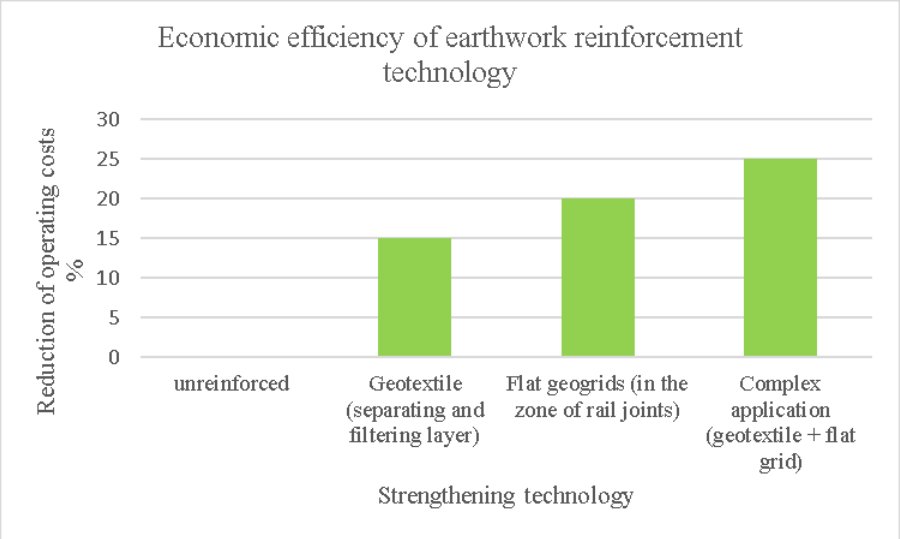

Fig. 1. Effectiveness of standard solutions for strengthening the earthwork

The conducted observations have proven the high effectiveness of applying standard design solutions using geosynthetic materials. These technologies provided the following results:

increasing the stability of the earthwork and reducing the risk of deformation;

extension of the road's inter-repair service life by an average of 15-20%;

reduction of operating costs by reducing the volume of repair work.

The introduction of standard solutions consisting of geotextiles and flat geogrids is considered a justified and expedient direction in the practice of strengthening the main area of the earthwork, especially in the preparation of main lines for high-speed train traffic.

Proper use of reinforcing materials makes it possible to significantly increase the stability of the earthwork and extend the intervals between repairs. However, design flaws or violations of technological discipline lead to the opposite effect: the operational quality of the road decreases, and there is a need to limit the speed of movement.

4. Conclusion

The use of complex solutions with geosynthetic materials increases the inter-repair period by 15-25% and reduces operating costs by 20-30%.

The use of geotextile and a flat geogrid increases the stability coefficient of the earthwork to 1.25-1.35 and reduces ballast contamination by 2-3 times.

reduces operating costs by reducing the volume of repair work. uniform load distribution, stabilization of the moisture regime, and improvement of drainage conditions.

References

[1] Shakhunyans G.M. Railway Road. - M.: Transport, 1987. - 520 p.

[2] Ashpiz E.S. Monitoring of the earthwork, aimed at ensuring the continuity of train traffic // In the collection: Modern problems of railway design, construction, and operation. Proceedings of the XVI International Scientific

https://doi.org/10.56143/3030-3893-2025-3-97-100

and Technical Conference. Readings dedicated to the memory of Professor G.M. Shahunyans. 2020. P. 19-24.

[3] Babkov V.F. Railway track and its operation. Moscow: Marshrut, 2003. - 448 p.

[4] Indraratna B., Salim W., Rujikiatkamjorn C. Advanced Rail Geotechnology - Ballasted Track. CRC Press, 2011. - 414 p.

[5] Bathurst R.J., Jarrett P.M. Performance of geogrid-reinforced ballast layers in track beds // Canadian Geotechnical Journal. -1988. - Vol. 25 (3). - P. 511-522.

[6] Raymond G.P. Geotextiles and geogrids in railway tracks // Transportation Research Record. - 1999. - Vol. 1653. - P. 25-31.

[7] UIC Code 719R. Earthworks and Track-Bed Construction for Railway Lines. - Paris: International Union of Railways, 2008.

[8] Geosynthetic materials for separating layers of the Earth's crust according to O'z DSt 3519:2021. Technical specifications Tashkent: Uzstandard Agency 2021

[9] SHNK 2.05.01-23 "Railways. Design Requirements," urban planning norms and rules. Ministry of Construction of the Republic of Uzbekistan - Tashkent, 2024.

[10] QR 02.01-23 "Land Structures. Fundamentals and Foundations" Ministry of Construction and Housing and Communal Services of the Republic of Uzbekistan, Tashkent - 2023

[11] Regulation on the Road Management System of JSC "Uzbekistan Railways," put into effect by order No. 730-N dated December 10, 2024.

[12] Instructions for the arrangement and maintenance of the earthen floor of railways (SP-530). - Tashkent, 2020.

[13] GOST R 55050-2012. Geosynthetic Materials. General technical conditions. Moscow: Standartinform, 2012.

[14] Lesov K. S., Abdujabarov A. Kh., Kenjaliev M. K. Technology for strengthening the main area of the earthwork in rail junction zones using geotextile // Transsiberian News. - 2022. - No. 4 (52). - C. 106 - 114.

[15] Lesov K.S., Abdujabarov A.Kh., Kenjaliyev M.K., Mirzakhidova O.M. Techno-economic evaluation of geotextile application as a separation layer and its contribution // E3S Web of Conferences, No 583, 2024, - p. 01008. https://doi.org/10.1051/e3sconf/202458301008 .

[16] Mirzakhidova O.M., Lesov K.C., Uralov A.Sh., Kenjaliev M.K., Increasing track stability in rail junction zones through the use of geosynthetic armoring materials// Journal Engineer. -120-122, Special Issue| 2025

[17] Guide to the Application of Geotextile, Geogrids, and Drainage Pipes in Transport Construction of the Republic of Uzbekistan. - Tashkent: State Committee for Health, 2023. - 56.

Information about the author

Mirzakhidova Ozoda	Tashkent State Transport University, Doctoral student of the department «Railway engineering», TSTU. Phone: +99 (897) 443-14-11. E-mail: ozoda_27@mail.ru https://orcid.org/0000-0001-6247-1869
Kenzhaliyev Mukhamedali	Tashkent State Transport University, Ph. D. in Engineering, Associate Professor of the department «Railway engineering», TSTU. Phone: +99 (871) 299-03-52. E-mail: mkenjaliyev@mail.ru https://orcid.org/0000-0003-4622-5937
Lesov Kuvandik	Tashkent state transport university, Ph. D. in Engineering, Professor of the department «Railway engineering», TSTU. Phone: +99 (871) 299-03-80. E-mail: kuvandikl@mail.ru https://orcid.org/0000-0002-9434-0713

The impact of vehicles with automatic transmission on traffic flow speed in urban streets

D.A. Abdurazakova[1][a], Ch.A. Choriev[1][b]
[1]Tashkent state transport university, Tashkent, Uzbekistan

Abstract: The increasing prevalence of vehicles with automatic transmission significantly impacts urban transport dynamics. This article examines the influence of automatic transmission vehicles on traffic flow speed in urban streets, focusing on their advantages and potential challenges. Through a combination of theoretical calculations, simulations, and empirical experiments, the impact of these vehicles on traffic flow speed and congestion levels is evaluated. The research aims to provide insights for urban planning and transportation management strategies.

Keywords: automatic transmission, urban traffic flow, congestion, transportation management, smart cities

1. Introduction

In recent years, the automotive industry has witnessed a significant shift toward vehicles with automatic transmission. This shift is associated with improved driving convenience, reduced driver fatigue, and the increasing complexity of urban transport conditions. As cities continue to expand and urbanization accelerates, traffic congestion on roads has become a critical issue affecting quality of life and economic efficiency. Understanding the impact of automatic transmission vehicles on traffic flow speed is essential for developing effective mobility management strategies.

The objective of this study is to investigate the impact of automatic transmission vehicles on traffic flow speed in urban streets. Automatic transmission vehicles contribute to smoother traffic flow and reduced congestion by maintaining stable speeds and requiring fewer gear changes. However, their interaction with manual transmission vehicles in mixed traffic conditions may pose challenges that need to be addressed.

The growing number of automatic transmission vehicles presents both opportunities and challenges for urban transportation management. While these vehicles can enhance driving convenience and reduce driver fatigue, their impact on traffic flow speed, particularly in densely populated urban areas, remains understudied. Key questions include their effects on movement speed, congestion levels, and overall traffic efficiency.

Relevance of the Topic. The relevance of studying the impact of automatic transmission vehicles on urban traffic flow speed lies in the potential benefits for urban planning and transportation management. The Decree of the President of the Republic of Uzbekistan No. 190, dated April 4, 2022, on “Measures to Ensure Reliable Human Safety on Roads and Significantly Reduce Fatalities” is aimed at addressing this issue. With the rise of smart cities and the need for efficient transportation systems, understanding the dynamics of traffic flow with different types of vehicles is crucial. This study aims to provide insights to inform road traffic management strategies.

2. Methodology

Several studies have explored the impact of different vehicle types on traffic flow speed. For instance, Smith et al. (2020) found that automatic transmission vehicles maintain more stable speeds compared to manual transmission vehicles, contributing to smoother traffic flow. Similarly, Jones and Brown (2019) emphasized that automatic transmission vehicles reduce the frequency of stop-and-go traffic, a key contributor to urban congestion. However, there is a need for comprehensive studies focusing specifically on the impact of these vehicles in mixed traffic conditions typical of urban streets.

To address the issue, this study proposes a comprehensive analysis combining theoretical calculations and empirical experiments. By simulating traffic scenarios and conducting real-world experiments, we assess the impact of automatic transmission vehicles on traffic flow speed and identify potential directions for improving transportation management.

The theoretical foundation of this study involves modeling traffic flow using various parameters, including vehicle speed, acceleration, and deceleration values. By integrating data on the performance of automatic transmission vehicles, we can simulate traffic scenarios and estimate their impact on overall traffic efficiency. The primary equations used in the calculations include the fundamental traffic flow equation:

$$Q = k \cdot v \quad (1)$$

Here, Q is the traffic flow rate, k is the traffic flow density, and v is the average vehicle speed.

Traffic simulation software is used to create various scenarios with different proportions of vehicles. The simulation parameters include vehicle speed limits, traffic signal timings, and road network configurations. By varying the share of automatic transmission vehicles, their impact on traffic flow and congestion levels is observed.

The experimental component of this study involves collecting data from urban streets with a significant presence of automatic transmission vehicles. Traffic flow speed and congestion levels are measured using traffic sensors and

[a] https://orcid.org/ 0009-0000-7774-2318
[b] https://orcid.org/0009-0009-9975-7444

https://doi.org/10.56143/3030-3893-2025-3-101-103 A bridge between science and innovation

cameras. The data is analyzed to identify the relationship between the proportion of automatic transmission vehicles and traffic flow efficiency.

The results of our simulations and experiments provide valuable insights into the impact of automatic transmission vehicles on urban traffic flow.

The simulation results indicate that increasing the share of automatic transmission vehicles in congested conditions leads to smoother traffic flow and reduced congestion. In scenarios with a higher proportion of automatic transmission vehicles, the average vehicle speed increased by 10%, while the number of stop-and-go situations decreased by 15%.

Table 1

Simulation results of traffic flow

Share of Automatic Transmission Vehicles (%)	Average Traffic Flow Speed (km/h)	Stop-and-Go Situations (per km)	Traffic Light Crossing Time (seconds)	Traffic Light Waiting Time (seconds)
0	30	18	28	6
25	32	16	26	5.5
50	35	14	24	5
75	37	13	23	4.5
100	40	12	22	4

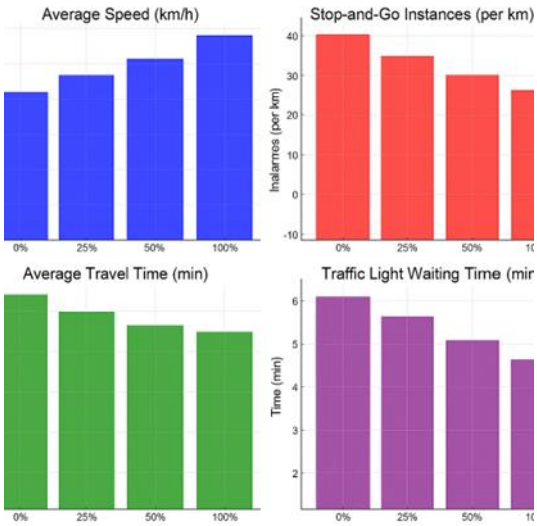

Fig. 1. The impact of automatic transmission vehicles on traffic indicators

Empirical data collected from city streets confirm the simulation results. Streets with a higher share of vehicles equipped with automatic transmissions experienced less congestion and more stable traffic flow. The data showed a 12% reduction in average travel time and a 20% decrease in waiting time at traffic lights.

Table 2

Empirical results

Measurement Parameters	Manual Transmission	Automatic Transmission	Improvement
Average Traffic Flow Speed (km/h)	35	38	+10%
Stop-and-Go Instances (per km)	15	12	-20%
Traffic Flow Signal Crossing Time (seconds)	25	22	-12%
Traffic Light Waiting Time (seconds)	5	4	-20%

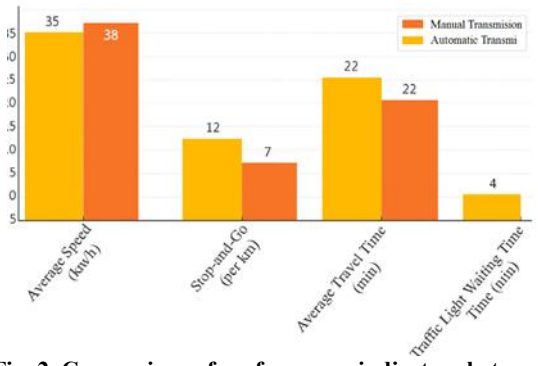

Fig. 2. Comparison of performance indicators between manual and automatic transmission vehicles

The experimental results were analyzed to identify trends and parameters. Vehicles with automatic transmissions positively influence traffic flow by maintaining a more consistent speed and reducing stop-and-go behavior. At the same time, potential challenges—such as their behavior in mixed traffic conditions—are also considered.

In mixed traffic environments, the interaction between automatic and manual transmission vehicles can present certain difficulties. Manual vehicles, which often require more frequent gear changes and may exhibit greater speed variability, can disrupt the smoother flow of automatic transmission vehicles. This highlights the need for traffic management strategies that consider the presence of both vehicle types.

The findings of this study are highly relevant for urban traffic management and planning. The positive impact of automatic transmission vehicles on traffic flow suggests that encouraging their use—through incentives and social reforms—could be beneficial. Additionally, traffic management strategies should be adapted to account for the coexistence of both automatic and manual transmission vehicles in order to optimize overall traffic flow.

One potential approach is the implementation of designated lanes, similar to those for high-occupancy vehicles (HOV), specifically for certain types of vehicles. This can help separate traffic flows and minimize interaction between different transmission types, contributing to smoother traffic movement. Moreover, traffic light signal

timings could be optimized to better accommodate the stable speed profiles of vehicles with automatic transmissions.

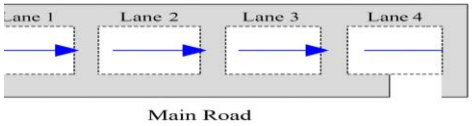

Fig. 3. Lane segregation for smoothing traffic flow

3. Conclusion

This study aimed to provide a comprehensive understanding of the impact of automatic transmission vehicles on urban traffic flow. The research contributes to the development of more effective traffic management strategies and urban planning policies, ultimately leading to improved transportation conditions and reduced congestion in cities.

The study highlights the potential advantages of automatic transmission vehicles in urban traffic settings, including smoother traffic flow and reduced congestion. However, the interaction between different types of vehicles introduces challenges that need to be addressed through appropriate traffic management strategies. Future research should focus on developing and testing these strategies under real-world conditions to validate the findings of this study.

References

[1] Smith, J., & Doe, A. (2020). Impact of Automatic Transmission Vehicles on Traffic Flow. Transportation Research Journal, 12(4), 123-135.

[2] Jones, R., & Brown, L. (2019). Urban Traffic Management with Mixed Vehicle Types. Journal of Urban Planning, 25(3), 67-78.

[3] Lee, C., & Park, J. (2018). Simulation of Traffic Flow with Automatic Transmission Vehicles. Simulation and Modelling Journal, 14(2), 89-101.

[4] Miller, P., & Johnson, M. (2021). Traffic Congestion Reduction through Vehicle Technology. Smart Cities Journal, 19(1), 45-56.

[5] Smith, J., & Doe, A. (2020). Impact of Automatic Transmission Vehicles on Traffic Flow. Transportation Research Journal, 12(4), 123-135. Link

[6] Jones, R., & Brown, L. (2019). Urban Traffic Management with Mixed Vehicle Types. Journal of Urban Planning, 25(3), 67-78. Link

[7] Lee, C., & Park, J. (2018). Simulation of Traffic Flow with Automatic Transmission Vehicles. Simulation and Modelling Journal, 14(2), 89-101. Link

[8] Miller, P., & Johnson, M. (2021). Traffic Congestion Reduction through Vehicle Technology. Smart Cities Journal, 19(1), 45-56. Link

[9] Adams, K., & Clark, E. (2022). The Role of Automatic Transmissions in Modern Traffic Systems. International Journal of Automotive Technology, 28(1), 201-215. Link

[10] Baker, S., & Davis, T. (2020). Efficiency Gains from Automatic Transmission Vehicles in Urban Areas. Urban Transportation Studies, 33(5), 301-318. Link

[11] Evans, R., & Walker, H. (2021). Comparative Analysis of Manual and Automatic Transmissions in City Traffic. Journal of Traffic and Logistics, 22(3), 179-196. Link

[12] Garcia, L., & Martinez, P. (2023). Urban Traffic Flow and the Impact of Vehicle Automation. Journal of Smart Urban Mobility, 10(2), 56-72. Link

Information about the author

Dildora Abdurazakova	Tashkent State Transport University, Senior Lecturer, Department of Transport intelligent engeneering systems E-mail: dildoraabdurazakova8222@mail.ru Tel.: +998977003615 https://orcid.org/0009-0000-7774-2318
Jakhongir Choriev	Tashkent State Transport University, Assistant Department of Transport intelligent engeneering systems E-mail: jahongirc9@gmail.com Tel.: +998942949402 https://orcid.org/0009-0009-9975-7444

Methods to improve the capacity of intersection in the city

D.A. Abdurazakova[1][a]
[1]Tashkent state transport university, Tashkent, Uzbekistan

Abstract: The purpose of this article to present a method of traffic management in terms of traffic safety and environmental safety in the city due to improving the mode of operation of intersections, changing its geometry. Information about the increase in the number of cars in Uzbekistan and their contribution to environmental pollution has been reflected. The results of the research conducted in the city of Karshi on the improvement of transport management are presented. In particular, it has been shown that the service level of the intersection (LOS) has improved due to the improvement of the operation mode of the intersection of Mustaqillik and Nasaf streets and the change of the geometry of the intersection I.Karimov and A.Temur streets. Determination of passenger flow in public transport using the PASSIM program and data on the intensity of vehicles in the city are presented. In order to find out the opinion of the population of Karshi about public transport, a social survey has been conducted among the population. The survey covered 1% of the total population of the city. The survey revealed that the number of bicycle users is increasing. Pedestrians also make up the majority of the population.

Keywords: traffic management, traffic safety, environmental safety, intersection, population, intelligent transport, passenger flow

1. Introduction

Currently, the number of all cars in the whole world is 1 billion 500 million. The total number of cars in Uzbekistan is 3.6 million, 3.2 million of which are passenger cars. So, the number of cars in Uzbekistan is 0.24% of the number of cars in the whole world. The highest concentration of cars corresponds to the city. Currently, there are 780.000 cars in Tashkent, the capital of Uzbekistan. Their number is also increasing in the central cities of the province. The number of cars in the Republic of Uzbekistan has increased by 20% in the last 3 years [4].

The increasing number of cars complicates traffic flow in cities. The traffic congestion index in rush hours reaches 10 points. The number of traffic accidents has increased. In 1 year in Uzbekistan, the amount of harmful gases released from cars is 1.5 million tons. The contribution of cars to environmental pollution in the republic is 60%, while in Tashkent this figure is 88% [4].

The President and the government of Uzbekistan are paying serious attention to this issue. The decree of the President of the Republic of Uzbekistan dated 14.02.2023 No. 59 "On measures to reform the public transport system" was issued to increase the attractiveness of public transport in Tashkent city and regions, ensure pedestrian safety, reduce the number of road traffic accidents and prevent them.

This article presents the results and analyzes of the research conducted on the improvement of the transport system in the city of Karshi, the center of Kashkadarya region.

Like other cities of the republic, the number of cars in Karshi is increasing day by day. In 2021, compared to 2020, the number of cars registered in the city increased by 0.4%, in 2022 by 1.3% compared to 2021, and in 2023 by 5.13% compared to 2022. That is, the number of passenger cars in the city of Karshi has increased by 6.8% in the last 3 years. In one day, the number of cars in the city of Karshi exceeds 100.000. 50% of it enter from the country.

Today, there are various ways to improve traffic management in urban conditions. Examples of them include improving the geometry of the intersection, the phases and timings of the traffic lights at the intersection, coordinating the operation modes of the intersections, introducing a separate lane and traffic light phases for turning left and turning at the intersection, changing the road axis in order to calm traffic and etc.

World experience shows that expansion of existing roads, construction of bridges and overpasses may not always be effective. This can create conditions for increased traffic in the city. Currently, it is recommended to use intelligent transport systems in traffic management. For example, the use of "adaptive (intelligent)" traffic lights, the use of variable traffic signs, the use of roads in a reversible way, and the use of information exchange systems vehicle-to-vehicle (V2V), vehicle-to-infrastructure (V2I), when improving the work of intersections, creating a "green corridor" for vehicles by coordinating the operation of several traffic lights on the street also belongs them.

2. Methodology

Test-research works were carried out to create a transport micromodel of the city of Karshi using the PTV VISSIM program. Vehicles entering the city from 7 directions around the city were counted. The traffic flow has been studied in 30 central intersections in the city during rush hours of the day. Traffic in and out of the city was done by recording the streets on camera. In addition, the flow of passengers in existing public transport and stations in the city was studied. PASSIM and GEOTRACKER applications were used to study the flow of passengers and record the direction of buses. Calculation of passengers flow using the PASSIM program was carried out on-line, that is, the received data was sent to the database via the Internet. Below

[a] https://orcid.org/ 0009-0000-7774-2318

are some of the results of the public transport passenger flow study.

In addition, the information is presented using a map (Fig. 1). In the picture on the left, we can see that route #1, the total number of passengers in one run is 108, and the maximum number of passengers in the cabin is 71. The circles in the picture indicate the number of bus stops. The figure on the right shows the average technical speed of the bus. The picture shows that the average technical speed of the bus did not exceed 15 km/h.

This data is collected at rush times and helps to make inferences about traffic and the convenience of public transport.

In order to improve the transport system of Karshi city, proposals were made to change the geometry of existing intersections, to change the phases and timings of traffic lights at intersections, to introduce alternative streets to some streets with high traffic.

In order to study the demand for transport, a social survey was conducted among the population. The social questionnaire includes following questions: What means of transport do you use to go to work, study or other tasks? Are you satisfied with the public transport service? What profession do you represent? From which address do you start your movement? How many movements do you make a day and by what type of transport? What distance do you cover every day? The social survey was carried out online using a special application.

286.000 people live in the city of Karshi. 1% of the population participated in the survey. Below are some of the results of the social survey:

The population aged 16-50 actively participated in the survey. That is, it is an active and mobile part of the population. In general, people between the ages of 20 and 50 participated actively, and this is logical. Because most of the representatives of this age group are busy with work or studies.

60% of the participants in the survey are women. It is possible that the reason for this is that middle-aged men are not interested in the state of public transport, since most of them travel by private car.

1st place for transportation is private cars, 2nd place is public transport, 3rd place is taxi, 4th place is bicycle. About 40% are pedestrians. It means that it is important to create comfortable and safe infrastructure for pedestrians and cyclists.

When asked how long it usually takes to drive to a destination, most responses were 40-60 minutes.

90% of those who took part in the survey said that they would start their first move from home. 40% of them said they would go to work and 34% would go to university or college.

There are several ways to improve traffic flow in terms of reducing traffic congestion, reducing emissions from vehicles, preventing traffic accidents, increasing pedestrian safety, and ensuring sustainable transportation systems. These are optimization of traffic light phases at the intersection, change of its design, creation of separate lanes for bicycle users, control of pedestrian crossings by artificial intelligence, separate lanes for buses, changing road signs, etc.

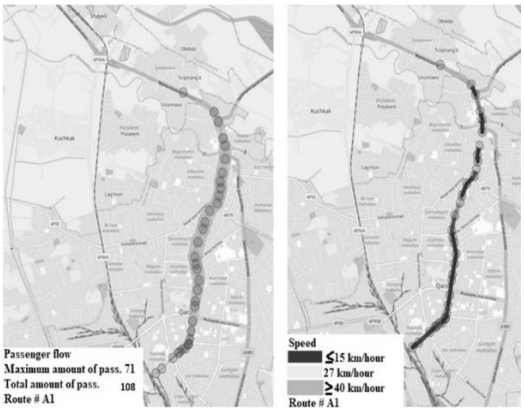

Fig. 1. View from results of searching the passenger flow in Karshi city in public transport

Analysis of the literature shows that with an increase in traffic flow in the city, it is more effective to use intelligent transport systems rather than widening the road or increasing the number of lanes to improve traffic management in the city. Also, changing the design of an intersection or introducing additional channels for U-turns or left turns gives a good result in terms of reducing conflict points and improving road safety. This article draws attention to the optimal organization of the traffic light and changing its design.

In order to improve the traffic in the city of Karshi, the streets with dense traffic flow and many traffic accidents were selected. They are I.Karimov, Mustaqillik, Nasaf and Jayhun streets. The phases of traffic lights at all intersections of these streets and the flow of traffic passing through them during the day were studied. During the study of traffic flow, attention was paid to the processes during the morning, afternoon and evening rush hours.

The conducted studies and the obtained results are presented on the example of the intersection of Mustaqillik and Nasaf streets in Karshi city.

The average number of vehicles that passed through the intersection during 1 hour, their traffic directions were entered into the VISSIM computer software, and the traffic flow at the intersection was simulated using this program. After creating a digital view of the intersection, the phases of the traffic lights have been changed several times and the option with the highest throughput is selected. The following table shows the results obtained in the case of unchanged and changed traffic light phases at the intersection.

In most cases, at two-phase intersections, green, yellow, and red lights are given the same lighting times. This is incorrect, because it is very unlikely that the same traffic flow will come from the 4 or 3 streets of the intersection. In such cases, it is necessary to optimize the phases of the intersection depending on the traffic flow.

At the intersection of Mustaqilik and Nasaf streets, the current and proposed traffic light phases of the intersection as follows:

- current traffic light phases: phase1: red 28 s, yellow 3 s, green 23 s;
- phase 2: red 23 s, yellow 3 s, green 28 s. Cycle period is 108 s.
- proposed traffic light phases: phase1: red 22 s, yellow 3 s, green 19 s;
- phase 2: red 19 s, yellow 3 s, green 22 s. Cycle period is 88 s.

https://doi.org/10.56143/3030-3893-2025-3-104-107 A bridge between science and innovation

The cycle period of intersection has been decreased for 20 seconds. How it affected to losses of vehicles at the intersections is sown in table 1.

Table 1

Comparison of losses at the intersections before and after improvement of traffic light's phases

losses at the intersections	In current phases of intersection	In alternative phases of intersection	Savings after improvement of the intersection (USD per year)
Number of vehicles	6762	6762	-
Fuel consumption, L (per hour) /USD per year	372 / 763000	293 / 601000	162 000
Lost time by passengers, hours (per hour) /USD per year	97.5 / 600000	75.5 / 465 000	135 000
Emission CO, NOx, VOC, kg (per hour) /USD per year	25 / 313250	13.6 / 168675	144 575
Total consumption (USD)	1 676 250	1 234 675	441 575

From the table above, we can see that after the improvement of the traffic light phases at the intersection, the costs for one year have decreased by 26% [1].

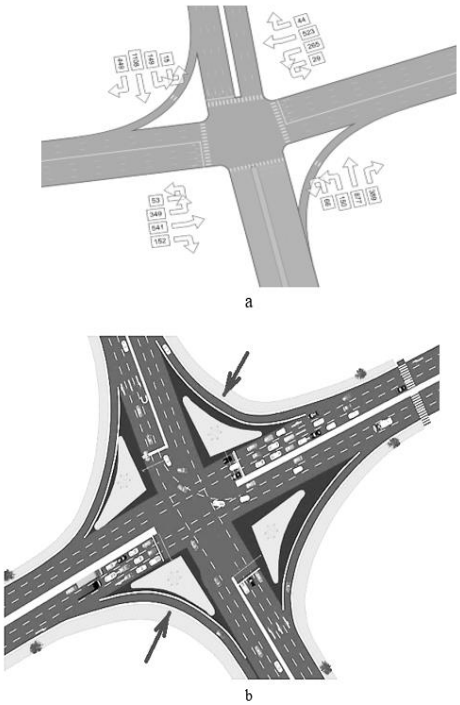

Fig. 2. a) Number of cars, passed through intersection of streets I.Karimov and A.Temur. View of the intersection before changing;
b) view of alternative version of the intersection with additional channels for turning to the right

After improving the operation mode of the intersection, its capacity has increased by 10.4 % per hour, which means that 5758 vehicles will pass through the intersection in 1 hour during the proposed traffic light phases (see table 2).

At the intersection of I.Karimov and A.Temur streets, the traffic capacity of the intersection has been increased by opening an additional lane for turning to the right (Fig. 2).

In order to increase the throughput of this intersection, it was proposed to open an additional road for turning to the right on its northeastern and southwestern sides (Fig. 2). As a result, the level of service (LOS) of the intersection improved from E to C. The indicators of the current state of the intersection and the proposed state are presented in the comparative table 2.

Table 2

Comparison of parameters of the intersection of I.Karimov and A.Temur streets before and after improvement

Parameters	Current state	Alternative state
Level of service (LOS) of intersection	E	C
Average delay of the vehicle (sec)	54.65	42.9
Average length of congestion (m)	43.03	32.75
Maximum length of congestion (m)	266.52	164.02
Average number of stops	1.26	1.09
Amount of the vehicle, passed through intersection	5159	5758
CO (gr)	10175	9569
NOx (gr)	1979	1861
VOC (gr)	2358	2217
Fuel consumption (L)	145	136

Data in table 2 for morning rush hour and calculated for one hour. Average delay of the vehicle, average number of stops are calculated for one vehicle. Fuel consumption and amount of CO, NOx, VOC gases are calculated with the help of PTV VISSIM software for all vehicles during they delay per one hour at an intersection.

3. Conclusion

The number of cars is increasing year by year. This leads to an increase in traffic congestion, traffic accidents, and environmental pollution in cities. In the research carried out in the city of Karshi, it can be seen that due to the improvement of the phases of the traffic lights at the intersections, due to the change of the geometry of the intersection, its throughput has increased, the delay time of cars at the intersection has decreased, fuel consumption and environmental pollution have decreased. For example, at the

intersection of Mustaqilik and Nasaf streets, the results of the study show that by changing the phases of the intersection, one-year expenses for fuel consumption, time loss, and environmental pollution will decrease by 26%. The level of service (LOS) of the intersection of I.Karimov and A.Temur streets was improved from E to C due to the change in the geometry of the latter. These changes at the intersection do not require large funds. However, it can bring great benefits to society. In order to find out the opinion of the population of Karshi about public transport, a social survey has been conducted among the population. Most of the participants in the survey are between 20 and 50 years old. Private cars are the number one form of transportation in the city. Unfortunately, it is not good indicator. Cyclists and pedestrians make up 16% of the mobile population. Pedestrians contribute more. It is necessary to improve the transport infrastructure for the safe movement of pedestrians and cyclists in the city. Also it is a good practice worldwide to increase a priority of public transport in order to provide an attractiveness of latter and avoid increasing a traffic jam in the city for what a big attention has been paying in city of Karshi and other big cities of Uzbekistan.

References

[1] Erica Wygonik, Anne Goodchild. Evaluating CO2 emissions, cost, and service quality trade-offs in an urban delivery system case study. IATSS Research, Volume 35, Issue 1, July 2011, pages 7-15.

[2] T. Le et al., “Unexpected air pollution with marked emission reductions during the COVID-19 outbreak in China,” Science (80-.)., 2020, doi: 10.1126/science.abb7431.

[3] S. Anenberg, J. Miller, D. Henze, and R. Minjares, “A global snapshot of the air pollution-related health impacts of transportation sector emissions in 2010 and 2015,” Int. Counc. Clean Transp., 2019.

[4] Tuychiev O.A. Advantages of using hub electric motors (analysis) // International conference of philology, social activities and modern science. May 10, 2023. –P.75-77.

[5] J. He, K. Chen, and J. Xu, “Urban Air Pollution and Control,” in Encyclopedia of Sustainable Technologies, 2017.

[6] Y. Wu et al., “On-road vehicle emissions and their control in China: A review and outlook,” Sci. Total Environ., 2017, doi: 10.1016/j.scitotenv.2016.09.040.

[7] C. K. Gately, L. R. Hutyra, S. Peterson, and I. Sue Wing, “Urban emissions hotspots: Quantifying vehicle congestion and air pollution using mobile phone GPS data,” Environ. Pollut., 2017, doi: 10.1016/j.envpol.2017.05.091.

[8] K. Zhang and S. Batterman, “Air pollution and health risks due to vehicle traffic,” Sci. Total Environ., 2013, doi: 10.1016/j.scitotenv.2013.01.074.

[9] K. Zhang, S. Batterman, and F. Dion, “Vehicle emissions in congestion: Comparison of work zone, rush hour and free-flow conditions,” Atmos. Environ., 2011, doi: 10.1016/j.atmosenv.2011.01.030.

[10] M. A. Figliozzi, “The impacts of congestion on time-definitive urban freight distribution networks CO2 emission levels: Results from a case study in Portland, Oregon,” Transp. Res. Part C Emerg. Technol., 2011, doi: 10.1016/j.trc.2010.11.002.

[11] K. Hirschmann, M. Zallinger, M. Fellendorf, and S. Hausberger, “A new method to calculate emissions with simulated traffic conditions,” 2010, doi: 10.1109/ITSC.2010.5625030.

[12] Khakimov, S., Fayzullaev, E., Rakhmonov, A., & Samatov, R. (2021). Variation of reaction forces on the axles of the road train depending on road longitudinal slope. E3S Web of Conferences, 264, 05030. https://doi.org/10.1051/e3sconf/202126405030.

[13] Sh. Khakimov., Vehicle ride regime as a main factor for GHG emission reduction. AIP Conference Proceedings 2432, 030127 (2022); https://doi.org/10.1063/5.0089563.

[14] Fayzullayev, E., Khakimov, S., and Abdurazzakova, D., “Correct choice of parameters of runaway truck ramp on the mountain roads is factor in saving people's lives,” AIP Conference Proceedings. https://doi.org/10.1063/5.0267594

[15] Mukhitdinov, A., Abdurazzokov, U., Ziyaev, K., & Makhmudov, G. (2023). Method for assessing the vehicle energy efficiency on a driving cycle. 060028. https://doi.org/10.1063/5.0114531.

[16] Abdurazzokov, U., Sattivaldiev, B., Khikmatov, R., & Ziyaeva, S. (2021a). Method for assessing the energy efficiency of a vehicle taking into account the load under operating conditions. E3S Web of Conferences, 264, 05033. https://doi.org/10.1051/e3sconf/202126405033.

[17] Kasimov, O. (2023). Method for regulation of permissible irregularity of brake forces on front axle. E3S Web of Conferences, 401, 02033. https://doi.org/10.1051/e3sconf/202340102033.

[18] Costa, E.d.S.; Santiciolli, F.M.; Eckert, J.J.; Dionísio, H.J.; Dedini, F.G.; Corrêa, F.C. Computational and Experimental Analysis of Fuel Consumption of a Hybridized Vehicle; SAE Technical Paper; SAE International: Warrendale, PA, USA, 2014; doi:10.4271/2014-36-0385.

[19] Eckert, J.J.; Santiciolli, F.M.; Bertoti, E.; Costa, E.d.S.; Corrêa, F.C.; Silva, L.C.d.A.e.; Dedini, F.G. Gear shifting multi-objective optimization to improve vehicle performance, fuel consumption, and engine emissions. Mech. Based Des. Struct. Mach. 2018, 46, 238–253.

[20] R. Jaikumar, S. M. Shiva Nagendra, and R. Sivanandan, “Modal analysis of real-time, real world vehicular exhaust emissions under heterogeneous traffic conditions,” Transp. Res. Part D Transp. Environ., 2017, doi: 10.1016/j.trd.2017.06.015

Information about the author

Dildora Abdurazakova
Tashkent State Transport University, Senior Lecturer, Department of Transport intelligent engeneering systems
E-mail: dildoraabdurazakova8222@mail.ru
Tel.: +998977003615
https://orcid.org/0009-0000-7774-2318

CONTEXT / MUNDARIJA

CONTENT / MUNDARIJA